THE ROLE OF HEAT SHOCK FACTOR 1 IN GERMINAL CENTER B CELLS AND LYMPHOMA

A Dissertation

Presented to the Faculty of the Weill Cornell Graduate School

of Medical Sciences

in Partial Fulfillment of the Requirements for the Degree of

Doctor of Philosophy

by

Tharu M. Fernando

May 2015

THE ROLE OF HSF1 IN GERMINAL CENTER B CELLS AND LYMPHOMA

Tharu M. Fernando, Ph.D.

Cornell University 2015

Diffuse large B cell lymphomas (DLBCLs) are a heterogeneous group of molecularly complex malignancies. The majority of DLBCL tumors arise from cells that are arrested in or have passed through the germinal center (GC). During the GC response, B cells undergo massive clonal expansion and somatic hypermutation of their immunoglobulin loci to produce high-affinity antibodies. Therefore GC B cells need to tolerate replicative and genotoxic stress without inducing cell cycle arrest, suggestive of a specialized stress response. Consistent with this hypothesis, we have discovered that a dominant regulator of the conserved stress response, heat shock factor 1 (HSF1), is important for the GC response. HSF1 regulates the stress-dependent induction of BCL6, an essential factor for GC formation that represses genes involved in DNA damage sensing and checkpoint activation. *Hsf1*$^{-/-}$ mice have smaller GCs and defects in the production of high-affinity antibodies. Because coordinate expression of genes is required for the GC response and post-GC differentiation, deregulation of certain genes, including BCL6, can lead to lymphomagenesis. Therefore the same pathways sustaining the GC response may be involved in maintaining DLBCL survival. We find that HSF1 controls a transcriptional program during the GC reaction that is necessary to tolerate stress associated with rapid replication and genomic instability. HSF1 is required to maintain the malignant phenotype in DLBCL due the regulation of genes involved in protein homeostasis and cell cycle control. We demonstrate that the stress axis of HSF1 and BCL6 is an

evolutionarily conserved feature of vertebrates and BCL6 acts as a stress response gene. BCL6 mediates stress tolerance through a lateral groove on its BTB domain that forms docking sites for NCOR, SMRT, and BCOR corepressors. Genetic or pharmacologic disruption of this motif abrogated the stress tolerance function of BCL6. Notably, a survey of human tumor cells revealed that HSF1-dependent expression of *BCL6* enables them to tolerate exposure to cytotoxic agents. Taken together, the evolutionarily conserved role of BCL6 and its BTB domain in mediating tolerance to stress in vertebrates provides the basis for using BCL6 BTB domain inhibitors as a broadly relevant therapeutic approach for cancer.

BIOGRAPHICAL SKETCH

Tharu M. Fernando earned her Bachelor of Science degree *summa cum laude* in Biological Sciences from Wright State University in December 2007. She completed a Master of Science degree in Pharmacology & Toxicology in June 2009 from Wright State University under the supervision of Dr. Courtney Sulentic. Her thesis research focused on understanding how an environmental contaminant, dioxin, affects the activity of a polymorphic enhancer region downstream of the immunoglobulin heavy chain locus. In August 2009, she joined the graduate program at Weill Cornell Graduate School of Medical Sciences in the department of Pharmacology and started her thesis research in the laboratory of Dr. Ari Melnick the following year. In April 2012, she was awarded the Ruth L. Kirschstein National Research Service Award Individual Predoctoral Fellowship from the National Cancer Institute to support her research training. Her dissertation, presented here, identified a role for HSF1 in the germinal center response and diffuse large B cell lymphoma, a disease that commonly arises from cells arrested in or have passed through the germinal center. Manuscripts describing her work are currently under preparation for publication in peer-reviewed journals. In addition, she has presented her work at several international conferences including the Society of Toxicology, Gordon Research Conference, Keystone Symposia, and American Society of Hematology.

ACKNOWLEDGMENTS

The past six years of painstaking research, many late nights, and countless experimental failures that were sprinkled with rare moments of success and sheer joy are finally culminating in the award of this doctoral degree. While it merely adds three slightly insignificant letters to the end of my name, I have achieved something greater, something that cannot be described, a mental feat of enduring epic battles with science and still standing to tell my tale of discovery. I could not have achieved this without the support of my family, friends and colleagues, and with them, I share this degree. First and foremost, I would like to thank my mentor, Dr. Ari Melnick, for the continuous support both scientifically and personally. Not only has he provided me with an incredible lab environment that has allowed me to broaden my technical expertise, but he has also been instrumental in my training and career development as an academic scientist. He has given me priceless insight into how to effectively communicate scientific concepts both in writing and giving talks. In addition I have learned so much from his remarkable ability to think outside the box and ask interesting questions. Most importantly he has supported me in times when I felt like I was mentally exhausted and broken, which happened on a few occasions. He somehow picked me up and gave me the energy to fight through it. His enthusiasm and excitement for science is near palpable and infectious, and it has driven me when I thought I had none left.

I owe a special thanks to Dr. Leandro Cerchietti, who is like a second mentor to me. From the time of my lab rotation to now, he has helped me every step

of the way. Our countless scientific discussions lead me to pursue research interests in such a diverse set of topics that spanned RNA modifications to the evolutionary conservation of stress response. By working together on such different projects, he kept me motivated and enthusiastic during those times that some projects weren't going very well. His constant support and encouragement have carried me through some of the roughest times in my PhD for which I cannot thank him enough.

I would also like to thank the members of my thesis committee, Dr. Lorraine Gudas, Dr. Yariv Houvras, and Dr. Olivier Elemento, for giving their time and intellectual input on my work over these past few years. Their thoughtful advice and encouragement contributed to both my scientific and personal growth. I also owe thanks to Dr. Gilbert Privé for all the help he has provided these past few months in finishing up my manuscript. I would like to thank him for flying to New York to attend my defense and am honored to have him on my examining committee.

I am indebted to all the current and former members of the Melnick lab. They are a talented group of scientists that have helped me both scientifically and personally. They are the reason I joined the lab and they are the reason I keep coming back despite all the failed experiments. This group has been an amazing support system through all these years, providing not only scientific advice but also endless amounts of encouragement and great times. I owe a special thanks to Dr. Katerina Hatzi who has been incredibly helpful through these past few years. I thank her for the countless times she has sat with me to help me analyze ChIP-seq data or run a unix command from the beginning

of my PhD and to this day. She has been invaluable and without her, an entire chapter of my dissertation would be missing. I would also like to thank my partner in crime, Rebecca Goldstein. We started our PhD's together in the Melnick lab and together we have finally completed them. I would like to thank her for always being there to celebrate moments of achievement and forget moments of failure. We have pushed each other to succeed despite all the frustration associated with being a student in the Melnick lab. She has been a constant and now that our PhD's are coming to an end, we will most likely part ways. I wish her every success with her future endeavors wherever they may take her.

I could not have made it these past few years without the love and support of my friends and family. I am incredibly grateful for all of my friends both in New York, Ohio, and around the world. While certainly challenging, these past few years have been filled with many happy moments, funny stories, and good times. I would not have been able to complete this dissertation without them. I would especially like to thank my parents for the constant encouragement and support. I am indebted to them for uprooting their lives in Sri Lanka and immigrating to the US so that my siblings and I could have more opportunities for a better life. They always pushed me to reach higher and so incredibly happy when I got this opportunity to come to New York for my PhD. Since then, they have provided an endless amount of encouragement, love, and support. For this, I am eternally grateful.

Finally, I have the utmost gratitude for my future husband, Justin Maurer. Together we have achieved many milestones including this dissertation. At the

present moment, he has helped me achieve a bachelor's degree, a master's degree, and finally a PhD. These achievements have often been preceded with many challenges, frustrations, and a few psychological breakdowns. He has helped me get past all of these struggles by providing infinite amounts of support, encouragement, and love. If it was accompanying me to lab late at night or cheering me up because of a failed experiment, he is a constant source of strength, support, and happiness. Without him, I could not have accomplished any of this. Thank you.

TABLE OF CONTENTS

LIST OF FIGURES

LIST OF TABLES

CHAPTER ONE
INTRODUCTION

1. Heat shock response

The heat shock response is a highly conserved mechanism shared by all organisms in response to a variety of chemical and physiological stresses. It was first described in 1962, when Ferrucio Ritossa noticed a distinct pattern of temperature- and chemical-induced puffing in polytene chromosomes of *Drosophila* larvae (Ritossa, 1962). These puffs were later shown to be transcriptionally active loci, encoding a set of conserved polypeptides collectively referred to as heat shock proteins (HSPs) (Lindquist, 1986; Lindquist and Craig, 1988). This effect was also observed in prokaryotes and in other eukaryotes implying an ancient and conserved mechanism for stress response (Kelley and Schlesinger, 1978; Lemaux et al., 1978; McAlister and Finkelstein, 1980). Most HSPs are abundant proteins expressed under normal conditions and function as molecular chaperones that facilitate the folding, translocation, and higher order assembly of client proteins. HSPs also protect the cell from general protein damage caused by denaturation and aggregation, either facilitating protein repair and refolding or inducing degradation. A family of transcription factors, aptly termed heat shock factors (HSFs), mediates the expression of *HSPs* and the response to stress. It was later found that HSFs not only have an essential role to play during stress response but they also have normal physiological functions and are important for development.

Effects of heat shock

Heat stress has detrimental effects on the cell, affecting both nuclear and cytoplasmic processes. Nucleoli become less condensed, and large deposits of ribosomal RNAs and aggregating ribosomal proteins are observed (Welch and Suhan, 1985) (**Figure 1.1A**). There is a complete block of DNA replication and transcription (Jamrich et al., 1977; Warters and Stone, 1983, 1984; Wong and Dewey, 1982). Heat shock transiently inhibits pre-mRNA splicing and mRNA export and induces the formation of distinct subnuclear structures referred to as nuclear stress bodies (Biamonti and Vourc'h, 2010; Boulon et al., 2010; Vogel et al., 1995). Nuclear stress bodies sequester pre-mRNA processing factors and a subset of splicing factors (Biamonti and Vourc'h, 2010). Early characterization of nuclear stress bodies demonstrated that these structures were initiated through an interaction between HSF1 and large regions of pericentromeric heterochromatin that contained tandem repeats of *satellite III* (*SatIII*) sequences (GGAAT) (Denegri et al., 2002; Jolly et al., 2002; Jolly et al., 2004; Rizzi et al., 2004). It was demonstrated in later studies that these *SatIII* sequences are transcribed and are required for the formation of nuclear stress bodies (Jolly et al., 2004; Metz et al., 2004; Rizzi et al., 2004; Shevtsov and Dundr, 2011). However the function of these nuclear stress bodies has yet to be determined.

Heat shock also induces cytoplasmic structures called stress granules, which are distinct from other cytoplasmic processing bodies (Collier and Schlesinger, 1986; Nover et al., 1989). This distinct compartment accumulates cellular mRNAs, pre-initiation and translation-related factors, and other RNA-binding proteins that affect translational control and mRNA stability (Anderson and Kedersha, 2006). Organelles are also affected as mitochondria undergo

several structural changes (**Figure 1.1B**). These induce metabolic changes as the total numbers of mitochondria decrease and ATP levels dramatically drop (Findly et al., 1983; Patriarca and Maresca, 1990; Welch and Suhan, 1985). Cells undergo a massive restructuring of the cytoskeleton with mild heat stress altering actin filaments into stress fibers and more severe stress resulting the aggregation of vimentin and other filament-forming proteins. This can result in the breakdown of the intermediate filament, actin, and tubulin networks and organelle relocalization (Toivola et al., 2010; Welch and Suhan, 1985, 1986). Fragmentation of the endoplasmic reticulum and Golgi complexes are observed, leading to a complete breakdown of intracellular transport processes (**Figure 1.1C**) (Welch and Suhan, 1985).

Collectively these effects lead to cell cycle arrest, decreased growth and reduced proliferation. If the duration and severity of stress is great enough, the cell will eventually accumulate enough defects that will result in cell death. However if the heat stress is not lethal, the cell will survive and become resistant to more severe and otherwise fatal stresses in a phenomenon known as thermotolerance (Gerner and Schneider, 1975). The increased levels of HSPs that are synthesized in response to stress conditions are thought to be the basis for this resistance (Lindquist, 1986).

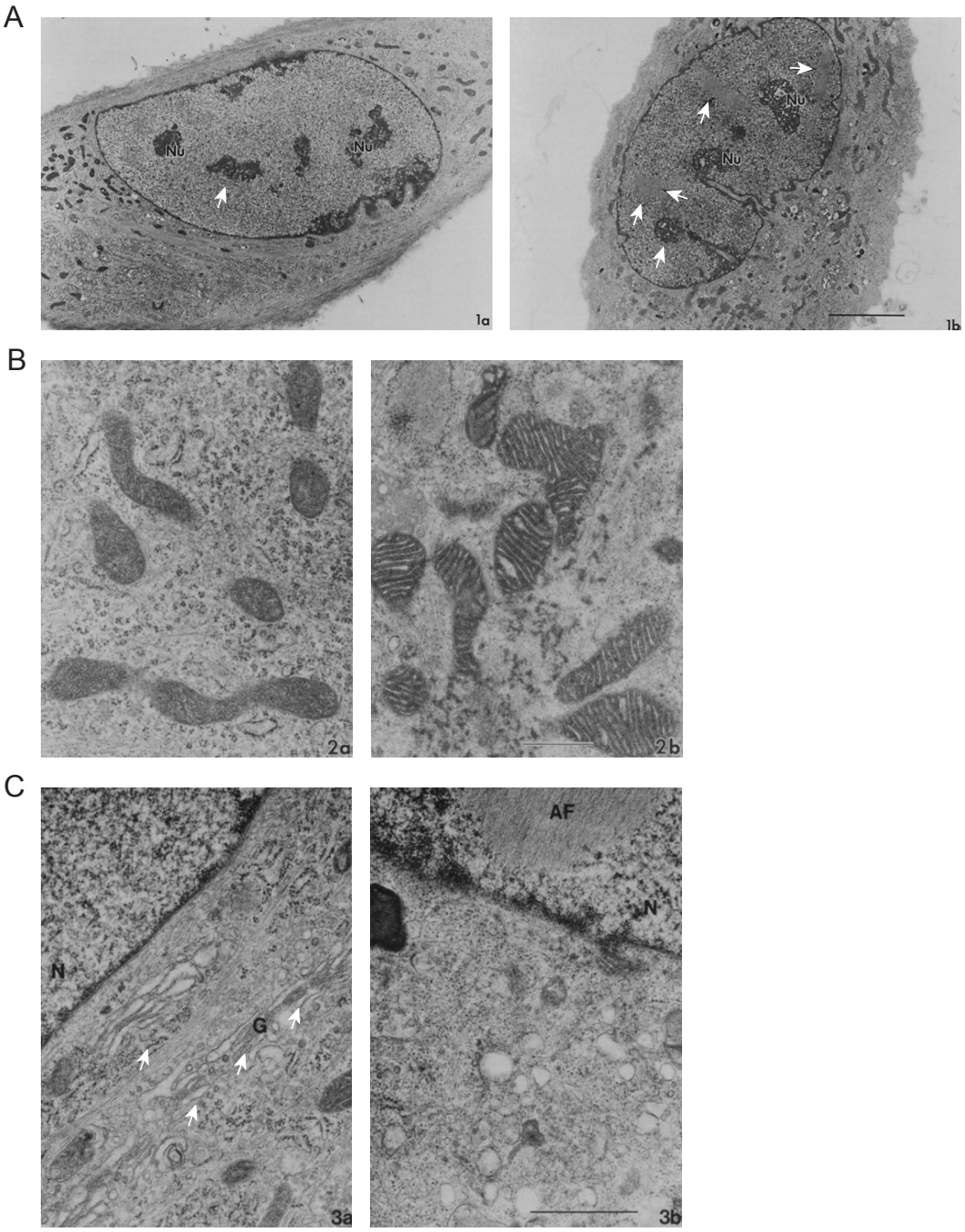

Figure 1.1 Detrimental effects of heat shock in rat embryo fibroblasts. Electron micrographs of cells incubated at normal temperature (37 °C, left) or after heat shock (3 h at 42 °C, right). (A) White arrows point to changes in the nucleoli and the formation of nuclear inclusion bodies. (B) Structural changes in mitochondria. (C) Heat shock induces fragmentation of the Golgi network. Adapted from Welch and Suhan (1985).

Heat shock proteins (HSPs)

Many studies have evaluated the heat shock response in several cell types and organisms on a genome-wide scale using differential display, gene expression profiling, and proteomics (Eisen et al., 1998; Gasch et al., 2000; GuhaThakurta et al., 2002; Larkindale and Vierling, 2008; Matsuura et al., 2010; Richmond et al., 1999; Rohlin et al., 2005; Tabuchi et al., 2008; Trinklein et al., 2004). These studies have demonstrated that 25-200 genes are significantly induced in different model organisms. In addition to the induction of molecular chaperones, other proteins that fall under the categories of metabolic enzymes, components of the proteolytic system, regulatory proteins like transcription factors and kinases, DNA- and RNA-modifying enzymes, and transport, detoxifying, and membrane-modulating proteins are also significantly upregulated upon heat stress (Richter et al., 2010). While the increased need for chaperones and proteases is intuitive in a cellular system that requires its protein homeostasis network to be maintained, the induction of other proteins in response to stress likely occurs to repair specific damages.

The predominant class of stress-inducible proteins is comprised of the molecular chaperones, HSPs. There are several major conserved families that are often classified by their molecular weight: HSP100s, HSP90s, HSP70s, HSP60s, HSP40s and small HSPs (or crystallins). HSPs are needed during both *de novo* protein folding and refolding of nonnative polypeptides (Lindquist and Craig, 1988; Richter et al., 2010; Saibil, 2013). In addition, HSPs can also mark misfolded proteins for degradation through coordination with ubiquitin ligases and the proteasome system (Arndt et al., 2007; Lanneau et al., 2010). While molecular chaperones are generally not thought to contribute structural

information for folding, they do prevent unwanted intermolecular interactions by binding to extended patches of hydrophic surfaces that can promote non-specific protein aggregation, specific peptide sequences, or structural elements. Chaperones do this by a cycle of controlled binding and release of nonnative proteins, which is triggered by multiple rounds of ATP hydrolysis with the exception of small HSPs that bind ATP but do not hydrolyze it (Bakthisaran et al., 2015; Hartl and Hayer-Hartl, 2009). While some molecular chaperones are only expressed after exposure to proteotoxic stress, most chaperones are ubiquitously expressed at high levels under physiological conditions. Some HSPs like HSP70 have forms that are both constitutive and stress inducible (HSC70 vs HSP70). Other HSPs like HSP90 complexes encompass as much as 1-2% of total cellular protein content and is further upregulated after stress (Borkovich et al., 1989).

HSP70 is one of the most highly conserved chaperones with more than 60% sequence identity with its prokaryotic version, DnaK (Richter et al., 2010). The HSP70 family has multiple genes, which are present in different cellular compartments and associated with a wide variety of physiological processes. The HSP70 family is involved in de novo protein folding, refolding of unfolded proteins, and preventing aggregation of unfolding proteins. HSP70 is indispensible for both normal growth and growth at higher temperatures (Lindquist and Craig, 1988). HSP70 functions together with cofactors like HSP40, which binds nonnative proteins, shuttles them to HSP70, and stimulates HSP70 ATPase activity (Kampinga and Craig, 2010; Richter et al., 2010; Saibil, 2013).

Similar to HSP70, HSP90 is also very well conserved with 40% identity shared with its bacterial homolog, htpG (Lindquist and Craig, 1988). Interestingly while the *HSP90* gene family is essential in *S. cerevisiae* for growth at high temperatures, the deletion of the *HtpG* gene in *E. coli* is not lethal (Bardwell and Craig, 1987; Borkovich et al., 1989; Lindquist and Craig, 1988). HSP90 is also found in almost every compartment of a eukaryotic cell. While it does not bind fully denatured polypeptides like HSP60 and HSP70, HSP90 binds partially folded protein intermediate conformations, suggesting it acts at the later stages of substrate folding (Jakob et al., 1995; Pearl and Prodromou, 2006; Taipale et al., 2010). HSP90 has a large number of diverse clients, which includes protein kinases, nuclear steroid receptors, transcription factors, protein trafficking and secretion components, and RNA processing factors (Taipale et al., 2010). In addition to its wide range of substrates, HSP90 also has a large cohort of co-chaperones that influence the dynamics of conformational equilibrium, the rate of ATP hydrolysis, recruitment of clients, or catalyze downstream enzymatic reactions. These include ATPase I (AHAI), HSP70-HSP90 organizing protein (HOP/STIP1), CDC37, p23 (PTGES3), FKBP51, FKBP52, and CHIP (Eckl and Richter, 2013).

Regulators of the heat shock response

In prokaryotes, the expression of *HSPs* is under the transcriptional control of σ32, which directs the bacterial RNA polymerase core enzyme to the promoters of *HSPs* (Grossman et al., 1987; Straus et al., 1987). In the absence of stress, DnaK the prokaryotic ortholog of HSP70 is bound to σ32, preventing σ32 from associating with the RNA polymerase core enzyme. After exposure to stress, DnaK disassociates from σ32, enabling the formation of

the RNA polymerase holoenzyme, which in turn is recruited to the consensus sites TTGAAA in the -35 region and CCCCATNT in the -10 region of *HSP* promoters (Nonaka et al., 2006; Wade et al., 2006; Zhao et al., 2005).

In eukaryotes, the expression of *HSPs* is tightly regulated by a family of transcription factors called heat shock factors (HSFs). HSFs bind to the upstream DNA regulatory regions of HSP genes as trimers, where each individual DNA-binding domain recognizes the pentameric sequence, nGAAn. Thus, a functional heat shock response element (HSE) is composed of at least three nGAAn repeats, and the promoters of most *HSP* genes contain more than one HSE, allowing for multiple HSF trimers to bind simultaneously. Thermal denaturation experiments demonstrated that orientation of the pentamers significantly drives stable HSF1-HSE interactions with cooperative binding only occurring when there are continuous inversions of the nGAAn sequence (Jaeger et al., 2014). While yeast and fruit flies have a single HSF, vertebrates express multiple HSFs (HSF1-4). In mammals, HSF1 is the dominant regulator of the heat shock response whereas this response is controlled by HSF3 in avian cells (Nakai, 1999). Orthologous *HSF3* gene segments were found in the human and mouse genome (Fujimoto et al., 2010). However only the mouse *HSF3* gene produced transcripts suggesting that the orthologous genomic region in humans is an *HSF3* pseudogene (Fujimoto et al., 2010). Interestingly the murine HSF3 failed to activate the *HSP70* gene during heat shock and was dispensable for thermotolerance (Fujimoto et al., 2010).

A large body of evidence has demonstrated that in addition to governing the heat shock response, the HSFs play many roles in normal physiology and development (Akerfelt et al., 2010). In *Drosophila*, deletion experiments demonstrated that the *Hsf* gene was important for oogenesis and larvae development, and these effects were not related to major changes in HSP expression (Jedlicka et al., 1997). Mice lacking HSF1 are not embryonic lethal, survive to adulthood, and have normal basal expression of *HSPs* (McMillan et al., 1998; Xiao et al., 1999). However *Hsf1*$^{-/-}$ mice exhibit multiple developmental defects including prenatal lethality, decreased body weight, growth retardation, failed zygotic cell division, placental defects, and female infertility (Christians et al., 2000; Xiao et al., 1999). *Hsf1*$^{-/-}$ oocytes also fail to mature as they are completely devoid of HSP90α, suggesting that maternal expression of HSF1 is required for the normal progression of meiosis in oocytes (Metchat et al., 2009). In addition *Hsf1*$^{-/-}$ mice exhibit abnormal brain morphology including enlarged ventricles, astriogliosis, neurodegeneration, progressive myelin loss, and defective olfactory neurogenesis (Homma et al., 2007; Santos and Saraiva, 2004; Takaki et al., 2006). In addition to developmental defects, Hsf1 null mice also display defects in the immune system including increased susceptibility to bacterial infections, impaired IgG production, reduced expression of cytokines and chemokines, and impaired T cell expansion after activation (Chen et al., 2012; Gandhapudi et al., 2013; Inouye et al., 2004).

The developmental functions of the HSF family are not limited to HSF1 as HSF2 and -4 also play important roles as developmental regulators. Unlike HSF1 that is ubiquitously expressed, HSF2 expression predominantly occurs

in the brain and testes, and its role in the development of these organs was apparent in the knockout mouse (Alastalo et al., 1998; Fiorenza et al., 1995; Goodson et al., 1995). *Hsf2*$^{-/-}$ mice have normal HSP expression but exhibit increased prenatal lethality, reduced female fertility, reduced testis size and sperm count, and brain abnormalities that include enlarged ventricles, abnormal neuronal migration, and defects in cortical lamination (Chang et al., 2006; Kallio et al., 2002; Wang et al., 2003). While *Hsf2* inactivation resulted in obvious defects, spermatogenesis was not completely arrested, indicating compensatory mechanisms. Indeed double disruption of *Hsf1* and *Hsf2* lead to a more pronounced phenotype: a complete lack of spermatozoa and male sterility (Wang et al., 2004). Unlike HSF1 and HSF2, HSF4 expression is undetectable in most tissues except in the brain, heart, lung, muscle, lens, and in splenic T cell subsets (Jin et al., 2011a; Tanabe et al., 1999). HSF4 has two isoforms, *HSF4a* and *HSF4b*, derived from alternative splicing of the same transcript and is a constitutive trimer (Nakai et al., 1997; Tanabe et al., 1999). *HSF4* mutations are associated with dominant inherited cataracts in humans, and *Hsf4* inactivation in mice results in cataracts shortly after birth most likely due to decreased expression of γ-crystallins and failure to repress fibroblast growth factors (Bu et al., 2002; Fujimoto et al., 2004; Min et al., 2004). The lens phenotype was more severe in the double knockout of *Hsf1* and *Hsf4* (Fujimoto et al., 2004; Min et al., 2004).

Although HSFs have both distinct and overlapping functions, HSF1 is the master regulator of the inducible heat shock response. This was demonstrated by a complete abrogation of HSP induction in *Hsf1*$^{-/-}$ mice after heat shock and a failure to acquire thermotolerance in *Hsf1*$^{-/-}$ embryonic cells (McMillan et al.,

1998; Xiao et al., 1999). Recent work has suggested a specific interplay between HSF1 and HSF2 in stress-inducible transcription. HSF2 can form heterotrimers with HSF1 and colocalize to stress-induced nuclear granules, but the stress-related functions of HSF2 are strictly dependent on HSF1 (Alastalo, 2003; Ostling et al., 2006; Sandqvist et al., 2009). Under basal conditions, trimerization of HSF1 is inhibited by a repressive HSP90-based multi-chaperone complex (Ali et al., 1998; Zou et al., 1998). In response to proteotoxic stress, HSPs are recruited to damaged proteins, allowing HSF1 to form homotrimers and undergo extensive post-translational modifications, both of which are essential for high-affinity DNA binding activity and transactivation.

Functional domains HSF1

The highly conserved DNA-binding domain (DBD) lies at the N-terminal region of the HSF1 protein (**Figure 1.2**) (Wu, 1995). The crystal structure (Harrison et al., 1994) and the two solution structures (Damberger et al., 1994; Vuister et al., 1994) of the HSF DBD resembles the winged helix-turn-helix family of DNA-binding proteins and consists of a three helix bundle capped by four antiparallel β-sheets. Physical and genetic studies show that the third helix of the HSF DBD acts as the recognition helix (Vuister et al., 1994). The oligomerization domain is C-terminal of the DBD and consists of arrays of hydrophobic heptad repeats (HR-A and HR-B) that are thought to form an unusual triple-stranded coiled-coil configuration (Peteranderl and Nelson, 1992). An additional C-terminal hydrophobic heptad repeat (HR-C) negatively regulates HSF1 trimerization by directly interacting with HR-A/B to form an intramolecular coiled-coil, maintaining the monomeric HSF1 in the absence of stress (**Figure 1.2**) (Farkas et al., 1998; Rabindran et al., 1993; Sarge et al.,

1993; Zuo et al., 1994; Zuo et al., 1995). The human HSF4, in addition to the HSF of *Saccharomyces cerevisiae* and *Kluvermonyces lactis*, lacks a conserved HR-C, which may explain their constitutive trimerization and DNA-binding activity (Chen et al., 1993; Nakai et al., 1997). The transactivation domain is located at the extreme C-terminal end of the HSF1 protein and is composed of two modules: AD1 and AD2, which are kept inactive by a regulatory domain found between HR-A/B and HR-C under basal conditions (**Figure 1.2**) (Green et al., 1995). While the isolated TAD has constitutive transcriptional activity, fusion with the regulatory domain restores stress-inducible activation (Green et al., 1995; Newton et al., 1996).

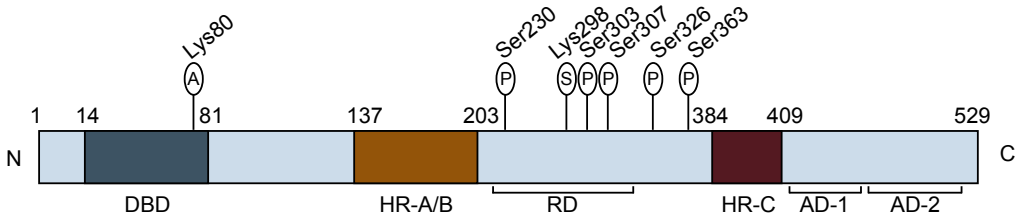

Figure 1.2 HSF1 organization. Functional domains of HSF1 include the DNA binding (DBD), heptad repeats (HR-A/B and HR-C), a regulatory domain (RD), and two activation domains (AD-1 and AD-2). HSF1 can be acetylated (A), phosphorylated (P), and sumoylated (S).

Activation and attenuation of HSF1

In the absence of stress, HSF1 is kept inactive in a multi-chaperone complex with HSP90, co-chaperone p23 (PTGES3), immunophilin FK506 binding protein 5 (FKBP52), HDAC6, and chaperone-like AAA ATPase p97/VCP (**Figure 1.3**) (Bharadwaj et al., 1999; Boyault et al., 2006; Boyault et al., 2007; Duina et al., 1998; Guo et al., 2001; Pratt and Toft, 1997; Zou et al., 1998). It is

predicted that HSP90 prevents the formation of HSF1 trimers by interacting with portions of the hydrophobic repeat regions (HR-A/B and HR-C) and a linker sequence N-terminal to the HR-A/B since those regions are involved in the repression of HSF1 oligomerization (Liu and Thiele, 1999; Orosz et al., 1996). Likewise treatment with HSP90 inhibitors has been demonstrated to activate HSF1 (Hegde et al., 1995; Zou et al., 1998). After heat shock, HSP90 and HSF1 dissociate (**Figure 1.3**). The mechanism of release is thought to rely on the dynamic nature of associations between HSPs and their substrates. Proteotoxic stress induces more protein unfolding, increasing the concentration of nonnative proteins that serve as substrates for HSP90. Due to the competition of HSF1 and misfolded proteins for HSP90, the rate of assembly of the HSF1-HSP90 complex is reduced, and unbound HSF1 monomers will rapidly trimerize (Voellmy, 2004). Zhou et al. (1998) experimentally demonstrated this when he showed that the addition of chemically denatured proteins to an *in vitro* system of Hela cells triggered HSF1 oligomerization. While HSF1 trimers gain DNA-binding activity, transactivation can only occur after the protein is extensively modified post-translationally (**Figure 1.3**).

Upon heat shock, HSF1 is hyperphosphorylated although the regulation of the effect of each phospho-residue on transcriptional competence is more complex. In addition to phosphorylation, HSF1 undergoes other post-translation modifications, including sumoylation, acetylation, and ubiquitinylation (**Figure 1.3**). Mass spectrometry analysis has revealed at least 12 serine residues that are phosphorylated within the regulatory domain of HSF1 (Guettouche et al., 2005). While stress-induced phosphorylation of both

Ser230 and Ser326 have been associated with increased transcriptional activity, Guettouche et al. (2005) demonstrated that Ser326 but no other serines residues specifically enhances HSF1 transcriptional competence (Holmberg et al., 2001). HSF1 is also phosphorylated under non-stress conditions. For instance, phosphorylation of Ser303 and Ser307 by GSK3β and ERK1 maintains HSF1 in a transcriptionally inactive state and may also mediate a protein-protein interaction with the scaffolding protein 14-3-3, which sequesters HSF1 in the cytoplasm (Chu et al., 1996; He et al., 1998; Kline and Morimoto, 1997; Knauf et al., 1996; Wang et al., 2004; Wang et al., 2003; Xavier et al., 2000). In addition to cytoplasmic sequestration, phosphorylation of Ser303/307 has been recently shown to facilitate an interaction with FBXW7α, a substrate-targeting unit of the Skp1-Cul1-F box ubiquitin ligase complex, which results in poly-ubiquitinylation, nuclear clearance, and degradation of HSF1 (Kourtis et al., 2015). Phosphorylation of Ser303 is also a prerequisite for a small ubiquitin-related modifier (SUMO) to be conjugated to Lys298, resulting in the repression of HSF1 transcriptional activity (Hietakangas et al., 2003). Unlike the rapid phosphorylation and sumoylation events that occur after heat shock, the acetylation of HSF1 at Lys80 by CBP/p300 is delayed and occurs when HSF1 activity is attenuated after activation (**Figure 1.3**) (Ghosh et al., 2011; Raychaudhuri et al., 2014; Westerheide et al., 2009). Lys80 is located in a short domain connecting the DNA recognition helix with the solvent-exposed loop and forms a hydrogen bond with the DNA phosphate backbone. Therefore, the neutralization of the positively charged Lys side chain would disrupt the DNA-HSF1 interaction. Deacetylation of HSF1 by SIRT1 enhances and prolongs DNA binding activity (Westerheide et al., 2009).

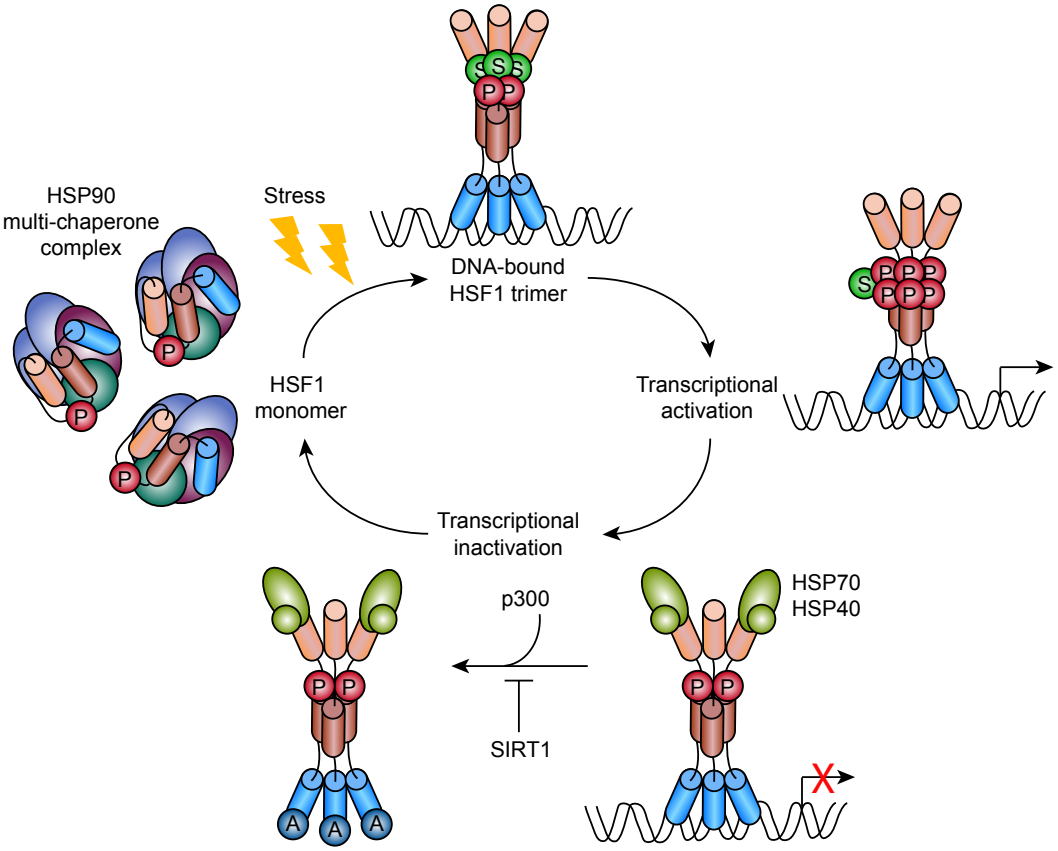

Figure 1.3 The HSF1 activation and attenuation cycle. Under basal conditions, HSF1 is a monomer and phosphorylated (P) in a complex with HSP90. After stress, HSF1 dissociates from the HSP90 complex, trimerizes, and binds to heat shock elements in its target genes. It undergoes other post-translational modifications that regulate its transactivation capacity like sumolyation (S) and phosphorylation (P). HSF1 attains transcriptional activity and induces the expression of its targets. HSF1 attenuation occurs by negative feedback from other HSPs that inhibits transactivation and by acetylation of Lys80 in the HSF1 DBD that inhibits DNA binding. SIRT1 antagonizes the actions of p300 by deacetylating HSF1. Adapted from Akerfelt et al. (2010).

After a cell has overcome stress and is returning to homeostasis, the oligomerization and activity of HSF1 must return to basal conditions. This is likely mediated by chaperones, as there is a decreased pool of unfolded proteins, which will shift chaperone complexes to form with HSF1. HSP70 and its co-chaperone HSP40 have been shown to interact with HSF1 to reduce its transactivation capacity without altering DNA binding (**Figure 1.3**) (Abravaya et al., 1992; Baler et al., 1992; Shi et al., 1998). In addition, the HSP90-multichaperone complex is able to associate with HSF1 trimers through its regulatory domain, which is distinct from the interaction HSP90 has with monomeric HSF1 (Guo et al., 2001).

HSF1-induced transcriptional regulation

Much of work that has provided insight into the transcriptional regulation of the heat shock response by HSF has been accomplished by extensive studies of the *HSP70* promoter in *Drosophila*. RNA polymerase II (Pol II) is transcriptionally engaged but paused downstream at the transcriptional start site of the *HSP70* promoter (Core and Lis, 2008). After heat shock, HSF binds HSEs within the *HSP70* promoter and recruits transcriptional coactivator Mediator, which collaborates with positive transcription elongation factor-b (P-TEFb) (Lis et al., 2000; Park et al., 2001). P-TEFb then phosphorylates the C-terminal domain (CTD) of Pol II, allowing for productive elongation (Marshall et al., 1996). In addition to P-TEFb, HSF1 also recruits histone-modifying enzymes, like Trithorax and CREB-binding protein (CBP), Spt6, a nucleosome chaperone, and Topoisomerase (Topo) I, which removes supercoils generated by transcription (Boehm et al., 2003; Ni et al., 2008; Smith et al., 2004). A recent study has demonstrated that the recruitment of HSF after heat shock

occurs rapidly while the recruitment of Pol II, Spt6, and Topo I occur much later (Zobeck et al., 2010). In addition to these transcriptional regulators, decondensation and nucleosome loss at the *HSP70* locus are dependent on poly(ADP)-ribose polymerase (PARP) (Petesch and Lis, 2008). After heat shock, PARP is rapidly redistributed along the *HSP70* locus (Petesch and Lis, 2012). The activation of PARP and accumulation of its catalytic product, PAR, at *HSP70* induce the formation of a localized compartment that retains Pol II for sustained transcriptional activation (Zobeck et al., 2010). This process is dependent on HSF1, which directs the acetylation of H2AK5 by the histone acetyltransferase TIP60, an event that is required for PARP activation, nucleosome loss, and transcriptional activation of *HSP70* (Petesch and Lis, 2012).

The mammalian *HSP70* promoter also houses paused Pol II. In fact, *HSP70* is bookmarked by HSF2, preventing its compaction by condensin and maintaining the gene in a transcriptionally competent or poised state (Xing, 2005). This allows HSF1 to bind and activate *HSP70* expression if cells in the early G1 phase were suddenly exposed to stress. Fujimoto et al. (2012) also demonstrated that low levels of HSF1 are bound to the *HSP70* locus and other HSF1 targets under normal physiological conditions in a complex with Replication Protein A (RPA), a protein known to stabilize single stranded DNA during DNA replication (Wold, 1997). The RPA-HSF1 complex opens the chromatin structure of the *HSP70* promoter by recruiting a histone chaperone FACT, which displaces histones, facilitating the preloading of Pol II (Fujimoto et al., 2012; VanDemark et al., 2006). This mechanism was found to be required for basal expression of HSF1 targets (Fujimoto et al., 2012). During

heat shock, active HSF1 recruits ATF1 and mitochondrial SSBP1 to the *HSP70* promoter (Takii et al., 2015; Tan et al., 2015). Both the HSF1-ATF1 and HSF1-SSBPI complexes have been demonstrated to be required for maximal recruitment of coactivators, lysine acetyltransferase CBP/p300 (Xu et al., 2008) and the BRG1-containing ATP-dependent chromatin-remodelling complex SWI/SNF, and optimal induction of *HSP70* (Corey, 2003; Sullivan et al., 2001; Takii et al., 2015; Tan et al., 2015; Xu et al., 2008). ATF1 also attenuates HSF1 activity by promoting acetylation of HSF1 via p300/CBP thereby decreasing its DNA binding activity (Ghosh et al., 2011; Raychaudhuri et al., 2014; Takii et al., 2015; Westerheide et al., 2009). Similar to the *HSP70* locus, HSF1 was shown to bind the *IL*-6 promoter and induce the opening of its chromatin structure by recruiting CBP and the SWI/SNF complex (Inouye et al., 2007). However unlike *HSP70*, HSF1 recruits a negative regulator of *IL-6*, ATF3, which inhibits *IL-6* expression (Takii et al., 2010).

Although heat shock increases the transcription of *HSP*s and other cytoprotective proteins, it also induces a global downregulation of many other housekeeping genes. This is partially mediated by the noncoding RNAs (ncRNAs) transcribed from mouse B2 and human Alu short interspersed elements (SINEs), which act as general transcriptional repressors by associating with Pol II complexes at promoters (Espinoza et al., 2004; Mariner et al., 2008). In addition to ncRNAs, HSF1 may also play a role in the downregulation of genes by potentially inducing changes in chromatin architecture or recruiting corepressors although the precise mechanisms have yet to be defined. However, HSF1 has been demonstrated to interact with and increase the activity of HDAC1 and HDAC2 after heat shock, resulting in a

global deacetylation of core histones (Fritah et al., 2009). An interaction between HSF1, HDAC1/2, and MTA1 has also been reported in breast cancer cells (Khaleque et al., 2008). Moreover, CoREST, an integral component of a histone deacetylase complex also containing HDAC1/2, interacts with HSP70 in a negative feedback loop that regulates *HSP70* gene expression (Gomez et al., 2008). Through this interaction, CoREST has been shown to repress HSF1-dependent transactivation.

Heat shock response and cancer

HSPs have been implicated in tumor initiation and survival, stabilizing many of the signaling pathways that are frequently hijacked to induce and maintain a malignant phenotype (Workman et al., 2007; Zuehlke and Johnson, 2010). In addition, tumor cells become addicted to HSPs because of oncoproteins that need a high degree of chaperoning because they are aberrantly expressed (HER2), mutated (B-RAF), or chimeric due to a genetic translocation (BCR-ABL) (Trepel et al., 2010; Workman et al., 2007; Zuehlke and Johnson, 2010). This is further confirmed by the fact that tumor-specific HSP90 participates in higher-order multi-chaperone complexes and has higher affinity for HSP90 inhibitors relative to normal tissues (Kamal et al., 2003; Moulick et al., 2011). This most likely represents a stress-specific form of HSP90 chaperone complexes in tumor cells that is necessary for executing functions required to maintain a malignant lifestyle. In fact many HSP90 inhibitors preferentially accumulate in the tumor and exhibit surprisingly low toxicity (Kamal et al., 2003; Moulick et al., 2011; Vilenchik et al., 2004). Thus several HSP90 inhibitors have been developed since the concept of targeting HSP90 first arose in the 1990s with the discovery of geldanamycin (Whitesell et al., 1994).

While geldanamycin proved too toxic and unstable for clinical use, geldanamycin analogs were promising and demonstrated proof-of-concept anti-tumor activity but with hepatic toxicity due to their quinone metabolism (Jhaveri et al., 2014; Neckers and Workman, 2012). Geldanamycin and many other HSP90 inhibitors all take advantage of the core network of hydrogen-bonding interactions to anchor the drug into the N-terminal ATP-binding pocket of HSP90 (Prodromou et al., 1997; Roe et al., 1999; Stebbins et al., 1997). High throughput screening and structure-based design methods have been employed to find newer HSP90 inhibitors that can be administered more frequently, achieve higher maximal doses, and lack significant hepatotoxicity, which was limiting for geldanamycin chemotypes. Many of these inhibitors fall into the purine scaffold series, with candidates BBIIB021, BIIB028, PU-H71, and the resorcinols, which include NVP-AUY922 (Cheung et al., 2005; Chiosis et al., 2001; Eccles et al., 2008; Neckers and Workman, 2012).

Due to its role in regulating the stress response, HSF1 has also been implicated in allowing cells to tolerate the imbalances of protein homeostasis that occurs during malignancy. While elevated HSP levels have been noted in several tumor types, increased HSF1 expression has also been found in human prostate carcinoma cell lines and HSF1 depletion sensitizes cells to proteasome and HSP90 inhibitors (Jolly and Morimoto, 2000; Tang et al., 2005; Zaarur et al., 2006). Susan Lindquist and colleagues demonstrated that genetic elimination of HSF1 protects mice against tumorigenesis in cancer models driven by loss-of-function *TP53* mutations and chemical carcinogens (Dai et al., 2007; Jin et al., 2011b; Min et al., 2007). While overexpression of HSF1 alone is unable to induce transformation in immortalized mouse

embryonic fibroblasts (MEFs), HSF1 enables cellular transformation initiated by oncogenic *RAS* and *PDGF-B* (Dai et al., 2007). These results are concordant with another study demonstrating a role for HSF1 in HER2-induced transformation of a breast epithelial cell line (Khaleque et al., 2008; Meng et al., 2010). Furthermore knockdown of HSF1 results in decreased cell viability in a number of malignant cell lines including breast, cervical, prostate, and kidney cancer (Dai et al., 2012; Dai et al., 2007; Meng et al., 2010; Min et al., 2007; Santagata et al., 2012; Zhao et al., 2011). Although HSF1 acts neither as a classical oncogene or tumor suppressor, HSF1 seems to govern a broad network of signaling pathways to support the tumorigenic environment.

Many studies have demonstrated that HSF1 regulates the expression of other genes in addition to *HSPs* (Dai et al., 2007; Khaleque et al., 2008; Mendillo et al., 2012; Trinklein et al., 2004). HSF1 modulates a number of cellular processes including signal transduction, proliferation, glucose metabolism, and protein translation (Dai et al., 2007; Lee et al., 2008; Zhao et al., 2011; Zhao et al., 2009). Therefore it was possible that HSF1 plays a larger role to directly rewire the transcriptome to maintain the malignancy of cancer cells. By using isogenic human breast cancer cell lines with different tumorigenic and metastatic potential and transforming them, Mendillo et al. (2012) demonstrated that the highly metastatic and tumorigenic cells have stronger HSF1 nuclear staining and were more dependent on HSF1. By using chromatin immunoprecipitation (ChIP) followed by next-generation sequencing (ChIP-seq) in heat shocked or transformed cell lines, Mendillo et al. (2012) went on to show that the HSF1 transcriptional program in malignant cells was distinct from cells exposed to heat shock. While many HSF1 gene targets

enrich in protein folding and stress response categories, other HSF1 regulated genes fall under categories of protein translation, RNA binding, metabolism, immune processes, cell cycle/proliferation, and cell adhesion (Mendillo et al., 2012). Activation of the HSF1-cancer program is associated with disease progression and can predict poor prognosis in breast, colon, lung, and hepatocellular carcinoma patients (Fang et al., 2012; Mendillo et al., 2012; Santagata et al., 2011).

While many studies have shown a clear role for HSF1 in maintaining a malignant phenotype in cancer cells, HSF1 also plays a part reprogramming tumor stroma to further enable tumor growth in a non-cell autonomous manner (Scherz-Shouval et al., 2014). HSF1 has been demonstrated to be active in cancer-associated fibroblasts (CAFs) (Scherz-Shouval et al., 2014). This specific subset of fibroblasts and myofibroblasts are recruited by the tumor to support proliferation, invasion, metastasis, angiogenesis and drug resistance by secreting extracellular matrix components, chemokines, cytokines, and growth factors. (Erez et al., 2010; Kalluri and Zeisberg, 2006; Lu et al., 2012; Olumi et al., 1999; Orimo et al., 2005; Pickup et al., 2013; Siegel and Massague, 2003; Straussman et al., 2012; Wilson et al., 2012). HSF1 activation in CAFs induces the expression and secretion of TGF-β and SDF1, which have been previously demonstrated to enhance the protumorigenic phenotype (Kojima et al., 2010; Scherz-Shouval et al., 2014). These results were further confirmed by the observation that HSF1 depletion in CAFs results in decreased growth of the tumor in a xenograft model (Scherz-Shouval et al., 2014). Interestingly the HSF1 transcriptional program in stromal cells was profoundly different from the transcriptional program it drives in cancer cells,

suggesting that HSF1 can drive highly divergent transcriptional responses depending on the cellular context (Scherz-Shouval et al., 2014).

2. B cell activation and lymphomagenesis

The immune system has two arms that protect an organism from pathogens: innate and adaptive immunity. The first line of defense is the innate immune system, which plays an essential role to mount an inflammatory response and activate the complement system. This controls the infection until the adaptive immune response can take effect. However the effectors of the innate immune response are limited in that they can only recognize some (not all) pathogens because they rely on germline-encoded receptors that identify microorganisms that may evolve more rapidly than the host they infect. In addition, innate immunity effectors lack immunological memory and are unable to provide long-lasting immunity. The adaptive immune response on the other hand has lymphocytes that undergo genetic recombination of variable regions within their germline antigen receptor genes during development to produce a clonally diverse repertoire of antigen receptors. While each lymphocyte will carry only one antigen specificity, millions of lymphocytes are produced to allow for the recognition of an almost infinite number of pathogens. After encountering an antigen, lymphocytes adapt their receptors to bind the antigen with higher affinity by undergoing additional somatic mutations and clonally expand to allow for the differentiation of enough effector cells to clear the antigen. After the antigen has been removed, many of the lymphocytes specific to that antigen will undergo apoptosis, leaving a few antigen-specific cells that remain and act as memory cells. These cells provide lasting protective immunity by allowing for a more rapid and enhanced response to

later encounters with the same pathogen. The humoral immune response, an important feature of adaptive immunity that is mediated by immunoglobulin molecules (or antibodies), protects extracellular spaces and prevents the spreading of intracellular infections. This response requires the coordinated efforts of both B and T cells for the maximal production of high-affinity antibodies by B cells.

B cell development

B cells are derived from a common lymphoid progenitor in the bone marrow by the concerted action of a network of stimulator molecules and transcriptional regulators that induces a specific lineage-defining gene expression program. In mice, the transition to the first step in B cell development, the pre-pro-B stage, is driven by interleukin (IL)-7 produced by stromal cells and signaling via the IL-7 receptor (**Figure 1.4**) (Milne and Paige, 2006). By activating the IL-7 receptor and STAT5, IL-7 induces the expression of *early B cell factor* (*EBF*) *1* (DeKoter et al., 2002; Dias et al., 2005; Kikuchi et al., 2005). EBF1 together with E2A and FOXO1 induce the expression of the essential B lineage-commitment factor, *PAX5*, which in turn participates in a positive feedback loop to further upregulate *EBF1* (Lin et al., 2010; Milne and Paige, 2006; Nutt and Kee, 2007). PAX5 activates genes necessary for subsequent B cell development while repressing genes involved in the development of non-B lineage cells (Delogu et al., 2006; Fuxa and Busslinger, 2007; Medvedovic et al., 2011).

The B cell antigen receptor (BCR) is a surface immunoglobulin (Ig) molecule consisting of two heavy and two light chains. Before the BCR can be

expressed on the surface of a B cell, the receptor must be assembled by DNA recombination events that join the variable (V), diversity (D), and joining (J) segments of the heavy (*IgH*) chain gene and V to J segments of the light chain (*Igκ* and *Igλ*) genes. This process is called V(D)J recombination, and it requires the endonucleases recombination activating genes (RAG) 1 and 2. RAGs introduce a double-strand break between a variable region segment and a nearby recombination signal sequence. This is followed by repair by nonhomologous end-joining (NHEJ) proteins, which generates a newly joined gene arrangement. To prevent aberrant recombination events, V(D)J recombination is tightly and temporally controlled during B cell development by (i) limiting the expression of *RAG1/2* to certain stages of B cell maturation and (ii) limiting RAG1/2 access to the different *Ig* gene segments by epigenetic mechanisms (Jhunjhunwala et al., 2009; Perlot and Alt, 2008).

D_H-J_H rearrangement of the *IgH* loci precedes V_H-DJ_H recombination and occurs in lymphoid progenitors in a mechanism dependent on E2A and EBF1 activating the expression of *RAG* genes (**Figure 1.4**) (Goebel et al., 2001; Perlot and Alt, 2008; Romanow et al., 2000). In committed pro-B cells, PAX5 mediates the contraction of the *IgH* locus, which is necessary for the juxtaposition of distal V_H genes to proximal DJ_H segments (Fuxa et al., 2004). Other studies have demonstrated that additional transcriptional regulators that include YY1, CCCTC-binding factor (CTCF), and members of the cohesin family also coordinate this event (Degner et al., 2009; Ebert et al., 2011; Liu et al., 2007). Upon productive rearrangement of one *IgH* allele, intact μ transcripts are expressed, which assemble with a surrogate light chain and accessory chains Igα and Igβ to form the pre-BCR (**Figure 1.4**) (Nishimoto et

al., 1991). Pre-BCR signaling acts to transiently downregulate the expression of *RAGs*, and attenuation of IL-7 receptor signaling also decreases the accessibility of the *IgH* locus to the RAGs (Chowdhury and Sen, 2003; Jung et al., 2006). If the first V_H-DJ_H rearrangement was nonproductive, V_H-DJ_H rearrangement occurs on the other chromosome. After successful *IgH* rearrangement and formation of the pre-BCR, B cells progress to the pre-B cell stage where they enlarge and receive signals to proliferate (**Figure 1.4**) (Melchers, 2005). Pro-B cells that have nonproductive rearrangements at both *IgH* alleles are unable to form the pre-BCR, making them incapable of receiving this proliferative signal, and undergo apoptosis.

The proliferating large pre-B cells eventually transition to small resting pre-B cells (**Figure 1.4**). This proliferative burst likely occurs to produce enough progeny so that each can produce a different light chain gene with differing antigen specificity thereby increasing BCR diversity. However pre-B cells must exit the cell cycle to allow for the reactivation of RAG expression and induction of light chain rearrangement (Lin and Desiderio, 1994). This occurs when the pre-B cells migrate away from IL-7-rich niches of the bone marrow (Tokoyoda et al., 2004). Light chain recombination tends to occur first on the *Igκ* locus and is driven by pre-BCR-dependent and -independent mechanisms and requires some of the same transcription factors involved in *IgH* rearrangement like PAX5 and E2A (Hamel et al., 2014; Lazorchak et al., 2006; Sato et al., 2004). Activated ERK induces *E2A*, which binds the *Igκ* enhancers to change the epigenetic landscape into a more open chromatin structure (Mandal et al., 2009). In addition, the loss of IL-7 receptor signaling leads to activation of PI3 kinase (PI3K)/Akt, resulting in increased *FOXO* expression (Amin and

Schlissel, 2008). FOXO1 directly induces the expression of the *RAGs* and kinases, *SYK* and *BLNK* (Amin and Schlissel, 2008; Ochiai et al., 2012). The SYK/BLNK module induces *IRF4* and *IRF8* expression, which also bind the *Igκ* enhancers and further increase *Igκ* accessibility (Johnson et al., 2008; Lu et al., 2003; Ma et al., 2008). Collectively, these events make the *Igκ* locus more accessible to transcription and recombination (Hamel et al., 2014). Once *Ig* light chains have been productively rearranged, they replace the surrogate light chain and combine with the rearranged heavy chain to form intact IgM molecules (**Figure 1.4**). IgM together with signaling accessory chains, Igα and Igβ, form the mature and fully functional BCR complex.

The now immature B cells undergo a negative selection process that will allow the cell to emigrate out of the bone marrow if it does not encounter a strong cross-linking antigen (i.e. self). Self-reactive B cells can undergo receptor editing, which requires additional rearrangement of their light chains to change their self-reactive receptors into non-self-reactive receptors (Gay et al., 1993; Tiegs et al., 1993). If they fail to edit their receptors appropriately, the cells will be deleted or silenced in a process referred to as anergy (Goodnow et al., 1988; Lederberg, 1959; Nemazee and Burki, 1989; Nossal and Pike, 1980). Immature B cells migrate out of the bone marrow and into secondary lymphoid organs like the spleen and lymph nodes. Secondary lymphoid organs have distinct compartments for B, T, and leukocyte and non-leukocyte stromal cells based on the expression patterns of chemoattractant receptors. Here the immature B cells compete for access to follicles formed by other B cells and attain signals for survival and maturation (Dal Porto et al., 2002). Once mature, resting B cells express both surface IgM and IgD (**Figure 1.4**). If they have not

encountered antigen, naïve B cells will leave the lymphoid organs via the efferent lymph (as in lymph nodes) or the marginal sinus (as in the spleen) to recirculate throughout the body or to another tissue in search for its antigen.

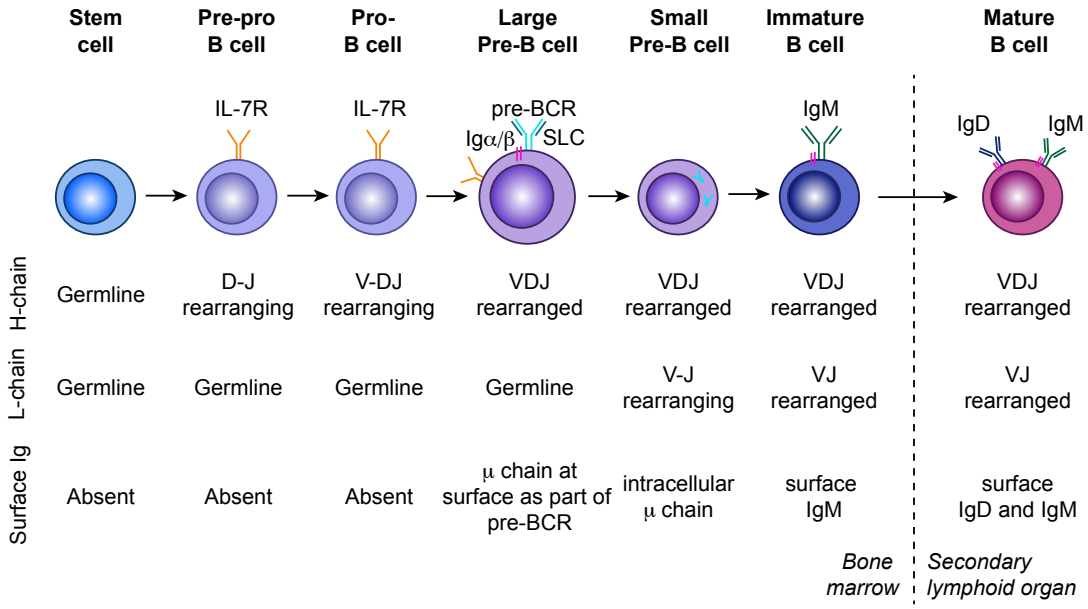

Figure 1.4 B cell development is marked by the rearrangement and expression of *Ig* genes. Pre-pro B cell differentiation from a stem cell is driven by IL-7 signaling through its receptor (IL-7R), which induces heavy chain rearrangement first. D_H-J_H rearrangement occurs in the pre-pro B cell followed by V_H-DJ_H rearrangement in the late pro-B cell stage. Once productive VDJ_H rearrangement has occurred, μ chain transcripts are expressed forming the pre-BCR with Igα/β and surrogate light chain (SLC). Pre-BCR signaling stimulates cells to grow and proliferate and also dampens IL-7R signaling. Large pre-B cells stop proliferating and become resting small pre-B cells to undergo light chain rearrangement. After productive light chain rearrangement, the fully functional BCR is formed from IgM, resulting in immature B cells. Immature B cells leave the bone marrow and migrate to peripheral secondary lymphoid organs to mature. At this stage, mature naïve B cells express both surface IgD and IgM from an alternative mRNA splicing mechanism. Adapted from Janeway et al. Immunobiology (2001).

B cell activation and the germinal center

Once a mature B cell encounters antigen in the lymphoid follicles either directly or through other antigen-presenting cells like macrophages, follicular or other local dendritic cells, its surface BCRs begin to cluster and crosslink with each other to induce a signaling cascade that results in the first stages of B cell activation (**Figure 1.5**). Then the B cell internalizes and processes the antigen for presentation by its major histocompatibility complex (MHC) class II proteins to T cells. Maximal B cell activation can only occur after additional signals from a specific subset of cognate T cells referred to as T follicular helper (T_{FH}) cells. Dendritic cells prime $CD4^+$ T cells to the T_{FH} cell fate through inducible costimulator (ICOS), various interleukins, and T cell receptor (TCR) signaling, which together upregulate the expression of B cell lymphoma 6 (BCL6) and other T_{FH} markers like CXC-chemokine receptor 5 (CXCR5) and programmed cell death protein 1 (PD1) (Choi et al., 2013; Choi et al., 2011; Crotty, 2014). Activated B cells and T_{FH} cells migrate to the borders of the follicle and T zone (i.e. the interfollicular zone) where they have long-lived interactions via MHC-TCR and CD40-CD40L interactions (**Figure 1.5**) (De Silva and Klein, 2015; Okada et al., 2005; Qi et al., 2008). Here activated B cells can undergo one of several fates. If the activated B cell has a BCR with high-affinity for the antigen, it will move to the extra-follicular regions and differentiate into short-lived plasma cells that secrete antibody (Jacob and Kelsoe, 1992; O'Connor et al., 2006; Paus et al., 2006). Alternatively, they can differentiate unto unswitched, recirculating memory B cells (Taylor et al., 2012). Finally a subset of B cells will be stimulated by T_{FH} cells to proliferate and migrate to the center of the B cell follicle where they will form distinct structures called secondary follicles or germinal centers (GCs) (**Figure 1.5**)

(Baumjohann et al., 2011; Choi et al., 2011; Kerfoot et al., 2011; Kitano et al., 2011; Pereira et al., 2009). GCs are the sites of affinity maturation where B cells clonally expand and are selected for producing high-affinity antibodies against antigen, and this process is highly dependent on BCL6, the master regulator of both the T_{FH} and GC B cell program (Basso and Dalla-Favera, 2010; Johnston et al., 2009; Nurieva et al., 2009).

Once B cells migrate into the center of the follicle, they grow and differentiate into blast-like cells (or centroblasts) that proliferate rapidly. The proliferation of centroblasts pushes naive B cells outward, forming the mantle zone that surrounds the GC (**Figure 1.5**) (De Silva and Klein, 2015; Victora and Nussenzweig, 2012). The GC becomes polarized into two discrete compartments referred to as the dark and light zone based on their histological appearance. The dark zone consists of densely packed centroblasts whereas the light zone has B cells interspersed in a network of follicular dendritic cells (FDCs), T_{FH}, and macrophages (De Silva and Klein, 2015; Victora and Nussenzweig, 2012). Apart from anatomical differences, chemokine gradients and the expression of their receptors also segregate GC cells into dark and light zone compartments. Dark zone B cells express high levels of CXCR4 and lower levels of CD83 and CD86 whereas light zone B cells express low levels of CXCR4 and high levels of CD83 and CD86 (Allen et al., 2004; Allen et al., 2007; Caron et al., 2009; Victora et al., 2010).

In the dark zone, centroblasts undergo somatic hypermutation (SHM) of their *IgV* regions by activation-induced cytidine deaminase (AID). AID deaminates deoxycytosines into deoxyuracils on single-stranded DNA producing

mismatches that are removed by base excision repair or mismatch repair mechanisms ultimately producing an Ig receptor with a spectrum of affinities for the antigen (Dominguez and Shaknovich, 2014; Zan and Casali, 2013). GC B cells then migrate to the light zone where they are positively selected if they express high-affinity antigen receptors and are signaled to re-enter the dark zone for further cell division and mutations. Many rounds of mutation and selection allow for the production of the highest-affinity antibodies (De Silva and Klein, 2015; Victora and Nussenzweig, 2012). Selection of GC B cells is dominated by T_{FH} cells, which have also homed to the light zone of the GC (**Figure 1.5**) (Victora et al., 2010). Many studies have demonstrated that T_{FH} cells provide survival and proliferative signals via its TCR to GC B cells through peptide-MHC complexes (De Silva and Klein, 2015; Victora and Nussenzweig, 2012). In fact GC B cells that present a higher density of antigen on MHC complexes have the largest and longest contacts with T_{FH} cells, and this is directly correlated to the number of times the cell divides after re-entering the dark zone and the accumulation of SHM (Gitlin et al., 2014; Shulman et al., 2014; Victora et al., 2010). While BCR affinity is directly associated to the amount of antigen captured and presented on MHC complexes, BCR signaling does not influence GC B cell selection by either T_{FH} cells or FDCs. In fact BCR signaling is quiescent due to increased phosphatase activity of SHP1 (Khalil et al., 2012; Victora et al., 2010). In addition to receiving proliferative signals from T_{FH} cells, GC B cells also provide signals to T_{FH} cells. Shulman et al. (2014) demonstrated that contact between T_{FH} and GC B cells results in increased calcium signaling and IL-4 and IL-21 production in T_{FH} cells, which enhances GC T_{FH} function (Shulman et al., 2014). In addition, GC B cells express ICOSL that enhances interactions

with ICOS-expressing T_{FH} cells (Liu et al., 2015). This in turn increases the surface display of CD40L on T_{FH} cells, which provides GC B cells with CD40 stimulation that induces more ICOSL on GC B cells (Liu et al., 2015). Once selected in the light zone, GC B cells can undergo class-switch recombination (CSR) of their *Ig* loci, which like SHM is also mediated by AID, to produce a different isotype of antibody for different effector function (De Silva and Klein, 2015; Victora and Nussenzweig, 2012). After CSR, GC B cells can re-circulate back to the dark zone or directly differentiate further. This process is regulated by T_{FH}-mediated production of IL-4 and IL-21 (Zotos and Tarlinton, 2012).

The end product of the GC response is the differentiation of B cells to two post-GC compartments: memory B cells or plasmablasts (**Figure 1.5**). Memory B cells recirculate in the periphery and will rapidly differentiate into plasma cells if they re-encounter the same antigen (Gray, 1993). Plasmablasts will differentiate further into long-lived plasma cells and home to the bone marrow (Shapiro-Shelef and Calame, 2005). The mechanisms governing the fate of GC B cells to the either cell compartments are not fully understood. Entry into the memory compartment is hypothesized to be a stochastic event in that if the GC B cell is selected and survives apoptosis, this might be sufficient for progression towards the memory cell fate (Victora and Nussenzweig, 2012; Zotos and Tarlinton, 2012). Commitment to the plasma cell fate has been demonstrated to occur through CD40 activation of the NF-κB pathway and induction of IRF4. IRF4 suppresses *BCL6* and induces the expression of *BLIMP1*, which is the master regulator of plasma cell differentiation (Oracki et al., 2010; Victora and Nussenzweig, 2012).

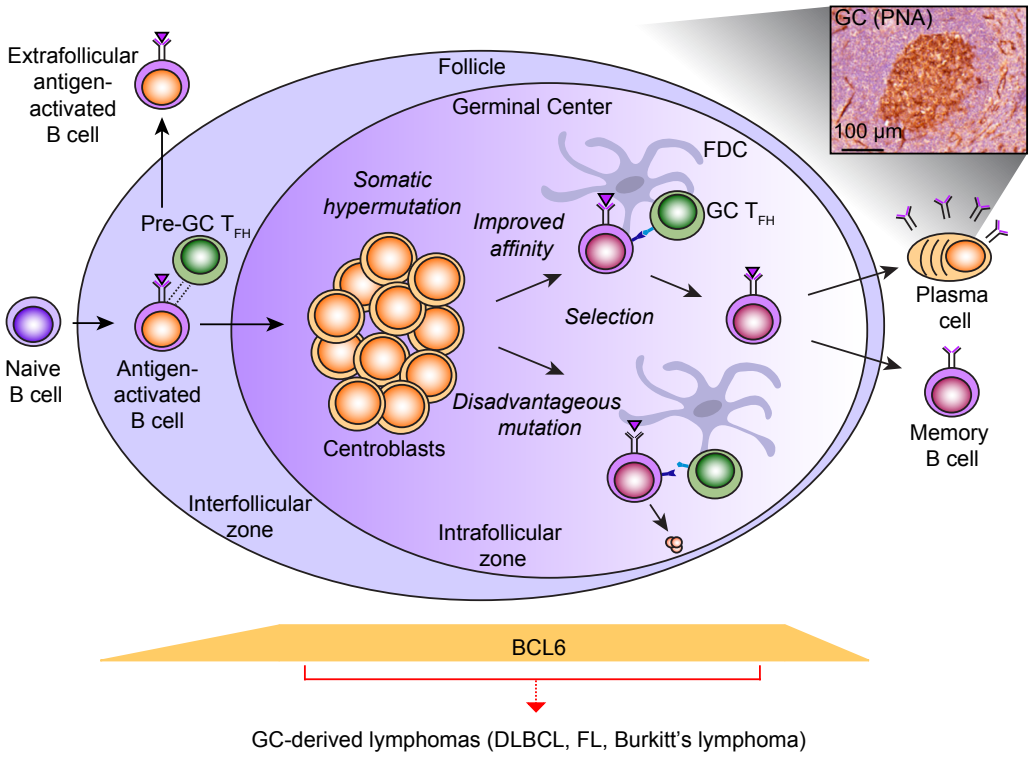

Figure 1.5 Germinal center formation. To generate high-affinity antibodies, antigen-activated B cells migrate to the interfollicular zone where T_{FH} cells stimulate them to move to the center of the follicle, proliferate, and differentiate into centroblasts, resulting in the formation of GCs. Centroblasts undergo clonal expansion and somatic hypermutation of the *IgV* loci to produce Ig of heterogeneous affinities to antigen. GC B cells with high-affinity antigen-specific Ig are selected by T_{FH} cells that provide them with proliferative and survival signals whereas those cells with mutations that encode low-affinity Ig are not selected and undergo apoptosis. After selection, GC B cells can differentiate further into either antibody-secreting plasma cells or memory B cells. BCL6 is the master regulator of the GC response in GC B cells and T_{FH} cells. However BCL6 expression must be downregulated to ensure post-GC exit and terminal differentiation, and constitutive expression of BCL6 can transform GC B cells into malignant lymphomas. GCs are detectable by immunohistochemistry using peanut agglutinin (PNA) to stain splenic tissues obtained from immunized mice (top right inset). Adapted from Bunting and Melnick (2013) and Beguelin et al. (2013).

GCs and B cell lymphomas

While GCs are necessary for the immune response, they need to be tightly regulated to prevent transformation into lymphomas. GC B cells undergo genotoxic and replicative stress due to SHM and CSR of their *Ig* loci and clonal expansion. Both processes are essential for the production high-affinity antibodies. However aberrant SHM and/or CSR can make the GC B cell susceptible to chromosomal translocations and deregulation of proto-oncogenes resulting in malignancy (Klein and Dalla-Favera, 2008; Lenz and Staudt, 2010). In fact the majority of human B cell lymphomas have somatic mutations in the *IgV* loci suggesting that they are either blocked in or have passed through the GC (Klein and Dalla-Favera, 2008; Seifert et al., 2013). GC B cells can give rise to a number of lymphomas, including follicular, Burkitt, and diffuse large B cell lymphomas.

Diffuse large B cell lymphoma (DLBCL) is the most common form of lymphoma, accounting for 30-40% of newly diagnosed lymphomas (Lenz and Staudt, 2010; Rodriguez-Abreu et al., 2007; Roschewski et al., 2014). They are aggressive but have a greater than 50% response rate to the current standard therapeutic regimen of cyclophosphamide, doxorubicin, vincristine, prednisone, and rituximab (R-CHOP) (Roschewski et al., 2014). DLBCL is a heterogeneous group of malignancies that can be subdivided into three molecular subtypes based on gene expression profiling studies: GC B cell-like (GCB), activated B cell-like (ABC), and primary mediastinal B cell lymphoma (PMBL) (Lenz and Staudt, 2010; Roschewski et al., 2014). Furthermore whole-genome and exome sequencing of DLBCL primary tumor samples have revealed a gamut of mutations that add an additional level of complexity to the

disease (Lohr et al., 2012; Morin et al., 2011; Pasqualucci et al., 2011b; Zhang et al., 2013). The three DLBCL subtypes have differing clinical presentations, cure rates, and therapeutic responsiveness (Lenz and Staudt, 2010; Roschewski et al., 2014). For example GCB DLBCL has a better prognosis than ABC DLBCL with R-CHOP treatment or a modified treatment regimen that adds dose-adjusted etoposide to R-CHOP (DA-EPOCH-R) (Roschewski et al., 2014). Patients with PMBL have an extremely high cure rate after treatment with DA-EPOCH-R relative to both GCB and ABC DLBCL patients (Dunleavy et al., 2013). In addition to clinical differences, these DLBCL subtypes also differ widely in mechanisms of oncogenic activation (Lenz and Staudt, 2010; Roschewski et al., 2014).

GCB DLBCLs have a genetic signature similar to normal GC B cells (Lenz and Staudt, 2010; Roschewski et al., 2014). GCB DLBCLs have highly mutated and switched *Ig* loci, and SHM is ongoing on malignant cells (Klein and Dalla-Favera, 2008; Lenz and Staudt, 2010; Roschewski et al., 2014). GCB-specific genetic lesions include the t(14;18) translocation, which results in ectopic expression of anti-apoptotic *BCL2*; the loss of *PTEN* and amplification of the microRNA *miR-17-92* cluster, which activate the PI3K/AKT pathways to promote growth and proliferation; and *TP53* mutations that result in increased genomic instability (Lohr et al., 2012; Morin et al., 2011; Pasqualucci et al., 2011b; Zhang et al., 2013). Somatic mutations that are GC-specific occur in *EZH2*, resulting in a proliferative effect and differentiation blockade by aberrant H3K27 trimethylation; *MEF2B*, which enhances the GC-phenotype by inducing *BCL6*; *BCL2*, resulting in the activation of anti-apoptotic pathways; and *GNA13*,

which results in the activation of AKT signaling (Beguelin et al., 2013; Caganova et al., 2013; Muppidi et al., 2014; Ying et al., 2013).

Unlike GCB DLBCLs, ABC DLBCLs have gene expression patterns that are more similar to B cells undergoing plasmacytic differentiation, and therefore the hallmark signature of ABC DLBCL is the constitutive activation of NFκB signaling (Lenz and Staudt, 2010; Roschewski et al., 2014). Persistent NFκB signaling leads to a host of downstream cellular processes involved in tumor development and progression (Lenz and Staudt, 2010; Roschewski et al., 2014; Staudt, 2010). ABC-specific somatic mutations frequently occur in *MYD88*, an adaptor protein that interacts with toll-like receptors (TLRs) (Morin and Gascoyne, 2013; Roschewski et al., 2014). This mutation induces rapid proliferation in the absence of TLR ligands by activating the NF-κB and JAK/STAT3 pathways (Ngo et al., 2011). Activating mutations can also occur in the *Igα*/*Igβ* co-stimulatory molecules of the BCR (CD79A/CD79B, respectively), inducing chronic BCR activation, and *CARD11*, a member of the CARD11/BCL10/MALT1 (CBM) complex that activates the IkB kinase (IKK) complex resulting in nuclear translocation of NF-κB dimers (Morin and Gascoyne, 2013; Roschewski et al., 2014). ABC DLBCLs also have genetic lesions that inactivate negative regulators of the NF-κB pathway. ABC DLBCLs have frequent nonsense mutations or genetic deletions of *TNFAIP3*, which encodes A20 a deubiquitinating enzyme that inactivates IKK (Roschewski et al., 2014; Staudt, 2010).

PMBL DLBCL genetic signatures are similar to Hodgkin lymphomas in that both rely heavily on NF-κB and JAK-STAT6 signaling. The characteristic

genetic lesion of PMBL DLBCL is the amplification of chromosome 9p24 (Lenz and Staudt, 2010; Roschewski et al., 2014; Shaffer et al., 2012). This results in amplification of *JAK2.* PMBL DLBCLs also frequently have deletions of *SOCS1*, a negative regulator of JAK2, and mutations in *STAT6*, collectively increasing the activity of the JAK-STAT pathway. PMBL DLBCL patients also have translocations of a transactivator of MHC class II genes (*CIITA*) that produce fusion proteins. These fusions result in the inactivation of CIITA and loss of MHC class II proteins thereby allowing tumor cells to evade immune surveillance (Jardin, 2014; Morin and Gascoyne, 2013; Roschewski et al., 2014; Shaffer et al., 2012).

While DLBCL sub-types differ cytogenetically and by mutational status, they all deregulate transcriptional mechanisms intended to control the GC response. Many of these mechanisms involve chromatin remodeling factors and epigenetic regulators and are also targets for aberrant regulation due to mutations. These mutations are not sub-type specific but do occur at different frequencies. Mutations in the methyltransferase *MLL2* are equally distributed between GCB and ABC DLBCL and result in a truncated form of the protein (Jardin, 2014; Morin and Gascoyne, 2013). The acetyltransferase genes, *CREBBP* and *EP300*, also have loss-of-function mutations, which are found in both GCB and ABC DLBCL and follicular lymphoma (Jardin, 2014; Morin and Gascoyne, 2013). As alluded to earlier, BCL6 is the master regulator of the GC program. Therefore it is one of the most commonly deregulated genes in DLBCLs (Ci et al., 2008). Chromosomal translocations involving *BCL6* at chromosome 3q27 are found in 30-40% of DLBCLs and interestingly occur more frequently in ABC versus GCB DLBCL (Ci et al., 2008). Moreover 70% of

DLBCLs display somatic mutations in the 5' regulatory regions of *BCL6* (Pasqualucci et al., 2001). Either of these genetic aberrations leads to constitutive *BCL6* expression and the maintenance of the proliferative and genetically unstable GC phenotype (Hatzi and Melnick, 2014).

3. The BCL6 transcriptional repressor

BCL6 is a transcriptional regulator that plays an important role in B cell development and the formation of GCs. Pre-B cells induce BCL6 during light chain rearrangement for its pro-survival functions (Duy et al., 2010). This is required for pre-B cells to generate an extensive repertoire of polyclonal B cells (Duy et al., 2010). BCL6 null mice fail to develop GCs and cannot generate affinity-matured antibodies (Dent et al., 1997; Ye et al., 1997). BCL6 allows GC B cells to sustain SHM and CSR of their *Ig* loci without inducing cell arrest or apoptosis by repressing genes involved in DNA damage sensing and response, apoptosis, and checkpoint activation (Phan and Dalla-Favera, 2004; Phan et al., 2005; Ranuncolo et al., 2007; Ranuncolo et al., 2008a). It also maintains the centroblast phenotype by repressing genes involved in premature B cell activation and plasma cell differentiation (Li et al., 2005; Shaffer et al., 2000; Tunyaplin et al., 2004). However BCL6 expression must be downregulated to enable post-GC differentiation and normal growth, and as discussed earlier, its deregulation is often associated with lymphomagenesis (Hatzi and Melnick, 2014). In addition to being essential for the survival of GC B cells, BCL6 is also critical for T_{FH} cell differentiation to repress genes that drive differentiation towards alternate T helper cell lineages (Crotty, 2014; Johnston et al., 2009; Nurieva et al., 2009).

BCL6 structure and function

BCL6 is a member of the bric-a-brac, tramtrack, broad complex/pox virus zinc finger (BTB/POZ) family of proteins. The human BCL6 protein is 706 amino acids and consists of an N-terminal BTB/POZ domain (residues 5-129) and six C-terminal Krüppel C_2H_2-type zinc finger (ZF) domains (residues 518-681) (**Figure 1.6**). The N-terminal and C-terminal domains are connected by a large, unstructured linker that contains another regulatory domain referred to as RD2 (residues 350-395) (**Figure 1.6**). Through its various protein domains, BCL6 is able to recruit a diverse set of chromatin-modifying complexes and therefore has multi-faceted biochemical mechanisms of gene repression (**Figure 1.6**).

The BCL6 BTB domain is an obligate homodimer and has autonomous repressor activity (Ahmad et al., 2003; Chang et al., 1996; Deweindt et al., 1995). The interface between monomers create two extended lateral grooves that serve as docking sites to corepressors NCOR1 (NCOR), NCOR2 (also known as SMRT), and BCOR (Ahmad et al., 2003; Dhordain et al., 1997; Ghetu et al., 2008; Huynh and Bardwell, 1998; Huynh et al., 2000). NCOR and SMRT have 45% sequence identity yet bind the BCL6 BTB domain with a highly similar sequence (Ahmad et al., 2003). In comparison, the BCOR BTB binding domain (BBD) is different in sequence and structure to NCOR and SMRT but binds to the same lateral groove on the BCL6 BTB domain (Ghetu et al., 2008). The BBD residues of NCOR, SMRT, and BCOR are specific for the BCL6 BTB domain, and conversely, the BCL6 BTB domain surface residues that interact with these corepressors are also unique to BCL6 (Stogios et al., 2010). It was thought that corepressor binding to the BCL6 BTB domain was mutually exclusive (Huynh et al., 2000). However Hatzi et al.

(2013) demonstrated that a ternary complex consisting of both BCOR and SMRT is able to bind simultaneously to symmetrical sites on the BCL6 domain. BCL6 BTB corepressors act as adaptor proteins for other chromatin modifying proteins. NCOR and SMRT form complexes with histone deacetylase 3 (HDAC3) whereas BCOR forms a Polycomb repressive complex 1 (PRC1)-like complex (Farcas et al., 2012; Gao et al., 2012; Gearhart et al., 2006; Karagianni and Wong, 2007; Sanchez et al., 2007). Mutating the residues (N21K and H116A) within the BCL6 BTB domain that make contact with the corepressors abrogates binding to NCOR and SMRT and diminishes BTB repressor activity in reporter assays (Ahmad et al., 2003).

BCL6 is a sequence-specific transcriptional repressor and binds DNA via its ZF domain (Baron et al., 1995; Chang et al., 1996; Deweindt et al., 1995; Kawamata et al., 1994). The BCL6 consensus core sequence is TTCCT(A/C)GAA but more degenerate sequences have been found by mapping BCL6 binding sites using chromatin immunoprecipitation (ChIP) (Baron et al., 1995; Chang et al., 1996; Ci et al., 2009; Kawamata et al., 1994). Mutational studies demonstrated that the first two ZFs are dispensable for DNA binding activity while mutations in the other four ZFs resulted in a complete inability of BCL6 to bind to its consensus motif (Mascle et al., 2003). In addition to being required for DNA binding, the BCL6 ZF domain can mediate transcriptional repression (Albagli et al., 1996; Lemercier et al., 2002). The BCL6 ZFs have been shown to interact with class II HDACs and the corepressor ETO to enhance its own repressor activity (Chevallier et al., 2004; Lemercier et al., 2002). It has also been demonstrated to bind AP-1 proteins and repress their transcriptional activity (Vasanwala et al., 2002).

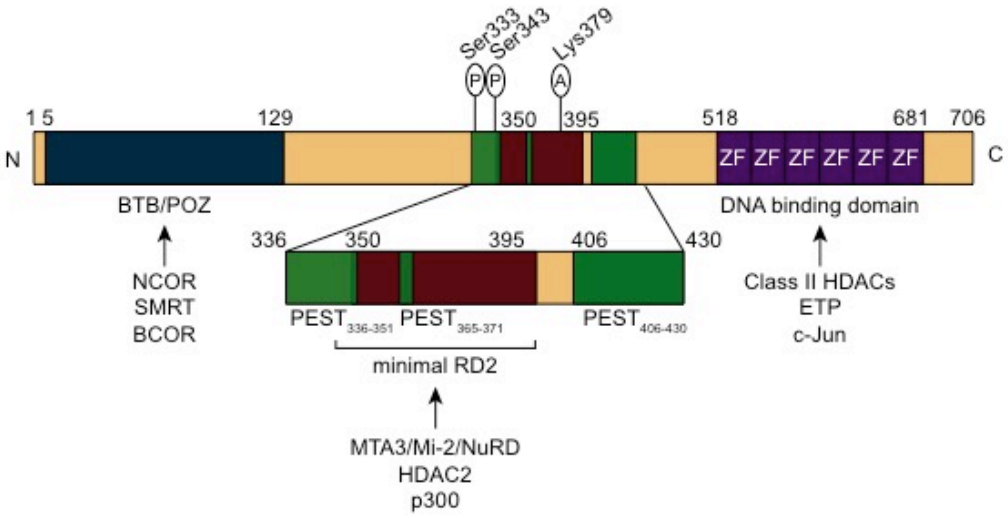

Figure 1.6 BCL6 organization. Functional domains of BCL6 include the BTB domain, the middle repressor domain (RD2), and six zinc finger (ZF) domains. BCL6 stability and repressor activity is regulated by post-translational modifications including acetylation (A) and phosphorylation (P) and three PEST sequences found in the middle linker region. Each BCL6 domain can mediate interactions with other proteins including corepressors and other chromatin-modifying proteins.

The RD2 domain of BCL6 is found between the BTB domain and ZF domains and, like them, has autonomous repressor activity (**Figure 1.6**) (Chang et al., 1996; Lemercier et al., 2002). The minimal residues of this linker region required for repressor activity were mapped to amino acids 350-395 (Huang et al., 2014). The RD2 domain has been shown to mediate transcriptional repression by interacting with MTA3, which recruits the Mi-2/NuRD complex to BCL6 targets and facilitates HDAC-dependent repression (Fujita et al., 2004; Huang et al., 2014). This interaction was dependent on the acetylation status of KKYK residues that map to amino acids 387-379 on the RD2 domain (Fujita et al., 2004). The acetyltransferase p300 binds to BCL6 and acetylates these residues, inactivating BCL6 (Bereshchenko et al., 2002). Therefore HDAC

complexes are important for BCL6-mediated transcriptional repression by maintaining its inhibitory capacity and by modifying chromatin to a more repressive state (Bereshchenko et al., 2002). Phosphorylation of the RD2 domain is another means to modulate BCL6 stability. MAP kinase can phosphorylate residues within proline-, glutamate-, serine-, and threonine-rich PEST sequences in the RD2 domain and mark it for degradation by the ubiquitin-proteasome pathway (Niu et al., 1998).

BCL6 repressive mechanisms in GC B cells and lymphoma

The formation of GCs is a sequential and coordinated process that relies heavily on BCL6 induction in both GC B cells and T_{FH} cells (Crotty, 2014; Hatzi and Melnick, 2014). BCL6 is critical for GC B cells to sustain DNA damage associated with SHM and CSR while proliferating rapidly because it silences DNA damage sensing and response, apoptosis, and cell cycle checkpoints genes like *ATR*, *ATM*, *TP53*, *CHECK1*, and *CDKN1A* (Phan and Dalla-Favera, 2004; Phan et al., 2005; Ranuncolo et al., 2007; Ranuncolo et al., 2008a). By generating mutant knock-in mice that have disrupted BTB or RD2 function, our lab was able to demonstrate that the BCL6 repressor domains mediate distinct steps in GC development (Huang et al., 2014; Huang et al., 2013). Mice with mutations in the BCL6 BTB domain (N21K and H116A) that abrogate the recruitment of NCOR, SMRT, and BCOR were able to form early GC clusters but unable to sustain the rapid proliferative and DNA damage-tolerant phenotype of GC B cells (Huang et al., 2013). These results were confirmed by ChIP-seq studies in human GC B cells that showed BCL6 recruited SMRT or BCOR to key cell cycle genes like *ATR*, *TP53*, and *CDKN1A* (Hatzi et al., 2013). The GC defects from BCL6 BTB mutant mice were B cell autonomous

and did not affect T_{FH} function (Huang et al., 2013). Interestingly, mutations in the RD2 domain (KKYK to QQYQ) that prevent the recruitment of MTA3/Mi-2/NuRD and HDAC2 complexes resulted in a failure to form nascent GCs due to impaired B cell trafficking to the GC (Huang et al., 2014). T_{FH} cells were partially impaired in RD mutant mice most likely due to decreased *IL-21* expression and derepression of *Blimp1* (Huang et al., 2014). These studies were the first to demonstrate that BCL6 can mediate distinct biological functions through its repressor domains.

The repression of BCL6 targets that enables a proliferative and pro-survival phenotype in GC B cells can also make them vulnerable to malignant transformation (Hatzi and Melnick, 2014). Transgenic mice that have constitutive expression of BCL6 in GC B cells develop GC hyperplasia and tumors similar to human DLBCL (Baron et al., 2004; Cattoretti et al., 2005). BCL6 expression is tightly regulated at the transcriptional and post-transcriptional level in GC B cells. The induction of *BCL6* is a complex process and several reports have identified multiple transcription factors involved including IRF8, STATs, and AP-1 (Arguni et al., 2006; Lee et al., 2006; Scheeren et al., 2005). However it has yet to be determined which factor plays the leading role in driving *BCL6* expression. Many proteins including HSP90, FBXO11, and p300 regulate BCL6 protein stability (Bereshchenko et al., 2002; Cerchietti et al., 2009a; Duan et al., 2012). Nuclear HSP90 is found in the majority of primary DLBCL patient samples and forms a complex with BCL6 at its target genes. FBXO11 controls the ubiquitinylation and degradation of BCL6, but it is mutated or deleted in many DLBCL cell lines, leading to increased levels and stability of BCL6 (Duan et al., 2012). Finally as discussed

earlier, p300 acetylates BCL6, inactivating its repressor function. However somatic, inactivating mutations in *EP300* and its closely related protein *CREBBP* occur frequently in lymphoma and might augment BCL6 activity (Pasqualucci et al., 2011a).

The transcriptional program mediated by the BCL6 BTB domain induces a stress-tolerant phenotype in GC B cells. DLBCL cells share this same program with GC B cells as 85% of BCL6-corepressor targets in DLBCL were also found in GC B cells (Hatzi et al., 2013). BCL6 mediates transcriptional repression in two ways: (i) by forming a potently, repressive ternary complex at promoters and (ii) by toggling enhancers from an active to a poised state by recruiting SMRT and HDAC3. BCL6 represses a subset of its bound promoters by forming a complex with both SMRT and BCOR (Hatzi et al., 2013). This subset of promoters have a repressive chromatin state associated with them: depletion of activating histone marks (H3K4me3, H3K9Ac, H3K79me2, and H3K27me3) and enrichment of repressive marks (H3K27me3 and DNA methylation) (Hatzi et al., 2013). In addition, these repressed genes had lower levels of elongated Pol II (Hatzi et al., 2013). 85% of BCL6-SMRT complexes occurred outside of promoters, and the majority were associated with transcriptional enhancers as defined by an enrichment of H3K4me1 and lack of H3K4me3 (Hatzi et al., 2013). BCL6-SMRT complexes at enhancers were found to regulate the most proximal gene by recruiting HDAC3 that deacetylated H3K27Ac, decommissioning the enhancer from an active to a poised state and antagonizing the H3K27-acetylating activity of p300 (Hatzi et al., 2013). Enhancer toggling is likely required to mediate rapid transcriptional changes in response to external stimuli as in the course of GC development.

However somatic mutations in *EP300* and *CREBBP* could lock the BCL6 transcriptional program by failing to activate genes necessary for post-GC exit and normal terminal differentiation (Pasqualucci et al., 2011a).

Inhibiting the BCL6 BTB domain

BCL6 is constitutively expressed in the majority of DLBCL and follicular lymphoma and it is required for lymphoma survival, making it a very attractive therapeutic target (Hatzi and Melnick, 2014). Structural studies of the BCL6 BTB domain and its corepressor BBDs demonstrated that the interface between the BBD and the BTB domain are specific to BCL6 and its corepressors (Stogios et al., 2010). Therefore the docking site on the lateral groove of the BCL6 BTB domain provided a unique chance for the rational design of both biological and chemical inhibitors specific for the BCL6 BTB domain without affecting other BTB proteins. Early studies demonstrated an effectiveness of cell-penetrating peptides that mimicked the SMRT BBD for BCL6 BTB inhibition (**Figure 1.7**) (Polo et al., 2004). The BCL6 peptide inhibitor (BPI) blocked the recruitment of BCL6 corepressors resulting in the loss of repressive chromatin modifications and reactivation of BCL6 targets (Polo et al., 2004). BPI treatment in vivo resulted in the loss of GCs and potent anti-lymphoma activity in DLBCL (Cerchietti et al., 2008; Cerchietti et al., 2009b; Parekh et al., 2007; Ranuncolo et al., 2008a; Ranuncolo et al., 2008b). This peptide was further improved to make it more stable and potent, resulting in a retro-inverso BCL6 peptide inhibitor (RI-BPI) (Cerchietti et al., 2009b). In addition to peptide inhibitors, computer-aided drug design allowed for the identification of small molecules that could specifically bind and inhibit BCL6 BTB domain repressor activity (**Figure 1.7**) (Cerchietti et al., 2010a). One

compound, 79-6, was found to dock in the lateral groove of the BCL6 BTB domain (**Figure 1.7**) (Cerchietti et al., 2010a). 79-6 treatment induces the de-repression of BCL6 targets and selective killing of BCL6-depedent DLBCL cell lines *in vitro* and *in vivo* in a xenograft model (Cerchietti et al., 2010a).

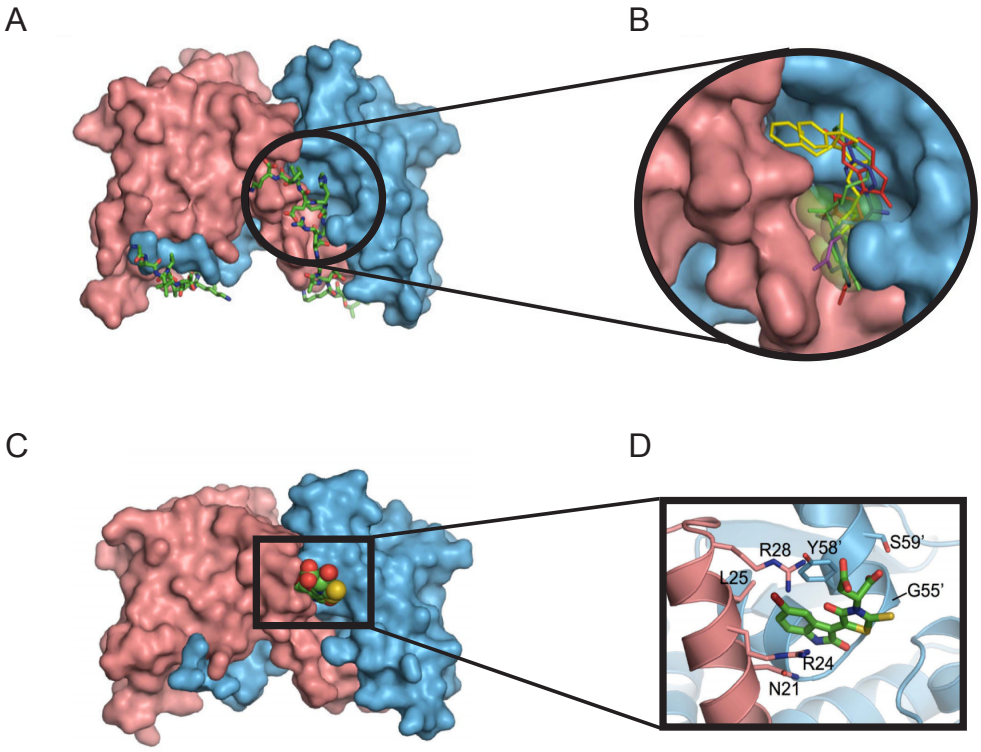

Figure 1.7 Targeting the BCL6 BTB domain with small molecule inhibitors. (A) Structure of the BCL6 BTB dimer with each monomer colored coded in red and blue with two SMRT peptides. The lateral groove of the BTB binding pocket is circled. (B) View of selected compounds in the same binding pocket shared with SMRT. (C) Compound 79-6 in the lateral groove of the BTB dimer. (D) A magnified view showing the molecular interactions between 79-6 and the BTB dimer. Residues on each BTB chain are distinguished with no primes or primes (‘). Adapted from Cerchietti et al. (2010).

A role for BCL6 outside of the GC

Although its role in GC B and T_{FH} cells is well characterized, BCL6 also mediates differentiation of other immune cells like T cell subtypes and macrophages (Bunting and Melnick, 2013). BCL6 null mice have a lethal inflammatory phenotype due to suppression of T_H2 and T_H17 differentiation (Dent et al., 1997; Mondal et al., 2010; Ye et al., 1997). In macrophages, BCL6 occupied genomic sites overlap with the NF-κB cistrome, suggesting that BCL6 has a role limiting the extent of NF-κB-directed inflammation (Barish et al., 2010; Barish et al., 2012). However both the BCL6 BTB or RD2 mutant mice had normal T helper responses, suggesting these domains are dispensable for suppressing inflammatory responses and likely rely on other functions of BCL6 (Huang et al., 2014; Huang et al., 2013).

BCL6 is also expressed in a number of cell-types with no immune-related function and in many cases acts as a cell survival factor (Bajalica-Lagercrantz et al., 1998; LaPensee et al., 2014; Meyer et al., 2009; Otaki et al., 2010; Tiberi et al., 2014; Tiberi et al., 2012; Zhang et al., 2007). A role for BCL6 in neurogenesis is emerging with recent studies (Otaki et al., 2010; Tiberi et al., 2014; Tiberi et al., 2012; Zhang et al., 2007). Tiberi et al. (2012, 2014) demonstrated that BCL6 is expressed in neuronal precursors and mediates neuronal differentiation in the cerebral cortex by altering the composition of transcriptional complexes to silence Notch targets despite active Notch signaling. BCL6 also promotes the survival of sensory neurons to allow them enough time for efficient differentiation into mature olfactory sensory neurons (Otaki et al., 2010). How BCL6 is induced and whether there is a common biological function shared by all cell types remain unanswered questions.

4. Hypothesis

In order to generate high-affinity antibodies, antigen-activated B cells are stimulated to proliferate and differentiate into centroblasts, resulting in the formation of GCs (Klein and Dalla-Favera, 2008). GC B cells are unique in that they have gained the ability to sustain genotoxic, replicative, metabolic, and oxidative stress associated with massive clonal expansion and SHM of their *Ig* loci that would otherwise be lethal (Doughty et al., 2006; Klein and Dalla-Favera, 2008). BCL6 maintains the survival and proliferate state of GC B cells by repressing genes involved in DNA damage sensing and checkpoint activation (Hatzi and Melnick, 2014). Because GC B cells undergo rapid cell division and tolerate genomic instability, the constitutive expression of factors required to maintain the GC phenotype can lead to lymphomagenesis (Hatzi and Melnick, 2014). Along these lines, GC-derived DLBCLs are heavily dependent on BCL6, and inhibition or knockdown of BCL6 kills DLBCLs. The distinctive characteristics of GC B cells suggest that they require a specialized stress response for the production affinity-matured Ig and this reliance may also be inherited in DLBCL.

In the context of the GC, the biological function of BCL6 is to mediate survival despite undergoing severe stress. To carry out its function, BCL6 requires a highly specialized form of HSP90 that is stress-specific and found to be enriched in tumor cells (teHSP90) (Cerchietti et al., 2009a; Moulick et al., 2011). TeHSP90 binds with BCL6 to its targets and is required for BCL6 transcriptional repression (Cerchietti et al., 2009a). HSP90 stabilizes both BCL6 mRNA and protein in DLBCL cells, suggesting that HSP90 may also be

required in GC B cells to facilitate BCL6 function (Cerchietti et al., 2009a). HSP expression is governed by HSF1, the dominant regulator of the stress response (Akerfelt et al., 2010). Because HSF1 contributes to maintaining homeostasis after exposure to various proteotoxic stress, it has been implicated in tumorigenesis and maintaining malignancy (Dai et al., 2007; Jin et al., 2011b; Min et al., 2007). Since GC B cells display a unique ability to withstand stress, it is hypothesized that HSF1 mediates a specialized stress response that is required for the survival of GC B cells. HSF1 likely drives a transcriptional program complementary to BCL6 that allows GC B cells to tolerate stress associated with rapid proliferation and genomic instability. These two items will be explored in chapter two and three. HSF1 dependency may also be required by GC-derived lymphomas to maintain the malignant phenotype, which will be investigated in chapter three. Because BCL6 is intimately linked to the stress response via HSP90 and it rescues cells from high-stress environments, it is postulated that BCL6 may have evolved as a stress response factor. This may point to a broader conserved role of BCL6 in inducing stress tolerance in a diverse set of cell types than previously confined to the GC. This idea will be examined in chapter four.

CHAPTER TWO

ROLE OF HSF1 IN GERMINAL CENTERS

1. Introduction

In order to produce high-affinity antibodies, antigen-stimulated B cells are activated to proliferate and differentiate, resulting in the formation of district structures in secondary lymphoid organs termed germinal centers (GCs) (Klein and Dalla-Favera, 2008). GC B cells clonally expand while simultaneously undergoing somatic hypermutation (SHM) of their immunoglobulin variable regions and later class-switch recombination (CSR), a non-homologous end-joining process that allows the expression of different classes of antibody. During this stage, GC B cells require the expression of BCL6 to tolerate the genotoxic stress associated with rapid proliferation and DNA damage events (SHM and CSR) without inducing cell cycle arrest or apoptosis (Klein and Dalla-Favera, 2008). BCL6 is a transcriptional repressor that maintains the GC phenotype by repressing several genes involved in DNA damage sensing, DNA damage response, apoptosis, checkpoint activation, premature activation of B cells, and plasma cell differentiation (Klein and Dalla-Favera, 2008). However, BCL6 expression is turned off to enable post-GC differentiation and normal cell growth, and its deregulation is often associated with lymphomagenesis (Hatzi and Melnick, 2014). Due to BCL6 control of transcriptional programs related to stress tolerance, GCs seemed to have acquired a specialized stress response.

Heat shock proteins (HSPs) are molecular chaperones that elicit several adaptive responses to help organisms survive a milieu of environmental

stressors, including heat, hypoxia, oxidative stress, ATP depletion, and pH changes (Richter et al., 2010). However, a large body of evidence also implicates HSPs in tumor initiation and survival, stabilizing many of the signaling pathways that are frequently hijacked to induce and maintain a malignant phenotype (Workman et al., 2007; Zuehlke and Johnson, 2010). In fact, our laboratory has recently shown that a specialized form of HSP90 that is enriched in tumors (teHSP90) stabilizes BCL6 at the mRNA and protein level in B cell lymphoma (Cerchietti et al., 2009a). TeHSP90 forms a complex with BCL6 at its target genes and is required for transcriptional repression of BCL6 targets (Cerchietti et al., 2009a). If BCL6 requires HSP90 for its biological function in DLBCL cells, it is likely that the same mechanism is used by BCL6 in GC B cells that are also highly stressed, suggesting that the entire heat shock response may also be active during the GC reaction.

HSP expression is transcriptionally regulated by a small family of proteins referred to as heat shock factors (HSFs) (Akerfelt et al., 2010). Within this family, HSF1 is the master regulator of the stress response. HSF1 is reported to be involved in affinity maturation as HSF1 knockout mice have decreased serum levels of class-switched Ig, especially IgG2a (Inouye et al., 2004). However a specific role for HSF1 in GC was not demonstrated. Due to the stress tolerant phenotype of GC B cells, we wondered if HSF1 and the heat shock response are important for the survival of GC B cells and required for the production of affinity-matured antibodies.

2. Results

2.1 BCL6 is transcriptionally regulated by HSF1 in B cells

BCL6 is the master regulator of the GC response and *BCL6* mRNA is strongly upregulated in GC B cells (Klein and Dalla-Favera, 2008). HSF1 is the dominant regulator of stress response and induces expression of *HSPs* after exposure to stress. These considerations led us to ask whether *BCL6* is an HSF1 target gene. To address this question we first examined the *BCL6* promoter for HSF1 binding sites, known as heat shock elements (HSEs). We identified two highly conserved HSEs consisting of three tandem inverted repeats of 5'-nGAAn-3' within the *BCL6* promoter. We also identified a third HSE that was less conserved (**Figure 2.1A**). To identify if these were bona fide HSEs, we designed an AlphaLisa assay to quantify HSF1 DNA binding with biotinylated oligonucleotides encoding both wild type and mutant versions of each of the three *BCL6* HSEs in the presence of a recombinant form of HSF1, which can spontaneously trimerize in the absence of HSP90 (**Figure 2.1B**) (Goodson and Sarge, 1995; Zhong et al., 1996). HSF1 exhibited concentration dependent specific binding to the wild type but not mutant probes corresponding to all three *BCL6* promoter HSEs (**Figure 2.1C**). A consensus *HSPA1A* HSE was used as a positive control.

We next performed quantitative ChIP analysis to determine if HSF1 binds to the *BCL6* promoter after heat shock in human tonsillar naïve B (NB) cells. Heat shock markedly increased HSF1 enrichment by 6-fold at the *BCL6* promoter (**Figure 2.1D**). Because *BCL6* expression is naturally induced in GC B cells undergoing massive stress, we also tested whether HSF1 binding is increased in primary human GC B cells under basal conditions (no exogenous stress). We found that HSF1 binding is more than 3-fold enriched at the *BCL6* promoter in GC B cells relative to NB cells (**Figure 2.1D**). Furthermore HSF1

binding was also increased at the *HSP90AA1* promoter in GC B cells relative to NB cells (**Figure 2.1D**), suggesting that the HSF1 becomes active and induces *BCL6* and *HSP90* expression during the GC response.

Because HSF1 becomes transcriptionally active and is present at the *BCL6* promoter in GC B cells, we wondered whether HSF1 is required for stress-dependent induction of *BCL6* transcripts. However, because teHSP90 can post-transcriptionally stabilize *BCL6* mRNA (Cerchietti et al., 2009a), it was necessary to specifically determine whether heat shock and HSF1 could induce the formation of newly transcribed *BCL6* mRNA. To this end, splenic $B220^{+}$ cells purified from $Hsf1^{+/+}$, $Hsf1^{+/-}$, and $Hsf1^{-/-}$ mice were heat shocked while simultaneously being pulsed with an alkyne-modified nucleotide analog (5'ethynyl uridine, EU), which would allow for the capture for newly transcribed EU-labeled transcripts by biotin-azide treatment and streptavidin pull-down. After heat shock, there was a 5-fold induction of nascent *Bcl6* transcripts in $Hsf1^{+/+}$ cells and an HSF1 dose-dependent decrease in $Hsf1^{+/-}$ cells with a complete lack of *Bcl6* induction in $Hsf1^{-/-}$ cells (**Figure 2.1E**). There was also a dose-dependent reduction of *Hspa1a* nascent transcripts, measured as positive controls. Because there are three HSF transcription factors (HSF1, -2, and -4), it is likely that one of the other HSFs could partially compensate for lack of HSF1 in inducing *Hspa1a* after heat shock explaining the residual induction of these transcripts.

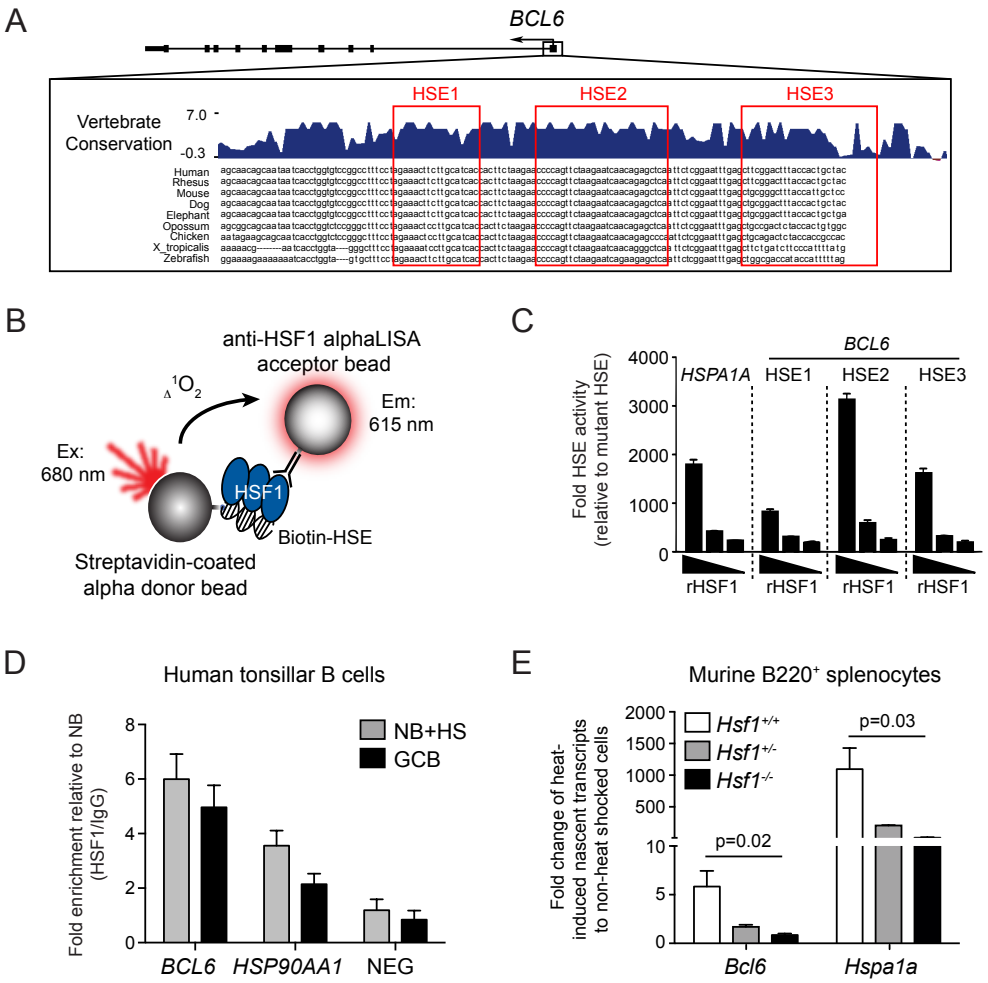

Figure 2.1 HSF1 transcriptionally regulates BCL6 expression. (A) UCSC genome browser plot of vertebrate conservation of the BCL6 promoter. Red boxes highlight potential heat shock elements (HSEs). (B) Schematic of alphaLISA detection of HSF1 binding activity. A biotinylated HSE is used to capture transcriptionally active HSF1 present in nuclear extracts on the streptavidin donor. After laser excitation at 680 nm, short-lived oxygen molecules produced by the donor bead can reach the anti-HSF1 coated alphaLISA acceptor bead and generate a chemiluminescent signal at 615 nm. (C) AlphaLISA activity of the consensus *HSPA1A* HSE and the three *BCL6* HSEs described in (A) with increasing concentrations of recombinant HSF1. (D) Quantitative ChIP of HSF1 in resting IgD+ naïve B cells (NB), heat shocked NBs, and resting GC B cells at the *BCL6* promoter, *HSP90AA1* promoter, and a negative control gene *HBB*. (E) qRT-PCR of nascent *Bcl6* and *Hspa1a* mRNA in heat shocked murine B220^{+} splenocytes of *Hsf1*$^{+/+}$, *Hsf1*$^{+/-}$, and *Hsf1*$^{-/-}$ mice. Data was normalized to murine *Hprt1*. Values in (C-E) are the mean of triplicates ± SEM. Values in (E) represent a mean of triplicates ± SEM (n = 2-3 mice per group). A t-test was used to assess significance.

2.2 HSF1 is activated in GC B cells

The fact that BCL6 is an HSF1 target gene led us to question whether HSF1 is active and important during the development of GC B cells, which is a canonical BCL6-dependent process. HSF1 gains transactivation capability after becoming hyperphosphorylated. Phosphorylation at Ser326 is the best indicator of HSF1 transcriptional activation (Guettouche et al., 2005). To determine whether HSF1 is activated in GC B cells, we performed immunofluorescence studies on tissue sections of human tonsils using antibodies to BCL6 and HSF1-pSer^{326}. Examination of GCs revealed colocalization of these two proteins in the majority of GC cells (**Figure 2.2A**). As a second line of evidence for HSF1 activation, we compared DNA binding activity of HSF1 in nuclear lysates of NB vs. GC B cells using the AlphaLisa quantitative DNA binding assay and probes corresponding to wild-type or mutant HSE. These experiments showed significant increase in HSF1 DNA binding in GC B cells vs. NB cells ($p<0.01$, **Figure 2.2B**). Note that this is not due to differential expression of HSF1 since the protein levels were identical in NB and GC B cells (**Figure 2.2C)**. Having established that HSF1 is active in GC B cells, we wondered whether this was purely due to stress or whether immune signaling linked to initiation of the GC reaction might also be involved. We therefore treated primary human NB cells with CD40L, IL-4, or IL-21 (signals linked to GC initiation) and compared HSF1 binding activity to that induced by the canonical heat shock response. All three of these signaling ligands induced a significant and similar degree of HSF1 activation as heat shock ($p<0.01$, **Figure 2.2D**).

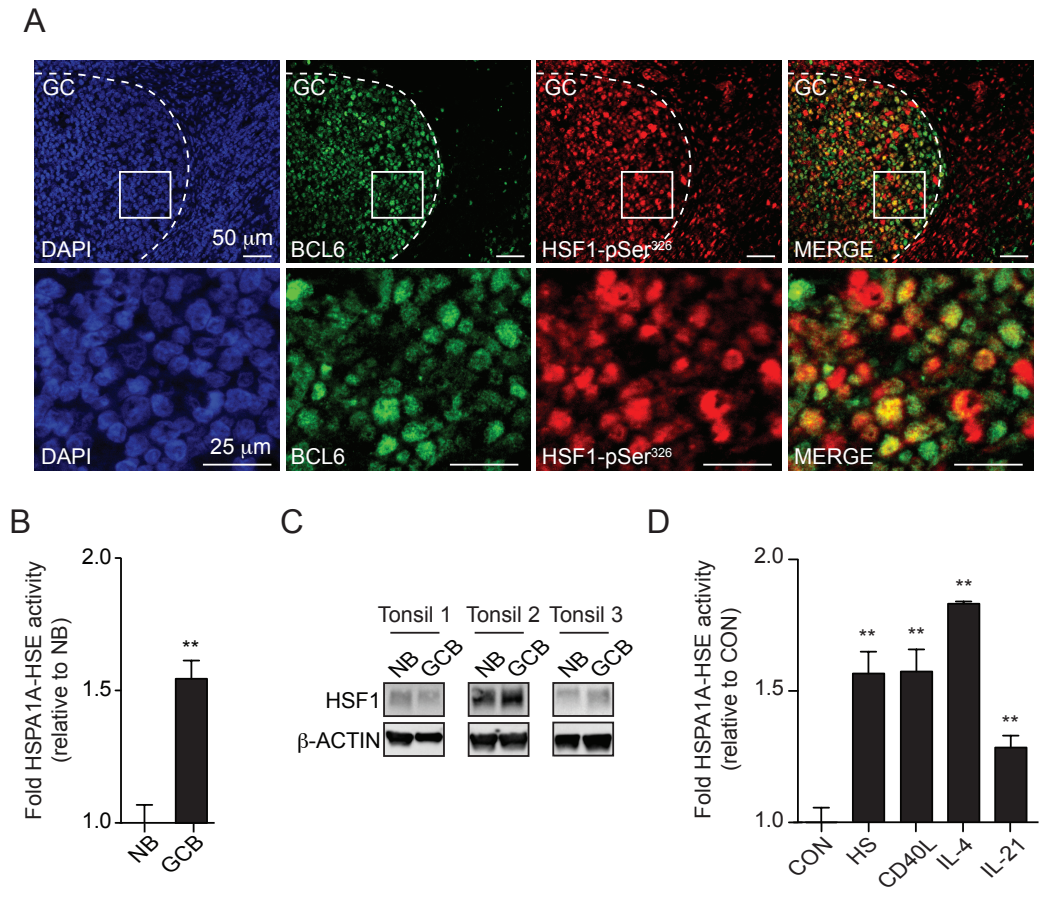

Figure 2.2 HSF1 is activated in GC B cells. (A) Immunofluorescence of paraffin-embedded serial human tonsillar sections. (B) AlphaLISA activity of the consensus *HSPA1A* HSE with nuclear extracts of naïve B cells (NB) and germinal center B cells (GCB) isolated from human tonsils. (C) Immunoblot of HSF1 protein levels in NB and GCB cells isolated from three independent human tonsils. (D) AlphaLISA activity of the consensus *HSPA1A* HSE with nuclear extracts from human splenic NB cells that were resting at 37 ºC (CON), heat shocked for 15 min at 43 ºC (HS), and treated for 1 h with 500 ng/mL CD40 ligand (CD40L), 100 ng/mL IL-4, or 100 ng/mL IL-21. Values in (B and D) are the mean of triplicates ± SEM. A t-test was used to assess significance, ** $p<0.01$.

2.3 Heat shock response is required for GC formation

To identify if the stress response becomes active during GC formation, we immunized mice with T cell-dependent antigen, sheep red blood cells (SRBC), and randomized pairs of mice to receive either 75 mg/kg body weight per day of an HSP90-specific inhibitor, PU-H71, that targets teHSP90 (Moulick et al., 2011) or vehicle. Mice were sacrificed at various time points after SRBC immunization, as early as 3 h later and up to 10 days later when the GC reaction is at its peak, and spleens were harvested for examination with a tissue microarray (TMA) (**Figure 2.3A**). Immunohistochemical analysis of the TMA revealed very few small peanut agglutinin (PNA) $^{+}$ and BCL6^{+} clusters (both of which specifically stain GC B cells) present as early as 6 h post-SRBC, suggesting basal levels of spontaneously formed GCs. Moderately sized clusters appear at day 5 post-SRBC and the largest clusters appear at 8-10 days post-SRBC (**Figure 2.3B**). Quantification of the PNA^{+} clusters of PU-H71-treated mice revealed a complete abrogation of GCs at early time points and very few, smaller GCs at day 10 post-SRBC (**Figure 2.3C**). The histologic appearance of the spleen was otherwise normal. These results demonstrate that the stress-specific form of HSP90 is required for the survival of GC B cells. In DLBCL cells, HSP90 binds with BCL6 at its target, and HSP90 is required for BCL6-mediated transcriptional repression (Cerchietti et al., 2009a). Therefore we wondered if HSP90 is also important for BCL6 function in normal GC B cells. Quantitative ChIP assays performed in human tonsillar CD77^{+} GC B cells revealed the presence of HSP90 at the promoters of BCL6 targets, *ATR*, *CCN1*, *TP53*, and *ZFP443* but not at a negative control region within the human *HBB* locus (**Figure 2.3D**). These results suggest that HSP90 is also required for BCL6 to repress its target genes in non-malignant GC B cells.

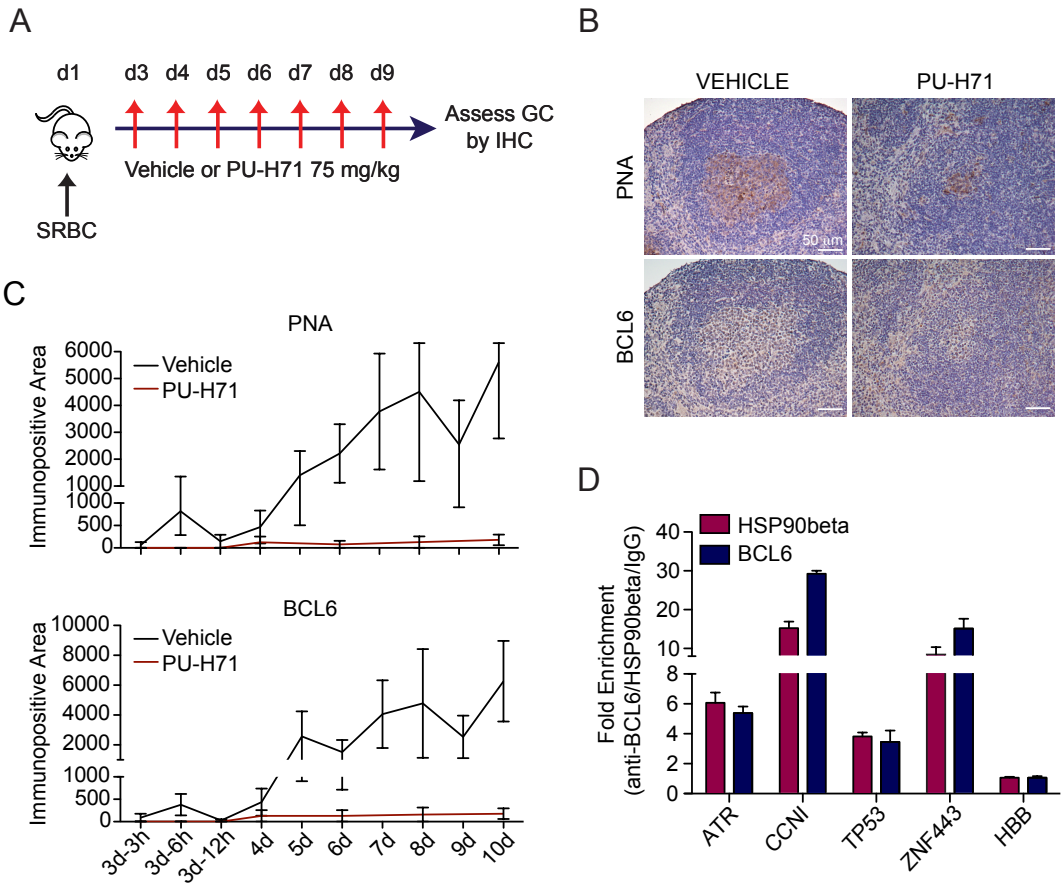

Figure 2.3 Heat shock response is required for GC formation. (A) Schematic representation of the PU-H71 treatment course after SRBC immunization of C57BL/6 mice. (B) Immunohistochemistry of paraffin-embeded spleen sections of C57BL/6 mice 8 d after SRBC immunization with vehicle or PU-H71. (C) Quantification of immunopositive area of PNA (top) and BCL6 (bottom) from a tissue microarray of splenic sections harvested from mice several time points after SRBC immunization. Values in (C) are the mean of 4-6 mice per group ± SEM. Values in (D) are the mean ± SEM of three independent experiments.

2.4 HSF1 is required for development of GC B cells

Hsf1$^{-/-}$ mice were shown to have decreased levels of class-switched antibodies (Inouye et al., 2004), suggesting a key role for HSF1 in humoral immunity. However it was not known whether HSF1 is required for the development of GC B cells or whether the affinity maturation defect was due to other effects in the immune system. Phenotypic analysis of *Hsf1*$^{-/-}$ mice showed normal early development of pro-B (B220^{+}, CD43^{+}, IgM^{-}), pre-B (B220^{+}, CD43^{-}, IgM^{-}), and immature B cells (B220^{+}, CD43^{-}, IgM^{+}) in the bone marrow and normal T (CD3^{+}) and B (B220^{+}) lymphocyte populations in spleens (**Figure 2.4A-B**). In addition, *Hsf1*$^{-/-}$ mice formed normal splenic lymphoid follicles (**Figure 2.4C**).

The fact that HSF1 is active in GC B cells indicates that it is functional. But to determine whether this activity translates into phenotypic effects, we first immunized *Hsf1*$^{-/-}$ or *Hsf1*$^{+/+}$ mice with a T cell dependent antigen (SRBC) and then examined spleens for GC formation 10 days later. Immunohistochemistry staining with PNA revealed that GCs were significantly reduced in numbers ($p<0.05$) and smaller in area relative to spleen size ($p<0.001$, **Figure 2.5A**). As additional confirmation of this finding, we performed flow cytometry to determine the percentage GC B cells (B220^{+}, FAS^{+}, GL7^{+}) among total splenic B220^{+} B cells. *Hsf1*$^{-/-}$ exhibited an approximately 50% reduction in the number of GC B cells compared to wild type ($p<0.05$, **Figure 2.5B**). Because the formation of GCs requires T follicular (T_{FH}) cells to stimulate and drive GC B cells (Victora and Nussenzweig, 2012), we next examined the development of total T_{FH} cells (CD4^{+}, CXCR5$^{lo\text{-}hi}$, PD1$^{lo\text{-}hi}$) and GC-specific T_{FH} cells (CD4^{+}, CXCR5^{hi}, PD1^{hi}). The frequency of T_{FH} cells in either compartment did not differ in *Hsf1*$^{-/-}$ mice relative to *Hsf1*$^{+/+}$ mice (**Figure 2.5C**). Because there was

no difference in overall numbers of B220^{+} B cells in *Hsf1*$^{-/-}$ mice (**Figure 2.4B-C**), the defect observed is specific to GC but not total B cells.

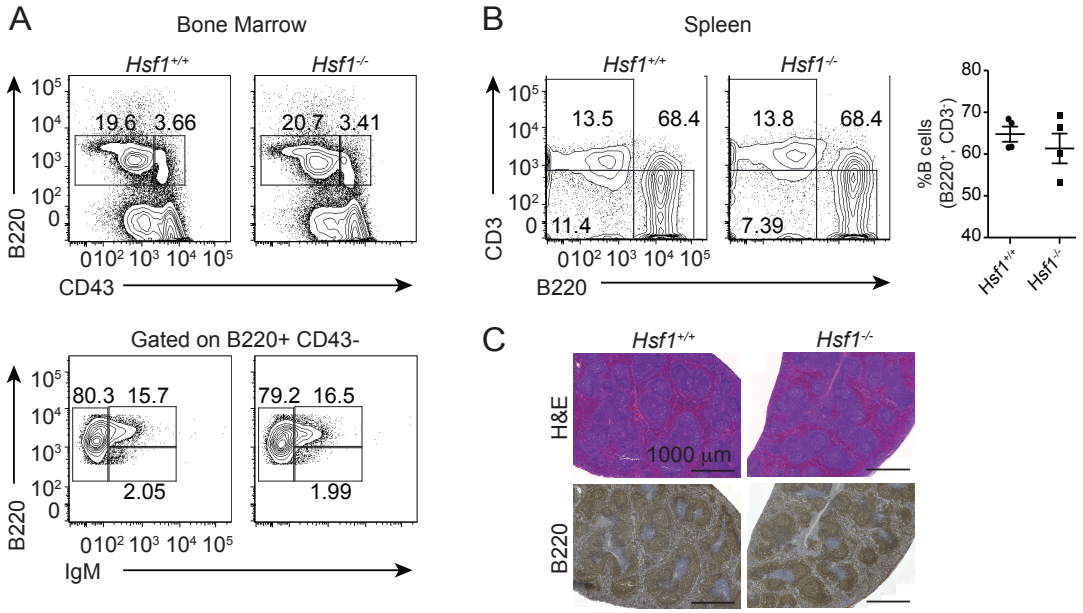

Figure 2.4 *Hsf1*$^{-/-}$ mice have normal development of B and T cells in bone marrow and splenic follicles. (A) Expression of B220, CD43, and IgM in bone marrow cells from *Hsf1*$^{+/+}$ and *Hsf1*$^{-/-}$ mice. Top panel distinguishes pro-B (B220^{+} CD43^{+}) and pre-B cells (B220^{+} CD43^{-}), and bottom panel distinguishes pre-B (B220^{+} CD43^{-} IgM^{-}) and immature B cells (B220^{+} CD43^{-} IgM^{+}). (B) Flow cytometry of CD3^{+} T cell and B220^{+} B cell populations in spleen. Quantification of the total number of B220^{+} cells (right). (C) Immunohistochemistry of paraffin-embdedded splenic sections from *Hsf1*$^{+/+}$ and *Hsf1*$^{-/-}$ mice stained for H&E and B220. Data in (A-C) are representative of at least two independent experiments (n=3-5 per group). Values in (B) the mean ± SEM of 4 mice per group.

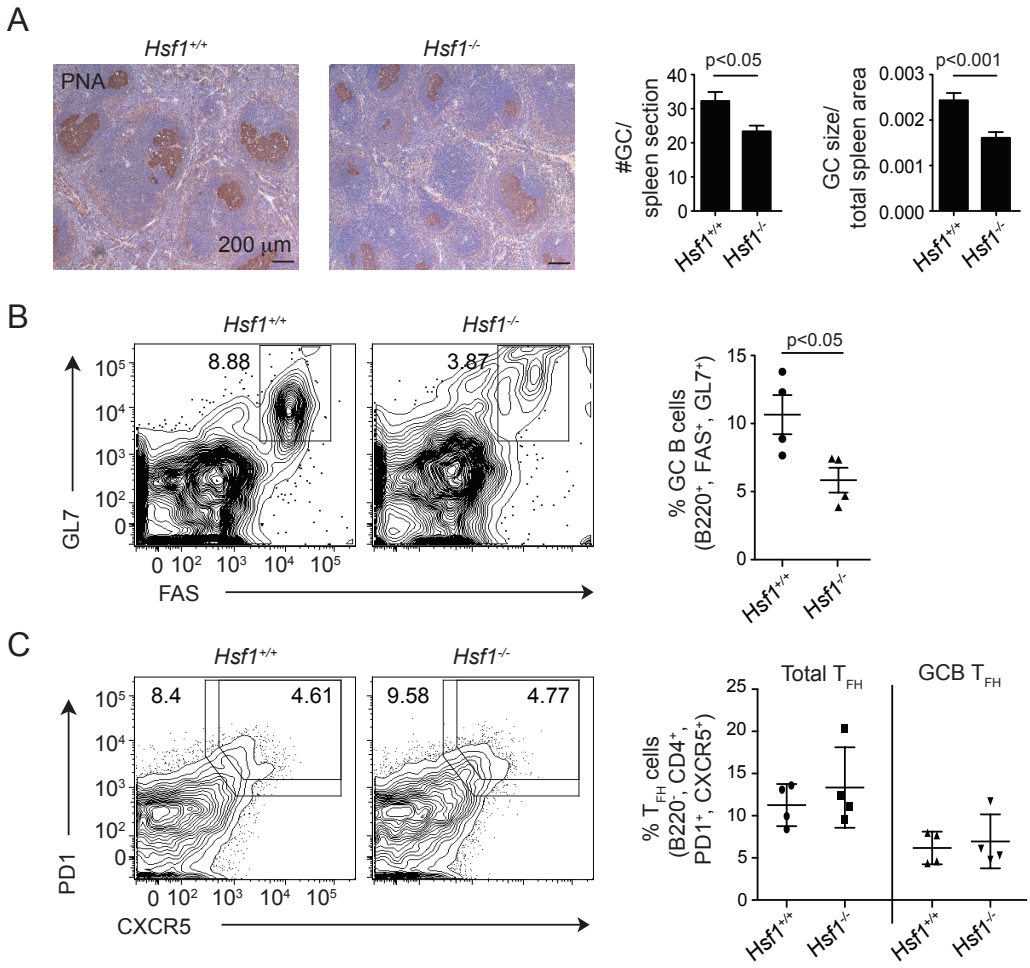

Figure 2.5 HSF1 is required for development of GCs. (A) Immunohistochemistry of paraffin-embeded spleen sections of *Hsf1*$^{+/+}$ and *Hsf1*$^{-/-}$ mice 10 d after SRBC immunization. Quantification of the number and size of GCs (right). (B) Flow cytometry (left) and quantification (right) of splenic GC B cells (FAS^{+} GL7^{+}) among live B220^{+} cells obtained from *Hsf1*$^{+/+}$ and *Hsf1*$^{-/-}$ mice 10 d after SRBC immunization. (C) Flow cytometry (left) and quantification (right) of splenic total T_{FH} cells (CXCR5$^{lo\text{-}hi}$ PD1$^{lo\text{-}hi}$) and GC-specific T_{FH} cells (CXCR5^{hi} PD1^{hi}) among live CD4^{+} B220^{-} cells obtained from *Hsf1*$^{+/+}$ and *Hsf1*$^{-/-}$ mice 10 d after SRBC immunization. Values in (A-C) are representative of at least two independent experiments (n=3-7 mice per group). Each symbol represents an individual mouse; error bars indicate the mean ± SEM. A t-test was used to assess significance.

To determine whether there is indeed a defect in affinity maturation linked to this GC phenotype (Inouye et al., 2004), we immunized *Hsf1*$^{-/-}$ and *Hsf1*$^{+/+}$ mice with the specific T cell dependent antigen, 4-hydroxy-3-nitrophenylacetyl chicken gamma globulin (NP-CGG), and measured the levels of antigen-specific GC B cells (NP^+, $GL7^+$). NP-specific GC B cells were severely reduced in *Hsf1*$^{-/-}$ compared to *Hsf1*$^{+/+}$ mice (**Figure 2.6A**). GC formation results in the production of plasma cells that secrete high-affinity Ig. Therefore we then investigated whether HSF1 was required for the formation of plasma cells. *Hsf1*$^{-/-}$ mice had lower total plasma cells ($B220^-$, $CD138^+$) and lower NP-specific plasma cells ($B220^-$, $CD138^+$, NP^+) vs wild-type mice (**Figure 2.6B**). Finally the titer of high-affinity antibodies was measured by NP4 ELISA with serum collected 14 d after immunization. *Hsf1*$^{-/-}$ mice generated significantly lower titers of high-affinity NP_4 IgG2a compared to wild type ($p<0.05$) and lower titers of NP_4 IgG1 although not significant ($p=0.06$, **Figure 2.6C**). These results demonstrate definitively that *Hsf1*$^{-/-}$ mice have defects in affinity maturation.

It is important to note that GC formation requires the intimate cooperation between GC B cells and GC T_{FH} cells (Victora and Nussenzweig, 2012). Loss of function of either one will result in reduced GC formation and affinity maturation. Hence the experiments above are not sufficient to prove that GC B cells are HSF1-dependent. T_{FH} cells do not undergo massive proliferation or SHM and do not undergo the level of stress that must be endured by GC B cells. Hence we predicted that the GC impairment phenotype was B cell autonomous. To determine if this is the case, we performed mixed chimera bone marrow transplantations using irradiated *Rag1*$^{-/-}$ mice (deficient in T and

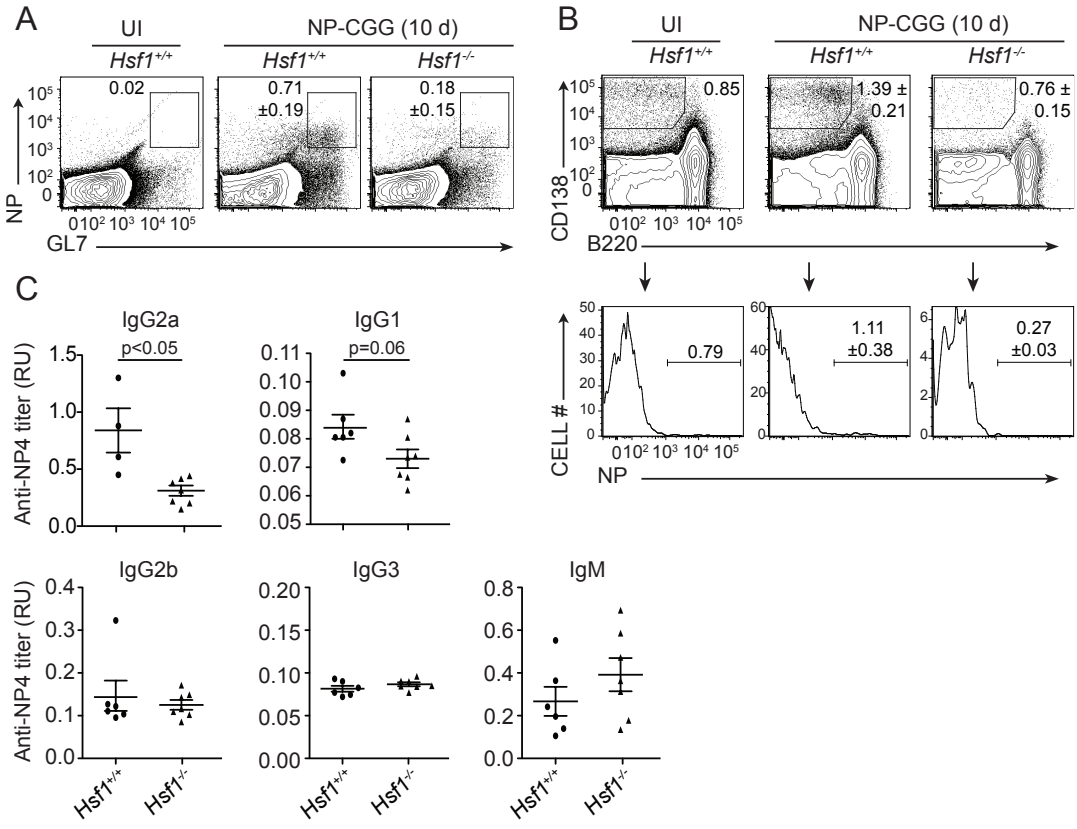

Figure 2.6 *Hsf1*$^{-/-}$ mice have defects in affinity maturation. (A) Flow cytometry analysis of NP-specific GC B cells (NP^{+} GL7^{+}) among live B220^{+} cells from mice left unimmunized (UI) or 10 d after immunization with NP-CGG. (B) Flow cytometry of total plasma cells (CD138^{+} B220^{dim}) among DAPI^{-} spleen cells with further gating of the NP^{+} compartment of total plasma cells (bottom) from mice left unimmunized (UI) or 10 d after immunization with NP-CGG. (C) Titers of NP-specific immunoglobulins, measured with NP_4-BSA in serum from mice 35 d after primary immunization with NP-CGG and presented as relative units (RU) as serial dilution of serum relative to antibody end-point titers. Values in (A-C) are representative of at least two independent experiments (n=3-7 mice per group). Each symbol represents an individual mouse; error bars indicate the mean ± SEM. A t-test was used to assess significance.

B cells) as recipients. *Rag1*$^{-/-}$ recipients were transplanted with CD45.1^{+} bone marrow from *Hsf1*$^{+/+}$ mice mixed with either CD45.2^{+} *Hsf1*$^{-/-}$ or CD45.2^{+} *Hsf1*$^{+/+}$ cells, at 50% ratio (**Figure 2.7A**). After engraftment, GC formation was

induced by immunization with SRBC and spleens examined 10 days later. While we detected no difference in CD45.1$^+$ GC B cells or GC T_{FH} cells between each chimera (**Figure 2.7B-C**, top), we again observed a significant, 50% reduction in the formation of GC B cells (B220$^+$, FAS$^+$, GL7$^+$) from CD45.2$^+$ *Hsf1*$^{-/-}$ as compared to CD45.2$^+$ *Hsf1*$^{+/+}$ cells ($p<0.01$, **Figure 2.7B**, bottom). In marked contrast there was no defect in GC T_{FH} cells (CD4$^+$, PD1$^+$, CXCR5$^+$, B220$^-$) (**Figure 2.7C**, bottom). Hence HSF1 effects in GC B cells are B cell autonomous.

2.5 HSF1 induces BCL6 expression in GC B cells

We demonstrated earlier that HSF1 induces *BCL6* expression after heat stress in B cells. BCL6 allows GC B cells to sustain replicative and genotoxic stress from clonal expansion and SHM. Because *Hsf1*$^{-/-}$ mice have defects in GC number and size and is this accompanied with defects in the production of high-affinity antibodies, we wondered if BCL6 induction is impaired in *Hsf1*$^{-/-}$ GC B cells. By using flow cytometry, we observed high levels of BCL6 staining intensity in *Hsf1*$^{+/+}$ GC B cells (B220$^+$, FAS$^+$, GL7$^+$) (**Figure 2.8A**). In stark contrast, *Hsf1*$^{-/-}$ GC B cells exhibited a higher percentage of cells with BCL6 intensity overlapping with the isotype controls, suggesting a population of cells with almost no BCL6 induction (**Figure 2.8A**). Notably there were populations of *Hsf1*$^{-/-}$ GC B cells that had similar levels of BCL6 staining to wild-type (**Figure 2.8A**). This might explain why a complete abrogation of GC formation is not observed in *Hsf1*$^{-/-}$ mice. Some cells must be able to overcome the HSF1 defect and perhaps rely on other transcription factors that respond to immune signaling like IRF8 to compensate and induce BCL6 (Bunting and Melnick, 2013).

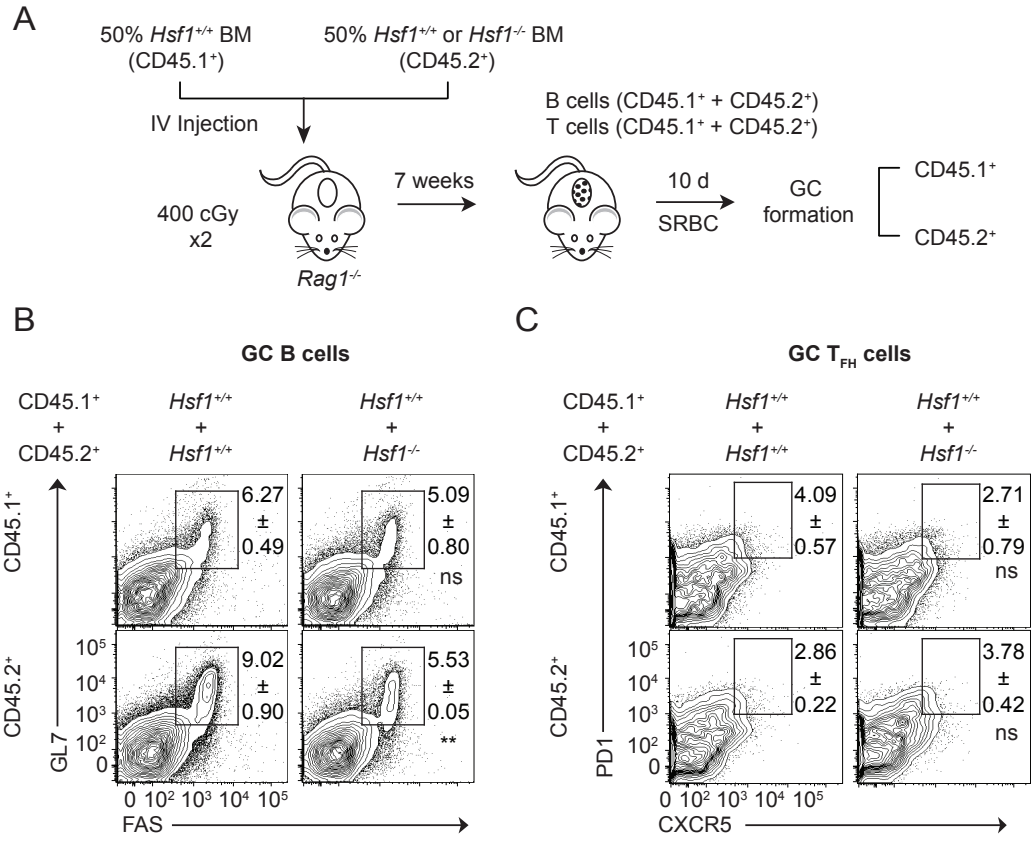

Figure 2.7 GC defect in *Hsf1*$^{-/-}$ are B cell autonomous. (A) Strategy for generating chimeras by transplantation of mixed bone marrow (BM). (B) Ratio of the frequency of GC B cells (FAS^{+} GL7^{+}) among live B220^{+} cells from CD45.1^{+} and CD45.2^{+} donors, quantified by flow cytometry 10 d after SRBC immunization. (C) Ratio of the frequency of GC T_{FH} cells (CXCR5^{hi} PD1^{hi}) among live B220^{-} CD4^{+} T cells from CD45.1^{+} and CD45.2^{+} donors, quantified by flow cytometry as in (B). Values in (B-C) are representative of two independent experiments (n = 3-5 mice per group). Error bars indicate the mean ± SEM. A t-test was used to assess significance, ** $p<0.01$.

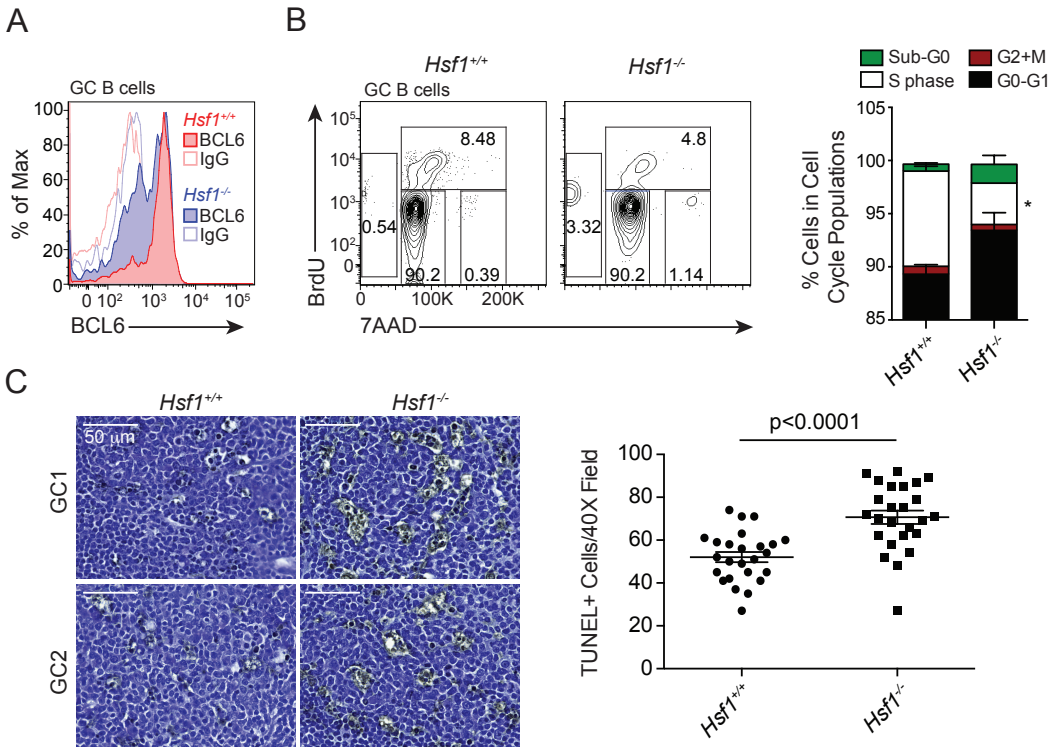

Figure 2.8 HSF1 is required for BCL6 induction in GC B cells. (A) Flow cytometry of intracellular levels of BCL6 in GC B cells (B220$^+$ FAS$^+$ GL7$^+$) from *Hsf1*$^{+/+}$ (red filled) and *Hsf1*$^{-/-}$ (blue filled) mice at 10 d after immunization with SRBC. IgG1 κ is used as an isotype control (red/blue outline). (B) Flow cytometry (left) and quantification (right) of BrdU incorporation in GC B cells (B220$^+$ FAS$^+$ GL7$^+$) from mice immunized with SRBC. (C) Immunhistochemistry of TUNEL staining in representative germinal centers (left) of paraffin-embedded splenic sections of *Hsf1*$^{+/+}$ and *Hsf1*$^{-/-}$ mice 10 d after SRBC immunization. Quantification of TUNEL$^+$ cells per 40X field. TUNEL$^+$ cells were counted in 5 fields per mouse with 5 mice per group. Values in (B-C) are representative of two independent experiments (n = 3-5 mice per group). Error bars indicate the mean ± SEM. A t-test was used to assess significance, * p<0.05.

Along the lines that BCL6 mediates the survival and proliferative state of GC B cells, we investigated whether *Hsf1*$^{-/-}$ GC B cells are unable to maintain GCs and instead undergo less cell division and more apoptosis. To determine effects on proliferation rates, we analyzed BrdU incorporation of GC B cells isolated from spleens of SRBC-immunized *Hsf1*$^{+/+}$ and *Hsf1*$^{-/-}$ mice. We observed a significant decrease in the number of *Hsf1*$^{-/-}$ GC B cells cycling in the S phase compared to wild-type controls ($p<0.05$, **Figure 2.8B**). We also noted an increased percentage of cells in sub-G1 (lower DNA content) although it was not significant (**Figure 2.8B)**. To more precisely determine if GC B cells in *Hsf1*$^{-/-}$ mice have increased levels of apoptosis, DNA fragmentation was measured using Terminal deoxynucleotidyl transferase dUTP nick-end labeling (TUNEL) immunohistochemistry, which specifically labels blunt ends of double-stranded DNA breaks and marks cells that are undergoing the last phase of apoptosis. TUNEL staining was performed on splenic sections from SRBC-immunized *Hsf1*$^{+/+}$ and *Hsf1*$^{-/-}$ mice, and the percentage of TUNEL-positive cells in the GCs were quantified in 5 high-powered fields per mouse (n=5). *Hsf1*$^{-/-}$ mice had a significantly higher number of TUNEL^{+} GC cells compared to *Hsf1*$^{+/+}$ mice ($p<0.0001$, **Figure 2.8C**). Taken together with the induction of HSF1 downstream of GC activation signals, our data suggest that the described HSF1-BCL6 stress response axis plays a cooperating and necessary role in formation of GCs integrated with canonical immune signaling events.

3. Discussion

Herein we demonstrate that HSF1 induces nascent transcription of *BCL6* in B cells exposed to thermal stress. The GC is a high-stress environment where B

cells proliferate rapidly while undergoing DNA damage events to mutate their *Ig* genes. GC B cells are therefore exposed to a variety of stressors associated with increased cell division, genomic instability, nutrient starvation, and hypoxia. We have shown that the conserved stress response is active in GC B cells and is necessary for their survival. It is interesting to note that while HSF1 null mice were only found to have a partial defect in GC formation, pharmacological inhibition of the stress-activated form of HSP90 (teHSP90) resulted in almost a complete lack of GCs. This discrepancy could be a measure of how each protein regulates BCL6. While HSF1 transcriptionally induces nascent *BCL6* transcripts, a number of other mechanisms exist in between the stages of mRNA and protein production that could compensate for decreased levels of nascent gene expression. HSP90 has a more of a direct role in regulating BCL6 because it is critical for maintaining BCL6 protein stability (Cerchietti et al., 2009a). Therefore inhibiting HSP90, an effector protein of the heat shock response, more effectively impedes BCL6 function whereas *Hsf1*$^{-/-}$ GC B cells likely rely on other mechanisms to induce BCL6 or HSP90.

It is interesting to speculate that the role of HSP90 in BCL6 transcriptional repression may be more complex than just effects on protein stability. While HSP90 forms a complex with BCL6 at its targets and is required for its repressor activity, HSP90 has been demonstrated to interact with and be essential for the function of other transcription factors and chromatin-modifying protein like the trithorax group proteins (Taipale et al., 2010). This presents an interesting scenario where BCL6 competes with these transcriptional regulators for a limited pool of HSP90. In this situation, an increase in BCL6 at

the transcriptional level (via HSF1) may tip the balance in favor of BCL6 repression programs. An alternative mechanism of HSP90 enhancing BCL6 function is linked to pausing RNA polymerase II (Pol II). HSP90 preferentially occupies the transcriptional start site (TSS) of genes with paused Pol II and stabilizes the negative elongation factor (NELF) (Sawarkar et al., 2012). Paused Pol II is found in genes that have to be rapidly induced in response to external stimuli (like in the GC where B cell must get cues from other cell types to proliferate or differentiate). HSP90 inhibition releases paused Pol II, allowing it to transcribe the entire gene (Sawarkar et al., 2012). Notably BCL6 ternary corepressor complexes that form in gene promoters suppress Pol II elongation, resulting in increased levels of paused Pol II (Hatzi et al., 2013). It is interesting to speculate that HSP90 may act as bridge between BCL6 and Pol II to tether Pol II at the TSS and increase pausing. This could result in enhanced suppression of Pol II elongation thereby increasing the repression of BCL6 targets.

The moderate defects in affinity maturation in immunized HSF1 null mice is in part explained due to the presence of *Hsf1*$^{-/-}$ GC B cells that efficiently upregulate BCL6 levels similar to wild-type cells. While we have demonstrated that *BCL6* induction after heat stress is HSF1-dependent and others have already established this for *HSP90*, their expression in the GC could be compensated by additional factors that also respond to immune stimuli. In fact *BCL6* regulation in the GC is complex and can be attributed to several factors that work in concerted fashion or independently at various stages of GC development (Bunting and Melnick, 2013). During the GC response, B cells encounter stimulation signals from many different cytokines including IL-4, IL-

21, and CD40. While we have shown that HSF1 undergoes transactivation after these stimuli, they can also activate a plethora of other transcription factors, some of which have been reported to regulate *BCL6* in B cells or other cell types (Bunting and Melnick, 2013). IL-21R signaling is required for GC B cells to induce and maintain the expression of *BCL6* (Bunting and Melnick, 2013). IL-21R signaling stimulates the phosphorylation and activation of STAT3, which induces its binding to the *BCL6* promoter (Arguni et al., 2006). Notably STAT binding sites closely resemble HSEs and therefore are the same sites found on the *BCL6* promoter (Arguni et al., 2006). STAT3 has also been observed to transcriptionally regulate the expression of *HSP90* in response to IL-6 (Stephanou and Latchman, 2011). Therefore STAT3 is a likely suspect for a compensatory factor that relieves defective *BCL6* and *HSP90* induction in HSF1 null mice. In addition to STATs, *BCL6* expression is also transcriptionally regulated by IRF8. IRF8 knockout mice have decreased GC formation and lower levels of *BCL6* although not completely absent, suggesting that other factors in these mice contribute to *BCL6* induction (like HSF1 and STAT3) (Lee et al., 2006).

It is important to note that while BCL6 is crucial for both GC B cell and T_{FH} cell lineage commitment, the GC defect in HSF1 null mice was B cell autonomous and T_{FH} cell defects were not observed. These results further corroborate our hypothesis that HSF1 is required for stress-mediated induction of *BCL6* in GC B cells, which are highly stressed due to clonal expansion and DNA damage events due to SHM. The circumstances that mediate BCL6 induction appear to be quite in different in T_{FH} cells compared to GC B cells. GC T_{FH} cells upregulate BCL6 expression in a mechanism independent of IL-21 and IL-6

(Bunting and Melnick, 2013). ICOS signaling has been implicated in the induction of BCL6 in the early steps of T_{FH} differentiation. In vitro studies have also demonstrated a potential role for STAT and FOXO proteins in regulating BCL6 to direct T_H1 differentiation to the T_{FH} lineage (Oestreich et al., 2012). These results suggest an HSF1-independent mechanism for BCL6 induction in T_{FH} cells.

Collectively we have demonstrated that HSF1 mediates stress-induced levels of *BCL6*. BCL6 is the master regulator of the GC response and is aberrantly expressed in DLBCL. For these reasons, HSF1 may also be important to maintain *BCL6* expression in DLBCL and other cell types that express *BCL6* in response to stress.

4. Materials and Methods

AlphaLISA

Biotinylated and standard oligonucleotides (Vuori et al., 2009) were purchased from Integrated DNA Technologies, diluted in Tris⁄EDTA buffer (pH 8.0) and annealed. Cells were treated and nuclear extracts were prepared using the Nuclear Extraction kit (Active Motif). For the entire assay, solutions were diluted to their working concentrations in Alphalisa Immunoassay buffer solution 5X (AL001F). Protein A acceptor beads (6760137, PerkinElmer) were incubated with polyclonal rabbit HSF1 antibody (ADI-SPA-901, Enzo Life Sciences) for 1 h at room temperature with agitation. Streptavidin donor beads (6760002, PerkinElmer) were added and the mixture was kept in the dark with agitation. Meanwhile, 2 μg of nuclear extract were incubated with annealed biotinylated HSPA1A HSE or mutated HSE for 30 min in white 384-well

Optiplates (6005620, PerkinElmer). The acceptor and donor beads mixture was added to each well and incubated for an additional 1 h. Luminescence was measured in an EnVision Multilabel Plate Reader (PerkinElmer) and then analyzed.

Primary cell isolation

Human tissues were obtained with approval of the Institutional Review Board (IRB), Office of Research Integrity of the Weill Cornell Medical College and in accordance with the Declaration of Helsinki. Human IgD^+ naïve B cells and $CD77^+$ GC B cells were isolated from de-identified human tonsillectomy specimens or spleens. After centrifugation in Fico/Lite-LymphoH density gradient media (Atlanta Biologicals), mononuclear cells were collected and affinity-purified using microbead cell separation via the autoMACS system (Miltenyi Biotec). Naïve and GC B cell purity was determined by flow cytometric analysis to be >90% $IgD^+/CD38^{low}$ and >90% $CD77^+/CD38^{high}$. Single-cell suspensions of mononuclear cells were generated from murine spleens using red blood cell lysis (Qiagen) or Fico/Lite-LM density gradient media (Atlanta Biologicals). For B220 purification, cells were affinity-purified using positive selection with anti-B220 microbeads or negative selection with anti-CD43 microbeads and the autoMACS (Miltenyi Biotec). Splenocytes were determined to be >95% $B220^+$ by flow cytometric analysis.

Nascent RNA capture

Murine $B220^+$ splenocytes or human cells transfected with HSF1-targeting siRNA for 48 h were heat shocked at 43 ºC for 2 h followed by recovery at 37 ºC for 2 h or treated with 100 nM doxorubicin for 4 h while simultaneously

pulsed with 0.2 mM ethnyl uridine (EU). EU-labeled RNA was captured with the Click-It Nascent RNA capture kit (Molecular Probes). Briefly, RNA was extracted using Trizol reagent (Invitrogen), resuspended with RNase-free H_2O, and quantified with the Nanodrop (Thermo Scientific). 1 μg total RNA was biotinylated by a click reaction with 0.5 μM biotin azide and re-precipitated with Glyco-blue (Ambion), ammonium acetate, and ice cold 100% ethanol. RNA was spun at 13,000xg for 15 min at 4 ºC, washed with 75% ethanol, dried for 5 min at room temperature, and resuspended in RNase-free H_2O. RNA concentration was re-measured by the Nanodrop (Thermo Scientific) and equal amounts of RNA (0.75-1 μg) were allowed to bind to 25 μL Dynabeads MyOne Streptavidin T1 beads (Invitrogen) in the presence of RNaseOUT recombinant ribonuclease inhibitor (Invitrogen) for 30 min at room temperature with gentle agitation. The bound RNA was washed with the provided Click-it wash buffers and resuspended in 12 μL RNase-free H_2O. The RNA bound to the beads was taken directly into a cDNA synthesis reaction using the SuperScript III first-strand synthesis system (Invitrogen). A fraction of the undiluted cDNA was used in real-time quantitative PCR and detected by fast SYBR Green (Quanta Biosciences) on the 7900HT Fast Real-Time PCR System (Applied Biosystems).

Immunofluorescence

De-identified human tonsillar specimens were fixed in 4% formaldehyde and embedded in paraffin. Sections were prepared, cleared in xylene, and hydrated through a descending alcohol series. Antigens were unmasked in rehydrated slides by boiling in 1 mM EDTA buffer pH 8.0 and incubating for 15 min at sub-boiling temperature. After cooling, slides were blocked with

blocking buffer (PBS, 5% normal goat serum, 0.3% Triton X-10). Primary antibodies (anti-BCL6 D8, Santa Cruz; anti-HSF1-pSer^{326} EP1713Y, Epitomics) were diluted in blocking buffer and applied overnight at 4 ºC. Slides were rinsed in PBS and fluorochrome-conjugated secondary antibodies (Alexa Fluor 488 goat anti-mouse IgG, Alexa Fluor 647 goat anti-rabbit IgG, Molecular Probes) were diluted in blocking buffer and applied for 1 h at room temperature. Slides were rinsed and mounted in Prolong Gold Antifade Reagent with DAPI (Molecular Probes) and imaged with an Axiovert 200M fluorscent microscope (Zeiss Inc).

Immunoblot

Whole cell lysate was prepared using lysis buffer (20mM Tris pH 8.0, 150 mM NaCl, 5 mM EDTA, 1% Triton X-100) supplemented with protease inhibitors and resolved by SDS-PAGE, transferred to PVDF membranes, probed with primary antibodies (anti-HSF1 E-4, Santa Cruz; anti-β-ACTIN AC-15, Sigma) followed by HRP-conjugated secondary antibodies (Santa Cruz) and detected with enhanced chemiluminescence (Pierce).

Animals

C57BL/6, *Hsf1*$^{+/+}$, *Hsf1*$^{-/-}$, CBy.SJL(B6)-*Ptprc*^{a}/J (CD45.1), and BALB/c *Rag1*$^{-/-}$ were obtained from Jackson Laboratories. The maintenance and procedures of all animals were in accordance with and approved by the Research Animal Resource Center of the Weill Cornell Medical College.

Germinal center formation

Age- and sex-matched mice were immunized intraperitoneally at 8 to 12 weeks of age with 0.5 mL 2% v/v sheep red blood cells (SRBC, Cocalico Biologicals) or a 1:1 mixture of 100 μg of NP-CGG (ratio 20-29, Biosearch Technologies) and Imject alum (Pierce). For PU-H71 experiments, C57BL/6 mice were randomized into two groups immediately after SRBC immunization and after 3 days, sterile PBS or 75 mg/kg PU-H71 (generously provided by Gabriela Chiosis) was administered via daily intraperitoneal injections for up to 7 days. Age- and sex-matched *Hsf1*$^{+/+}$ and *Hsf1*$^{-/-}$ mice were immunized with SRBC or NP-CGG and sacrificed at day 10.

Immunohistology

Mouse spleens were fixed in 4% formaldehyde and embedded in paraffin. Sections were prepared, cleared in xylene, and hydrated through a descending alcohol series. Slides were boiled with antigen retrieval buffer (10 mM sodium citrate buffer pH 6.4 or 1 mM EDTA buffer pH 8.0) and cooled. Endogenous peroxidase activity was quenched by treatment with 3% hydrogen peroxide in methanol and permeabilized (0.5% Triton X-100, 20mM HEPES pH 7.4, 50 mM NaCl, 3 mM $MgCl_2$, 30 mM Sucrose). Slides were blocked with 5% non-fat milk powder in PBS-Tween and then incubated with biotin-conjugated PNA (Vector Laboratories) or biotin-conjugated anti-B220 (Invitrogen RM2615). Avidin-horseradish peroxidase (HRP) was applied, and peroxidase activity was detected with DAB color substrates (Vector Laboratories) and counterstained with hematoxylin. Images were obtained using an Axioskop imaging microscope (Zeiss Inc) and ImageJ software (NIH) was used to quantify germinal centers.

Chromatin Immunoprecipitation (ChIP)

ChIP was performed as previously described (Hatzi et al., 2013). Briefly, naïve B cells that were heat shocked at 43 ºC for 30 min or GC B cells were fixed with 1% formaldehyde for 10 min at room temperature, quenched with 125 mM glycine, and lysed in modified RIPA buffer (150 mM NaCl, 1% v/v Nonidet P-40, 0.5% w/v deoxycholate, 0.1% w/v SDS, 50 mM Tris pH 8, 5 mM EDTA) supplemented with protease inhibitors. Cell lysates were sonicated using a tip sonicator (Branson) to generate fragments less than 400 bp. Precleared lysates were incubated overnight with 5 μg anti-HSF1 (ADI-SPA-901, Enzo Life Sciences), 5 μg anti- anti-BCL6 (N3, Santa Cruz), 100 uL of anti-HSP90β supernatant (H9010, Invitrogen) or control IgG antibody. Immunocomplexes were recovered, sequentially washed with increasing stringency of wash buffers (150 mM NaCl, 250 mM NaCl, 250 mM LiCl), and eluted with 1% SDS and 100 mM $NaHCO_3$. Crosslinks were reversed, and DNA was purified using a Qiaquick PCR purification kit (Qiagen). ChIP DNA was amplified with real-time quantitative PCR using SYBR Green (Quanta Biosciences) and 7900HT Fast Real-Time PCR System (Applied Biosystems). Input standard curves were used for estimation of relative enrichment.

Flow cytometric analysis

Single-cell suspensions of mononuclear cells were generated from bone marrow and murine spleens using red blood cell lysis (Qiagen) and Fico/Lite-LM density gradient media (Atlanta Biologicals), respectively. Mononuclear cells were washed with PBS with 1mM EDTA, filtered, and resuspended in staining buffer (PBS, 1% FBS, 0.09% sodium azide). Fluorescent-labeled antibodies (**Table 2.1**) were diluted in staining buffer and applied to cells for 20

min at 4 ºC. If primary antibodies were not conjugated to fluorochromes, cells were washed, and incubated with fluorochrome-conjugated secondary antibodies for 20 min at 4 ºC. Cells were washed and resuspended in stain buffer. Flow cytometry data was acquired with the Macsquant (Miltenyi Biotec) or FACS Canto II (BD Biosciences) flow cytometer and analyzed with FlowJo software package (TreeStar).

Table 2.1 Summary of antibodies used for flow cytometry.

Antigen	Host	Fluorophore	Clone	Manufacturer
Anti-mouse B220	Rat	PE/FITC/APC	RA3-6B2	BD Pharmingen
Anti-mouse B220	Rat	PE-Cy7	RA3-6B2	eBioscience
Anti-mouse CD43	Rat	FITC	eBioR2/60	eBioscience
Anti-mouse IgM	Rat	APC	II/41	eBioscience
Anti-mouse IgD	Rat	PE	11-26.ca2	BD Pharmingen
Anti-mouse CD3	Rat	APC	17A2	BioLegend
Anti-mouse FAS	Hamster	PE	Jo2	BD Pharmingen
Anti-mouse GL7	Rat	FITC	GL7	BD Pharmingen
Anti-mouse CD4	Rat	APC	GK1.5	eBioscience
Anti-mouse CXCR5	Rat	PE-Cy7	2G8	BD
Anti-mouse PD1	Hamster	PE/FITC	J43	eBioscience
NP		PE		Biosearch Technologies
Anti-mouse CD138	Rat	BV421	281-2	BioLegend
Anti-mouse CD45.1	Mouse	PerCP-Cy5.5	A20	eBioscience
Anti-mouse CD45.2	Mouse	PerCP-Cy5.5	104	eBioscience
Anti-human IgD	Mouse	FITC	IA6-2	BD Pharmingen
Anti-human CD77	Rat	Purified	38-13	AbD Serotec
Anti-rat IgM	Goat	PerCP	Poly	Jackson
Anti-human CD38	Mouse	APC	HB7	BD Biosciences

Enzyme-linked immunosorbent assay (ELISA)

Mice were immunized twice with NP-CGG, with the second NP-CGG immunization occurring at day 20-post the initial NP-CGG immunization. Serum samples were collected 15 days after the secondary NP-CGG immunization (which coincides with day 35-post primary immunization), and titers of isotype-specific high-affinity antibodies to NP were measured in plates coated with NP_4-BSA with the SBA Clonotyping System (Southern Biotech) in serial dilutions followed by incubation with HRP-labeled detection antibodies and ABTS substrate solution. Titers are presented as the greatest serum dilution that provided an average absorbance exceeding 2-fold above the average background absorbance at 405 nm.

Mixed-bone marrow chimera studies

For the generation of mixed bone marrow chimera, 4 x 10^6 cells from a 1:1 mixture of CBy.SJL(B6)-*Ptprc*^{a}/J bone marrow cells (CD45.1$^+$) and CD45.2$^+$ *Hsf1*$^{+/+}$ or *Hsf1*$^{-/-}$ bone marrow cells were injected into the tail veins of sub-lethally irradiated (400 cGy at 2 doses, 4 h apart) BALB/c *Rag1*$^{-/-}$ mice in collaboration with the MSKCC Antitumor Assessment Core Facility. Recipient mice were immunized with SRBC 7 weeks later and GC formation was assessed 10 days post-SRBC with flow cytometric analysis.

Intracellular staining for BCL6

For flow cytometric analysis of BCL6 levels, single-cell suspensions of mononuclear cells were generated from murine spleens using Fico/Lite-LM density gradient media (Atlanta Biologicals). Mononuclear cells were washed with PBS with 1mM EDTA, filtered, and fixed with CytoFix/CytoPerm

Fixation/Permeabilization buffer (BD Biosciences) for 10 min at 37 ºC. Cells were washed with stain buffer (PBS, 1% FBS, 0.09% sodium azide) and pelleted. Cells were permeabilized by vortexing gently while simultaneously adding drop wise cold BD Phosflow Perm Buffer III (BD Biosciences) and incubating on ice for 30 min. Cells were washed twice with stain buffer and stained with fluorescent-conjugated anti-BCL6 (K112-91, BD Pharmingen) or the same amount of isotype control (mouse IgG_1 κ, BD Pharmingen) for 1 h at room temperature. Cells were washed and stained with other fluorescent-labeled cell surface antibodies in stain buffer for 20 min at 4 ºC. Cells were washed and resuspended in stain buffer. Flow cytometry data was acquired with the Macsquant (Miltenyi Biotec) or FACS Canto II (BD Biosciences) flow cytometer and analyzed with FlowJo software package (TreeStar).

BrdU detection

For BrdU labeling, mice were injected intraperitoneally with 1-2 mg BrdU (Sigma-Aldrich) 2 h before sacrificing. Mononuclear cells were prepared using Fico/Lite-LM density gradient media (Atlanta Biologicals). Cells were stained with the appropriate cell surface markers. Then BrdU-positive cells were detected by BrdU Flow kits (BD Pharmingen) according to the manufacturer's protocol.

TUNEL assay

Apoptotoic cells were detected in situ by labeling and detecting DNA strand breaks by the terminal deoxynucleotidyl transferase dUTP nick end labeling (TUNEL) method using the ApopTag Peroxidase In Situ Apoptosis Detection Kit (Millipore). Briefly, formalin-fixed paraffin-embedded spleens were

deparaffinized and pre-treated with trypsin (Zymed) to expose DNA. Endogenous peroxidase was quenched using 3% hydrogen peroxide (Sigma) followed by incubation with TdT enzyme for 1 h. Then, anti-digoxigenin-peroxidase was applied to the slides. Color was developed with diaminobenzoate chromogen peroxidase substrate (Vector Laboratories) and counterstained with methyl green (Fisher Scientific). Images were obtained using an Axioskop imaging microscope (Zeiss Inc) and TUNEL-positive cells were counted in 40X high-powered fields of 5 germinal centers per mouse (n=5).

Statistical analysis

Student's *t*-test was used for statistical analysis unless otherwise stated. All statistical analyses were done using GraphPad Prism 5.

CHAPTER THREE

ROLE OF HSF1 IN DLBCL

1. Introduction

DLBCL is the most common form of aggressive lymphoid malignancy, accounting for nearly 40% of all non-Hodgkin lymphomas (Lenz and Staudt, 2010). Current therapy includes R-CHOP, the combination of a monoclonal antibody (rituximab), three chemotherapeutics (doxorubicin, vincristin, cyclophosphamide), and one steroid (prednisone). While more than 50% of DLBCL patients respond to this drug cocktail, up to one-third of patients remain incurable, and the chemotherapy drug regimen is not without its toxicities, highlighting a need for more targeted treatments (Roschewski et al., 2014). Understanding the etiology of DLBCL will provide additional avenues to improve existing therapies and facilitate the discovery of novel therapeutic targets. Somatically mutated *Ig* loci and gene expression profiles of DLBCL tumors suggest that the majority of them arise from B cells transiting or exiting the germinal center (GC) reaction (Klein and Dalla-Favera, 2008; Lenz and Staudt, 2010; Seifert et al., 2013). Dissecting the molecular mechanisms underlying the biology of GC B cells will help to further elucidate how GC B cells transform into DLBCL tumors.

The formation of GCs is essential for the generation of high-affinity antibodies. GC B cells undergo clonal expansion and SHM of their *Ig* variable regions without undergoing cell cycle arrest or apoptosis because of the induction of a B cell-specific stress response program (Klein and Dalla-Favera, 2008). BCL6 is the master regulator of this program and maintains the GC phenotype by

repressing several genes involved in DNA damage sensing, apoptosis, checkpoint activation, and plasma cell differentiation (e.g. *ATR*, *CHEK1*, *TP53*, *CDKN1A*, and *PRDM1*) (Hatzi and Melnick, 2014). *BCL6* expression must eventually be turned off to enable post-GC differentiation and normal cell growth, and its deregulation is often associated with lymphomagenesis (Hatzi and Melnick, 2014).

HSP90 was found to stabilize BCL6 mRNA and protein levels in DLBCL. Treatment of DLBCL cell lines with HSP90 inhibitors including the purine-scaffold molecule, PU-H71, results in the degradation of BCL6 and apoptosis of BCL6-dependent DLBCL cells (Cerchietti et al., 2009a). Furthermore PU-H71 treatment abrogates the GC response in mice, demonstrating that HSP90 may also function to stabilize BCL6 in the normal physiological setting. The master regulator of the conserved heat shock response is HSF1, which transcriptionally regulates the expression of *HSPs* and other stress proteins (Akerfelt et al., 2010). In fact HSF1 is active in GC B cells and regulates stress-dependent induction of *BCL6*. Moreover HSF1 null mice have smaller GCs and defects in affinity maturation demonstrating that HSF1 plays an important role in maintaining the GC program in normal B cells.

Because HSF1 contributes to maintaining homeostasis after exposure to various stressors, it has been implicated in cellular adaptation to the malignant phenotype (Whitesell and Lindquist, 2009). Increased HSF1 expression has been found in several tumor types, and HSF1 depletion results in decreased cell viability and chemosensitization (Dai et al., 2012; Dai et al., 2007; Jolly and Morimoto, 2000; Tang et al., 2005; Zaarur et al., 2006; Zhao et al., 2011).

Furthermore HSF1 is required for tumorigenesis and transformation by a number of oncogenes including *RAS*, *PDGF-B*, and *HER2* (Dai et al., 2007; Jin et al., 2011b; Khaleque et al., 2008; Meng et al., 2010; Min et al., 2007). Although HSF1 is not a classical oncogene, HSF1 seems to govern a broad network of signaling pathways to support the tumorigenic environment, and the activation of its cancer program is associated with disease progression and predicts poor prognosis in cancer patients (Fang et al., 2012; Mendillo et al., 2012; Santagata et al., 2011).

In the context of DLBCL, *BCL6* is the most frequently deregulated oncogene with 30-40% of patients bearing chromosomal translocations of the 3q27 region and 70% patients displaying somatic mutations in the 5' regulatory regions of *BCL6* (Ci et al., 2008; Pasqualucci et al., 2001). Because HSF1 regulates *BCL6* expression in GCs and is required for efficient affinity maturation, we therefore wondered if HSF1 is necessary for the maintenance of malignant phenotype and survival of DLBCL cells.

2. Results

2.1 HSF1 regulates BCL6 in DLBCL

During the GC response, HSF1 inducibly binds HSEs in the *BCL6* gene after immune stimuli and mediates the production of nascent transcripts from the *BCL6* locus. Because *BCL6* is highly expressed in DLBCL, we investigated if *BCL6* expression in DLBCLs is also mediated by HSF1. We first identified if HSF1 binds to *BCL6* by performing chromatin immunoprecipitation (ChIP) with an HSF1-specific antibody. We found HSF1 bound to the *BCL6* promoter basally in DLBCL cell lines, OCI-LY1 and OCI-LY7 (**Figure 3.1A**). To

determine if HSF1 transcriptionally regulates *BCL6* expression, we knocked down HSF1 by lentivirally transducing DLBCL cells with a puromycin-selectable HSF1-targeting shRNA (pLKO.1). After selecting cells for 48 h, we observed a decrease in BCL6 mRNA and protein levels in DLBCL cells (**Figure 3.1B-C**). In addition BCL6, HSP90 levels also dropped after HSF1 depletion, as expected since it is well-known target gene of HSF1 (**Figure**

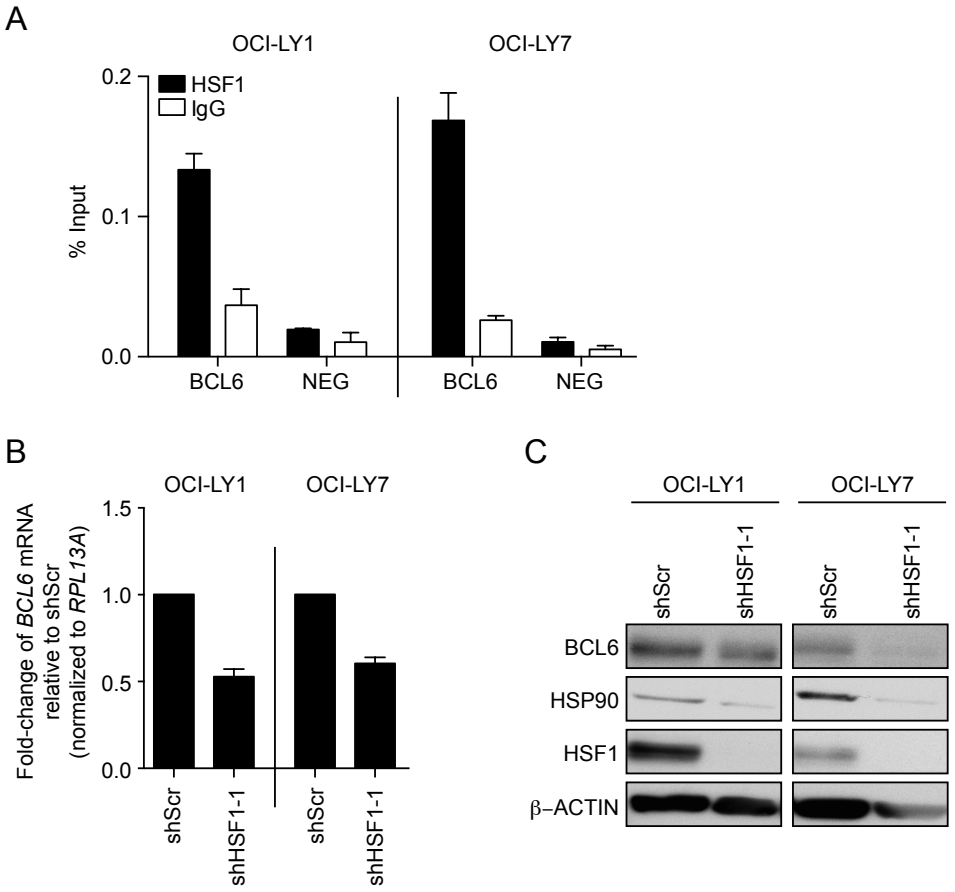

Figure 3.1 HSF1 regulates BCL6 expression in DLBCL cells. (A) Percent input of HSF1 ChIP at the *BCL6* gene and a negative control region in OCI-LY1 and OCI-LY7. (B) BCL6 expression in OCI-LY1 and OCI-LY7 cells transduced with HSF1 shRNA and a scrambled control (shScr) and selected for 2 d with puromycin. (C) Immunoblot of OCI-LY1 and OCI-LY7 cells transduced as described in (B). Values in (A-C) are representative of three independent experiments. Error bars indicate the mean ± SEM.

3.1C). However HSP90 stabilizes BCL6 post-transcriptionally, therefore the effect seen here may reflect an indirect mechanism of HSF1-mediated regulation of BCL6 (Cerchietti et al., 2009a).

2.2 HSF1 maintains DLBCL survival

DLBCL cells are highly dependent on BCL6 for their pathogenesis and survival (Hatzi and Melnick, 2014). In addition, pharmacological inhibition of HSP90 results in strong anti-lymphoma activity in *in vitro* and *ex vivo* models of DLBCL. Because HSF1 knockdown results in a decrease in both BCL6 and HSP90 levels, we next examined whether HSF1 knockdown affects DLBCL survival. We first transduced two DLBCL cell lines (OCI-LY1 and SU-DHL4) with 5 HSF1-targeting shRNAs in a tetracycline-inducible backbone and an empty vector control (pLVUTH-KRAB) (Szulc et al., 2006). After doxycycline (a more stable tetracycline derivative), shRNA expression is induced along with a GFP transgene. By measuring GFP-positive cells, cell viability and growth was assessed. In cells infected with the empty vector, GFP-positive cells continued to increase until d 3 where they plateaued to 25-30% even with continuous replenishment of doxycycline to the media (**Figure 3.2**). The percentages of GFP-positive cells transduced with HSF1 shRNAs were significantly lower compared to the empty vector in all five shRNAs in both OCI-LY1 and SU-DHL4 (**Figure 3.2**). These preliminary results suggest that DLBCL cells require HSF1 for their normal proliferation and survival. However infection efficiency after transduction with this inducible shRNA system was poor and difficult for downstream assays to more precisely answer these questions. Therefore the puromycin-selectable pLKO.1 shRNA backbone was used for all further experiments.

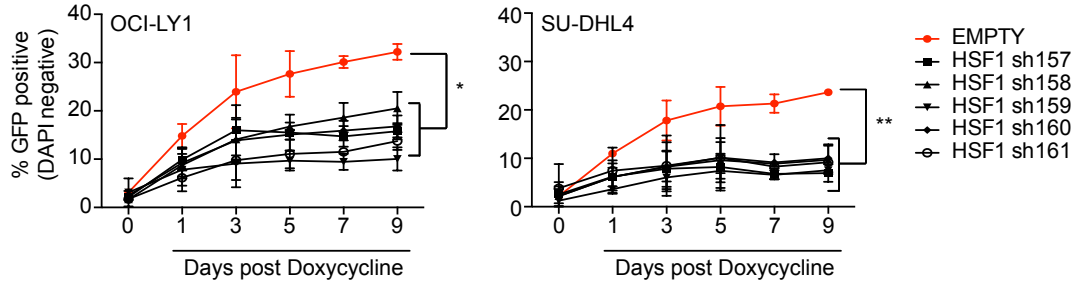

Figure 3.2 DLBCL cells require HSF1 for normal growth and proliferation. The % GFP+ DAPI- cells after doxycycline induction in OCI-LY1 and SU-DHL4 cells transduced with a tetracycline-inducible backbone with 5 HSF1-targeting shRNAs and an empty vector control. Values are representative of three independent experiments. Error bars indicate the mean ± SEM. A t-test was used to assess significance, * $p<0.05$ and ** $p<0.01$ at d 5, d 7, and d9.

While preliminary experiments demonstrated a potential dependency for HSF1, HSF1 knockdown was performed in a larger panel of DLBCL cell lines to better address this query. This panel included both GC B cell-like (GCB) and activated B cell-like (ABC) DLBCL cell lines. While they both arise from the GC, GCB and ABC DLBCL cells are thought to come from different cells of origin within GC development. GCB DLBCLs are highly dependent on BCL6 as they reflect more of a centroblast-phenotype whereas ABC DLBCLs have gene expression patterns that are more similar to B cells undergoing plasmacytic differentiation and are therefore in a later GC stage (Lenz and Staudt, 2010; Roschewski et al., 2014). Two HSF1-targeting shRNAs (shHSF1-1 and -2) and a scrambled control (shScr) were used to transduce 9 DLBCL cell lines. This panel included four GCB (OCI-LY1, OCI-LY7, SU-DHL4, SU-DHL6), two ABC (HBL1 and TMD), and three BCL6-independent (K422, PFEIFFER, TOLEDO)

cell lines. DLBCL cell lines were transduced and selected 48 h later with 1 μg/mL puromycin. Live cells were monitored by flow cytometry using Annexin V^- and $DAPI^-$ criteria. The percentage of live cells decreased as early as d 2 after puromycin with the most sensitive cell lines almost completely killed by d 4 and d 8 in shHSF1-1 and shHSF1-2, reflecting differences in HSF1 knockdown efficiency between the hairpins (**Figure 3.3A-B**). The most sensitive cell lines (SU-DHL6, TMD8, and PFEIFFER) had efficient HSF1 knockdown with both shRNAs and spanned all three categories of GCB, ABC, and BCL6-independent. The percentage of live cells also decreased in the other DLBCL cell lines with the greatest decrease occurring in cells transduced with shHSF1-1, the hairpin that was most effective at depleting HSF1 (**Figure 3.3A-B**). Decreases in cell viability were accompanied by an induction of apoptotic markers like cleaved PARP1 (cPARP1). All the cell lines transduced with shHSF1-1 had higher cPARP1 levels compared to shScr (**Figure 3.3B**). These results demonstrate HSF1 is required to maintain DLBCL survival.

Some DLBCL cell lines had minimal effects on cell viability, therefore we wondered if HSF1 knockdown may at least cause defects in the proliferation of cells. To test this, we examined BrdU incorporation 4 d after shRNA transduction. We found that shHSF1-1 expressing cells had decreased number of cells entering S phase and a subsequent increase of cells in G2/M-phase (**Figure 3.4A**). This experiment was complemented with additional studies using a proliferation dye, eFluor670. Three DLBCL cell lines (OCI-LY1, OCI-LY7, and the BCL6-independent TOLEDO) were transduced with shHSF1-2, the HSF1-targeting hairpin with moderate effects on viability to measure changes in proliferation rate. Cells were stained with eFluor670,

transduced, and selected with puromycin. The proliferation index was calculated based on the rate of eFluor670 dilution using flow cytometry. All three DLBCL cell lines irrespective of BCL6 dependence had significant decreases in proliferation index with shHSF1-2 relative to the control shScr, indicating a role for HSF1 in upholding the rapid proliferate state of DLBCL cells (**Figure 3.4B**). Collectively both BCL6-dependent and -independent cell lines were sensitive to HSF1 knockdown, suggesting that HSF1 has independent functions related to cell viability and cell cycle control distinct from BCL6.

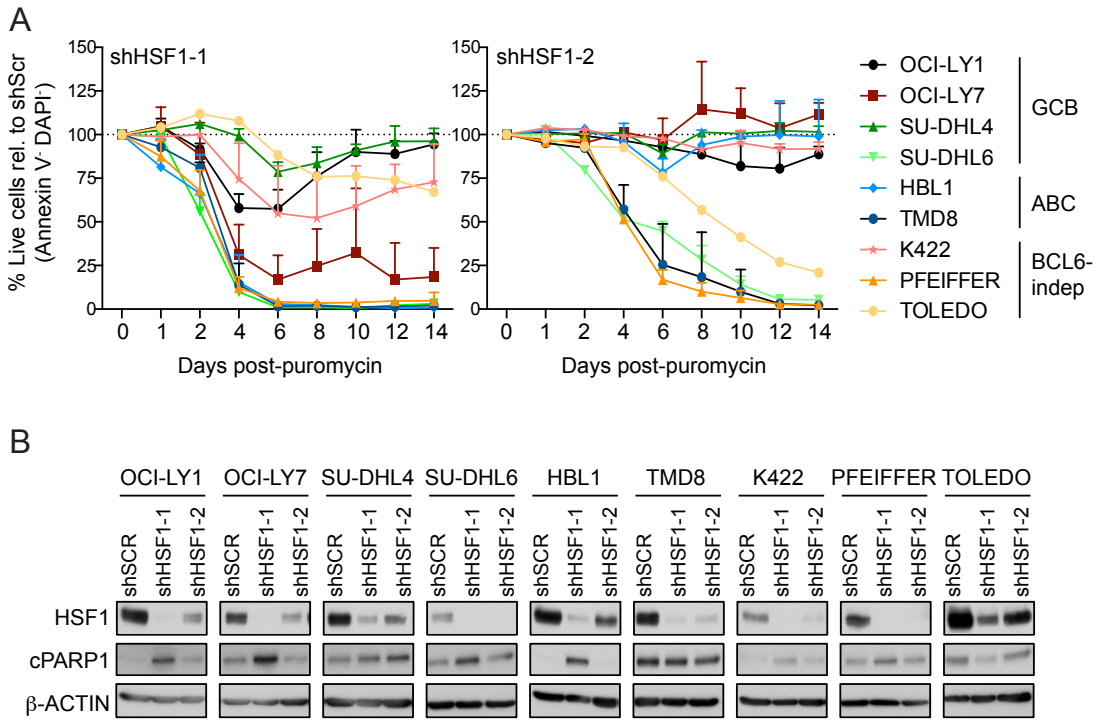

Figure 3.3 HSF1 is necessary for DLBCL survival. (A) % Live cells as measured by Annexin V- and DAPI- in a panel of DLBCL cell lines transduced with two HSF1-targeting shRNAs and control shScr and selected with puromycin. (B) Immunoblot was performed in (A) at d2 post-puromycin. Values in (A) are representative of three independent experiments. Error bars indicate the mean ± SEM.

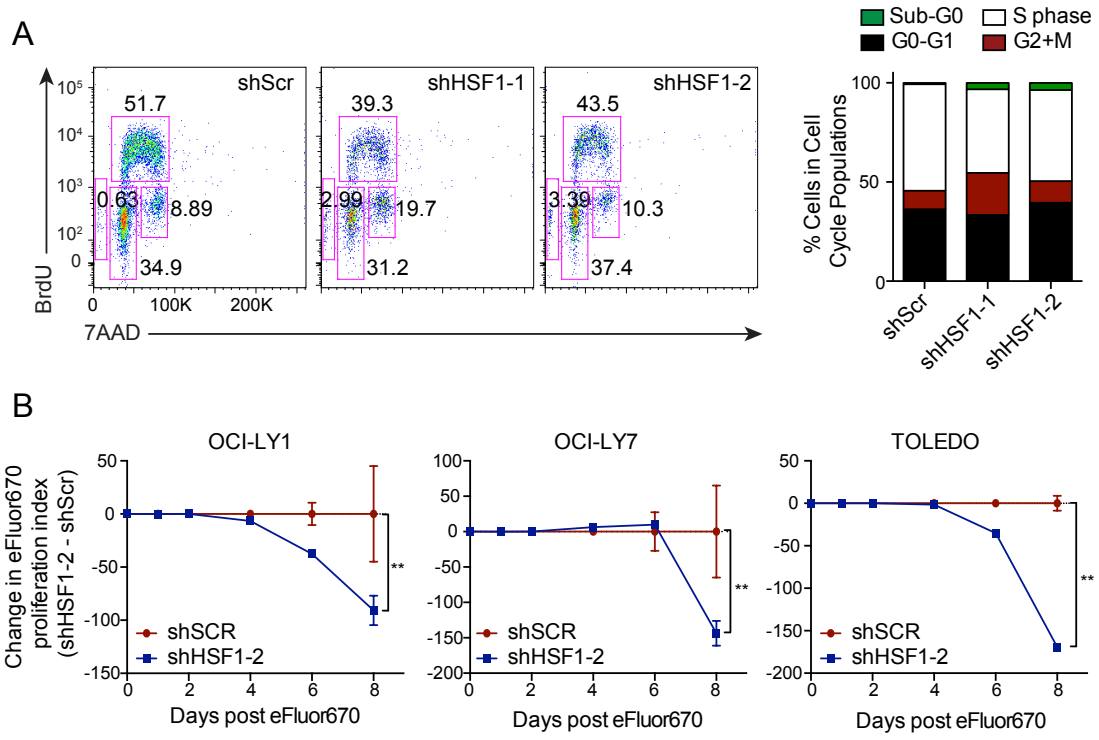

Figure 3.4 DLBCL cells require HSF1 for rapid proliferation. (A) BrdU incorporation in OCI-LY1 cells transduced with 2 HSF1-targeting shRNAs and shScr vector control 4 d after puromycin selection. Quantification of cell populations is shown on the right. (B) Rate of proliferation in OCI-LY1, OCI-LY7, and TOLEDO cells stained with eFluor670 and transduced with shHSF1-2 and selected with puromycin. Values are representative of three independent experiments. Error bars indicate the mean ± SEM. A t-test was used to assess significance, ** $p<0.01$.

2.3 Genome-wide patterns of HSF1 occupancy in DLBCL

HSF1 facilitates the survival and proliferation of DLBCL. However how it coordinates these effects is still unclear. HSF1 is a transcription factor that mediates its function by modulating gene expression of its targets. We have demonstrated that HSF1 regulates BCL6 expression in GC B cells and DLBCL, and HSF1 knockdown is followed with decreases in BCL6 levels. Interestingly many DLBCL cell lines that are not dependent on BCL6 also rely on HSF1, implying that HSF1 regulates additional genes important for DLBCL pathogenesis. To determine the genome-wide transcriptional program in DLBCL, we performed HSF1 ChIP followed by next-generation sequencing in two DLBCL cell lines, OCI-LY1 and OCI-LY7. HSF1 ChIP-seq was done in replicates, which were highly correlated in both cell lines (Pearson r 0.87 and 0.93 for OCI-LY1 and OCI-LY7 respectively) (**Figure 3.5A-B**). We identified HSF1 occupied sites with the ChIPseeqer peak detection tool (Giannopoulou and Elemento, 2011). We overlapped the replicates of each cell line and identified 147 and 675 reproducible peaks in both OCI-LY1 and OCI-LY7 respectively, which amounted to 167 and 664 genes, respectively (**Table 3.1**). In OCI-LY1, more than 40% of HSF1 peaks fell within promoter regions, 20% within gene bodies (mainly introns), and more than 30% fell within distal and intergenic regions (**Figure 3.5C**). In OCI-LY7, equal percentages of HSF1 peaks occupied both promoters and introns (30%), and almost 35% of peaks were found in distal and intergenic peaks (**Figure 3.5D**). The low number of peaks in OCI-LY1 is likely due to poor immunoprecipitation efficiency with this particular HSF1 antibody (Enzo). However this antibody outperformed others (Cell Signaling and Santa Cruz) for ChIP and these peak numbers are

consistent with other HSF1 genome-wide studies in cancer cell lines (Mendillo et al., 2012; Vihervaara et al., 2013).

Table 3.1 Summary of mapped reads and detected peaks in ChIP-seq experiments.

		CHIP	INPUT	CLONAL READS	PEAKS (T5F2)	OVERLAPPED PEAKS	GENES
OCI-LY1	R1	12,773,795	17,794,651	<10%	651	147	167
	R2	10,768,344	21,468,559	<10%	589		
OCI-LY7	R1	9,561,890	16,593,942	<10%	1609	675	664
	R2	10,741,011	13,678,363	<10%	1664		

HSF1 binds to its target through specific regulatory elements, termed heat shock response elements or HSEs. We next sought to determine if many of the HSF1 occupied genomic sites have HSEs using the de novo motif discovery tool FIRE (Elemento et al., 2007). In OCI-LY1, the HSE motif was the only motif identified to be over-represented by FIRE, localized close to the center of the HSF1 peak summit, and was present in almost 60% of HSF1 peaks (**Figure 3.6A**). In OCI-LY7, FIRE identified 3 motifs that were over-represented (**Figure 3.6B**). The motif with the highest z-score was the canonical HSE, which similarly to OCI-LY1 was found close to the peak summit and present in 55% of all HSF1 peaks (**Figure 3.6B**). The other two motifs over-represented appear to be degenerate HSEs. Interestingly one motif rich in A's was found to be under-represented in HSF1 peaks (**Figure 3.6B**). The presence of an HSE in the majority of HSF1 occupied genomic sites suggests that HSF1 directly binds its target loci to regulate their expression. Those HSF1-bound sites without canonical HSEs may have

degenerate HSEs, as found in OCI-LY7, or HSF1 may be recruited to those targets by another transcription factor.

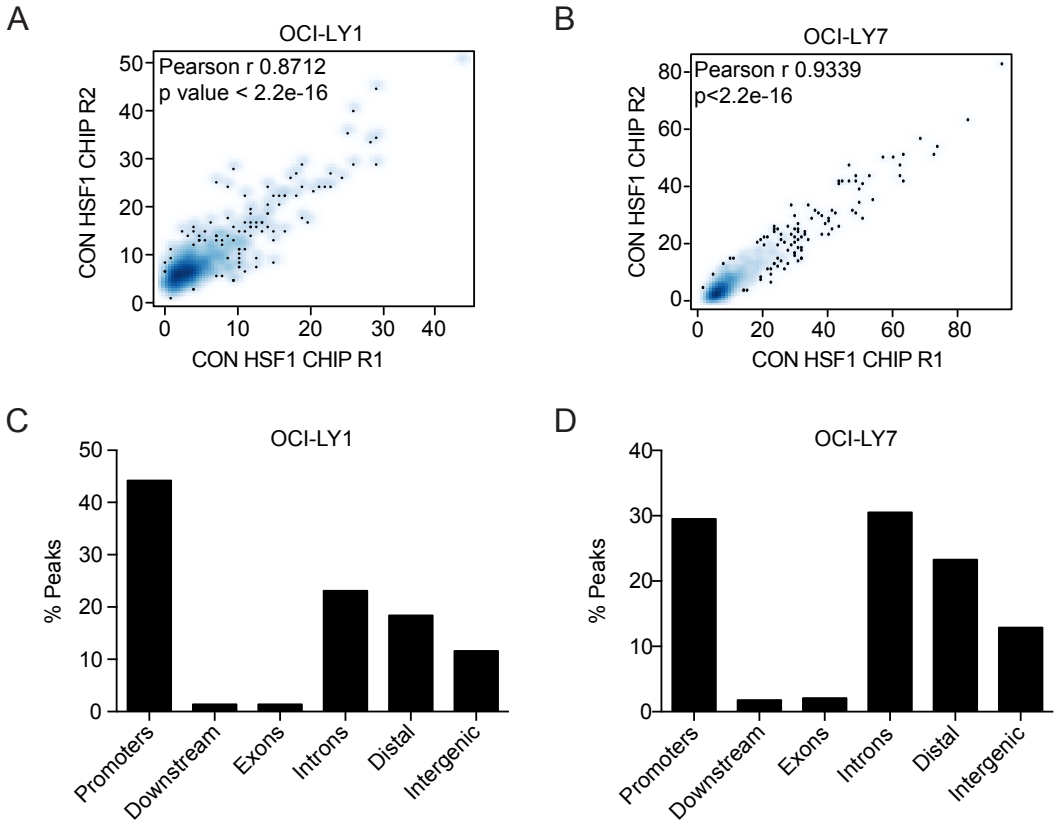

Figure 3.5 Genome-wide occupancy of HSF1 in DLBCL cells. Correlation of HSF1 ChIP-seq replicates in (A) OCI-LY1 and (B) OCI-LY7 cells. Each point represents the maximum peak height of each peak location in replicate (R1) and R2. Distribution of HSF1 ChIP-seq occupied regions in the genome in (C) OCI-LY1 and (D) OCI-LY7 cells.

2.4 HSF1 regulates the expression of its target loci

To determine the consequences of HSF1 occupancy on gene expression, we profiled OCI-LY1 and OCI-LY7 for global mRNA changes after HSF1 knockdown using next-gen sequencing. We transduced DLBCL cells with two

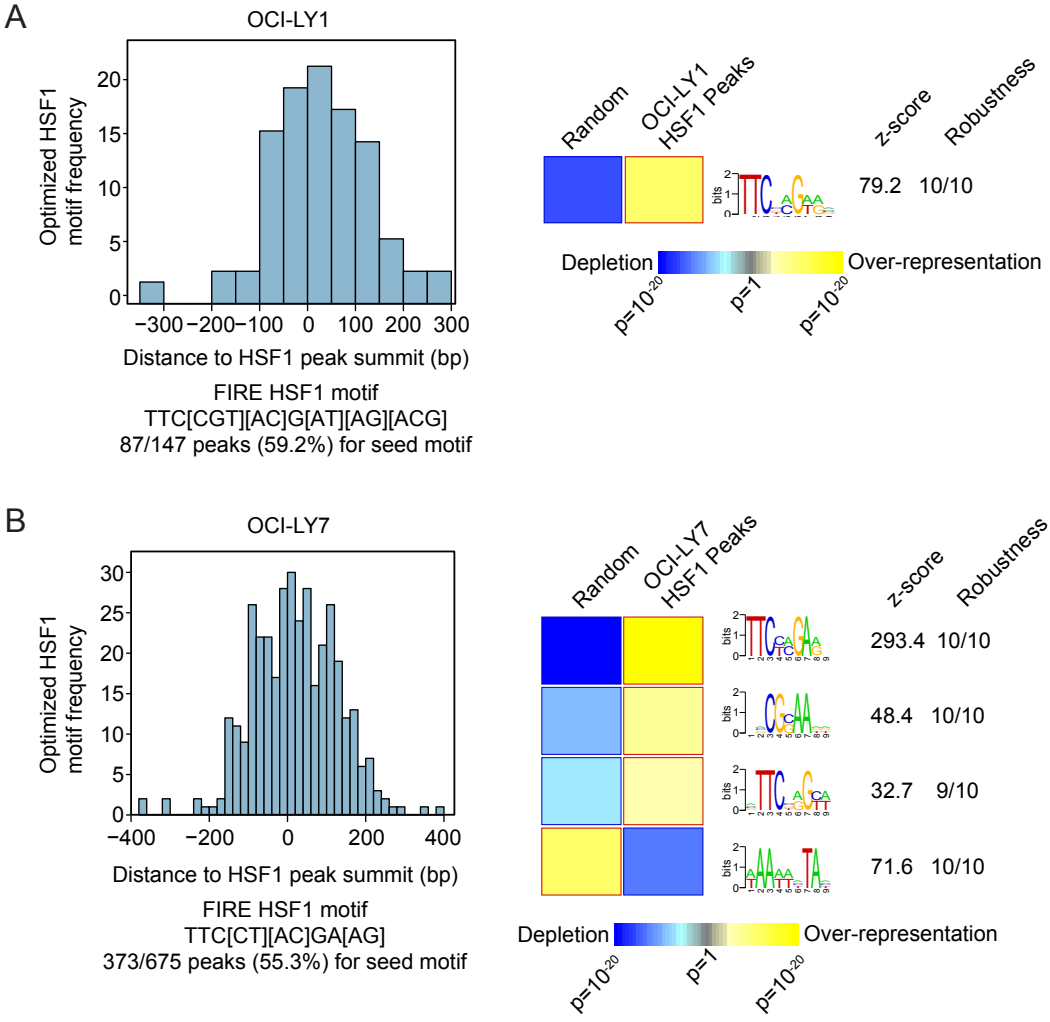

Figure 3.6 *De novo* motif discovery of HSF1 binding sites using FIRE. The location of the top motif identified by FIRE (resembling the canonical HSE) in relation to the HSF1 peak summit in (A) OCI-LY1 or (B) OCI-LY7 cells, left. Motifs identified by FIRE that are over- or under-represented in HSF1 binding sites in (A) OCI-LY1 or (B) OCI-LY7 cells, right.

HSF1-targeting (shHSF1-1 and -2) and a scrambled control shRNA (shScr) and analyzed mRNA expression 48 h post-puromycin selection when cell viability was not impaired. Differentially expressed genes were identified with the EdgeR package using FDR<0.05 (Robinson et al., 2010). The gene

expression changes resulting from both HSF1 shRNAs were well correlated in OCI-LY1 and OCI-LY7 (Pearson r values 0.69 and 0.66 respectively) (**Figure 3.7A-B**). As observed earlier with effects on cell viability, shHSF1-1 has more gene expression changes (4,646 and 6,721 differentially expressed genes in OCI-LY1 and OCI-LY7, respectively) than shHSF1-2 (2,118 and 2,561 differentially expressed genes in OCI-LY1 in OCI-LY7, respectively) again due to the differences in HSF1 knockdown efficiency, as shHSF1-1 is able to deplete HSF1 levels better than shHSF1-2 (**Figure 3.7C**). Moreover OCI-LY7 had more genes bound by HSF1, and this was reflected with more genes being mobilized after HSF1 depletion. HSF1 knockdown resulted in a large number of downregulated genes (2,890 in OCI-LY1 and 3,442 in OCI-LY7 with shHSF1-1), indicating that many were transcriptionally activated by HSF1. However many genes also increased (1,756 in OCI-LY1 and 3,279 in OCI-LY7 with shHSF1-1), suggesting that HSF1 can form repressive transcriptional complexes. Alternatively the de-repression of genes might be a secondary effect because of HSF1-mediated modulation of other genes that function as repressors like BCL6, which we demonstrated earlier is an HSF1 target. Genes downregulated in OCI-LY7 after shHSF1-1 were enriched in genesets associated with proliferation and B cell differentiation including genes repressed by BLIMP1, the master regulator of plasma cell differentiation (**Figure 3.7D**). These results are consistent with proliferation defects seen after HSF1 knockdown (**Figure 3.3-3.4**) but they also imply that HSF1 knockdown releases DLBCL cells from the centroblast-phenotype and allows them to differentiate to plasmacytic B cells.

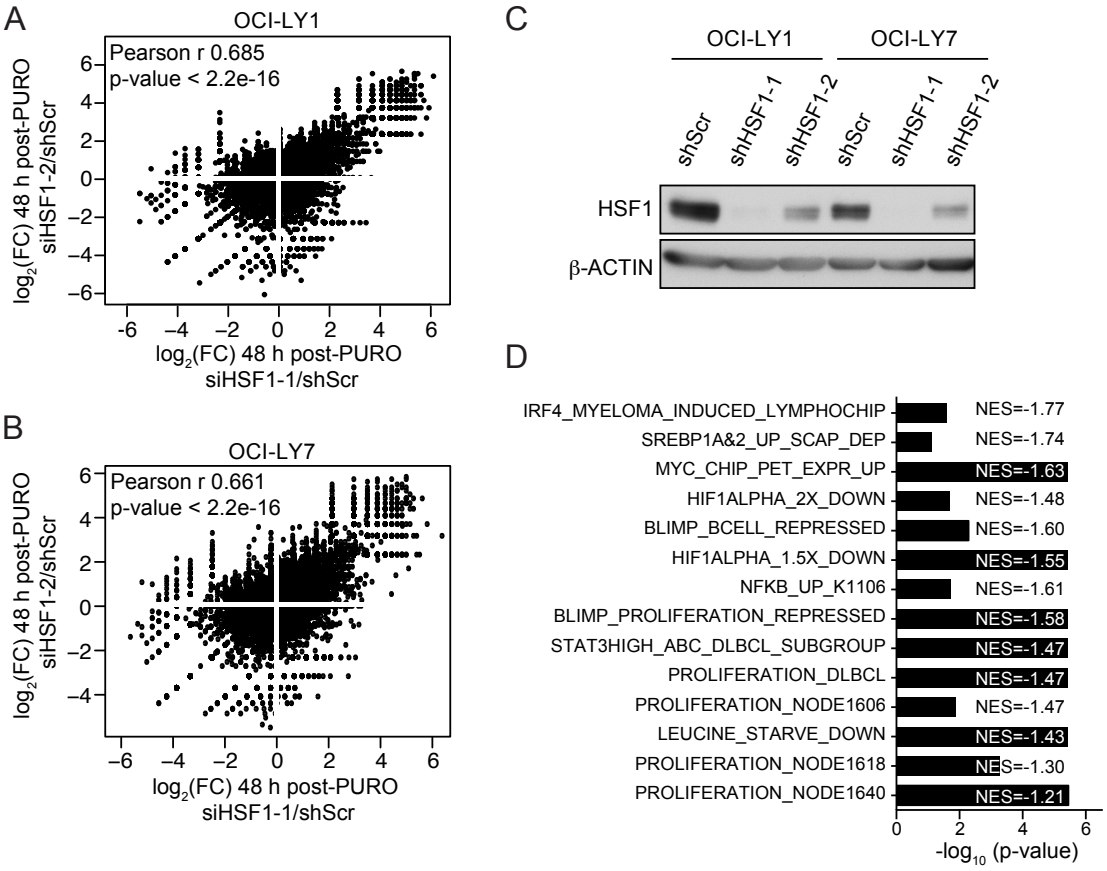

Figure 3.7 Gene expression profiling after HSF1 knockdown in DLBCL cells. OCI-LY1 and OCI-LY7 mRNA-seq after cells were transduced with two HSF1-targeting shRNAs and a control shScr and selected for 2 d with puromycin. Correlation of $\log_2$ fold-changes of each HSF1 shRNA to shScr. in (A) OCI-LY1 and (B) OCI-LY7 cells. (C) Immunoblot of cells described earlier. (D) Summary of Staudt gene signatures that significantly enrich with genes downregulated after shHSF1-1 in OCI-LY7 cells using GSEA.

To evaluate the effect of HSF1 binding on the expression of its target genes, we performed gene set enrichment analysis (GSEA) with a ranked list of all gene expression changes after HSF1 knockdown and HSF1 promoter targets. A significant enrichment was seen with HSF1-bound promoters and genes downregulated after HSF1 depletion with shHSF1-1 (the stronger shRNA) in both OCI-LY1 (NES=-1.83, FDR q-value=0.0002) and OCI-LY7 (NES=-1.42, FDR q-value=0.003) (**Figure 3.8A-B**). Enrichment was also seen between HSF1-bound promoters and genes downregulated after shHSF1-2 although with higher FDR q-values, most likely due to inefficient HSF1 knockdown (**Figure 3.8A-B**). Many of the genes bound and regulated by HSF1 were associated with gene ontology categories of molecular chaperones, chromatin binding, protein translation, and lymphocyte activation, suggesting that HSF1 controls a unique program that includes both canonical expression of *HSPs* but also other genes involved in DLBCL malignancy and survival (**Figure 3.8C**).

2.5 HSF1 transcriptional programs in normal GC B cells and DLBCLs are distinct

Considering that many of the molecular mechanisms governing the GC response are hijacked by DLBCL cells to maintain their highly proliferative and pro-survival phenotype, we wondered if the HSF1 transcriptional program is shared between DLBCL cells and GC B cells. To answer this question, we performed HSF1 ChIP-seq in human $CD77^{+}$ GC B cells affinity-purified from de-identified tonsillectomy specimens. HSF1 ChIP-seq replicates correlated with Pearson r values of 0.80, and the overlap of ChIP-seq replicates yielded 433 regions occupied by HSF1 with 454 unique genes potentially regulated.

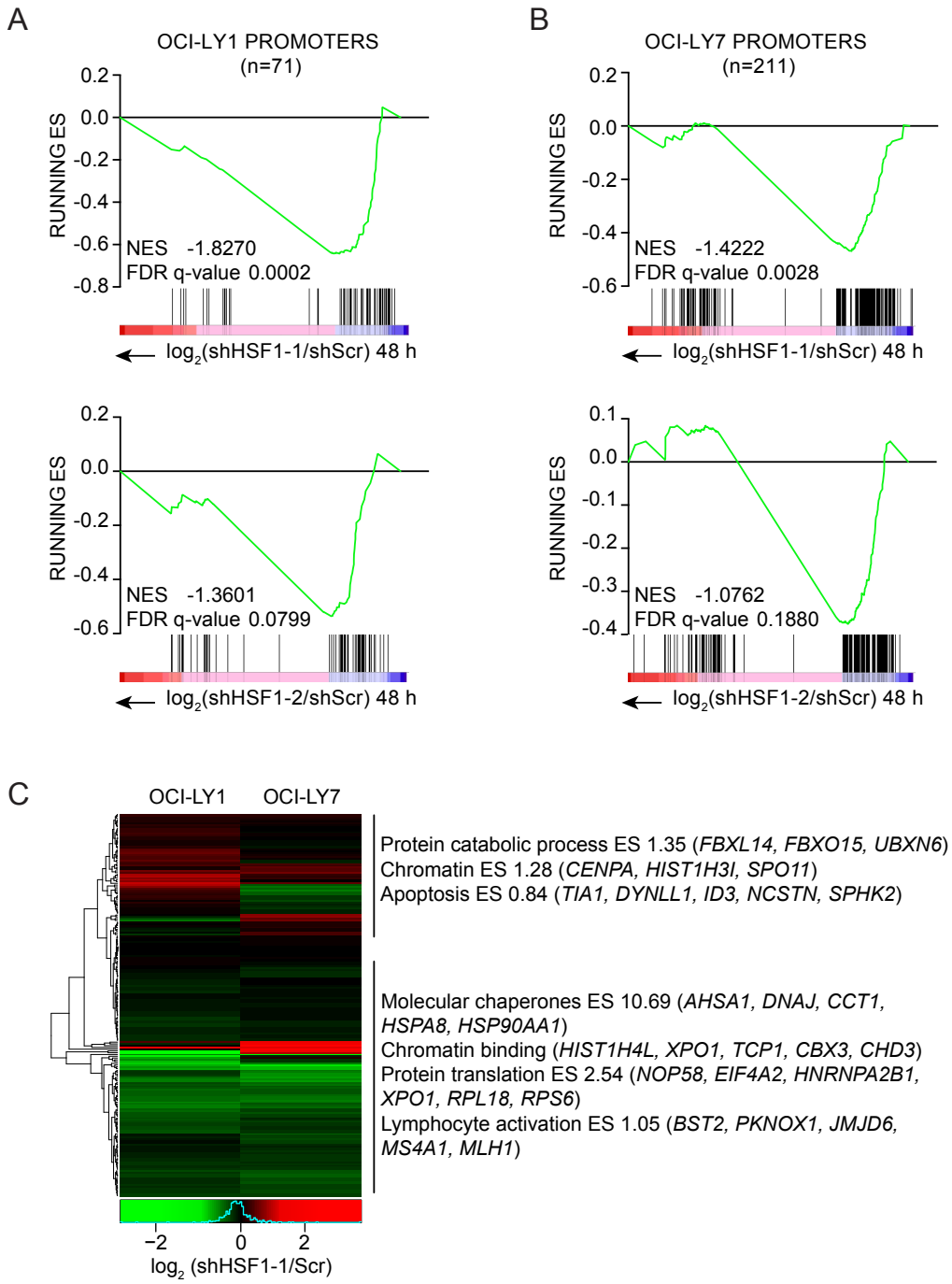

Figure 3.8 HSF1 regulates the expression of genes that it binds. GSEA with HSF1 promoter targets in (A) OCI-LY1 and (B) OCI-LY7 and a ranked list of all gene expression changes after shHSF1-1 (top) or shHSF1-2 (bottom). (C) Heatmap of HSF1-bound promoters and their gene expression changes with enriched gene ontology categories on the right.

GC HSF1 ChIP-seq demonstrated similar genome occupancy as DLBCL cell lines with more than 40% of HSF1-bound peaks falling within promoters (**Figure 3.9A-B**). Like in DLBCL cells, the canonical HSE was over-represented (found in 57% of total peaks) and localized to the center of the peak summit (**Figure 3.9C**). HSF1 promoter targets in GC B cells were also strongly enriched (NES=-1.29, FDR q-value=0.00 2) in genes downregulated after shHSF1-1 transduction in DLBCL cells, demonstrating that HSF1 in fact positively regulates many of its targets in GC B and DLBCL cells (**Figure 3.9D**).

To understand the differences in transcriptional programs between GC B cells and DLBCL cells, we overlapped the HSF1-bound targets in GC B cells and union of genes bound in DLBCL cells. We found 130 genes that were occupied by HSF1 in both GC B cells and DLBCL cells, but we also found genes that were specific to GC B cells or DLBCL cells (**Figure 3.10**). As expected, the shared HSF1 targets reflect the canonical functions of HSF1 in maintaining proteostasis and include genes involved protein folding, translation, and the ubiquitin-proteasome system. The shared HSF1 targets are also involved in gene expression, as many of them are transcription factors, chromatin-binding proteins, and long noncoding RNAs. HSF1 targets that are unique to GC B cells reflect tissue-specific targets as many genes are involved immune signaling and protein transport. DLBCL-specific targets reflect the pro-survival and proliferative function of HSF1 that are required by DLBCL for pathogenesis. Many of these targets are involved in cell cycle control for uncontrolled proliferation and modulation of chromatin that is

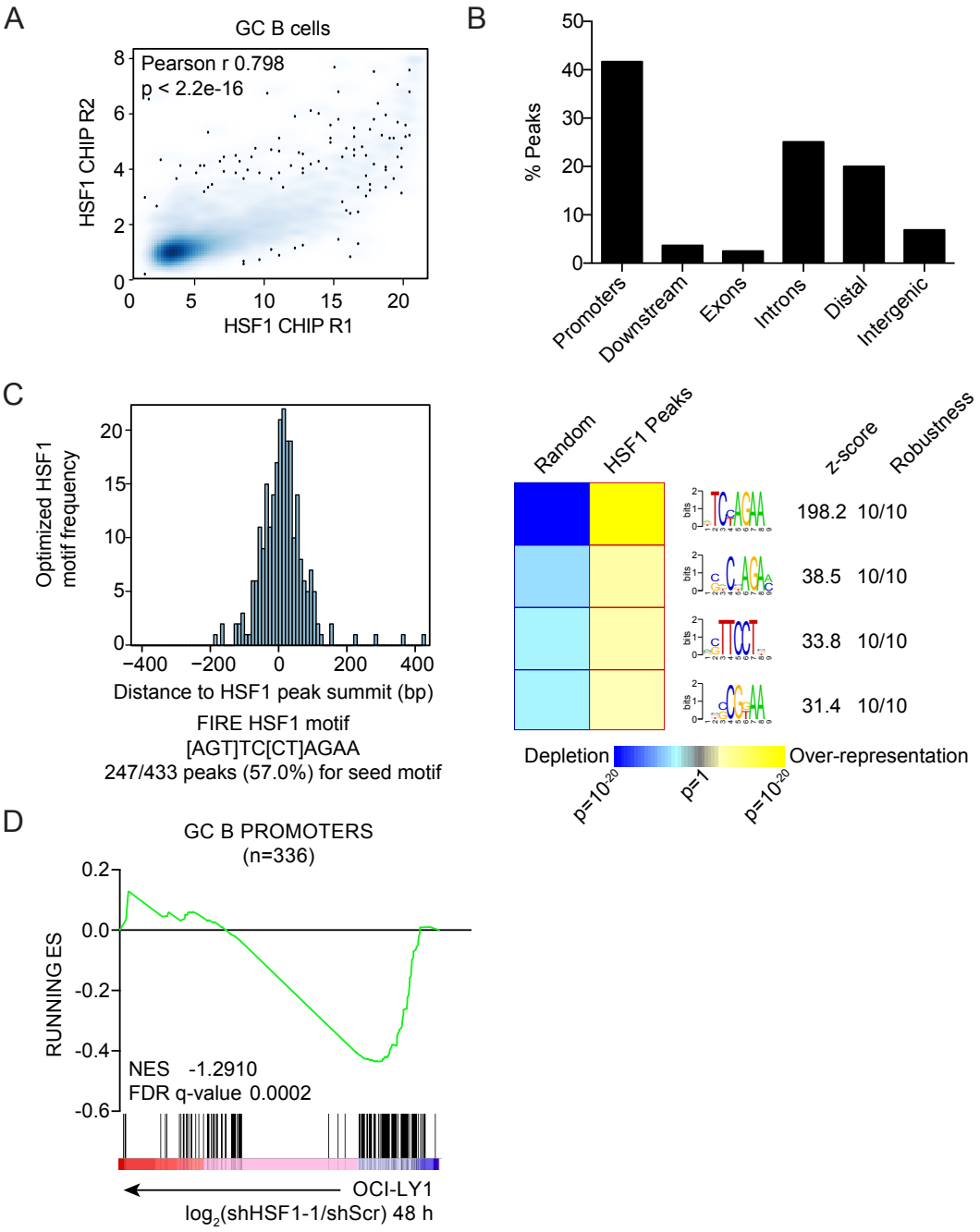

Figure 3.9 Genome-wide occupancy and de novo motif discovery of HSF1 binding sites in GC B cells. (A) Correlation of HSF1 ChIP-seq replicates in human tonsillar GC B cells. Each point represents the maximum peak height of each peak location in replicate (R1) and R2. (B) Distribution of HSF1 ChIP-seq occupied regions in the genome. (C) The location of the top motif identified by FIRE (resembling the canonical HSE) in relation to the HSF1 peak summit, left. Motifs identified by FIRE that are over- or underrepresented in HSF1 binding sites, right.

required for activation of additional transcriptional programs that maintain genomic instability and DLBCL malignancy.

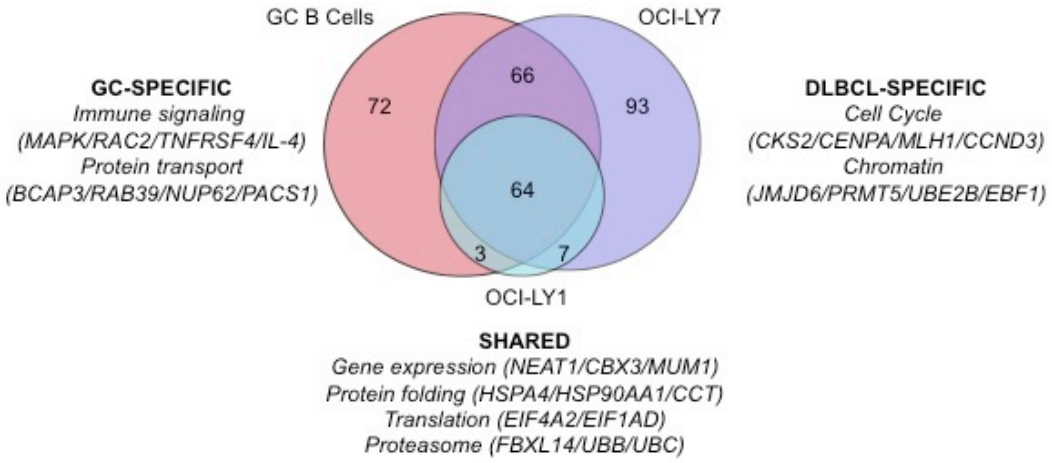

Figure 3.10 HSF1 transcriptional program in GC B cells and DLBCL cells. The overlap of HSF1-bound promoters in GC B cells and DLBCL cells, OCI-LY1 and OCI-LY7. Gene ontology categories that enrich in the GC B cell-specific, left; shared between GC B cells and DLBCLs, center; and DLBCL-specific, right are noted.

3. Discussion

In an earlier chapter, we have shown that HSF1 mediates the stress-dependent induction of *BCL6*. This occurs after heat shock and also in GC B cells that are highly stressed due to replicative, genotoxic, and metabolic stress. We demonstrate here that BCL6 induction in DLBCL is also stress-dependent as HSF1 depletion results in decreased levels of BCL6. BCL6 is the most frequently deregulated oncogene in DLBCL, and its constitutive expression in GC B cells can induce lymphomagenensis (Ci et al., 2008). Due to the regulation of BCL6, it was not surprising that our data indicate that DLBCL cells also require HSF1 to sustain their survival and rapid proliferation.

Our initial hypothesis was that this was facilitated by maintenance of BCL6 expression, and GCB DLBCL cells would therefore be more dependent on HSF1. However BCL6-independent and ABC DLBCL cell lines that express lower levels of BCL6 were also sensitive to HSF1 knockdown. These data suggest that HSF1 can complement other drivers of DLBCL malignancy by maintaining an oncogenic environment that allows cells to tolerate aberrant mutations, genomic instability, and a high replicative index.

To identify how HSF1 maintains an oncogenic environment, we sought to determine the HSF1-driven transcriptional program in DLBCL. We found that HSF1 is directly recruited to the majority of its targets by the presence of HSEs. HSF1 binds to the promoters, gene bodies, and intergenic regions of genes. We have determined that promoter binding greatly influences whether a gene will be regulated by HSF1 as the majority of promoter-bound genes are positively regulated by HSF1. However the significance of HSF1 binding to other genomic regions like introns and intergenic sites is still unclear. Many of these regions have HSEs suggesting that they are indeed bona fide targets and not artifacts. Intergenic regions are frequently associated with regulatory elements or enhancers. HSF1 binding at these regions could indicate potential enhancer regions that fine-tune gene expression.

Mendillo et al. (2012) found that genes that were negatively regulated by HSF1 were more frequently bound by HSF1 at intergenic than promoter regions, suggesting that intergenically-bound HSF1 participates in the repression of proximal genes. However GSEA with our datasets did not demonstrate an enrichment with intronic- or intergenic-bound regions with increased or

decreased gene expression changes after HSF1 knockdown (not shown). If intergenic HSF1 binding does truly participate in regressive complexes, the presence of a distinguishing factor that separates out the repressor functions of HSF1 has not yet been elucidated. Notably the HSF1 binding site is similar to the BCL6 motif ([AT]TC[CT][AT][AC]GA) (Ci et al., 2009; Hatzi et al., 2013). BCL6 is transcriptional repressor that mediates its functions at enhancer regions by recruiting the corepressors SMRT and HDAC3 to toggle enhancers from an active to a poised state (Hatzi et al., 2013). In fact the HSF1 binding site was overrepresented in genomic regions bound by both BCL6 and SMRT (Hatzi et al., 2013). These results suggest that HSF1 could act with BCL6 to toggle enhancer activity, revealing a novel role for HSF1 in modulating enhancer activity.

A large percentage of HSF1-occupied sites also fall within introns. Instead of regulating the expression of genes transcriptionally, HSF1 could potentially regulate genes post-transcriptionally by affecting differential splicing. A functional screen identified several HSF1 binding proteins that are involved in RNA splicing, including PRPF8, SNRNP200, and EFTUD2, which together form the U5 snRNP components of the spliceosome (Fujimoto et al., 2012). EFTUD2 is an RNA helicase that unwinds U4/U6 RNA and is required for spliceosome activation (Bartels et al., 2002). HSF1 could directly modulate alternative splicing events by targeting the U5 snRNP components for preferential intron retention or exon skipping. Alternatively HSF1 could facilitate exon usage indirectly by modulating chromatin at its binding sites. It was recently demonstrated that trimethylation of H3K36 on a histone variant (H3.3) associated with actively transcribed genes can recruit BS69, a

chromatin reader, which mediates intron retention by directly binding to EFTUD2 (Guo et al., 2014). By activating trimethylation of H3K36, HSF1 could recruit BS69 to induce intron retention at its targets.

While the exact biochemical mechanisms of HSF1 at its occupied genomic regions remain unclear, the transcriptional program driven by HSF1 in GC B cells and DLBCL has now been revealed. While many of the genes regulated by HSF1 are common to both GC B cells and DLBCL, there are specific subsets of genes uniquely found in one or the other. The gene expression program shared by GC B cells and DLBCL largely represents the canonical functions of HSF1 in maintaining protein homeostasis as many of these genes are molecular chaperones, components of the ubiquitin-proteasome system, and translational machinery. This is expected since both GC B and DLBCL cells are highly stressed, undergoing SHM, and therefore producing proteins with aberrant mutations that must be effectively chaperoned. This explains why DLBCL cells, independent of the oncogenic driver whether it is BCL6 or constitutive NF-κB signaling, are sensitive to HSF1 depletion. The HSF1-specific program in GC B cells seems to reflect normal GC biology as many of these genes are involved in immune signaling and protein transport, which is likely required by GC B cells to constantly shuttle their Ig receptors to the surface for antigen presentation. The DLBCL-specific HSF1 targets include genes involved in cell cycle control and proliferation. This is consistent with our results demonstrating cell cycle arrest and decreased cell proliferation after HSF1 knockdown. In addition to these expected targets, HSF1 also seems to regulate a number of transcription factors and chromatin-modifiers. While the exact reasons why they might be regulated by HSF1 is still unclear and likely

very complex, these data implicate them in the pathogenesis of DLBCL and suggest that they could be important for DLBCL survival.

We have found that HSF1 is critical for DLBCL survival and explored the transcriptional mechanisms mediating HSF1-induced malignancy. These studies elucidated HSF1 as a novel therapeutic target in lymphoma and also provided mechanistic insight into the transcriptional regulation of genes important for lymphoma development and survival. DLBCL is the most common lymphoid malignancy, accounting for almost 40% of all non-Hodgkin lymphomas (Lenz and Staudt, 2010). While more than 50% of DLBCL patients respond to current anti-lymphoma therapy, a third of patients remain incurable, demonstrating a need for better targeted treatments (Roschewski et al., 2014). A great deal of time and money has been spent to understand the molecular mechanisms underlying DLBCL in the hope of discovering novel therapeutic targets. One outcome of these efforts is the growing emergence of HSP-based therapies, which have proven extremely promising in animal studies and are currently in cancer clinical trials (Neckers and Workman, 2012). However targeting the upstream transcription factor that governs the expression of *HSPs* as well as multiple other pathways important for DLBCL survival may be a more effective way to reprogram the fundamental cellular processes that drive and maintain B cell malignancy. The identification of HSF1-mediated pathways involved in B cell transformation we present here will hopefully provide additional avenues to improve and specify both heat shock-targeted therapies and chemotherapeutic combinations for treatment of DLBCL.

4. Materials and Methods

Mammalian Cell Lines

The DLBCL cell lines OCI-LY1 and OCI-LY7 were grown in Isocove's medium supplemented with 10% FBS and penicillin G/streptomycin. SU-DHL4, SU-DHL6, K422, PFEIFFER, TOLEDO, HBL-1, and TMD8 were grown in RPMI 1640 supplemented with 10% FBS, penicillin G/streptomycin, L-glutamine, and HEPES. Cell lines were obtained from ATCC, DMSZ or the Ontario Cancer Institute and grown in 37 ºC with 5% CO_2.

Primary cell isolation

Human tissues were obtained with approval of the Institutional Review Board (IRB), Office of Research Integrity of the Weill Cornell Medical College and in accordance with the Declaration of Helsinki. $CD77^+$ GC B cells were isolated from de-identified human tonsillectomy specimens or spleens. After centrifugation in Fico/Lite-dLymphoH density gradient media (Atlanta Biologicals), mononuclear cells were collected and affinity-purified using microbead cell separation via the autoMACS system (Miltenyi Biotec). GC B cell purity was determined by flow cytometric analysis to be >90% $CD77^+/CD38^{high}$.

Chromatin Immunoprecipitation (ChIP)

ChIP was performed as previously described (Hatzi et al., 2013). Briefly, OCI-LY1, OCI-LY7, or GC B cells were fixed with 1% formaldehyde for 10 min at room temperature, quenched with 125 mM glycine, and lysed in modified RIPA buffer (150 mM NaCl, 1% v/v Nonidet P-40, 0.5% w/v deoxycholate, 0.1% w/v SDS, 50 mM Tris pH 8, 5 mM EDTA) supplemented with protease inhibitors. Cell lysates were sonicated using a tip sonicator (Branson) to generate

fragments less than 400 bp. Precleared lysates were incubated overnight with 5 μg anti-HSF1 (ADI-SPA-901, Enzo Life Sciences) or control IgG antibody. Immunocomplexes were recovered, sequentially washed with increasing stringency of wash buffers (150 mM NaCl, 250 mM NaCl, 250 mM LiCl), and eluted with 1% SDS and 100 mM $NaHCO_3$. Crosslinks were reversed, and DNA was purified using a Qiaquick PCR purification kit (Qiagen). ChIP DNA was amplified with real-time quantitative PCR using SYBR Green (Quanta Biosciences) and 7900HT Fast Real-Time PCR System (Applied Biosystems). Input standard curves were used for estimation of relative enrichment.

Lentiviral transduction

Lentivirus was produced in 293T by calcium phosphate transfection of pLKO.1-puromycin vectors (The RNAi Consortium) or tetracycline-inducible pLVUTH-KRAB vectors (Szulc et al., 2006) with the envelope and packaging vectors, VSV.G and Δ8.91. Lentivirus was collected 48 h after transfection and concentrated with PEG-it (Systems Biosciences). Cells were transduced and selected with 1 μg/mL puromycin or induced with 0.5 μg/mL doxycycline 48 h after infection.

Control shRNA sequences:

shSCR: 5'- CCTAAGGTTAAGTCGCCCTCG -3'

Human shRNA sequences:

sh157 (also shHSF1-1): 5'- GCAGGTTGTTCATAGTCAGAA -3'

sh158: 5'- GCACATTCCATGCCCAAGTAT -3'

sh159: 5'- CCAGCAACAGAAAGTCGTCAA -3'

sh160: 5'- GCCCAAGTACTTCAAGCACAA -3'

sh161 (also shHSF1-2) : 5'- CAGTGACCACTTGGATGCTAT -3'

mRNA isolation and real-time RT-qPCR

DLBCL cells were transduced with shRNAs and then selected 48 h later with 1 μg/mL puromycin. At d2 post-puromycin, cells were collected and resuspended in Trizol reagent (Invitrogen) and stored at -80 ºC until RNA extraction. After thawing, 1/5 volume of chloroform was added, and the samples were shaken vigorously for 15 sec. After 2 min incubation at room temperature, the samples were spun at 12,000xg for 15 min at 4 ºC. The aqueous phase was aspirated into a new tube, and 1 volume of isopropanol was added. Samples were mixed and incubated for 10 min at room temperature or overnight at -80 ºC. Tubes were spun again at 12,000xg for 10 min, and then washed with 75% ethanol. Tubes were spun at 7,500xg for 5 min, aspirated, and allowed to dry at room temperature for 5-10 min. RNA was resuspended in RNase-free H_2O and quantified with the Nanodrop (Thermo Scientific). cDNA was prepared using the Verso cDNA synthesis kit (Thermo Scientific) and detected by fast SYBR Green (Quanta Biosciences) on the 7900HT Fast Real-Time PCR System (Applied Biosystems). Gene expression was normalized to a housekeeping gene *RPL13A* and expressed as values relative to control using the ddCt method. Results were represented as fold change in expression with the standard error for 3 series of triplicates.

Immunoblot

Whole cell lysate was prepared from DLBCL cells with lysis buffer (20mM Tris pH 8.0, 150 mM NaCl, 5 mM EDTA, 1% Triton X-100) supplemented with protease inhibitors. Protein was cleared, quantified by Bradford reagent (Pierce) and resolved by SDS-PAGE, transferred to PVDF membranes,

probed with primary antibodies (anti-HSF1 E-4, Santa Cruz; anti-β-ACTIN AC-15, Sigma, anti-BCL6 D8, Santa Cruz; anti-cleaved PARP-1 5A5, Santa Cruz) followed by HRP-conjugated secondary antibodies (Santa Cruz) and detected with enhanced chemiluminescence (Pierce).

BrdU detection

For BrdU labeling, cells were plated several hours before being pulsed with 10 μM BrdU (Sigma-Aldrich) for 10 min without disturbing cells. BrdU-positive cells were detected by BrdU Flow kits (BD Pharmingen) according to the manufacturer's protocol.

Measuring the change in proliferation rate

DLBCL cells were stained with 0.1 μM eFluor670 (eBioscience) according to the manufacturer's instructions and then split for transduction with shRNAs. Cells were selected 48 h later with puromycin and monitored by flow cytometry for the rate of dye dilution every other day. The change in proliferation index at day x was measured by using the eFluor670 MFI in the formula below. Change in proliferation index that is less than 0 indicates decreased proliferation rate of shHSF relative to shScr.

Change in proliferation index = shHSF(MFI_{d0}/MFI_{dx})- shScr(MFI_{d0}/MFI_{dx})

Preparation of ChIP-seq libraries

ChIP-seq libraries were prepared using the Illumina TruSeq DNA library prep kit (Illumina) with minor modifications. Briefly 5-10 ng of purified ChIP DNA was end-repaired using the kit's enzymes and protocol and purified with minielute columns (Qiagen). A-tailing was performed to add A bases to the 3'

ends of the DNA fragments using the kit's enzymes and protocol and purified with minielute columns (Qiagen). Adapters were ligated using the Quick Ligation kit (New England Biolabs). Stop ligation solution was added and DNA was cleaned up using Ampure XP beads (Agencourt) at a 1:1 ratio of beads:DNA solution. Adaptor-modified ChIP DNA was size-selected using SPRIselect beads (Beckman Coulter) by adding a 0.5X volume of beads to allow fragments greater than 400 bp to bind the beads. The supernatant was collected and 1X volume of beads was added. The supernatant was aspirated, and the beads were washed 2X with 80% ethanol, dried, and eluted with resuspension buffer. Adaptor-modified ChIP DNA was amplified using 12 PCR cycles. Libraries were quantified using the Qubit (Life Technologies) and size was verified using the Bioanalyzer (Agilent). The library was cluster amplified and sequenced on the Illumina HiSeq2500 (Illumina). Reads were processed using CASAVA 1.8 and mapped to hg19.

ChIP-seq peak detection

Peak calling and all downstream analysis including annotation and FIRE was performed with the ChIPseeqer detection algorithm (Giannopoulou and Elemento, 2011). Each ChIP-seq dataset was normalized to its corresponding input lane. Peaks were annotated using the RefSeq database (hg19).

Preparation of mRNA-seq libraries

DLBCL cells were transduced with HSF1 shRNAs and shScr and selected for 48 h with puromycin. RNA was purified using Trizol extraction (Invitrogen) and treated with Dnase (Qiagen). RNA quality was verified using the Agilent 2100 Bioanalyzer (Agilent Technologies) and the RNA integrity number values were

greater than 8 for all samples. Sequencing libraries were generated with polyA+ RNA using the TruSeq RNA sample prep kit (Illumina). Libraries were cluster amplified and sequenced for 50 cycles using the Illumina HiSeq2000. Reads were aligned to hg19 using TopHat (Trapnell et al., 2009), and gene expression values were calculated by counting how many reads map uniquely to the union of all gene exons using HTseq-count. Samples were normalized for sequencing depth, and differentially expressed genes were identified with the edgeR package(Robinson et al., 2010). Genes with counts per million > -3 and an FDR value < 0.05 were considered differentially expressed.

Statistical analysis

Student's *t*-test was used for statistical analysis unless otherwise stated. All statistical analyses were done using GraphPad Prism 5.

CHAPTER FOUR

BCL6 IS AN EVOLUTIONARILY CONSERVED STRESS RESPONSE GENE

1. Introduction

BCL6 was initially identified because it was frequently translocated to heterologous promoters leading to its constitutive expression and linking it to the pathogenesis of diffuse large B cell lymphomas (DLBCL) (Ci et al., 2008). DLBCLs arise from GC B cells, which form transient structures in secondary lymphoid organs after exposure to T-cell dependent antigens (Klein and Dalla-Favera, 2008). The transition from resting to GC B cells requires a major phenotypic shift. GC B cells attain the unique ability to tolerate rapid cell proliferation while simultaneously undergoing DNA damage events in their *Ig* genes with the goal of producing high-affinity antigen-specific antibodies (Klein and Dalla-Favera, 2008). BCL6 is the master regulator of the GC transcriptional program that drives GC development and is essential for GC B cells to endure replicative and genotoxic stress (Basso and Dalla-Favera, 2010). BCL6 maintains the survival of these cells by directly repressing genes involved in DNA damage sensing and response and cell cycle checkpoint activation (Hatzi and Melnick, 2014). Therefore it is not surprising that DLBCL cells inherit the biological dependency on BCL6, which reflects the biology of GC B cells (Hatzi and Melnick, 2014). Consequently, BCL6 inhibition or knockdown rapidly kills DLBCL cells, underscoring the significance of BCL6 as a therapeutic target in the disease(Cerchietti et al., 2010b; Cerchietti et al., 2008; Cerchietti et al., 2009b; Parekh et al., 2007; Ranuncolo et al., 2008a; Ranuncolo et al., 2008b).

Although BCL6 is often thought of in the highly specialized context of the humoral immune response, its role in GC B cells is consistent with functionality linked to surviving severe stress. Along these lines, BCL6 is highly dependent on a fraction of HSP90 that is activated upon stress and enriched in GC B cells and DLBCL (teHSP90) (Cerchietti et al., 2009a). TeHSP90 is required for BCL6 stability and its transcriptional repressor function (Cerchietti et al., 2009a). In fact, it was demonstrated in an earlier chapter that HSF1, the dominant regulator of the stress response, is required for stress-mediated induction of BCL6 in B cells. Collectively these mechanistic associations are suggestive of an intimate role of BCL6 in the stress response. Along these lines, BCL6 has been shown to be induced in various cell types when they are submitted to stressful conditions such as the withdrawal of growth factors, exposure to drugs that target key survival factors, or oxidative stress (Duy et al., 2011; LaPensee et al., 2014; Meyer et al., 2009; Toney et al., 2000). Moreover BCL6 is often expressed in cell types that tolerate a great deal of stress under basal conditions such as cardiac and skeletal myocytes, dermal epithelial cells, and melanocytes (Kageshita et al., 2006; Miki et al., 1994; Yoshida et al., 1999; Yoshida et al., 1996).

These considerations prompted us to wonder about the forces of natural selection that resulted in the phylogenetic development of BCL6. Because of the connection between HSF1 and HSP90-mediated regulation of BCL6, its prominent role in the high-stress environment of the GC, and its function in rescuing several cell types from stress-induced growth arrest and death, it was postulated that BCL6 may have evolved as a stress response factor that might reprogram cells to operate under stress conditions. Such functionality might be

helpful in tissues that must maintain their integrity in spite of sustained stress and for complex organisms with relatively longer life spans and more limited reproductive capacity.

2. Results

2.1 The HSF1-BCL6 stress response axis is an evolutionarily conserved feature of vertebrate organisms

HSF1 is the master regulator of stress response and its binding sites at the BCL6 promoter are evolutionarily conserved. This notion led us to consider whether HSF1-mediated induction of BCL6 might be a general feature of stress response beyond GC B cells. We therefore subjected a variety of tissues to proteotoxic stress (in the form of heat shock) and measured relative *BCL6* transcript abundance by qRT-PCR. We observed significant upregulation of *BCL6* mRNA in mouse brain, kidney, and liver ($p<0.05$, **Figure 4.1A**). To determine if *BCL6* induction was dependent on HSF1, we next examined whether heat shock induced *BCL6* in brain, kidney and liver of *Hsf1*$^{+/-}$. In all cases there was profound impairment of *BCL6* upregulation after heat shock in *Hsf1*$^{+/-}$ vs. *Hsf1*$^{+/+}$ mice (**Figure 4.1A**). As a complementary approach, we used siRNA transfection to knock down HSF1 in human fibroblasts and then used heat shock to induce stress response and measured *BCL6* nascent transcripts compared to a control non-targeted siRNA. HSF1 knockdown significantly impaired heat shock-induced *BCL6* nascent transcripts ($p<0.01$, **Figure 4.1B**).

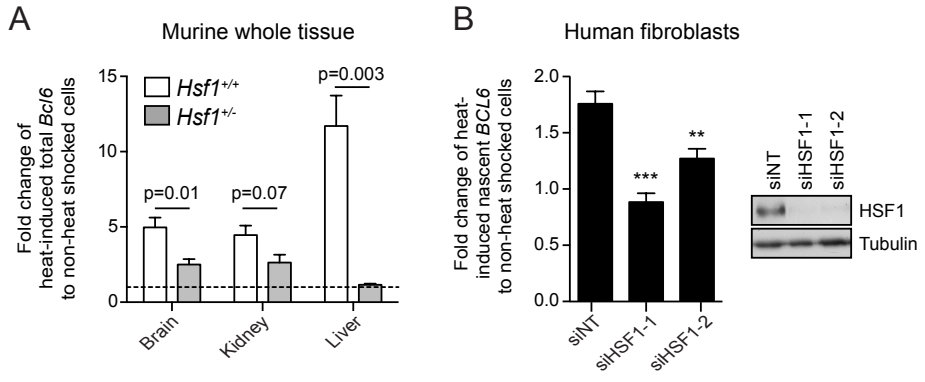

Figure 4.1 HSF1 mediates *BCL6* induction in response to stress in mammalian cells. (A) qRT-PCR of total *Bcl6* mRNA in heat shocked murine brain, kidney, and liver tissues of *Hsf1*$^{+/+}$ and *Hsf1*$^{+/-}$ mice normalized to GAPDH. (B) qRT-PCR of nascent *BCL6* mRNA in heat shocked human fibroblasts transfected with nontargeting (siNT) or HSF1 siRNA (siHSF1) for 48 h. Data was normalized to human *HPRT1* (left). Representative immunoblot of HSF1 knockdown in human fibroblasts 48 h after transfection with siNT and siHSF1 (right). Values in (A) represent a mean of triplicates ± SEM (n = 2 mice per group). Values in (B) are the mean of triplicates ± SEM. A t-test was used to assess significance, ** $p<0.01$, *** $p<0.001$.

Given the conservation of HSEs in the *BCL6* promoter and its general role as an HSF1 target gene in various distinct tissue types, we postulated that BCL6 evolved as a component of the HSF1 stress response pathway. HSF1 is conserved throughout eukaryotic evolution while BCL6 orthologs first appeared in chordates. BCL6 is a member of the BTB-ZF family, which are found throughout the metazoans. However clear BCL6 orthologs are restricted to the vertebrates. Notably jawless fish (agnathosomes) such as lampreys, the first vertebrates to evolve approximately 500 million years ago, contain a gene that encodes a protein with more than 40% sequence identity to human BCL6 (**Figure 4.2A**). Importantly lamprey BCL6 identifies with human BCL6 as the

top hit in a reciprocal blast search (G. Privé, unpublished results). BCL6 is also present in all jawed vertebrates (gnathosomes), which branched off from the agnathosomes in the Ordivician period (**Figure 4.2A**). Hence HSF1 preceded BCL6, which seems to have evolved through natural selection accompanying the appearance of vertebrate animals. As with other BTB-ZF proteins, BCL6 can be divided into three discrete regions: an N-terminal BTB domain that forms an obligate homodimer and mediates transcriptional repression; a middle region that is dynamically disordered but contains a 40 amino-acid autonomous repression domain (RD2); and a C-terminal cluster of C_2H_2-type zinc finger domains that binds to DNA. Examination of BCL6 sequence conservation by Shannon entropy analysis reveals high conservation of the BTB and zinc-finger domains whereas the RD2 domain is less conserved (**Figure 4.2B**) (provided by G. Privé).

To determine if BCL6 functions as a stress inducible gene in animal species representing the spectrum of vertebrate evolution, we induced heat shock in cells from mammals (humans, mice, dogs), birds (chicken), reptiles (iguana), ray-finned fish (zebrafish), and agnathosomes (lamprey). *BCL6* transcripts were detected by qRT-PCR and were significantly upregulated after proteotoxic stress in every species ($p<0.05$, **Figure 4.3A**). Given the amino acid conservation of the N-terminus, we used an N-terminal polyclonal antibody to perform western blots with lysate from cells exposed to stress from each species to detect BCL6 protein. In all cases we observed an increase in BCL6 protein abundance (**Figure 4.3B**). Collectively these data are consistent with the notion that BCL6 is a central component of vertebrate-specific stress response downstream of HSF1.

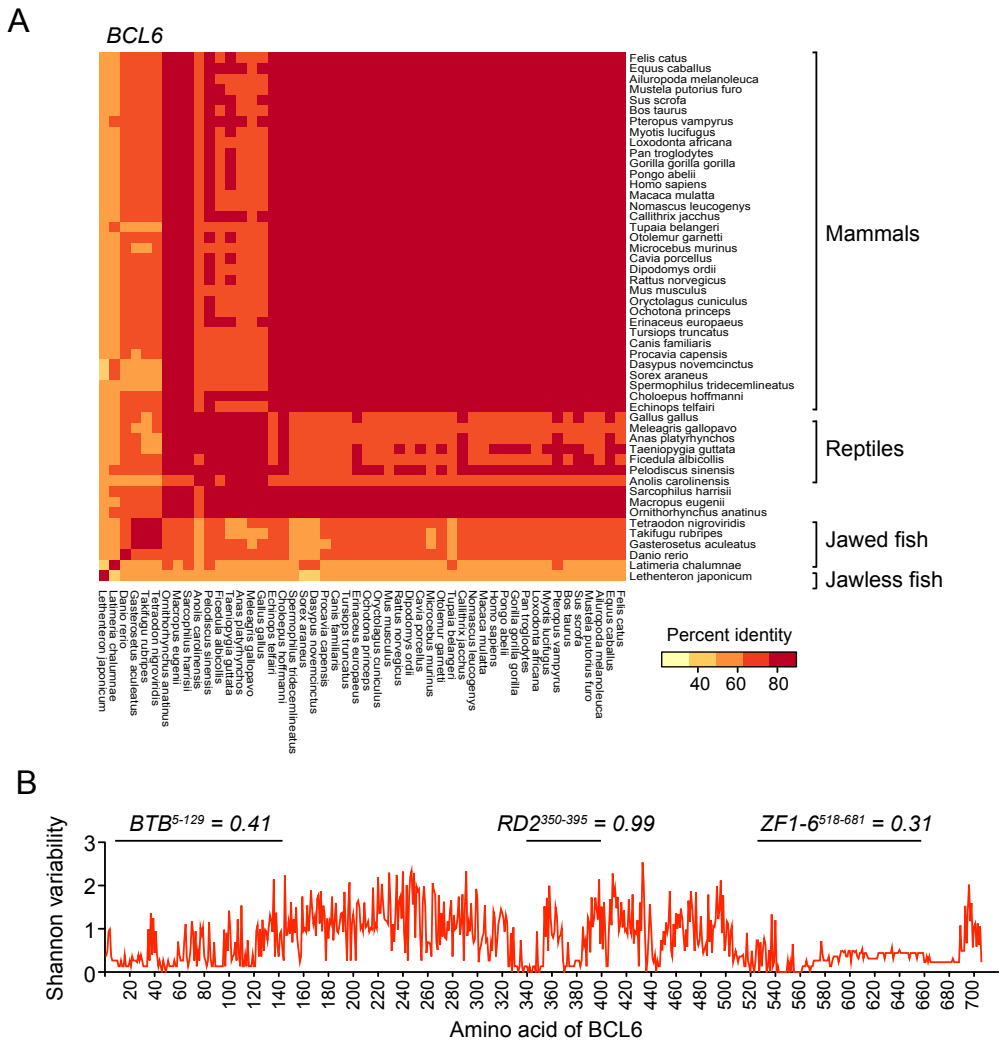

Figure 4.2 BCL6 protein is evolutionarily conserved in vertebrate organisms. (A) Heatmap representating percent identity of predicted BCL6 protein orthologs as defined by the orthologous matrix (OMA) group 26555 and the predicted sequence from Lethenteron japonicum. (B) Shannon protein variability per amino acid in multiple sequence alignments of BCL6. Average protein variability of the BTB, minimal RD2, and zinc finger (ZF) domains are reported above the plot. Provided by G. Privé.

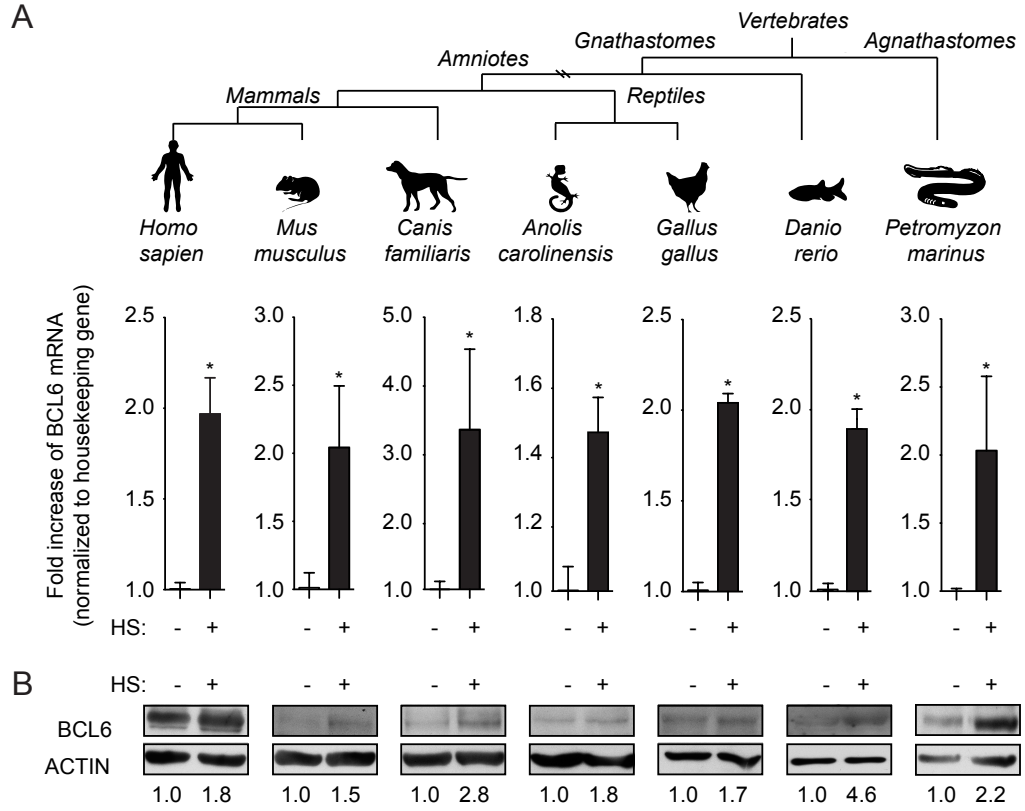

Figure 4.3 BCL6 induction after stress is an evolutionarily conserved feature of vertebrate organisms. (A) qRT-PCR of *BCL6* in heat shocked human adult fibroblasts, murine BCL1 B cells, dog Cf2Th thymocytes, iguana IgH-2 epithelial cells, chicken DT-40 B cells, zebra fish embryos, and sea lamprey typhlosole tissue and normalized to *HPRT1*, *ACTB* or *GAPDH*. (B) Representative immunoblots of BCL6 from whole cell extracts isolated from cells heat shocked as above and returned to resting temperature for 6 hrs. The average densitometry of immunoblots is below. Samples are separated by the phylogenetic relationship (Miller et al., 2007). Values in (A and B) represent the mean of triplicate experiments ± SEM and t-test was used to assess significance, * $p<0.05$.

2.2 BCL6 is required for stress tolerance

To further understand the significance of BCL6 in vertebrate stress response, we next performed functional assays to assess for a putative contribution to survival under stress conditions. To determine whether induction of BCL6 was required for cells to survive exposure to proteotoxic stress, we isolated purified naïve B cells from wild type and *Bcl6*$^{-/-}$ mice, exposed them to heat shock, and measured viability relative to control cells by trypan blue exclusion. Both *Bcl6*$^{+/+}$ and *Bcl6*$^{-/-}$ exhibited approximately 25% loss of viability (**Figure 4.4A**). Hence loss of BCL6 did not affect survival after acute stress exposure.

During the GC reaction, B cells are repeatedly exposed to stress as they undergo rapid sequential replication cycles and somatic hypermutation. Moreover, unlike HSF1, which is present under basal conditions and is rapidly activated by stress conditions, BCL6 must first be transcribed and translated in order to carry out any biological function. Hence we wondered whether BCL6 stress function might engage at a later stage, for example in enabling cells to adapt to recurrent or ongoing stress. Therefore we exposed primary murine resting B cells to sequential proteotoxic stress and then measured cell viability after the second stress exposure. In this case, we observed a significant, 5-fold reduction in the percentage of dead cells after repeated heat shocks in *Bcl6*$^{+/+}$ B cells ($p<0.001$) relative to *Bcl6*$^{-/-}$ B cells (**Figure 4.4B**), suggesting that BCL6 is indeed required for stress tolerance. To determine whether this function is evolutionarily conserved, we performed similar experiments with zebrafish embryos depleted of BCL6. The zebrafish embryos injected with BCL6 or control morpholinos were exposed to either single or repeated proteotoxic stress and then examined for viability. In this case, depletion of

BCL6 was associated with a trend towards increased embryo death after the first heat shock (p=0.06, **Figure 4.4C**). However the difference was much more dramatic and significant after the second heat shock, where we again observed a five fold increase in cell death in BCL6 depleted vs. control embryos (p=0.01, **Figure 4.4D**). Hence BCL6 mediates adaptation of

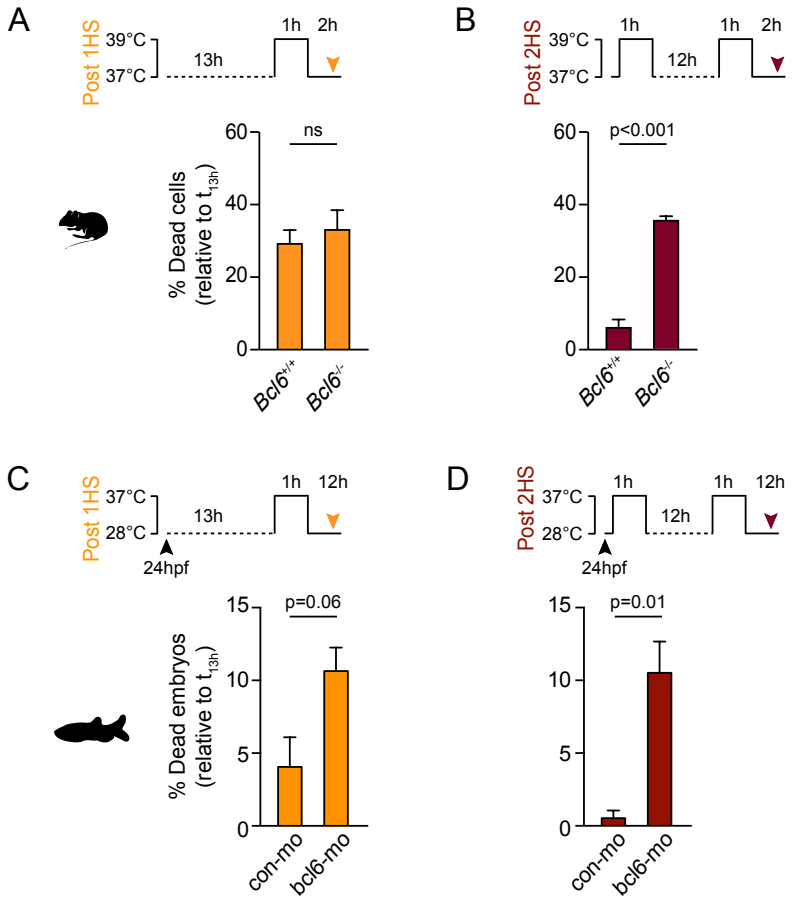

Figure 4.4 BCL6 is required for stress tolerance. (A-B) Murine B220^{+} splenocytes from *Bcl6*$^{+/+}$ and *Bcl6*$^{-/-}$ and (C-D) zebrafish embryos injected with control or *bcl6* mo were heat shocked either (A, C) once (Post 1HS, orange) or (B, D) serially heat shocked (Post 2HS, red) according to the schematics on top of each graph. Viability of B220^{+} splenocytes was measured by trypan blue exclusion. Viability of zebrafish embryos was measured by the absence of opaque tissues. Values in (A and B) represent the mean of triplicate experiments ± SEM and t-test was used to assess significance.

vertebrate cells to repeated stress conditions.

2.3 BCL6 mediates vertebrate stress tolerance through a lateral groove on its BTB domain

Human BCL6 is a potent transcriptional repressor, and to determine the biochemical mechanism through which BCL6 mediates vertebrate adaptation to stress, we turned to the conserved BTB domain as a prime candidate for conferring similar functions in other species as the RD2 domain is less conserved (**Figure 4.5A**). The repression functions of the BTB domain are mediated through the binding of a 17-residue BCL6 binding domain (BBD) motif in the NCOR, SMRT, and BCOR corepressors to the lateral groove surface of the BTB dimer and are highly conserved (Ahmad et al., 2003; Ghetu et al., 2008). Notably the residues lining the lateral groove are not conserved in other BTB-ZF proteins (Stogios et al., 2010). Point mutations of BCL6 BTB lateral groove residues that disrupt corerepressor binding but do not affect protein folding ablate repressor activity of the BCL6 BTB domain (Ahmad et al., 2003). It is important to note that these BTB point mutations do not diminish the activity of the RD2 domain in the linker region and have no effect on BCL6 binding to its target genes (Huang et al., 2013). When engineered into the endogenous *BCL6* locus in mice, these BTB point mutations result in specific loss of the ability of BCL6 to maintain the survival and proliferation of GC B cells but do not affect BCL6 functions in T cells or macrophages (Huang et al., 2013).

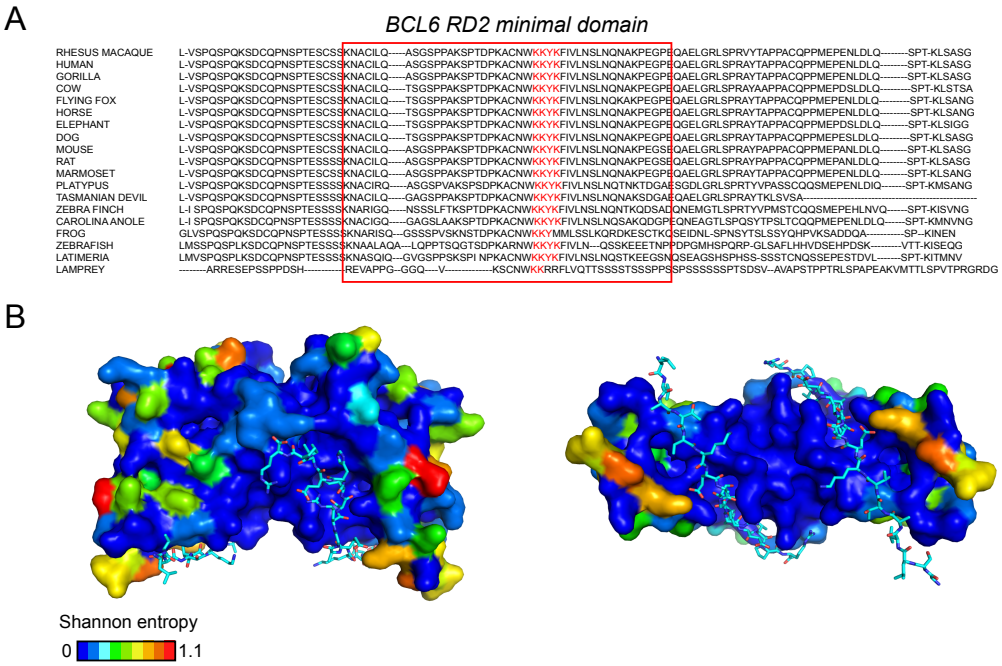

Figure 4.5 The lateral groove of the BCL6 BTB domain is highly conserved in vertebrates. (A) Protein sequence alignment of the BCL6 RD2 minimal domain with KKYK cluster highlighted in red. (B) Shannon entropy values were calculated by MUSCLE multiple sequence alignment (v3.8) and mapped onto the structure of the BCL6 BTB domain, protein data bank entry 1R2B. Provided by G. Privé.

Collectively, these data led us to consider whether the BCL6 BTB lateral groove is responsible for the conserved stress adaptation function of BCL6. To address this question, we first mapped the sequence conservation of the BCL6 BTB domain from a wide selection of vertebrates on to the surface of the structure (**Figure 4.5B).** Strikingly, we observed that all residues from the lateral groove that contact the NCOR, SMRT, and BCOR corepressors were conserved, even in the lamprey sequence. In contrast other regions of the surface were highly variable (**Figure 4.5B**). Likewise the NCOR, SMRT, and

BCOR BBDs are also highly conserved in these species (**Figure 4.6A-B**). To determine whether the lateral groove of the BTB domain mediates the stress adaptation function of BCL6, we performed proteotoxic stress response experiments using B cells from wild-type mice and mice engineered to contain point mutations that disrupt corepressor binding to the BTB domain lateral groove. As an additional control, we performed the same experiments using B cells from mice where the *Bcl6* locus was engineered to express a form of BCL6 with point mutations that disrupt the function of the less conserved RD2 domain (**Figure 4.5A**) but leave the BTB domain intact. After the first heat shock, there was no difference in cell death in wild-type, *Bcl6*^{BTBMUT} or *Bcl6*^{RD2MUT} (**Figure 4.7A**). After the second heat shock there was again a five-fold reduction in cell death in the wild-type and *Bcl6*^{RD2MUT} mice (**Figure 4.7A**). However in marked contrast, cell death was equivalent at both time points in the *Bcl6*^{BTBMUT} mice. Hence the highly conserved BCL6 BTB domain lateral groove mediates the stress adaptation function of BCL6.

In order to extend this paradigm to other vertebrate species, we took advantage of a second orthogonal approach that we developed to disrupt corepressor binding to the BCL6 BTB lateral groove. This involves the use of a peptidomimetic compound that was shown to penetrate cells, localize to the nucleus, bind specifically to the BCL6 BTB lateral groove but not to other BTB proteins, and blocks BCL6 from binding and recruiting SMRT and NCOR to its target genes (Cerchietti et al., 2009b; Polo et al., 2004). This retro-inverso BCL6 peptide inhibitor (RI-BPI) was also shown to phenocopy the *Bcl6*^{BTBMUT} mice (Cerchietti et al., 2009b; Polo et al., 2004). Because the BCL6 lateral

groove binding site is conserved throughout vertebrate evolution (**Figure 4.5B**), RI-BPI would be expected to be suitable for experiments in other species.

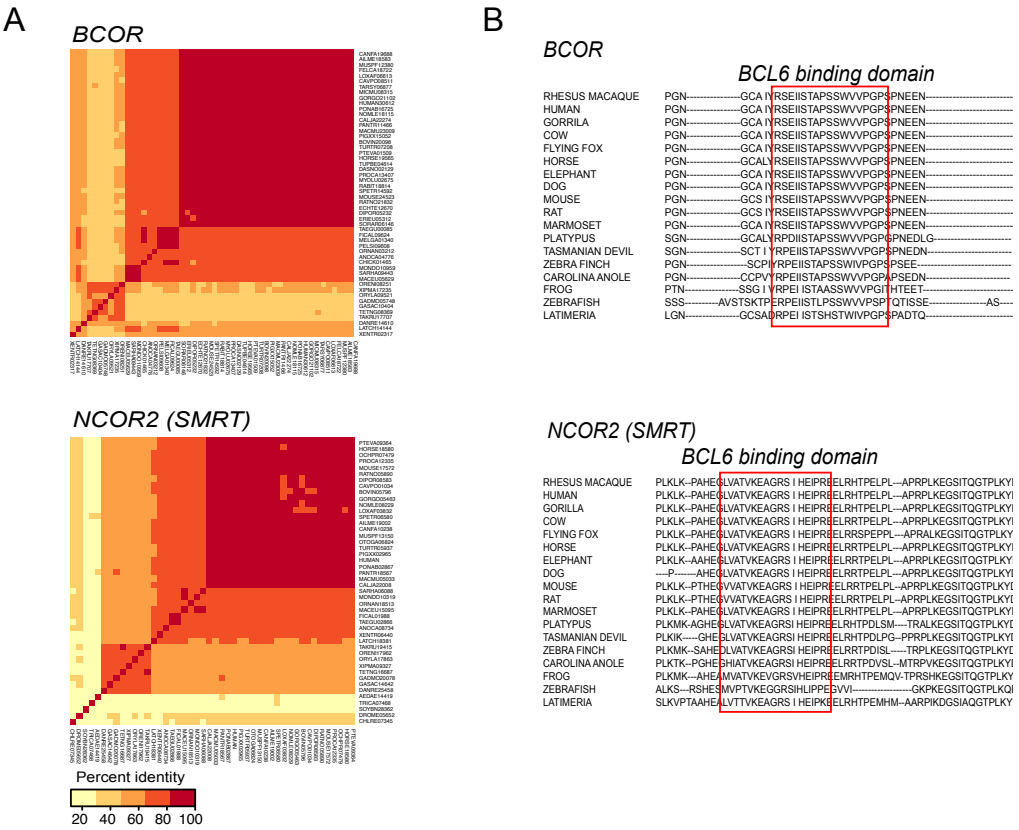

Figure 4.6 BCOR and SMRT are conserved in vertebrates. (A) Heatmap representing percent identify of predicted full-length BCOR (top) and NCOR2 (SMRT) (bottom) protein orthologs. (B) Protein sequence alignment of the BCL6 binding domain of BCOR (top) and NCOR2 (SMRT) (bottom).

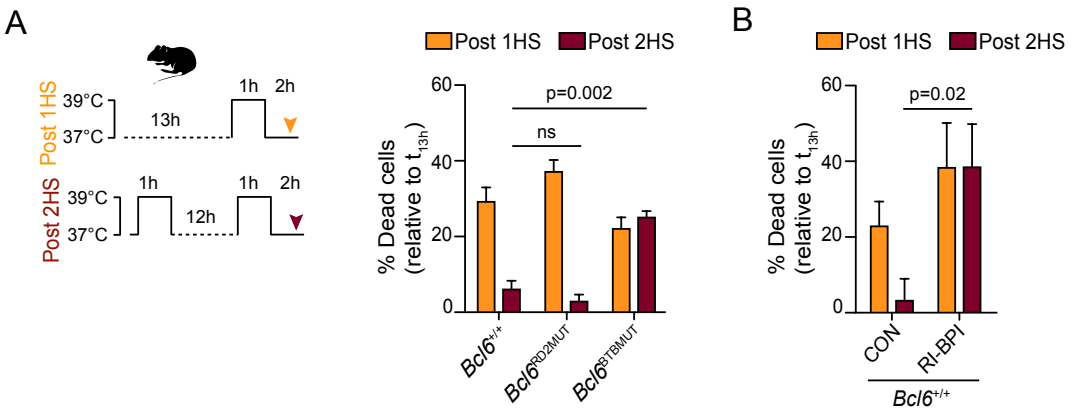

Figure 4.7 BCL6 mediates stress tolerance through a lateral groove on its BTB domain. (A) Murine B220^{+} splenocytes were isolated from *Bcl6*$^{+/+}$, *Bcl6*^{RD2MUT}, and *Bcl6*^{BTBMUT} mice and heat shocked either once (Post 1HS, orange) or serially heat shocked (Post 2HS, red) according to the schematic on the left. (B) *Bcl6*$^{+/+}$ cells were treated with vehicle (CON) or 1 μM RI-BPI. Cells were heat shocked as described in (A). Cell viability was measured by trypan blue or DAPI exclusion. Values in (A-B) are a mean of triplicates ± SEM. A t-test was used to assess significance.

To determine whether RI-BPI could abrogate stress adaptation similar to the BTB mutations, we first performed single and sequential proteotoxicity experiments in murine B cells. Exactly like in *Bcl6*^{BTBMUT} mice, exposure to RI-BPI had no effect on cell death after a single stress exposure but completely abrogated the ability of B cells to become stress tolerate (p=0.02, **Figure 4.7B**). The same experiments were performed in two additional branches of vertebrates (avian and reptile) and invertebrate cells (*Drosophila melanogaster* S2 cells) as insects do not have a BCL6 paralog or the vertebrate corepressor BBD motifs. Again, exposure to RI-BPI had no effect on cell viability after a single stress exposure but abrogated stress adaptation response in both avian

(p<0.001) and reptile cells (p<0.01, **Figure 4.8A)**. In *Drosophila* $S2^+$ cells, RI-BPI did increase cell death after a single stress exposure (**Figure 4.8B**). However S2 cells were able to acquire stress tolerance after serial proteotoxic stress in the presence of RI-BPI (**Figure 4.8B**). Taken all together, these data suggest that the BCL6 BTB domain lateral groove is the effector mechanism for BCL6-mediated stress adaption throughout vertebrate evolution. Because the lateral groove is the most highly conserved protein interaction motif on BCL6, it seems likely that a major reason for the development of BCL6 during evolution was to enable vertebrate cells to better withstand continuous or repeated stress conditions.

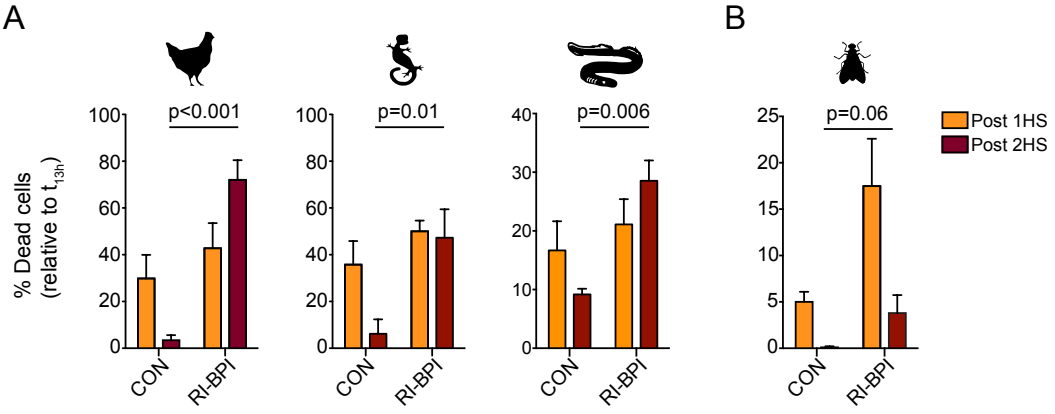

Figure 4.8 RI-BPI inhibits the acquisition of stress tolerance in vertebrates. (A) Chicken DT40 B cells, iguana IgH-2 epithelial cells, and sea lamprey typhlosole cells were treated with vehicle (CON) or 1 μM RI-BPI and heat shocked either once (Post 1HS, orange) or serially heat shocked (Post 2HS, red) according to the schematic above. (B) Drosophila $S2^+$ cells were treated with vehicle (CON) or 1 μM RI-BPI. Cells were heat shocked as described in (A). Cell viability was measured by trypan blue or DAPI exclusion. Values in (A-B) are a mean of triplicates ± SEM. A t-test was used to assess significance.

2.4 A stress and cell growth transcriptional program is controlled through the BTB domain

We speculated that BCL6-mediated repression of target genes that are dependent on its BTB domain function must be essential for its role in stress adaptation. To identify this gene set in mammalian cells, we performed mRNA-seq in *Bcl6*$^{+/+}$ and *Bcl6*^{BTBMUT} B220^{+} cells before and 12 h after proteotoxic shock and compared and contrasted the resulting gene expression profiles. Multidimensional scaling analysis showed that replicate gene expression profiles were highly reproducible. The first principle component clearly distinguished specimens based on exposure to stress, and the second distinctly divided BTB mutant from WT expression profiles (**Figure 4.9A**). Likewise unsupervised analysis of post-stress gene expression profiles showed clustering of BCL6 wild type vs. BTB mutant into distinct nodes. (**Figure 4.9B**).

As would be expected, a majority of genes downregulated (FDR<0.05) after heat shock were repressed in both wild type and BTB mutant cells (~70%). However, we also identified a set of 510 genes that were downregulated in *Bcl6*$^{+/+}$ but not in *Bcl6*^{BTBMUT} cells (**Figure 4.9C**). This gene set was further investigated for possible links to the actions of BCL6 in stress tolerance. These genes were significantly enriched in functional categories involved in stress response and cell cycle (**Figure 4.9D**), including acute inflammatory response (GO: 0050000), activation of immune response (GO: 0002526), and cell proliferation (GO: 0008283, GO: 0008284). Notably, this set of genes that were not repressed after heat shock in *Bcl6*^{BTBMUT} cells were significantly more upregulated after BCL6 knockdown in B cell lines than genes that did not

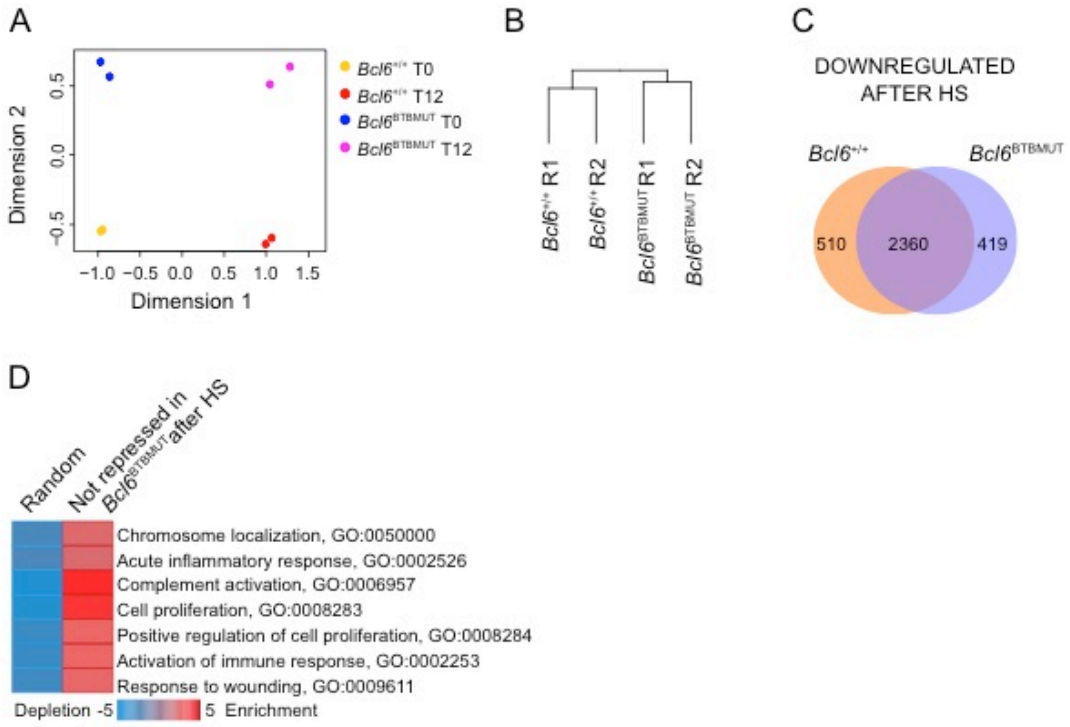

Figure 4.9 Gene expression profiling of *Bcl6*^{BTBMUT} cells after heat shock. (A) Multi-dimensional scaling plot of the leading biological coefficient of variation between samples using 500 genes with the most heterogeneous expression in *Bcl6*$^{+/+}$ and *Bcl6*^{BTBMUT} B220^{+} splenocytes before (T0) and 12 h after a single heat shock (1 h at 43 °C, T12). (B) Clustering of the union of differentially expressed genes in *Bcl6*$^{+/+}$ and *Bcl6*^{BTBMUT} B220^{+} cells after heat shock as described in (A) using complete linkage clustering with Euclidean distance measure. The exact test (Robinson et al., 2010) was used to identify differentially expressed genes at FDR < 0.05. (C) Venn diagram of genes significantly (FDR < 0.05) downregulated after heat shock that are common and unique to *Bcl6*$^{+/+}$ and *Bcl6*^{BTBMUT} B220^{+} cells. (D) Heatmap of overrepresented gene ontology categories among genes that were not repressed in *Bcl6*^{BTBMUT} B220^{+} splenocytes after heat shock relative to a randomly generated set of genes. Enrichment and depletion was measured by hypergeometric p values.

change after heat shock in *Bcl6*^{BTBMUT} cells (Wilcoxon test, p=0.003, **Figure 4.10A**). GSEA analysis also showed strong enrichment of this gene set (FDR=0.02) among genes derepressed after BCL6 siRNA (**Figure 4.10B**)

(Hatzi et al., 2013). The genes in the leading edge of the GSEA represent the genes that are dependent on the BTB domain for their repression after heat shock and are highly derepressed after BCL6 siRNA. A subset of these were strongly derepressed after heat shock in *Bcl6*^{BTBMUT} cells relative to *Bcl6*$^{+/+}$ cells including *Ifitm2, Npas4, Nr4a2, Prickle1, Rab34, Rasbp1* and *Tox* (**Figure 4.11A**). To validate these genes in an independent experiment and an additional tissue type, we exposed B cells and brain tissue from wild-type and *Bcl6*^{BTBMUT} mice to heat shock and performed qRT-PCR. We observed consistent derepression of several of these genes after heat shock including *Tox, Nr4a2* and *Npas4* (**Figure 4.11B**), all three of which are transcription factors.

2.5 Repression of TOX is required for the BCL6-mediated stress adaptive phenotype

It is likely that repression of many target genes is necessary for the biological effect of BCL6. Yet as proof-of-principle to determine if one of these candidate genes was important for the actions of BCL6, we selected TOX, a transcription factor that has been mostly studied in T cells. To determine if repression of *Tox* contributes to the stress tolerance effect mediated by the BCL6 BTB domain, we performed serial stress response experiments in purified B cells from the spleens of *Tox*$^{-/-}$ mice. If there were rescue of the BCL6 loss-of-function phenotype, we would expect *Tox* deletion to compensate. We used RI-BPI to prevent BCL6 BTB domain-mediated repression in *Tox*$^{-/-}$ or wild type B cells. *Tox*$^{-/-}$ B cells were indeed more stress tolerant relative to *Tox*$^{+/+}$ B cells (**Figure 4.12A**). Similarly, *Tox*-depletion by two independent shRNAs in the murine B cell line, BCL1, enabled the cells to retain their ability to tolerate

serial heat shock despite the presence of RI-BPI, whereas a non-targeting control could did not rescue BCL6 function (**Figure 4.12B**). In summary these data indicate that BCL6 mediates its stress tolerance function through BTB-dependent transcriptional repression of a set of target genes, including *Tox*.

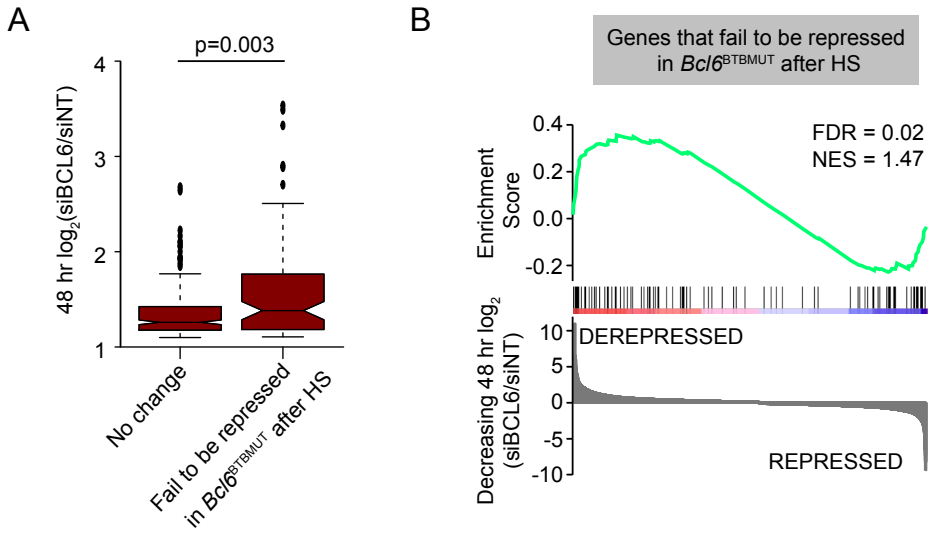

Figure 4.10 Genes that fail to be repressed after stress in *Bcl6*^{BTBMUT} cells are BCL6-regulated genes. (A) Comparison of fold gene induction in DLBCL OCI-LY1 cells after siBCL6 (log_2 siBCL6/siNT, 48hr) (Hatzi et al., 2013) of genes that did not change after heat shock or failed to be repressed in *Bcl6*^{BTBMUT} B220$^+$ splenocytes relative to *Bcl6*$^{+/+}$ splenocytes. Values represent the mean ± SEM. Mann-Whitney test was used to evaluate significance. (B) GSEA of genes that fail to be repressed in *Bcl6*^{BTBMUT} B220$^+$ splenocytes after heat shock relative to *Bcl6*$^{+/+}$ splenocytes with genes ranked based on decreasing log_2 RPKM at 48hr post-BCL6 knockdown as described in (A). FDR was used to measure significance of enrichment (5000 permutations, weighted statistic).

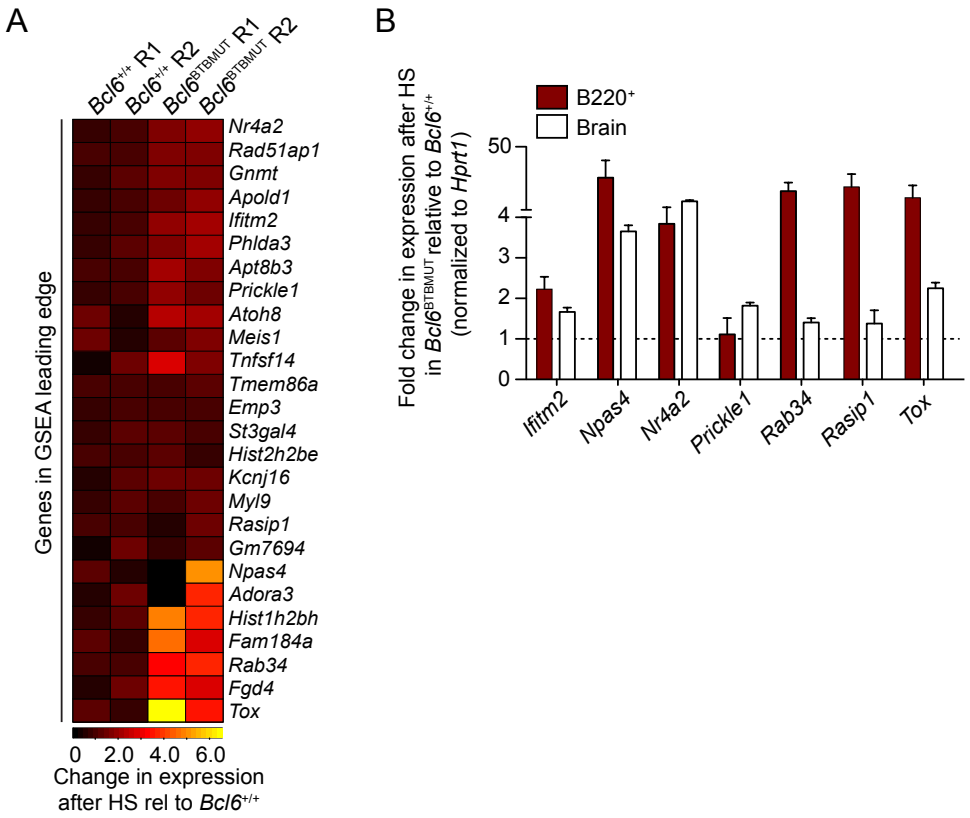

Figure 4.11 A subset of BCL6 regulated genes are strongly derepressed after heat shock in *Bcl6*^{BTBMUT} cells. (A) Heatmap representing the expression changes after heat shock of the GSEA leading edge genes described in Figure 4.10B in *Bcl6*^{BTBMUT} relative to *Bcl6*$^{+/+}$ B220^{+} splenocytes. (B) Validation of gene expression changes after heat shock in B220^{+} splenocytes and brain tissue of *Bcl6*^{BTBMUT} relative to *Bcl6*$^{+/+}$.

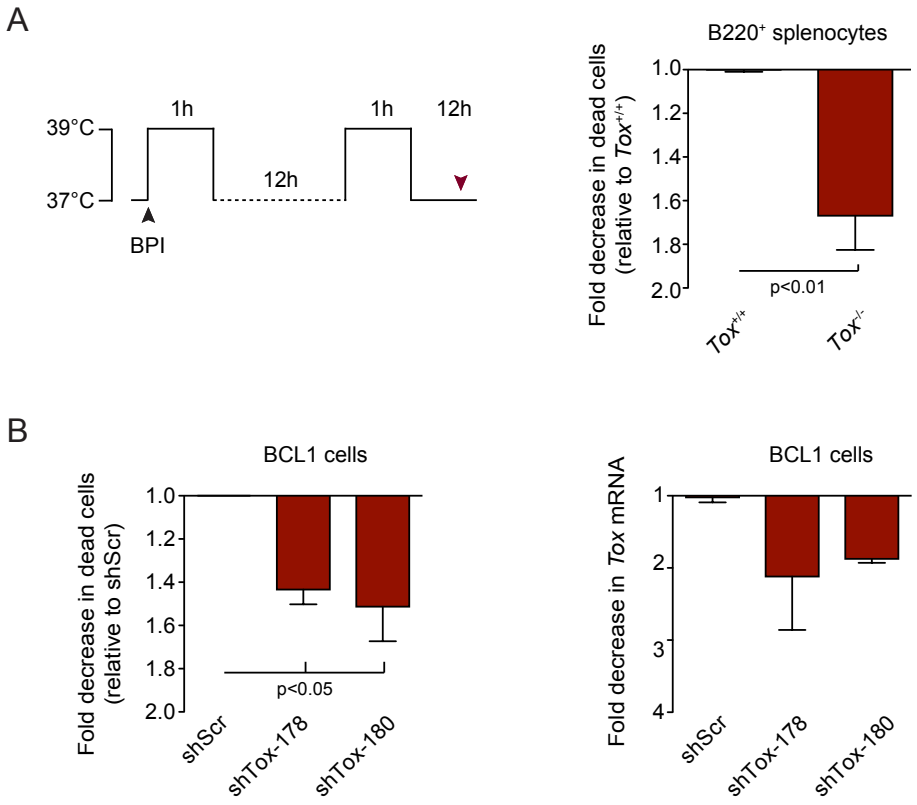

Figure 4.12 TOX repression is required for BCL6 to mediate thermotolerance through its BTB domain. (A) Fold decrease in dead B220^{+} splenocytes from *Tox*$^{+/+}$ and *Tox*$^{-/-}$ (left) or (B) Tox-deficient BCL1 cells (left) treated with 1 μM BPI and serially heat shocked. (B) Tox knockdown efficiency is shown on the right. Viability was measured by DAPI exclusion. Values represent mean of triplicates ± SEM. A t-test was used to evaluate significance.

2.6 Tumor cells upregulate BCL6 after exposure to stress

The general function of BCL6 in protecting normal cells from stress led us to wonder whether tumor cells might also rely on this evolutionarily conserved mechanism to facilitate their survival when exposed to potentially lethal stress, such as cytotoxic chemotherapy. To address this question, we exposed a panel of tumor cell lines of different histological origin to proteotoxic or

cytotoxic stress through exposure to heat shock or low dose (100 nM) doxorubicin, respectively. We observed an increase in *BCL6* mRNA both after heat shock and low dose doxorubicin (**Figure 4.13A**). There was also a strong positive correlation (Spearman *r* 0.8321, $p<0.001$) between *BCL6* and *HSPA1B* induction after low dose doxorubicin (**Figure 4.13B**), consistent with the notion that *BCL6* was induced as part of the stress response transcriptional program. Along these lines and to determine whether HSF1 mediates doxorubicin-induced BCL6 expression, we used two independent siRNAs to deplete HSF1 expression in the breast and lung cancer cell lines, MDA-MB-468 and H460, respectively. Measurement of *BCL6* nascent transcript induction revealed significant impairment after HSF1 knockdown (**Figure 4.13C**). Induction of BCL6 protein was also blunted upon HSF1 knockdown in both cell lines (**Figure 4.13D**).

2.7 BCL6 mediates stress tolerance in tumor cells

To test whether BCL6 enables tumors to tolerate exposure to cytotoxic drugs, we investigated whether increasing concentrations of RI-BPI and doxorubicin resulted in enhanced cell killing in solid tumor and DLBCL cells. In almost every cell line tested, the concentration of RI-BPI required to yield 50% growth inhibition was reduced with concurrent treatment with doxorubicin (**Figure 4.14A**). From the clinical perspective, BCL6 inhibitors are likely to be tested first in the context of DLBCL, a tumor type derived from GC B cells that are clearly dependent on BCL6 BTB stress signaling functions (Cerchietti et al., 2008; Cerchietti et al., 2009b; Parekh et al., 2007; Ranuncolo et al., 2008a; Ranuncolo et al., 2008b). Therefore we more extensively combined RI-BPI with classes of drugs commonly used in DLBCL cytotoxic therapy including

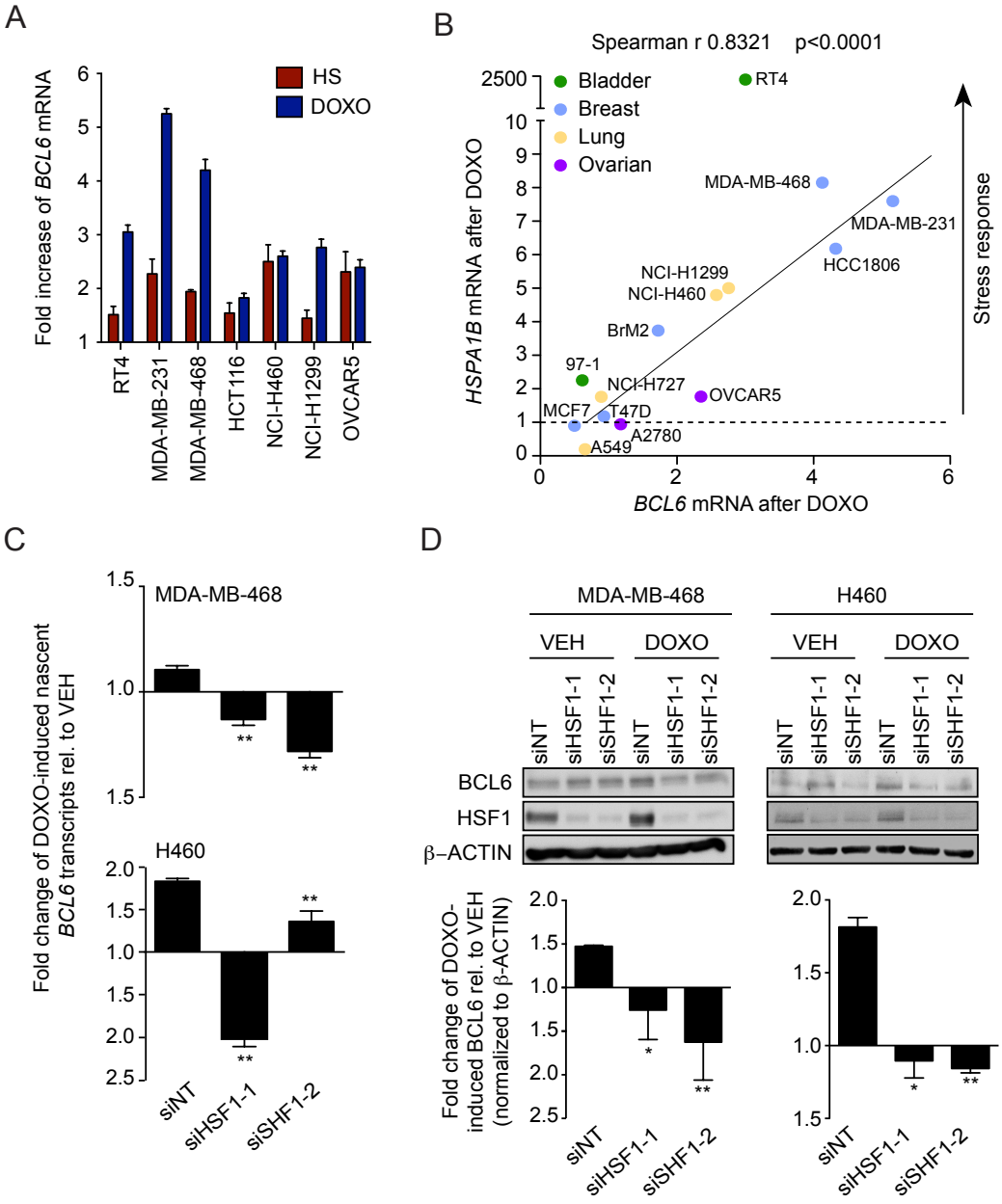

Figure 4.13 HSF1 induces BCL6 in response to chemotherapy. (A) qRT-PCR of *BCL6* mRNA after heat shock (HS, 2 h at 43 °C followed by 2 h at 37 °C) and 100 nM doxorubicin (DOXO, 4 h treatment). (B) *BCL6* and *HSPA1B* induction after heat shock in a panel of cancer cell lines. (C) Nascent *BCL6* mRNA in MDA-MB-468 and H460 cells transfected with 50 nM control (siNT) or HSF1-targeting siRNAs for 48 h and then treated with vehicle (VEH) or 100 nM DOXO for 4 h. (D) Representative immunoblot of BCL6 protein levels in MDA-MB-468 and H460 cells transfected as in (C) and treated with vehicle (VEH) or 100 nM DOXO for 8 h. Quantification of BCL6 levels after doxorubicin normalized to β-ACTIN and relative to siNT.

vincristine, dexamethasone, mechloretamine, and their combination (mechlorethamine, doxorubicin, vincristine, and dexamethasone), which is similar to the CHOP chemotherapy regimen. These combinations yielded

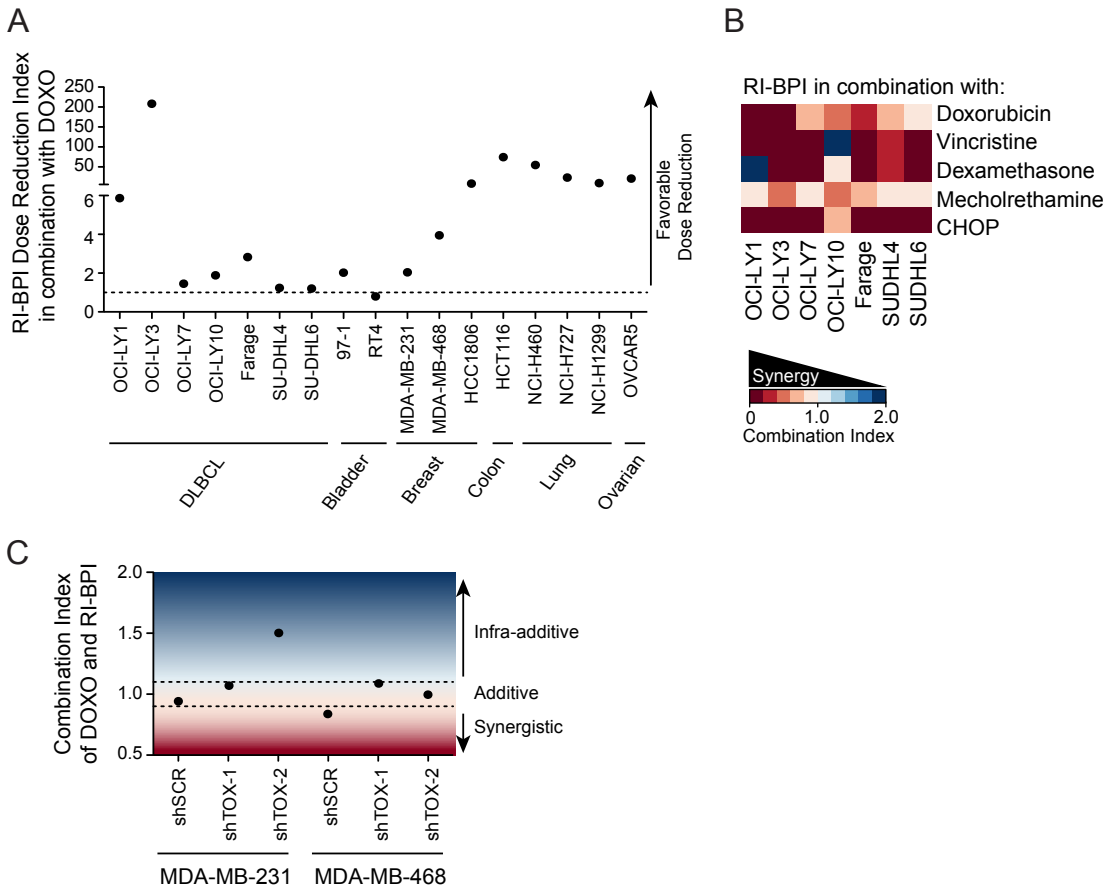

Figure 4.14 Therapeutically target BCL6-stress dependence in tumor cells with BTB inhibitors. (A) Dose reduction index for RI-BPI at the concentration that inhibited growth by 50% (GI_{50}) after concurrent exposure of cells to increasing concentrations of DOXO for 48 h. (B) Heatmap representing the combination index of doxorubicin, vincristine, dexamethasone, mechlorethamine, and CHOP (the combination of cyclophosphomide, doxorubicin, vincristine, and prednisone) with RI-BPI at the GI_{50} in DLBCL cell lines treated for 48 h. A combination index below 0.9 is synergistic; between 0.9 and 1.1 is additive; and above 1.1 is infra-additive. Provided by L. Cerchietti and S. Yang. (C) Combination index of concurrent administration of DOXO and RI-BPI at the GI_{50} in MDA-MB-231 and MDA-MB-468 cells transduced with a scrambled or two TOX-targeting shRNAs treated for 48 h.

mostly synergistic anti-tumor effects (**Figure 4.14B**).

We previously demonstrated that TOX repression by BCL6 was required for cells to acquire thermotolerance, and if we depleted RI-BPI-treated cells of TOX, they could reacquire thermotolerance (**Figure 4.12A-B**). Because of its role in mediating cell death after BCL6 BTB inhibition, we hypothesized that TOX derepression plays a crucial role in the anti-tumor activity of RI-BPI and other chemotherapies. We knocked down TOX in triple-negative MDA-MB-231 and MDA-MB-468 breast cancer cell lines and found that the combination index of RI-BPI and doxorubicin increased with TOX knockdown, demonstrating that the combination was less effective at cell killing (**Figure 4.14C**). These results suggest that the derepression of TOX that occurs after CL6 BTB inhibition is required to hinder thermotolerance and chemotolerance.

To determine whether targeting BCL6 might also yield more potent antitumor effects when combined with cytotoxic drugs *in vivo*, we engrafted human OCI-LY7 DLBCL cells in mice and evaluated whether RI-BPI enhanced the anti-tumor effect of chemotherapy. Once tumors reached 100 mm^3 in size mice were assigned to a schedule of RI-BPI (25 mg/kg), doxorubicin (0.6 mg/kg), the combination or vehicle only. Doxorubicin or RI-BPI alone each had significant antitumor activity as compared to vehicle ($p=0.02$ and $p=0.0001$, respectively). However the combination of doxorubicin with RI-BPI was the most potent and yielded significantly greater antitumor effect ($p<0.001$) (**Figure 4.15A**).

Cell lines maintained for years in culture may not fully reflect the biological dependencies of primary tumor cells from patients. Therefore we purified lymphoma cells from DLBCL biopsy specimens by enriching for $CD19^+$ cells obtained from lymph node biopsies of 21 $BCL6^+$ DLBCL patients. The specimens were plated using a dual-chamber co-culture system with a feeder layer of HK dendritic cells. $CD19^+$ cells were then exposed to increasing concentrations of RI-BPI or the combination of mechlorethamine, doxorubicin, vincristine and dexamethasone that mimic the CHOP regimen. The Webb fractional product of the drug combination was determined for each patient sample. 62% (13/21) of patient specimens manifested synergistic antitumor effects after exposure to the combination, and an additional four patients showed additive effect for a total response rate of 80% (**Figure 4.15B**). Taken

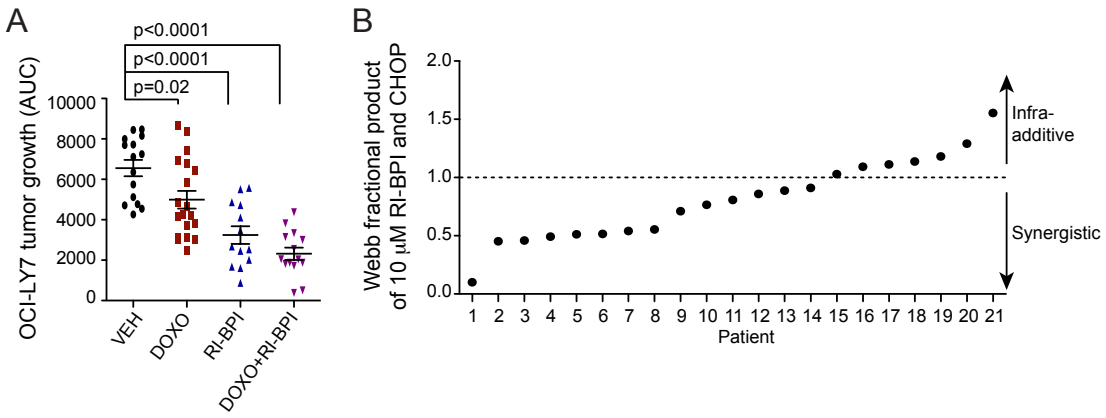

Figure 4.15 BCL6 BTB inhibitors have anti-lymphoma activity in preclinical and clinical models. (A) Area under the curve (AUC) of tumor growth curves for 14 days in OCI-LY7 xenografted mice treated with vehicle (DMSO, 10% in saline, n=15), DOXO (0.6 mg/kg, n=19), RI-BPI (25mg/kg, n=13), or the combination of RI-BPI and DOXO (n=14). (B) The webb fractional product of 10 μM BPI and CHOP at GI_{50} in primary DLBCL patient samples. Values in (A) represent the mean of two independent experiments ± SEM. A t-test was used to measure significance. Provided by L. Cerchietti and S. Yang.

together, the evolutionarily conserved role of BCL6 and its BTB domain in mediating tolerance to stress in vertebrates provides the basis for the rational translation of therapies that target the BCL6 BTB domain to induce chemosensitization of solid tumors that have limited therapeutic options. The combinatorial effect of BCL6 BTB inhibition and other chemotherapies would more effectively eradicate DLBCLs, a tumor type derived from a stress-dependent cell of origin.

3. Discussion

BCL6 is multi-faceted protein due to its multiple and distinct repressor domains. Here we demonstrate a more primitive role for BCL6 as a stress response gene. Like HSP90 and other stress response proteins, BCL6 mRNA and protein is induced after heat stress by HSF1, the master regulator of the heat shock response, in mammalian, avian, and reptilian cells in addition to a model of jawless vertebrates, the sea lamprey. We find that BCL6 mediates its stress tolerant phenotype through its BTB domain while its second repressor domain, RD2, is dispensable for this function. The BCL6 BTB domain is highly conserved in all vertebrates whereas the BCL6 RD2 domain, particularly the KKYK residues that facilitate interactions with HDAC2 and MTA3-NuRD are not conserved in jawless vertebrates, which are basal to jawed vertebrates. Because we have demonstrated that RD2 repressor activity is lost when KKYK residues are mutated, it is possible that the BCL6 RD2 domain has no function in these organisms, and BCL6 mediates its entire biological output through only the BTB domain. Thus the original function of BCL6 may have been to confer stress resistance after exposure to environmental stress stimuli. While

HSPs are induced to repair damaged and misfolded proteins, BCL6 may be induced because of its complementary role in tolerating DNA damage.

Both jawed and jawless vertebrates share the feature of recombinatorial rearrangement of their antigen-binding modules to generate a diverse repertoire of antigen receptors albeit employing structurally distinct types of receptors (Ig vs leucine-rich repeat, LRR, modules). In lampreys, flanking LRR coding units are randomly inserted into the germline VLR genes through short homology sequences at the ends of the modular LRR units as they lack recombinatorial signal sequences and RAG proteins (Boehm et al., 2012). *BCL6* expression has been found in VLR-B+ cells, which are similar to B-lymphocytes in jawed vertebrates (Hirano et al., 2013). The presence of BCL6 likely allows the VLR-B+ cells to tolerate the genomic damage associated with the rearrangement of LRR coding units, as it does in GC B cells. If this were true, BCL6 inhibition by either peptidomimetic or small molecule inhibitors would disrupt the LRR immune response and decrease LRR receptor diversification. It is interesting to note that a more divergent BCL6 ortholog can be identified in *C. intestionalis* a member of urochordates (G. Privé unpublished results). Given its role in mediating stress tolerance, it is tempting to speculate that the emergence of BCL6 in vertebrates might have been an influential event that allowed cells to tolerate genomic recombination events, which is the basis for generating antigen receptor diversity and thus the adaptive immune response.

The repression of TOX by BCL6 is critical for cells to adapt and survive repeated rounds of stress. TOX is markedly increased after heat shock in

Bcl6^{BTB} mutant cells, and TOX depletion can restore stress tolerance in BPI-treated cells. TOX is a member of the HMG-box family of DNA binding proteins that are structure-dependent but not sequence-dependent (O'Flaherty and Kaye, 2003). TOX homologs are found in lampreys and in arthropods. Although TOX has been previously described to be required for the development of the CD4 T cell lineage, it is not yet clear how TOX mediates its effects (Aliahmad and Kaye, 2008). HMG-box proteins bind to chromatin and modify the architecture of DNA (O'Flaherty and Kaye, 2003). TOX may act in a similar manner to modulate gene expression changes during thymocyte selection and stress response. BCL6 regulates TOX in DLBCL cells as demonstrated by TOX derepression after BCL6 knockdown in DLBCL cell lines. TOX is deleted in a subset of DLBCL, childhood acute lymphatic leukemia (4%) and prostate cancer (48%). Given its role in reducing stress tolerance and as a chromatin architecture protein, we postulate that TOX may act as a tumor suppressor by functioning as a rheostat of genomic damage.

The stress tolerance axis of HSF1 and BCL6 is conserved between heat stress and chemotherapy. Like what occurs after heat shock, HSF1 induces BCL6 in tumor cells treated with chemotherapy agents. We have previously demonstrated that BCL6 is required for the survival of imatinib-resistant ALL cells (Duy et al., 2011). The results of the current study suggest that the mechanisms that mediate thermotolerance are the same at play in chemotolerance. We find that we can harness this therapeutically by combining conventional chemotherapy with BCL6 BTB inhibitors. Moreover when we test the relevance of the BCL6 target, TOX, we find that its repression is also required for an effective anti-tumor combination of

chemotherapy and RI-BPI. While *BCL6* is the most frequently deregulated oncogene in DLBCL, it is also amplified in 30% of lung cancer, 24% of ovarian cancer, 22% of cervical cancer, and 19% of head and neck cancers. While DLBCL has a relatively high response rate to therapy, patients with solid tumors have a worse prognosis and are sometimes more refractory to treatment, particularly patients with triple-negative breast cancer and bladder cancer. Although BCL6 inhibitors have been described to have potent anti-lymphoma activity, our study provides a basis for the rational translation of BCL6 inhibitors to induce chemosensitization of solid tumors that have otherwise limited therapeutic options.

4. Materials and Methods

Animals

Hsf1$^{+/+}$ and *Hsf1*$^{+/-}$ were obtained from Jackson Laboratories. *Bcl6*$^{-/-}$ mice were kindly provided by Dr. Hilda Ye (Albert Einstein Medical College). *Bcl6*^{BTBMUT} *and Bcl6*^{RD2MUT} mice were generated by Dr. Chuaxin Huang from the Melnick lab (Huang et al., 2014; Huang et al., 2013). *Tox*$^{+/+}$ and *Tox*$^{-/-}$ mice were maintained at Cedars-Sinai Medical Center by the laboratory of Dr. Jonathan Kaye (Cedars-Sinai Medical Center). SCID mice were obtained from the National Cancer Institute. The maintenance and procedures of all animals were in accordance with and approved by the Research Animal Resource Center of the Weill Cornell Medical College.

Mammalian Cell Lines

Normal human adult dermal fibroblasts (ATCC) were grown in fibroblast blast medium supplemented with the serum-free fibroblast growth kit (ATCC).

Murine BCL1 cells (ATCC) were grown in RPMI 1640 supplemented with 10% FBS, penicillin G/streptomycin, and 0.05 mM 2-ME. Dog Cf2Th cells (ATCC) were grown in DMEM with 20% FBS, penicillin G/streptomycin, and non-essential amino acids. The DLBCL cell lines OCI-LY1, OCI-LY7, and OCI-LY10 were grown in Isocove's medium supplemented with 10% or 20% (OCI-LY10) FBS and penicillin G/streptomycin; OCI-LY3, Farage, SU-DHL4, and SU-DHL6 were grown in RPMI 1640 supplemented with 10% FBS, penicillin G/streptomycin, L-glutamine, and HEPES. The bladder cancer cell line RT4 was grown in McCoy's 5a medium supplemented with 10% FBS and penicillin G/streptomycin; 97-1 was grown in Ham's F-12 medium supplemented with 10% FBS and penicillin G/streptomycin. The breast cancer cell lines MCF7, T47D, HCC1806, MDA-MB-231, and MDA-MB-468 were grown in DMEM supplemented with 10% FBS and penicillin G/streptomycin. The colon cancer cell line HCT116 was grown in DMEM supplemented with 10% FBS and penicillin G/streptomycin. The lung cancer cell lines A549, NCI-H727, NCI-H460, and NCI-H1299 were grown in DMEM supplemented with 10% FBS, penicillin G/streptomycin, and L-glutamine. The ovarian cancer cell lines A2780 and OVCAR-5 were grown in RPMI 1640 supplemented with 10% FBS, penicillin G/streptomycin, and L-glutamine. Cell lines were obtained from ATCC, DMSZ or the Ontario Cancer Institute and grown in 37 ºC with 5% CO_2.

Non-mammalian cell lines

Iguana IgH-2 cells were grown in EMEM with 10% FBS, penicillin G/streptomycin, L-glutamine, and non-essential amino acids. Chicken DT40 cells were grown in DMEM with 10% FBS, 5% chicken serum, 10% tryptose phosphate broth, penicillin G/streptomycin, and 0.05 mM 2-ME. IgH-2 and

DT40 cell lines were obtained from ATCC and grown at 37 ºC with 5% CO_2. Drosophila S2+ cells were kindly provided by Dr. Eric Lai (Memorial Sloan Kettering Cancer Center) and grown in Schneider's Drosophila medium, 10% FBS, and penicillin G/streptomycin at 25-26 ºC with ambient CO_2.

Real-time RT-qPCR

Tissues from *Hsf1*$^{+/+}$ and *Hsf1*$^{+/-}$ mice, zebrafish embryos, lamprey typhlosole, or cells were heat shocked (43 ºC for 2 h followed by recovery at 37 ºC for 2 h, with the exception of zebrafish embryos that were heat shocked at 37 ºC followed by recovery at 28 ºC) or treated with 100 nM doxorubicin (Sigma) for 4 h. Cells were resuspended in Trizol reagent (Invitrogen) and stored at -80 ºC until RNA extraction. After thawing, 1/5 volume of chloroform was added, and the samples were shaken vigorously for 15 sec. After 2 min incubation at room temperature, the samples were spun at 12,000xg for 15 min at 4 ºC. The aqueous phase was aspirated into a new tube, and 1 volume of isopropanol was added. Samples were mixed and incubated for 10 min at room temperature or overnight at -80 ºC. Tubes were spun again at 12,000xg for 10 min, and then washed with 75% ethanol. Tubes were spun at 7,500xg for 5 min, aspirated, and allowed to dry at room temperature for 5-10 min. RNA was resuspended in RNase-free H_2O and quantified with the Nanodrop (Thermo Scientific). cDNA was prepared using the Verso cDNA synthesis kit (Thermo Scientific) and detected by fast SYBR Green (Quanta Biosciences) on the 7900HT Fast Real-Time PCR System (Applied Biosystems). Gene expression was normalized to a housekeeping gene, *RPL13A* (human), *Hprt1* (mouse, dog), *Actb* (chicken, iguana, zebrafish), or *GAPDH* (lamprey), and expressed

as values relative to control using the ddCt method. Results were represented as fold change in expression with the standard error for 3 series of triplicates.

siRNA transfection

Normal adult dermal fibroblasts and MDA-MB-468 cells were transfected using Lipofectamine 2000 (Invitrogen) with 50 nM siRNAs targeting HSF1 (Hs_HSF1_6/9, Qiagen) and a non-targeting control (Stealth RNAi medium GC duplex, Invitrogen).

siRNA sequences:

siHSF1-1 (Hs_HSF1_6): 5'-GCUUCGUGCGGCAGCUCAATT-3'

siHSF1-1 (Hs_HSF1_9): 5'-GGUUGUUCAUAGUCAGAAUTT-3'

Nascent RNA capture

Human cells transfected with HSF1-targeting siRNA for 48 h were heat shocked at 43 ºC for 2 h followed by recovery at 37 ºC for 2 h or treated with 100 nM doxorubicin for 4 h while simultaneously pulsed with 0.2 mM ethnyl uridine (EU). EU-labeled RNA was captured with the Click-It Nascent RNA capture kit (Molecular Probes). Briefly, RNA was extracted using Trizol reagent (Invitrogen), resuspended with RNase-free H_2O, and quantified with the Nanodrop (Thermo Scientific). 1 μg total RNA was biotinylated by a click reaction with 0.5 μM biotin azide and re-precipitated with Glyco-blue (Ambion), ammonium acetate, and ice cold 100% ethanol. RNA was spun at 13,000xg for 15 min at 4 ºC, washed with 75% ethanol, dried for 5 min at room temperature, and resuspended in RNase-free H_2O. RNA concentration was re-measured by the Nanodrop (Thermo Scientific) and equal amounts of RNA (0.75-1 μg) was allowed to bind to 25 μL Dynabeads MyOne Streptavidin T1

beads (Invitrogen) in the presence of RNaseOUT recombinant ribonuclease inhibitor (Invitrogen) for 30 min at room temperature with gentle agitation. The bound RNA was washed with the provided Click-it wash buffers and resuspended in 12 μL RNase-free H_2O. The RNA bound to the beads was taken directly into a cDNA synthesis reaction using the SuperScript III first-strand synthesis system (Invitrogen). A fraction of the undiluted cDNA was used in real-time quantitative PCR and detected by fast SYBR Green (Quanta Biosciences) on the 7900HT Fast Real-Time PCR System (Applied Biosystems).

Immunoblot

Cell suspensions or sonicated tissue samples (in the case of lamprey typhlosole) were used to prepare whole cell lysate with lysis buffer (20mM Tris pH 8.0, 150 mM NaCl, 5 mM EDTA, 1% Triton X-100) supplemented with protease inhibitors. Protein was cleared, quantified by Bradford reagent (Pierce) and resolved by SDS-PAGE, transferred to PVDF membranes, probed with primary antibodies (anti-HSF1 E-4, Santa Cruz; anti-β-ACTIN AC-15, Sigma, anti-BCL6 N3/D8, Santa Cruz; anti-GAPDH FL-335, Santa Cruz; anti-αTUBULIN DM1A, Sigma) followed by HRP-conjugated secondary antibodies (Santa Cruz) and detected with enhanced chemiluminescence (Pierce).

Protein sequence variability analysis

BCL6, BCOR, and NCOR2 (SMRT) orthologs were found with the orthologous matrix browser and aligned with the multiple sequence comparison by log-expectation (MUSCLE) (Edgar, 2004). The protein variability server (Garcia-

Boronat et al., 2008) was used for a sequence variability analysis (Shannon Diversity Index) of the multiple sequence alignment. Sequence entropy values were mapped onto the structure of Protein database entry 1R2B.

Primary isolation of murine B220+ cells

Single-cell suspensions of mononuclear cells were generated from murine spleens using red blood cell lysis (Qiagen) or Fico/Lite-LM density gradient media (Atlanta Biologicals). Splenocytes were purified using B220 positive selection or CD43 depletion using the autoMACS cell separation system (Miltenyi Biotec).

Thermotolerance

(i) Thermotolerance of cells grown at 37 ºC: Primary murine splenic $B220^+$ cells, BCL1 cells, DT40 cells, and IgH-2 cells were left untreated or treated with control or 1 μM RI-BPI peptide. Cells were heat shocked at 43 ºC for 1 h, allowed to recover at 37 ºC for 12 h, heat shocked again at 43 ºC for 1 h, and allowed to recover at 37 ºC for 1 h. Cell viability was monitored with Trypan blue exclusion or flow cytometry using DAPI exclusion.

(ii) Thermotolerance of zebrafish embryos grown at 28 ºC: 2 ng control morpholino (mo) (GeneTools) or bcl6 mo (Open Biosystems) were injected into the yolk of 1-2 cell stage embryos. At 24 h post-fertilization (hpf), embryos were separated into petri dishes and heat shocked in a water bath at 37 ºC for 1 h, allowed to recover at 28 ºC for 12 h, heat shocked again at 37 ºC for 1 h, and allowed to recover at 28 ºC for 12 h. Zebrafish embryos were counted non-viable if there was an absence of opaque tissues.

Morpholino sequences:

Control mo: 5'- CCTCCTACCTCAGTTACAATTTATA -3'

Bcl6 mo: 5'- TCTACAAATGAAAATATACCTGGAC -3'

(iii) Thermotolerance of lamprey typhlosole cells grown at 16 ºC: Cells from lamprey typhlosole were isolated and treated with 1 μM control or RI-BPI peptide. Cells were heat shocked at 29 ºC for 1 h, allowed to recover at 16 ºC for 12 h, heat shocked again at 29 ºC for 1 h, and allowed to recover at 16 ºC for 12 h. Cell viability was monitored flow cytometry using DAPI exclusion.

(iv) Thermotolerance of Drosophila cells grown at 25-26 ºC: Drosophila S2+ cells treated with control or 1 μM RI-BPI peptide were heat shocked at 37 ºC for 1 h, allowed to recover at 25 ºC for 12 h, heat shocked again at 37 ºC for 1 h, and allowed to recover at 25 ºC for 1 h. Cell viability was monitored with Trypan blue exclusion.

mRNA-seq

B220^{+} splenocytes from *Bcl6*$^{+/+}$ (n=2) and *Bcl6*^{BTBMUT}(Huang et al., 2013) (n=2) mice were heat shocked at 43 ºC for 1 h and allowed to recover at 37 ºC for 12 h. RNA was purified using Trizol extraction (Invitrogen) and treated with Dnase (Qiagen). RNA quality was verified using the Agilent 2100 Bioanalyzer (Agilent Technologies) and the RNA integrity number values were greater than 8 for all samples. Sequencing libraries were generated with polyA+ RNA using the TruSeq RNA sample prep kit (Illumina). Libraries were cluster amplified and sequenced for 50 cycles using the Illumina HiSeq2000. Reads were aligned to mm10 using Tophat (Trapnell et al., 2009), and gene expression values were calculated by counting how many reads map uniquely to the union of all gene exons using HTseq-count. Samples were normalized for sequencing depth, and differentially expressed genes were identified with the edgeR package

(Robinson et al., 2010). Genes with counts per million > -3 and an FDR value < 0.05 were considered differentially expressed. mRNA-seq data was validated using splenic $B220^{+}$ cells and brain tissue from *Bcl6*^{BTBMUT} *and* *Bcl6*^{RD2MUT} mice, using the same experimental plan discussed earlier in this section.

Lentiviral transduction

Lentivirus was produced in 293T by calcium phosphate transfection of pLKO.1-puro vectors (The RNAi Consortium) and envelope and packaging vectors. Lentivirus was collected 48 h after transfection and concentrated with PEG-it (Systems Biosciences). Cells were transduced and selected with 1 μg/mL puromycin 48 h after infection. Murine BCL1 cells were transduced with shSCR, shTox-1, and shTox-2. Human MDA-MB-231 and MDA-MB-468 cells were transduced with a non-targeting control shRNA, shTOX-1, and shTOX-2. Puromycin-resistant cells were selected for at least 4 days prior to thermotolerance or cell viability experiments.

Control shRNA sequences:

shSCR: 5'- CCTAAGGTTAAGTCGCCCTCG -3'

Murine shRNA sequences:

shTox-1: 5'- CCATTCTGATTTCTGTTGGTT -3'

shTox-1: 5'- CTGTACCTAAGTTCTCACTAT -3'

Human shRNA sequences:

shTOX-1: 5'- CCCTACTATTGCAACAAGTTT -3'

shTOX-2: 5'- CGATGATACCTCTAAGATCAA -3'

Drugs

Doxorubicin, dexamethasone, vincristine, mechlorethamine, cyclophosphamide, and prednisone were purchased from Sigma. Drugs were dissolved in DMSO (Sigma) or distilled pure water. RI-BPI (retro-inverted BCL6 peptidomimetic inhibitor) and control peptides were produced by Biosynthesis Inc from published sequences (Cerchietti et al., 2010b).

Growth inhibition

DLBCL and solid tumor cell lines were grown at concentrations sufficient to keep untreated cells in exponential growth over the complete drug exposure time. Cell lines were exposed concurrently to 6 concentrations of RI-BPI and drug for 48 h and analyzed for cell viability using a fluorometric reduction method (CellTiter-Blue, Promega) or ATP quantitation (CellTiter-Glo, Promega). Fluorescence ($560_{Ex}/590_{Em}$) or luminescence was determined with the Synergy4 microplate reader (Biotek). The number of viable cells was calculated using the linear least-squares regression of the standard curve. The fluorescence/luminescence was determined for three replicates per treatment condition and normalized to their respective controls (vehicle-treated). CompuSyn software (Biosoft) was used to plot dose-effect curves, determine the drug concentrations that inhibit the growth of the cell lines by 50% and 75% compared to control (Fa_{50} and Fa_{75}, respectively), and calculate the dose reduction index (DRI) at the Fa_{50} and Fa_{75}. The DRI is a measure of how many fold the dose of each drug in a combination may be reduced at a given effect level compared to the dose of each drug alone. DRI is based on the following equation: $DRI = (D_x)_1 / (D)_1$, where $(D_x)_1$ represents the dose of drug 1 for a given effect x and were $(D)_1$ represents the dose of drug 1 given in combination to reach the same effect x.

Mice xenotransplant

Six- to eight-week old male SCID mice housed in a barrier environment were subcutaneously injected in the left flank with 10^7 human DLBCL cells (OCI-LY7). Tumor volume was monitored every other day using electronic digital calipers in 2 dimensions. Tumor volume was calculated using the following formula: tumor volume (mm^3) = (smallest diameter^2 × largest diameter)/2. When tumors reached a palpable size (approximately 75 to 100 mm^3 after 21 days after injection), the mice were randomized to 4 different treatment arms. One group was injected intraperitoneally with vehicle (10% DMSO) and the other group received 0.6 mg/kg doxorubicin for 1 day. On day 2 of treatment, the mice were randomized to 2 arms, generating 4 different treatment arms. One group received intraperitoneal injections of sterile PBS or 25 mg/kg RI-BPI daily for 3 days. The schedule of 1 dose of doxorubicin followed by 3 days of RI-BPI was repeated 2 times. RI-BPI was stored lyophilized at -20 °C until reconstituted with sterile pure water immediately before use. Mice were weighed twice a week. All mice were euthanized by cervical dislocation under anesthesia when at least 2 out of 10 tumors reached 20 mm in any dimension (equivalent to 1 gram), which was generally on day 14 of the treatment schedule.

Primary isolation and growth inhibition of human lymphoma samples

Human $CD19^+$ B cells were affinity-purified from de-identified lymph node biopsies of confirmed DLBCL specimens in accordance with and approval from the Institutional Review Board (IRB) of Weill Cornell Medical College. Single-cell suspensions were obtained from lymph node biopsies by physical

disruption of tissues followed by cell density gradient separation with Fico-Lite LmphoH (Atlanta Biologicals). CD19 cells were affinity-purified from mononuclear cells using anti-CD19 microbeads and the autoMACS cell separator (Miltenyi Biotec). Primary DLBCL cells were co-cultured with HK dendritic cells in 96-well chambers with two compartments separated by 0.4 μm porous polyester membrane (Corning Inc) as previously described (Cerchietti et al., 2010b). Cells were grown in advanced RPMI medium with 10% human serum supplemented with antibiotics, l-glutamine, and HEPES for 48 hours. Primary cells were seeded in HK-conditioned medium for 2 hours followed by 2 hours of drug exposure and transferred to the coculture system for the remainder of the experiment. Cells were treated with 10 μM of BPI, a combination of the drugs, or vehicle in 4 replicates. After 48 hours of exposure, viability was determined by using an ATP-based luminescent method (CellTiter-Glo; Promega) and by Trypan blue exclusion. To determine synergism in primary cells, we used the Webb fractional product method (Prichard and Shipman, 1990). This method is based on the equation $Z = X + Y (1 - X)$, where Z is the expected effect of the combination and X and Y represent the effect of each drug alone. If Z is equal to the actual effect of the combination, then the relation is additive; if Z is higher then it is less than additive, and if Z is lower then it is more than additive (synergistic).

Statistical analyses

Student's *t*-test was used for statistical analysis unless otherwise stated. All statistical analyses were done using GraphPad Prism 5.

CHAPTER FIVE

REFERENCES

Abravaya, K., Myers, M.P., Murphy, S.P., and Morimoto, R.I. (1992). The human heat shock protein hsp70 interacts with HSF, the transcription factor that regulates heat shock gene expression. Genes & development *6*, 1153-1164.

Ahmad, K.F., Melnick, A., Lax, S., Bouchard, D., Liu, J., Kiang, C.-L., Mayer, S., Takahashi, S., Licht, J.D., and Privé, G.G. (2003). Mechanism of SMRT corepressor recruitment by the BCL6 BTB domain. In Molecular cell, pp. 1551-1564.

Akerfelt, M., Morimoto, R.I., and Sistonen, L. (2010). Heat shock factors: integrators of cell stress, development and lifespan. In Nature reviews Molecular cell biology, pp. 545-555.

Alastalo, T.-P. (2003). Formation of nuclear stress granules involves HSF2 and coincides with the nucleolar localization of Hsp70. In Journal of cell science, pp. 3557-3570.

Alastalo, T.P., Lonnstrom, M., Leppa, S., Kaarniranta, K., Pelto-Huikko, M., Sistonen, L., and Parvinen, M. (1998). Stage-specific expression and cellular localization of the heat shock factor 2 isoforms in the rat seminiferous epithelium. Experimental cell research *240*, 16-27.

Albagli, O., Dhordain, P., Bernardin, F., Quief, S., Kerkaert, J.P., and Leprince, D. (1996). Multiple domains participate in distance-independent LAZ3/BCL6-mediated transcriptional repression. Biochemical and biophysical research communications *220*, 911-915.

Ali, A., Bharadwaj, S., O'Carroll, R., and Ovsenek, N. (1998). HSP90 interacts with and regulates the activity of heat shock factor 1 in Xenopus oocytes. Molecular and cellular biology *18*, 4949-4960.

Aliahmad, P., and Kaye, J. (2008). Development of all CD4 T lineages requires nuclear factor TOX. The Journal of experimental medicine *205*, 245-256.

Allen, C.D., Ansel, K.M., Low, C., Lesley, R., Tamamura, H., Fujii, N., and Cyster, J.G. (2004). Germinal center dark and light zone organization is mediated by CXCR4 and CXCR5. Nature immunology *5*, 943-952.

Allen, C.D., Okada, T., Tang, H.L., and Cyster, J.G. (2007). Imaging of germinal center selection events during affinity maturation. Science *315*, 528-531.

Amin, R.H., and Schlissel, M.S. (2008). Foxo1 directly regulates the transcription of recombination-activating genes during B cell development. Nature immunology *9*, 613-622.

Anderson, P., and Kedersha, N. (2006). RNA granules. The Journal of cell biology *172*, 803-808.

Arguni, E., Arima, M., Tsuruoka, N., Sakamoto, A., Hatano, M., and Tokuhisa, T. (2006). JunD/AP-1 and STAT3 are the major enhancer molecules for high Bcl6 expression in germinal center B cells. International immunology *18*, 1079-1089.

Arndt, V., Rogon, C., and Hohfeld, J. (2007). To be, or not to be--molecular chaperones in protein degradation. Cellular and molecular life sciences : CMLS *64*, 2525-2541.

Bajalica-Lagercrantz, S., Piehl, F., Farnebo, F., Larsson, C., and Lagercrantz, J. (1998). Expression of the BCL6 gene in the pre- and postnatal mouse. In Biochem Biophys Res Commun, pp. 357-360.

Bakthisaran, R., Tangirala, R., and Rao, C.M. (2015). Small heat shock proteins: Role in cellular functions and pathology. Biochimica et biophysica acta *1854*, 291-319.

Baler, R., Welch, W.J., and Voellmy, R. (1992). Heat shock gene regulation by nascent polypeptides and denatured proteins: hsp70 as a potential autoregulatory factor. The Journal of cell biology *117*, 1151-1159.

Bardwell, J.C., and Craig, E.A. (1987). Eukaryotic Mr 83,000 heat shock protein has a homologue in Escherichia coli. Proceedings of the National Academy of Sciences of the United States of America *84*, 5177-5181.

Barish, G.D., Yu, R.T., Karunasiri, M., Ocampo, C.B., Dixon, J., Benner, C., Dent, A.L., Tangirala, R.K., and Evans, R.M. (2010). Bcl-6 and NF-kappaB cistromes mediate opposing regulation of the innate immune response. Genes & development *24*, 2760-2765.

Barish, G.D., Yu, R.T., Karunasiri, M.S., Becerra, D., Kim, J., Tseng, T.W., Tai, L.J., Leblanc, M., Diehl, C., Cerchietti, L.*, et al.* (2012). The Bcl6-SMRT/NCoR cistrome represses inflammation to attenuate atherosclerosis. Cell metabolism *15*, 554-562.

Baron, B.W., Anastasi, J., Montag, A., Huo, D., Baron, R.M., Karrison, T., Thirman, M.J., Subudhi, S.K., Chin, R.K., Felsher, D.W.*, et al.* (2004). The human BCL6 transgene promotes the development of lymphomas in the mouse. Proceedings of the National Academy of Sciences of the United States of America *101*, 14198-14203.

Baron, B.W., Stanger, R.R., Hume, E., Sadhu, A., Mick, R., Kerckaert, J.P., Deweindt, C., Bastard, C., Nucifora, G., Zeleznik-Le, N.*, et al.* (1995). BCL6 encodes a sequence-specific DNA-binding protein. Genes, chromosomes & cancer *13*, 221-224.

Bartels, C., Klatt, C., Luhrmann, R., and Fabrizio, P. (2002). The ribosomal translocase homologue Snu114p is involved in unwinding U4/U6 RNA during activation of the spliceosome. EMBO reports *3*, 875-880.

Basso, K., and Dalla-Favera, R. (2010). BCL6: master regulator of the germinal center reaction and key oncogene in B cell lymphomagenesis. In Advances in immunology, pp. 193-210.

Baumjohann, D., Okada, T., and Ansel, K.M. (2011). Cutting Edge: Distinct waves of BCL6 expression during T follicular helper cell development. In The Journal of Immunology, pp. 2089-2092.

Beguelin, W., Popovic, R., Teater, M., Jiang, Y., Bunting, K.L., Rosen, M., Shen, H., Yang, S.N., Wang, L., Ezponda, T.*, et al.* (2013). EZH2 is required for germinal center formation and somatic EZH2 mutations promote lymphoid transformation. Cancer cell *23*, 677-692.

Bereshchenko, O.R., Gu, W., and Dalla-Favera, R. (2002). Acetylation inactivates the transcriptional repressor BCL6. In Nature genetics, pp. 606-613.

Bharadwaj, S., Ali, A., and Ovsenek, N. (1999). Multiple components of the HSP90 chaperone complex function in regulation of heat shock factor 1 In vivo. Molecular and cellular biology *19*, 8033-8041.

Biamonti, G., and Vourc'h, C. (2010). Nuclear stress bodies. Cold Spring Harbor perspectives in biology *2*, a000695.

Boehm, A.K., Saunders, A., Werner, J., and Lis, J.T. (2003). Transcription factor and polymerase recruitment, modification, and movement on dhsp70 in vivo in the minutes following heat shock. Molecular and cellular biology *23*, 7628-7637.

Boehm, T., McCurley, N., Sutoh, Y., Schorpp, M., Kasahara, M., and Cooper, M.D. (2012). VLR-based adaptive immunity. Annual review of immunology *30*, 203-220.

Borkovich, K.A., Farrelly, F.W., Finkelstein, D.B., Taulien, J., and Lindquist, S. (1989). hsp82 is an essential protein that is required in higher concentrations for growth of cells at higher temperatures. Molecular and cellular biology *9*, 3919-3930.

Boulon, S., Westman, B.J., Hutten, S., Boisvert, F.-M., and Lamond, A.I. (2010). The Nucleolus under Stress. In Molecular cell, pp. 216-227.

Boyault, C., Gilquin, B., Zhang, Y., Rybin, V., Garman, E., Meyer-Klaucke, W., Matthias, P., Muller, C.W., and Khochbin, S. (2006). HDAC6-p97/VCP controlled polyubiquitin chain turnover. The EMBO journal *25*, 3357-3366.

Boyault, C., Zhang, Y., Fritah, S., Caron, C., Gilquin, B., Kwon, S.H., Garrido, C., Yao, T.-P., Vourc'h, C., Matthias, P.*, et al.* (2007). HDAC6 controls major cell response pathways to cytotoxic accumulation of protein aggregates. In Genes & development, pp. 2172-2181.

Bu, L., Jin, Y., Shi, Y., Chu, R., Ban, A., Eiberg, H., Andres, L., Jiang, H., Zheng, G., Qian, M.*, et al.* (2002). Mutant DNA-binding domain of HSF4 is associated with autosomal dominant lamellar and Marner cataract. Nature genetics *31*, 276-278.

Bunting, K.L., and Melnick, A.M. (2013). New effector functions and regulatory mechanisms of BCL6 in normal and malignant lymphocytes. In Current opinion in immunology, pp. 339-346.

Caganova, M., Carrisi, C., Varano, G., Mainoldi, F., Zanardi, F., Germain, P.L., George, L., Alberghini, F., Ferrarini, L., Talukder, A.K.*, et al.* (2013). Germinal center dysregulation by histone methyltransferase EZH2 promotes lymphomagenesis. The Journal of clinical investigation *123*, 5009-5022.

Caron, G., Le Gallou, S., Lamy, T., Tarte, K., and Fest, T. (2009). CXCR4 expression functionally discriminates centroblasts versus centrocytes within human germinal center B cells. Journal of immunology *182*, 7595-7602.

Cattoretti, G., Pasqualucci, L., Ballon, G., Tam, W., Nandula, S.V., Shen, Q., Mo, T., Murty, V.V., and Dalla-Favera, R. (2005). Deregulated BCL6 expression recapitulates the pathogenesis of human diffuse large B cell lymphomas in mice. In Cancer cell, pp. 445-455.

Cerchietti, L.C., Ghetu, A.F., Zhu, X., Da Silva, G.F., Zhong, S., Matthews, M., Bunting, K.L., Polo, J.M., Fares, C., Arrowsmith, C.H.*, et al.* (2010a). A small-molecule inhibitor of BCL6 kills DLBCL cells in vitro and in vivo. Cancer cell *17*, 400-411.

Cerchietti, L.C., Hatzi, K., Caldas-Lopes, E., Yang, S.N., Figueroa, M.E., Morin, R.D., Hirst, M., Mendez, L., Shaknovich, R., Cole, P.A.*, et al.* (2010b). BCL6 repression of EP300 in human diffuse large B cell lymphoma cells provides a basis for rational combinatorial therapy. In The Journal of clinical investigation.

Cerchietti, L.C., Lopes, E.C., Yang, S.N., Hatzi, K., Bunting, K.L., Tsikitas, L.A., Mallik, A., Robles, A.I., Walling, J., Varticovski, L.*, et al.* (2009a). A purine scaffold Hsp90 inhibitor destabilizes BCL-6 and has specific antitumor activity in BCL-6–dependent B cell lymphomas. In Nature medicine, pp. 1369-1376.

Cerchietti, L.C., Polo, J.M., Da Silva, G.F., Farinha, P., Shaknovich, R., Gascoyne, R.D., Dowdy, S.F., and Melnick, A. (2008). Sequential transcription factor targeting for diffuse large B-cell lymphomas. Cancer research *68*, 3361-3369.

Cerchietti, L.C., Yang, S.N., Shaknovich, R., Hatzi, K., Polo, J.M., Chadburn, A., Dowdy, S.F., and Melnick, A. (2009b). A peptomimetic inhibitor of BCL6 with potent antilymphoma effects in vitro and in vivo. Blood *113*, 3397-3405.

Chang, C.C., Ye, B.H., Chaganti, R.S., and Dalla-Favera, R. (1996). BCL-6, a POZ/zinc-finger protein, is a sequence-specific transcriptional repressor. Proceedings of the National Academy of Sciences of the United States of America *93*, 6947-6952.

Chang, Y., Ostling, P., Akerfelt, M., Trouillet, D., Rallu, M., Gitton, Y., El Fatimy, R., Fardeau, V., Le Crom, S., Morange, M.*, et al.* (2006). Role of heat-shock factor 2 in cerebral cortex formation and as a regulator of p35 expression. In Genes & development, pp. 836-847.

Chen, S., Zuo, X., Yang, M., Lu, H., Wang, N., Wang, K., Tu, Z., Chen, G., Liu, M., Liu, K.*, et al.* (2012). Severe multiple organ injury in HSF1 knockout mice induced by lipopolysaccharide is associated with an increase in neutrophil infiltration and surface expression of adhesion molecules. Journal of leukocyte biology *92*, 851-857.

Chen, Y., Barlev, N.A., Westergaard, O., and Jakobsen, B.K. (1993). Identification of the C-terminal activator domain in yeast heat shock factor: independent control of transient and sustained transcriptional activity. In The EMBO journal, pp. 5007-5018.

Cheung, K.M., Matthews, T.P., James, K., Rowlands, M.G., Boxall, K.J., Sharp, S.Y., Maloney, A., Roe, S.M., Prodromou, C., Pearl, L.H.*, et al.* (2005). The identification, synthesis, protein crystal structure and in vitro biochemical evaluation of a new 3,4-diarylpyrazole class of Hsp90 inhibitors. Bioorganic & medicinal chemistry letters *15*, 3338-3343.

Chevallier, N., Corcoran, C.M., Lennon, C., Hyjek, E., Chadburn, A., Bardwell, V.J., Licht, J.D., and Melnick, A. (2004). ETO protein of t(8;21) AML is a corepressor for Bcl-6 B-cell lymphoma oncoprotein. Blood *103*, 1454-1463.

Chiosis, G., Timaul, M.N., Lucas, B., Munster, P.N., Zheng, F.F., Sepp-Lorenzino, L., and Rosen, N. (2001). A small molecule designed to bind to the adenine nucleotide pocket of Hsp90 causes Her2 degradation and the growth arrest and differentiation of breast cancer cells. Chemistry & biology *8*, 289-299.

Choi, Y.S., Eto, D., Yang, J.A., Lao, C., and Crotty, S. (2013). Cutting edge: STAT1 is required for IL-6-mediated Bcl6 induction for early follicular helper cell differentiation. Journal of immunology *190*, 3049-3053.

Choi, Y.S., Kageyama, R., Eto, D., Escobar, T.C., Johnston, R.J., Monticelli, L., Lao, C., and Crotty, S. (2011). ICOS receptor instructs T follicular helper cell versus effector cell differentiation via induction of the transcriptional repressor Bcl6. In Immunity, pp. 932-946.

Chowdhury, D., and Sen, R. (2003). Transient IL-7/IL-7R signaling provides a mechanism for feedback inhibition of immunoglobulin heavy chain gene rearrangements. Immunity *18*, 229-241.

Christians, E., Davis, A.A., Thomas, S.D., and Benjamin, I.J. (2000). Maternal effect of Hsf1 on reproductive success. Nature *407*, 693-694.

Chu, B., Soncin, F., Price, B.D., Stevenson, M.A., and Calderwood, S.K. (1996). Sequential Phosphorylation by Mitogen-activated Protein Kinase and Glycogen Synthase Kinase 3 Represses Transcriptional Activation by Heat Shock Factor-1. In The Journal of biological chemistry, pp. 30847-30857.

Ci, W., Polo, J.M., Cerchietti, L., Shaknovich, R., Wang, L., Yang, S.N., Ye, K., Farinha, P., Horsman, D.E., Gascoyne, R.D.*, et al.* (2009). The BCL6 transcriptional program features repression of multiple oncogenes in primary B cells and is deregulated in DLBCL. Blood *113*, 5536-5548.

Ci, W., Polo, J.M., and Melnick, A. (2008). B-cell lymphoma 6 and the molecular pathogenesis of diffuse large B-cell lymphoma. Current opinion in hematology *15*, 381-390.

Collier, N.C., and Schlesinger, M.J. (1986). The dynamic state of heat shock proteins in chicken embryo fibroblasts. The Journal of cell biology *103*, 1495-1507.

Core, L.J., and Lis, J.T. (2008). Transcription Regulation Through Promoter-Proximal Pausing of RNA Polymerase II. In Science, pp. 1791-1792.

Corey, L.L. (2003). Localized recruitment of a chromatin-remodeling activity by an activator in vivo drives transcriptional elongation. In Genes & development, pp. 1392-1401.

Crotty, S. (2014). T follicular helper cell differentiation, function, and roles in disease. Immunity *41*, 529-542.

Dai, C., Santagata, S., Tang, Z., Shi, J., Cao, J., Kwon, H., Bronson, R.T., Whitesell, L., and Lindquist, S. (2012). Loss of tumor suppressor NF1 activates HSF1 to promote carcinogenesis. In The Journal of clinical investigation.

Dai, C., Whitesell, L., Rogers, A.B., and Lindquist, S. (2007). Heat shock factor 1 is a powerful multifaceted modifier of carcinogenesis. In Cell, pp. 1005-1018.

Dal Porto, J.M., Haberman, A.M., Kelsoe, G., and Shlomchik, M.J. (2002). Very low affinity B cells form germinal centers, become memory B cells, and participate in secondary immune responses when higher affinity competition is reduced. The Journal of experimental medicine *195*, 1215-1221.

Damberger, F.F., Pelton, J.G., Harrison, C.J., Nelson, H.C., and Wemmer, D.E. (1994). Solution structure of the DNA-binding domain of the heat shock transcription factor determined by multidimensional heteronuclear magnetic resonance spectroscopy. In Protein Science, pp. 1806-1821.

De Silva, N.S., and Klein, U. (2015). Dynamics of B cells in germinal centres. Nature reviews Immunology *15*, 137-148.

Degner, S.C., Wong, T.P., Jankevicius, G., and Feeney, A.J. (2009). Cutting edge: developmental stage-specific recruitment of cohesin to CTCF sites throughout immunoglobulin loci during B lymphocyte development. Journal of immunology *182*, 44-48.

DeKoter, R.P., Lee, H.J., and Singh, H. (2002). PU.1 regulates expression of the interleukin-7 receptor in lymphoid progenitors. Immunity *16*, 297-309.

Delogu, A., Schebesta, A., Sun, Q., Aschenbrenner, K., Perlot, T., and Busslinger, M. (2006). Gene repression by Pax5 in B cells is essential for blood cell homeostasis and is reversed in plasma cells. Immunity *24*, 269-281.

Denegri, M., Moralli, D., Rocchi, M., Biggiogera, M., Raimondi, E., Cobianchi, F., De Carli, L., Riva, S., and Biamonti, G. (2002). Human chromosomes 9, 12, and 15 contain the nucleation sites of stress-induced nuclear bodies. Molecular biology of the cell *13*, 2069-2079.

Dent, A.L., Shaffer, A.L., Yu, X., Allman, D., and Staudt, L.M. (1997). Control of Inflammation, Cytokine Expression, and Germinal Center Formation by BCL-6. In Science, pp. 589-592.

Deweindt, C., Albagli, O., Bernardin, F., Dhordain, P., Quief, S., Lantoine, D., Kerckaert, J.P., and Leprince, D. (1995). The LAZ3/BCL6 oncogene encodes a sequence-specific transcriptional inhibitor: a novel function for the BTB/POZ domain as an autonomous repressing domain. Cell growth & differentiation : the molecular biology journal of the American Association for Cancer Research *6*, 1495-1503.

Dhordain, P., Albagli, O., Lin, R.J., Ansieau, S., Quief, S., Leutz, A., Kerckaert, J.P., Evans, R.M., and Leprince, D. (1997). Corepressor SMRT binds the BTB/POZ repressing domain of the LAZ3/BCL6 oncoprotein. Proceedings of the National Academy of Sciences of the United States of America *94*, 10762-10767.

Dias, S., Silva, H., Jr., Cumano, A., and Vieira, P. (2005). Interleukin-7 is necessary to maintain the B cell potential in common lymphoid progenitors. The Journal of experimental medicine *201*, 971-979.

Dominguez, P.M., and Shaknovich, R. (2014). Epigenetic function of activation-induced cytidine deaminase and its link to lymphomagenesis. Frontiers in immunology *5*, 642.

Doughty, C.A., Bleiman, B.F., Wagner, D.J., Dufort, F.J., Mataraza, J.M., Roberts, M.F., and Chiles, T.C. (2006). Antigen receptor-mediated changes in glucose metabolism in B lymphocytes: role of phosphatidylinositol 3-kinase signaling in the glycolytic control of growth. Blood *107*, 4458-4465.

Duan, S., Cermak, L., Pagan, J.K., Rossi, M., Martinengo, C., di Celle, P.F., Chapuy, B., Shipp, M., Chiarle, R., and Pagano, M. (2012). FBXO11 targets BCL6 for degradation and is inactivated in diffuse large B-cell lymphomas. Nature *481*, 90-93.

Duina, A.A., Kalton, H.M., and Gaber, R.F. (1998). Requirement for Hsp90 and a CyP-40-type cyclophilin in negative regulation of the heat shock response. The Journal of biological chemistry *273*, 18974-18978.

Dunleavy, K., Pittaluga, S., Maeda, L.S., Advani, R., Chen, C.C., Hessler, J., Steinberg, S.M., Grant, C., Wright, G., Varma, G.*, et al.* (2013). Dose-adjusted EPOCH-rituximab therapy in primary mediastinal B-cell lymphoma. The New England journal of medicine *368*, 1408-1416.

Duy, C., Hurtz, C., Shojaee, S., Cerchietti, L., Geng, H., Swaminathan, S., Klemm, L., Kweon, S.M., Nahar, R., Braig, M.*, et al.* (2011). BCL6 enables Ph+ acute lymphoblastic leukaemia cells to survive BCR-ABL1 kinase inhibition. Nature *473*, 384-388.

Duy, C., Yu, J.J., Nahar, R., Swaminathan, S., Kweon, S.M., Polo, J.M., Valls, E., Klemm, L., Shojaee, S., Cerchietti, L.*, et al.* (2010). BCL6 is critical for the development of a diverse primary B cell repertoire. The Journal of experimental medicine *207*, 1209-1221.

Ebert, A., McManus, S., Tagoh, H., Medvedovic, J., Salvagiotto, G., Novatchkova, M., Tamir, I., Sommer, A., Jaritz, M., and Busslinger, M. (2011). The distal V(H) gene cluster of the Igh locus contains distinct regulatory elements with Pax5 transcription factor-dependent activity in pro-B cells. Immunity *34*, 175-187.

Eccles, S.A., Massey, A., Raynaud, F.I., Sharp, S.Y., Box, G., Valenti, M., Patterson, L., de Haven Brandon, A., Gowan, S., Boxall, F.*, et al.* (2008). NVP-AUY922: a novel heat shock protein 90 inhibitor active against xenograft tumor growth, angiogenesis, and metastasis. Cancer research *68*, 2850-2860.

Eckl, J.M., and Richter, K. (2013). Functions of the Hsp90 chaperone system: lifting client proteins to new heights. International journal of biochemistry and molecular biology *4*, 157-165.

Edgar, R.C. (2004). MUSCLE: multiple sequence alignment with high accuracy and high throughput. Nucleic acids research *32*, 1792-1797.

Eisen, M.B., Spellman, P.T., Brown, P.O., and Botstein, D. (1998). Cluster analysis and display of genome-wide expression patterns. Proceedings of the

National Academy of Sciences of the United States of America *95*, 14863-14868.

Elemento, O., Slonim, N., and Tavazoie, S. (2007). A universal framework for regulatory element discovery across all genomes and data types. Molecular cell *28*, 337-350.

Erez, N., Truitt, M., Olson, P., Arron, S.T., and Hanahan, D. (2010). Cancer-Associated Fibroblasts Are Activated in Incipient Neoplasia to Orchestrate Tumor-Promoting Inflammation in an NF-kappaB-Dependent Manner. Cancer cell *17*, 135-147.

Espinoza, C.A., Allen, T.A., Hieb, A.R., Kugel, J.F., and Goodrich, J.A. (2004). B2 RNA binds directly to RNA polymerase II to repress transcript synthesis. In Nature structural & molecular biology, pp. 822-829.

Fang, F., Chang, R., and Yang, L. (2012). Heat shock factor 1 promotes invasion and metastasis of hepatocellular carcinoma in vitro and in vivo. Cancer *118*, 1782-1794.

Farcas, A.M., Blackledge, N.P., Sudbery, I., Long, H.K., McGouran, J.F., Rose, N.R., Lee, S., Sims, D., Cerase, A., Sheahan, T.W.*, et al.* (2012). KDM2B links the Polycomb Repressive Complex 1 (PRC1) to recognition of CpG islands. eLife *1*, e00205.

Farkas, T., Kutskova, Y.A., and Zimarino, V. (1998). Intramolecular repression of mouse heat shock factor 1. Molecular and cellular biology *18*, 906-918.

Findly, R.C., Gillies, R.J., and Shulman, R.G. (1983). In vivo phosphorus-31 nuclear magnetic resonance reveals lowered ATP during heat shock of Tetrahymena. Science *219*, 1223-1225.

Fiorenza, M.T., Farkas, T., Dissing, M., Kolding, D., and Zimarino, V. (1995). Complex expression of murine heat shock transcription factors. Nucleic acids research *23*, 467-474.

Fritah, S., Col, E., Boyault, C., Govin, J., Sadoul, K., Chiocca, S., Christians, E., Khochbin, S., Jolly, C., and Vourc'h, C. (2009). Heat-shock factor 1

controls genome-wide acetylation in heat-shocked cells. In Molecular biology of the cell, pp. 4976-4984.

Fujimoto, M., Hayashida, N., Katoh, T., Oshima, K., Shinkawa, T., Prakasam, R., Tan, K., Inouye, S., Takii, R., and Nakai, A. (2010). A novel mouse HSF3 has the potential to activate nonclassical heat-shock genes during heat shock. In Molecular biology of the cell, pp. 106-116.

Fujimoto, M., Izu, H., Seki, K., Fukuda, K., Nishida, T., Yamada, S.-I., Kato, K., Yonemura, S., Inouye, S., and Nakai, A. (2004). HSF4 is required for normal cell growth and differentiation during mouse lens development. In The EMBO journal, pp. 4297-4306.

Fujimoto, M., Takaki, E., Takii, R., Tan, K., Prakasam, R., Hayashida, N., Iemura, S., Natsume, T., and Nakai, A. (2012). RPA assists HSF1 access to nucleosomal DNA by recruiting histone chaperone FACT. Molecular cell *48*, 182-194.

Fujita, N., Jaye, D.L., Geigerman, C., Akyildiz, A., Mooney, M.R., Boss, J.M., and Wade, P.A. (2004). MTA3 and the Mi-2/NuRD complex regulate cell fate during B lymphocyte differentiation. Cell *119*, 75-86.

Fuxa, M., and Busslinger, M. (2007). Reporter gene insertions reveal a strictly B lymphoid-specific expression pattern of Pax5 in support of its B cell identity function. Journal of immunology *178*, 8222-8228.

Fuxa, M., Skok, J., Souabni, A., Salvagiotto, G., Roldan, E., and Busslinger, M. (2004). Pax5 induces V-to-DJ rearrangements and locus contraction of the immunoglobulin heavy-chain gene. Genes & development *18*, 411-422.

Gandhapudi, S.K., Murapa, P., Threlkeld, Z.D., Ward, M., Sarge, K.D., Snow, C., and Woodward, J.G. (2013). Heat shock transcription factor 1 is activated as a consequence of lymphocyte activation and regulates a major proteostasis network in T cells critical for cell division during stress. Journal of immunology *191*, 4068-4079.

Gao, Z., Zhang, J., Bonasio, R., Strino, F., Sawai, A., Parisi, F., Kluger, Y., and Reinberg, D. (2012). PCGF homologs, CBX proteins, and RYBP define functionally distinct PRC1 family complexes. Molecular cell *45*, 344-356.

Garcia-Boronat, M., Diez-Rivero, C.M., Reinherz, E.L., and Reche, P.A. (2008). PVS: a web server for protein sequence variability analysis tuned to facilitate conserved epitope discovery. Nucleic acids research *36*, W35-41.

Gasch, A.P., Spellman, P.T., Kao, C.M., Carmel-Harel, O., Eisen, M.B., Storz, G., Botstein, D., and Brown, P.O. (2000). Genomic expression programs in the response of yeast cells to environmental changes. Molecular biology of the cell *11*, 4241-4257.

Gay, D., Saunders, T., Camper, S., and Weigert, M. (1993). Receptor editing: an approach by autoreactive B cells to escape tolerance. The Journal of experimental medicine *177*, 999-1008.

Gearhart, M.D., Corcoran, C.M., Wamstad, J.A., and Bardwell, V.J. (2006). Polycomb group and SCF ubiquitin ligases are found in a novel BCOR complex that is recruited to BCL6 targets. Molecular and cellular biology *26*, 6880-6889.

Gerner, E.W., and Schneider, M.J. (1975). Induced thermal resistance in HeLa cells. Nature *256*, 500-502.

Ghetu, A.F., Corcoran, C.M., Cerchietti, L., Bardwell, V.J., Melnick, A., and Privé, G.G. (2008). Structure of a BCOR corepressor peptide in complex with the BCL6 BTB domain dimer. In Molecular cell, pp. 384-391.

Ghosh, S.K., Missra, A., and Gilmour, D.S. (2011). Negative elongation factor accelerates the rate at which heat shock genes are shut off by facilitating dissociation of heat shock factor. Molecular and cellular biology *31*, 4232-4243.

Giannopoulou, E.G., and Elemento, O. (2011). An integrated ChIP-seq analysis platform with customizable workflows. BMC bioinformatics *12*, 277.

Gitlin, A.D., Shulman, Z., and Nussenzweig, M.C. (2014). Clonal selection in the germinal centre by regulated proliferation and hypermutation. Nature *509*, 637-640.

Goebel, P., Janney, N., Valenzuela, J.R., Romanow, W.J., Murre, C., and Feeney, A.J. (2001). Localized gene-specific induction of accessibility to V(D)J

recombination induced by E2A and early B cell factor in nonlymphoid cells. The Journal of experimental medicine *194*, 645-656.

Gomez, A.V., Galleguillos, D., Maass, J.C., Battaglioli, E., Kukuljan, M., and Andres, M.E. (2008). CoREST represses the heat shock response mediated by HSF1. Molecular cell *31*, 222-231.

Goodnow, C.C., Crosbie, J., Adelstein, S., Lavoie, T.B., Smith-Gill, S.J., Brink, R.A., Pritchard-Briscoe, H., Wotherspoon, J.S., Loblay, R.H., Raphael, K.*, et al.* (1988). Altered immunoglobulin expression and functional silencing of self-reactive B lymphocytes in transgenic mice. Nature *334*, 676-682.

Goodson, M.L., Park-Sarge, O.K., and Sarge, K.D. (1995). Tissue-dependent expression of heat shock factor 2 isoforms with distinct transcriptional activities. Molecular and cellular biology *15*, 5288-5293.

Goodson, M.L., and Sarge, K.D. (1995). Heat-inducible DNA binding of purified heat shock transcription factor 1. The Journal of biological chemistry *270*, 2447-2450.

Gray, D. (1993). Immunological memory. Annual review of immunology *11*, 49-77.

Green, M., Schuetz, T.J., Sullivan, E.K., and Kingston, R.E. (1995). A heat shock-responsive domain of human HSF1 that regulates transcription activation domain function. Molecular and cellular biology *15*, 3354-3362.

Grossman, A.D., Straus, D.B., Walter, W.A., and Gross, C.A. (1987). Sigma 32 synthesis can regulate the synthesis of heat shock proteins in Escherichia coli. Genes & development *1*, 179-184.

Guettouche, T., Boellmann, F., Lane, W.S., and Voellmy, R. (2005). Analysis of phosphorylation of human heat shock factor 1 in cells experiencing a stress. BMC biochemistry *6*, 4.

GuhaThakurta, D., Palomar, L., Stormo, G.D., Tedesco, P., Johnson, T.E., Walker, D.W., Lithgow, G., Kim, S., and Link, C.D. (2002). Identification of a novel cis-regulatory element involved in the heat shock response in

Caenorhabditis elegans using microarray gene expression and computational methods. Genome research *12*, 701-712.

Guo, R., Zheng, L., Park, J.W., Lv, R., Chen, H., Jiao, F., Xu, W., Mu, S., Wen, H., Qiu, J.*, et al.* (2014). BS69/ZMYND11 reads and connects histone H3.3 lysine 36 trimethylation-decorated chromatin to regulated pre-mRNA processing. Molecular cell *56*, 298-310.

Guo, Y., Guettouche, T., Fenna, M., Boellmann, F., Pratt, W.B., Toft, D.O., Smith, D.F., and Voellmy, R. (2001). Evidence for a mechanism of repression of heat shock factor 1 transcriptional activity by a multichaperone complex. The Journal of biological chemistry *276*, 45791-45799.

Hamel, K.M., Mandal, M., Karki, S., and Clark, M.R. (2014). Balancing Proliferation with Igkappa Recombination during B-lymphopoiesis. Frontiers in immunology *5*, 139.

Harrison, C., Bohm, A.A., and Nelson, H.C.M. (1994). Crystal structure of the DNA binding domain of the heat shock transcription factor. In Science, pp. 224.

Hartl, F.U., and Hayer-Hartl, M. (2009). Converging concepts of protein folding in vitro and in vivo. Nature structural & molecular biology *16*, 574-581.

Hatzi, K., Jiang, Y., Huang, C., Garrett-Bakelman, F., Gearhart, M.D., Giannopoulou, E.G., Zumbo, P., Kirouac, K., Bhaskara, S., Polo, J.M.*, et al.* (2013). A hybrid mechanism of action for BCL6 in B cells defined by formation of functionally distinct complexes at enhancers and promoters. Cell reports *4*, 578-588.

Hatzi, K., and Melnick, A. (2014). Breaking bad in the germinal center: how deregulation of BCL6 contributes to lymphomagenesis. Trends in molecular medicine *20*, 343-352.

He, B., Meng, Y.H., and Mivechi, N.F. (1998). Glycogen synthase kinase 3beta and extracellular signal-regulated kinase inactivate heat shock transcription factor 1 by facilitating the disappearance of transcriptionally active granules after heat shock. Molecular and cellular biology *18*, 6624-6633.

Hegde, R.S., Zuo, J., Voellmy, R., and Welch, W.J. (1995). Short circuiting stress protein expression via a tyrosine kinase inhibitor, herbimycin A. Journal of cellular physiology *165*, 186-200.

Hietakangas, V., Ahlskog, J.K., Jakobsson, A.M., Hellesuo, M., Sahlberg, N.M., Holmberg, C.I., Mikhailov, A., Palvimo, J.J., Pirkkala, L., and Sistonen, L. (2003). Phosphorylation of Serine 303 Is a Prerequisite for the Stress-Inducible SUMO Modification of Heat Shock Factor 1. In Molecular and cellular biology, pp. 2953-2968.

Hirano, M., Guo, P., McCurley, N., Schorpp, M., Das, S., Boehm, T., and Cooper, M.D. (2013). Evolutionary implications of a third lymphocyte lineage in lampreys. In Nature, pp. 435-438.

Holmberg, C.I., Hietakangas, V., Mikhailov, A., Rantanen, J.O., Kallio, M., Meinander, A., Hellman, J., Morrice, N., MacKintosh, C., Morimoto, R.I.*, et al.* (2001). Phosphorylation of serine 230 promotes inducible transcriptional activity of heat shock factor 1. The EMBO journal *20*, 3800-3810.

Homma, S., Jin, X., Wang, G., Tu, N., Min, J., Yanasak, N., and Mivechi, N.F. (2007). Demyelination, astrogliosis, and accumulation of ubiquitinated proteins, hallmarks of CNS disease in hsf1-deficient mice. The Journal of neuroscience : the official journal of the Society for Neuroscience *27*, 7974-7986.

Huang, C., Gonzalez, D.G., Cote, C.M., Jiang, Y., Hatzi, K., Teater, M., Dai, K., Hla, T., Haberman, A.M., and Melnick, A. (2014). The BCL6 RD2 Domain Governs Commitment of Activated B Cells to Form Germinal Centers. In Cell reports, pp. 1497-1508.

Huang, C., Hatzi, K., and Melnick, A. (2013). Lineage-specific functions of Bcl-6 in immunity and inflammation are mediated by distinct biochemical mechanisms. In Nature immunology.

Huynh, K.D., and Bardwell, V.J. (1998). The BCL-6 POZ domain and other POZ domains interact with the co-repressors N-CoR and SMRT. Oncogene *17*, 2473-2484.

Huynh, K.D., Fischle, W., Verdin, E., and Bardwell, V.J. (2000). BCoR, a novel corepressor involved in BCL-6 repression. Genes & development *14*, 1810-1823.

Inouye, S., Fujimoto, M., Nakamura, T., Takaki, E., Hayashida, N., Hai, T., and Nakai, A. (2007). Heat Shock Transcription Factor 1 Opens Chromatin Structure of Interleukin-6 Promoter to Facilitate Binding of an Activator or a Repressor. In The Journal of biological chemistry, pp. 33210-33217.

Inouye, S., Izu, H., Takaki, E., Suzuki, H., Shirai, M., Yokota, Y., Ichikawa, H., Fujimoto, M., and Nakai, A. (2004). Impaired IgG production in mice deficient for heat shock transcription factor 1. The Journal of biological chemistry *279*, 38701-38709.

Jacob, J., and Kelsoe, G. (1992). In situ studies of the primary immune response to (4-hydroxy-3-nitrophenyl)acetyl. II. A common clonal origin for periarteriolar lymphoid sheath-associated foci and germinal centers. The Journal of experimental medicine *176*, 679-687.

Jaeger, A.M., Makley, L.N., Gestwicki, J.E., and Thiele, D.J. (2014). Genomic heat shock element sequences drive cooperative human heat shock factor 1 DNA binding and selectivity. The Journal of biological chemistry *289*, 30459-30469.

Jakob, U., Lilie, H., Meyer, I., and Buchner, J. (1995). Transient interaction of Hsp90 with early unfolding intermediates of citrate synthase. Implications for heat shock in vivo. The Journal of biological chemistry *270*, 7288-7294.

Jamrich, M., Greenleaf, A.L., and Bautz, E.K. (1977). Localization of RNA polymerase in polytene chromosomes of Drosophila melanogaster. Proceedings of the National Academy of Sciences of the United States of America *74*, 2079-2083.

Jardin, F. (2014). Next generation sequencing and the management of diffuse large B-cell lymphoma: from whole exome analysis to targeted therapy. Discovery medicine *18*, 51-65.

Jedlicka, P., Mortin, M.A., and Wu, C. (1997). Multiple functions of Drosophila heat shock transcription factor in vivo. In The EMBO journal, pp. 2452-2462.

Jhaveri, K., Ochiana, S.O., Dunphy, M.P., Gerecitano, J.F., Corben, A.D., Peter, R.I., Janjigian, Y.Y., Gomes-DaGama, E.M., Koren, J., 3rd, Modi, S.*, et al.* (2014). Heat shock protein 90 inhibitors in the treatment of cancer: current status and future directions. Expert opinion on investigational drugs *23*, 611-628.

Jhunjhunwala, S., van Zelm, M.C., Peak, M.M., and Murre, C. (2009). Chromatin architecture and the generation of antigen receptor diversity. Cell *138*, 435-448.

Jin, X., Eroglu, B., Moskophidis, D., and Mivechi, N.F. (2011a). Methods in Molecular Biology, pp. 1-20.

Jin, X., Moskophidis, D., and Mivechi, N.F. (2011b). Heat shock transcription factor 1 is a key determinant of HCC development by regulating hepatic steatosis and metabolic syndrome. Cell metabolism *14*, 91-103.

Johnson, K., Hashimshony, T., Sawai, C.M., Pongubala, J.M., Skok, J.A., Aifantis, I., and Singh, H. (2008). Regulation of immunoglobulin light-chain recombination by the transcription factor IRF-4 and the attenuation of interleukin-7 signaling. Immunity *28*, 335-345.

Johnston, R.J., Poholek, A.C., DiToro, D., Yusuf, I., Eto, D., Barnett, B., Dent, A.L., Craft, J., and Crotty, S. (2009). Bcl6 and Blimp-1 are reciprocal and antagonistic regulators of T follicular helper cell differentiation. In Science, pp. 1006-1010.

Jolly, C., Konecny, L., Grady, D.L., Kutskova, Y.A., Cotto, J.J., Morimoto, R.I., and Vourc'h, C. (2002). In vivo binding of active heat shock transcription factor 1 to human chromosome 9 heterochromatin during stress. In The Journal of cell biology, pp. 775-781.

Jolly, C., Metz, A., Govin, J., Vigneron, M., Turner, B.M., Khochbin, S., and Vourc'h, C. (2004). Stress-induced transcription of satellite III repeats. The Journal of cell biology *164*, 25-33.

Jolly, C., and Morimoto, R.I. (2000). Role of the heat shock response and molecular chaperones in oncogenesis and cell death. Journal of the National Cancer Institute *92*, 1564-1572.

Jung, D., Giallourakis, C., Mostoslavsky, R., and Alt, F.W. (2006). Mechanism and control of V(D)J recombination at the immunoglobulin heavy chain locus. Annual review of immunology *24*, 541-570.

Kageshita, T., Kuwahara, K., Oka, M., Ma, D., Ono, T., and Sakaguchi, N. (2006). Increased expression of germinal center-associated nuclear protein (GANP) is associated with malignant transformation of melanocytes. Journal of dermatological science *42*, 55-63.

Kallio, M., Chang, Y., Manuel, M., Alastalo, T.P., Rallu, M., Gitton, Y., Pirkkala, L., Loones, M.T., Paslaru, L., Larney, S.*, et al.* (2002). Brain abnormalities, defective meiotic chromosome synapsis and female subfertility in HSF2 null mice. The EMBO journal *21*, 2591-2601.

Kalluri, R., and Zeisberg, M. (2006). Fibroblasts in cancer. Nature reviews Cancer *6*, 392-401.

Kamal, A., Thao, L., Sensintaffar, J., Zhang, L., Boehm, M.F., Fritz, L.C., and Burrows, F.J. (2003). A high-affinity conformation of Hsp90 confers tumour selectivity on Hsp90 inhibitors. Nature *425*, 407-410.

Kampinga, H.H., and Craig, E.A. (2010). The HSP70 chaperone machinery: J proteins as drivers of functional specificity. Nature reviews Molecular cell biology *11*, 579-592.

Karagianni, P., and Wong, J. (2007). HDAC3: taking the SMRT-N-CoRrect road to repression. Oncogene *26*, 5439-5449.

Kawamata, N., Miki, T., Ohashi, K., Suzuki, K., Fukuda, T., Hirosawa, S., and Aoki, N. (1994). Recognition DNA sequence of a novel putative transcription factor, BCL6. Biochemical and biophysical research communications *204*, 366-374.

Kelley, P.M., and Schlesinger, M.J. (1978). The effect of amino acid analogues and heat shock on gene expression in chicken embryo fibroblasts. Cell *15*, 1277-1286.

Kerfoot, S.M., Yaari, G., Patel, J.R., Johnson, K.L., Gonzalez, D.G., Kleinstein, S.H., and Haberman, A.M. (2011). Germinal center B cell and T follicular

helper cell development initiates in the interfollicular zone. Immunity *34*, 947-960.

Khaleque, M.A., Bharti, A., Gong, J., Gray, P.J., Sachdev, V., Ciocca, D.R., Stati, A., Fanelli, M., and Calderwood, S.K. (2008). Heat shock factor 1 represses estrogen-dependent transcription through association with MTA1. In Oncogene, pp. 1886-1893.

Khalil, A.M., Cambier, J.C., and Shlomchik, M.J. (2012). B cell receptor signal transduction in the GC is short-circuited by high phosphatase activity. Science *336*, 1178-1181.

Kikuchi, K., Lai, A.Y., Hsu, C.L., and Kondo, M. (2005). IL-7 receptor signaling is necessary for stage transition in adult B cell development through up-regulation of EBF. The Journal of experimental medicine *201*, 1197-1203.

Kitano, M., Moriyama, S., Ando, Y., Hikida, M., Mori, Y., Kurosaki, T., and Okada, T. (2011). Bcl6 Protein Expression Shapes Pre-Germinal Center B Cell Dynamics and Follicular Helper T Cell Heterogeneity. In Immunity, pp. 961-972.

Klein, U., and Dalla-Favera, R. (2008). Germinal centres: role in B-cell physiology and malignancy. In Nature reviews Immunology, pp. 22-33.

Kline, M.P., and Morimoto, R.I. (1997). Repression of the heat shock factor 1 transcriptional activation domain is modulated by constitutive phosphorylation. Molecular and cellular biology *17*, 2107-2115.

Knauf, U., Newton, E.M., Kyriakis, J., and Kingston, R.E. (1996). Repression of human heat shock factor 1 activity at control temperature by phosphorylation. In Genes & development, pp. 2782-2793.

Kojima, Y., Acar, A., Eaton, E.N., Mellody, K.T., Scheel, C., Ben-Porath, I., Onder, T.T., Wang, Z.C., Richardson, A.L., Weinberg, R.A.*, et al.* (2010). Autocrine TGF-beta and stromal cell-derived factor-1 (SDF-1) signaling drives the evolution of tumor-promoting mammary stromal myofibroblasts. Proceedings of the National Academy of Sciences of the United States of America *107*, 20009-20014.

Kourtis, N., Moubarak, R.S., Aranda-Orgilles, B., Lui, K., Aydin, I.T., Trimarchi, T., Darvishian, F., Salvaggio, C., Zhong, J., Bhatt, K.*, et al.* (2015). FBXW7 modulates cellular stress response and metastatic potential through HSF1 post-translational modification. Nature cell biology *17*, 322-332.

Lanneau, D., Wettstein, G., Bonniaud, P., and Garrido, C. (2010). Heat shock proteins: cell protection through protein triage. TheScientificWorldJournal *10*, 1543-1552.

LaPensee, C.R., Lin, G., Dent, A.L., and Schwartz, J. (2014). Deficiency of the transcriptional repressor B cell lymphoma 6 (Bcl6) is accompanied by dysregulated lipid metabolism. In PloS one, pp. e97090.

Larkindale, J., and Vierling, E. (2008). Core genome responses involved in acclimation to high temperature. Plant physiology *146*, 748-761.

Lazorchak, A.S., Schlissel, M.S., and Zhuang, Y. (2006). E2A and IRF-4/Pip promote chromatin modification and transcription of the immunoglobulin kappa locus in pre-B cells. Molecular and cellular biology *26*, 810-821.

Lederberg, J. (1959). Genes and antibodies. Science *129*, 1649-1653.

Lee, C.H., Melchers, M., Wang, H., Torrey, T.A., Slota, R., Qi, C.F., Kim, J.Y., Lugar, P., Kong, H.J., Farrington, L.*, et al.* (2006). Regulation of the germinal center gene program by interferon (IFN) regulatory factor 8/IFN consensus sequence-binding protein. The Journal of experimental medicine *203*, 63-72.

Lee, Y.-J., Kim, E.-H., Lee, J.S., Jeoung, D., Bae, S., Kwon, S.H., and Lee, Y.-S. (2008). HSF1 as a Mitotic Regulator: Phosphorylation of HSF1 by Plk1 Is Essential for Mitotic Progression. In Cancer research, pp. 7550-7560.

Lemaux, P.G., Herendeen, S.L., Bloch, P.L., and Neidhardt, F.C. (1978). Transient rates of synthesis of individual polypeptides in E. coli following temperature shifts. Cell *13*, 427-434.

Lemercier, C., Brocard, M.P., Puvion-Dutilleul, F., Kao, H.Y., Albagli, O., and Khochbin, S. (2002). Class II histone deacetylases are directly recruited by BCL6 transcriptional repressor. The Journal of biological chemistry *277*, 22045-22052.

Lenz, G., and Staudt, L.M. (2010). Aggressive lymphomas. In The New England journal of medicine, pp. 1417-1429.

Li, Z., Wang, X., Yu, R.Y., Ding, B.B., Yu, J.J., Dai, X.M., Naganuma, A., Stanley, E.R., and Ye, B.H. (2005). BCL-6 negatively regulates expression of the NF-kappaB1 p105/p50 subunit. Journal of immunology *174*, 205-214.

Lin, W.C., and Desiderio, S. (1994). Cell cycle regulation of V(D)J recombination-activating protein RAG-2. Proceedings of the National Academy of Sciences of the United States of America *91*, 2733-2737.

Lin, Y.C., Jhunjhunwala, S., Benner, C., Heinz, S., Welinder, E., Mansson, R., Sigvardsson, M., Hagman, J., Espinoza, C.A., Dutkowski, J.*, et al.* (2010). A global network of transcription factors, involving E2A, EBF1 and Foxo1, that orchestrates B cell fate. Nature immunology *11*, 635-643.

Lindquist, S. (1986). The heat-shock response. In Ann Rev Biochem, pp. 1151-1191.

Lindquist, S., and Craig, E.A. (1988). The heat-shock proteins, pp. 631-677.

Lis, J.T., Mason, P., Peng, J., Price, D.H., and Werner, J. (2000). P-TEFb kinase recruitment and function at heat shock loci. Genes & development *14*, 792-803.

Liu, D., Xu, H., Shih, C., Wan, Z., Ma, X., Ma, W., Luo, D., and Qi, H. (2015). T-B-cell entanglement and ICOSL-driven feed-forward regulation of germinal centre reaction. Nature *517*, 214-218.

Liu, H., Schmidt-Supprian, M., Shi, Y., Hobeika, E., Barteneva, N., Jumaa, H., Pelanda, R., Reth, M., Skok, J., Rajewsky, K.*, et al.* (2007). Yin Yang 1 is a critical regulator of B-cell development. Genes & development *21*, 1179-1189.

Liu, P.C., and Thiele, D.J. (1999). Modulation of human heat shock factor trimerization by the linker domain. The Journal of biological chemistry *274*, 17219-17225.

Lohr, J.G., Stojanov, P., Lawrence, M.S., Auclair, D., Chapuy, B., Sougnez, C., Cruz-Gordillo, P., Knoechel, B., Asmann, Y.W., Slager, S.L., *et al.* (2012). Discovery and prioritization of somatic mutations in diffuse large B-cell lymphoma (DLBCL) by whole-exome sequencing. Proceedings of the National Academy of Sciences of the United States of America *109*, 3879-3884.

Lu, P., Weaver, V.M., and Werb, Z. (2012). The extracellular matrix: a dynamic niche in cancer progression. The Journal of cell biology *196*, 395-406.

Lu, R., Medina, K.L., Lancki, D.W., and Singh, H. (2003). IRF-4,8 orchestrate the pre-B-to-B transition in lymphocyte development. Genes & development *17*, 1703-1708.

Ma, S., Pathak, S., Trinh, L., and Lu, R. (2008). Interferon regulatory factors 4 and 8 induce the expression of Ikaros and Aiolos to down-regulate pre-B-cell receptor and promote cell-cycle withdrawal in pre-B-cell development. Blood *111*, 1396-1403.

Mandal, M., Powers, S.E., Ochiai, K., Georgopoulos, K., Kee, B.L., Singh, H., and Clark, M.R. (2009). Ras orchestrates exit from the cell cycle and light-chain recombination during early B cell development. Nature immunology *10*, 1110-1117.

Mariner, P.D., Walters, R.D., Espinoza, C.A., Drullinger, L.F., Wagner, S.D., Kugel, J.F., and Goodrich, J.A. (2008). Human Alu RNA Is a Modular Transacting Repressor of mRNA Transcription during Heat Shock. In Molecular cell, pp. 499-509.

Marshall, N.F., Peng, J., Xie, Z., and Price, D.H. (1996). Control of RNA Polymerase II Elongation Potential by a Novel Carboxyl-terminal Domain Kinase. In The Journal of biological chemistry, pp. 27176-27183.

Mascle, X., Albagli, O., and Lemercier, C. (2003). Point mutations in BCL6 DNA-binding domain reveal distinct roles for the six zinc fingers. Biochemical and biophysical research communications *300*, 391-396.

Matsuura, H., Ishibashi, Y., Shinmyo, A., Kanaya, S., and Kato, K. (2010). Genome-wide analyses of early translational responses to elevated temperature and high salinity in Arabidopsis thaliana. Plant & cell physiology *51*, 448-462.

McAlister, L., and Finkelstein, D.B. (1980). Heat shock proteins and thermal resistance in yeast. Biochemical and biophysical research communications *93*, 819-824.

McMillan, D.R., Xiao, X., Shao, L., Graves, K., and Benjamin, I.J. (1998). Targeted disruption of heat shock transcription factor 1 abolishes thermotolerance and protection against heat-inducible apoptosis. The Journal of biological chemistry *273*, 7523-7528.

Medvedovic, J., Ebert, A., Tagoh, H., and Busslinger, M. (2011). Pax5: a master regulator of B cell development and leukemogenesis. Advances in immunology *111*, 179-206.

Melchers, F. (2005). The pre-B-cell receptor: selector of fitting immunoglobulin heavy chains for the B-cell repertoire. Nature reviews Immunology *5*, 578-584.

Mendillo, M.L., Santagata, S., Koeva, M., Bell, G.W., Hu, R., Tamimi, R.M., Fraenkel, E., Ince, T.A., Whitesell, L., and Lindquist, S. (2012). HSF1 Drives a Transcriptional Program Distinct from Heat Shock to Support Highly Malignant Human Cancers. In Cell, pp. 549-562.

Meng, L., Gabai, V.L., and Sherman, M.Y. (2010). Heat-shock transcription factor HSF1 has a critical role in human epidermal growth factor receptor-2-induced cellular transformation and tumorigenesis. Oncogene *29*, 5204-5213.

Metchat, A., Akerfelt, M., Bierkamp, C., Delsinne, V., Sistonen, L., Alexandre, H., and Christians, E.S. (2009). Mammalian heat shock factor 1 is essential for oocyte meiosis and directly regulates Hsp90alpha expression. The Journal of biological chemistry *284*, 9521-9528.

Metz, A., Soret, J., Vourc'h, C., Tazi, J., and Jolly, C. (2004). A key role for stress-induced satellite III transcripts in the relocalization of splicing factors into nuclear stress granules. Journal of cell science *117*, 4551-4558.

Meyer, R.D., Laz, E.V., Su, T., and Waxman, D.J. (2009). Male-specific hepatic Bcl6: growth hormone-induced block of transcription elongation in females and binding to target genes inversely coordinated with STAT5. In Molecular endocrinology, pp. 1914-1926.

Miki, T., Kawamata, N., Hirosawa, S., and Aoki, N. (1994). Gene involved in the 3q27 translocation associated with B-cell lymphoma, BCL5, encodes a Kruppel-like zinc-finger protein. Blood *83*, 26-32.

Miller, W., Rosenbloom, K., Hardison, R.C., Hou, M., Taylor, J., Raney, B., Burhans, R., King, D.C., Baertsch, R., Blankenberg, D.*, et al.* (2007). 28-way vertebrate alignment and conservation track in the UCSC Genome Browser. Genome research *17*, 1797-1808.

Milne, C.D., and Paige, C.J. (2006). IL-7: a key regulator of B lymphopoiesis. Seminars in immunology *18*, 20-30.

Min, J.N., Huang, L., Zimonjic, D.B., Moskophidis, D., and Mivechi, N.F. (2007). Selective suppression of lymphomas by functional loss of Hsf1 in a p53-deficient mouse model for spontaneous tumors. Oncogene *26*, 5086-5097.

Min, J.N., Zhang, Y., Moskophidis, D., and Mivechi, N.F. (2004). Unique contribution of heat shock transcription factor 4 in ocular lens development and fiber cell differentiation. Genesis *40*, 205-217.

Mondal, A., Sawant, D., and Dent, A.L. (2010). Transcriptional repressor BCL6 controls Th17 responses by controlling gene expression in both T cells and macrophages. Journal of immunology *184*, 4123-4132.

Morin, R.D., and Gascoyne, R.D. (2013). Newly identified mechanisms in B-cell non-Hodgkin lymphomas uncovered by next-generation sequencing. Seminars in hematology *50*, 303-313.

Morin, R.D., Mendez-Lago, M., Mungall, A.J., Goya, R., Mungall, K.L., Corbett, R.D., Johnson, N.A., Severson, T.M., Chiu, R., Field, M.*, et al.* (2011). Frequent mutation of histone-modifying genes in non-Hodgkin lymphoma. Nature *476*, 298-303.

Moulick, K., Ahn, J.H., Zong, H., Rodina, A., Cerchietti, L., Gomes DaGama, E.M., Caldas-Lopes, E., Beebe, K., Perna, F., Hatzi, K.*, et al.* (2011). Affinity-based proteomics reveal cancer-specific networks coordinated by Hsp90. Nature chemical biology *7*, 818-826.

Muppidi, J.R., Schmitz, R., Green, J.A., Xiao, W., Larsen, A.B., Braun, S.E., An, J., Xu, Y., Rosenwald, A., Ott, G.*, et al.* (2014). Loss of signalling via Galpha13 in germinal centre B-cell-derived lymphoma. Nature *516*, 254-258.

Nakai, A. (1999). New aspects in the vertebrate heat shock factor system: Hsf3 and Hsf4. Cell stress & chaperones *4*, 86-93.

Nakai, A., Tanabe, M., Kawazoe, Y., Inazawa, J., Morimoto, R.I., and Nagata, K. (1997). HSF4, a New Member of the Human Heat Shock Factor Family Which Lacks Properties of a Transcriptional Activator. In Molecular and cellular biology, pp. 469-481.

Neckers, L., and Workman, P. (2012). Hsp90 molecular chaperone inhibitors: are we there yet? Clinical cancer research : an official journal of the American Association for Cancer Research *18*, 64-76.

Nemazee, D.A., and Burki, K. (1989). Clonal deletion of B lymphocytes in a transgenic mouse bearing anti-MHC class I antibody genes. Nature *337*, 562-566.

Newton, E.M., Knauf, U., Green, M., and Kinston, R.E. (1996). The Regulatory Domain of Human Heat Shock Factor 1 Is Sufficient To Sense Heat Stress. In Molecular and cellular biology, pp. 839-846.

Ngo, V.N., Young, R.M., Schmitz, R., Jhavar, S., Xiao, W., Lim, K.H., Kohlhammer, H., Xu, W., Yang, Y., Zhao, H.*, et al.* (2011). Oncogenically active MYD88 mutations in human lymphoma. Nature *470*, 115-119.

Ni, Z., Saunders, A., Fuda, N.J., Yao, J., Suarez, J.-R., Webb, W.W., and Lis, J.T. (2008). P-TEFb is critical for the maturation of RNA polymerase II into productive elongation in vivo. In Molecular and cellular biology, pp. 1161-1170.

Nishimoto, N., Kubagawa, H., Ohno, T., Gartland, G.L., Stankovic, A.K., and Cooper, M.D. (1991). Normal pre-B cells express a receptor complex of mu heavy chains and surrogate light-chain proteins. Proceedings of the National Academy of Sciences of the United States of America *88*, 6284-6288.

Niu, H., Ye, B.H., and Dalla-Favera, R. (1998). Antigen receptor signaling induces MAP kinase-mediated phosphorylation and degradation of the BCL-6 transcription factor. Genes & development *12*, 1953-1961.

Nonaka, G., Blankschien, M., Herman, C., Gross, C.A., and Rhodius, V.A. (2006). Regulon and promoter analysis of the E. coli heat-shock factor, sigma32, reveals a multifaceted cellular response to heat stress. Genes & development *20*, 1776-1789.

Nossal, G.J., and Pike, B.L. (1980). Clonal anergy: persistence in tolerant mice of antigen-binding B lymphocytes incapable of responding to antigen or mitogen. Proceedings of the National Academy of Sciences of the United States of America *77*, 1602-1606.

Nover, L., Scharf, K.D., and Neumann, D. (1989). Cytoplasmic heat shock granules are formed from precursor particles and are associated with a specific set of mRNAs. Molecular and cellular biology *9*, 1298-1308.

Nurieva, R.I., Chung, Y., Martinez, G.J., Yang, X.O., Tanaka, S., Matskevitch, T.D., Wang, Y.-H., and Dong, C. (2009). Bcl6 mediates the development of T follicular helper cells. In Science, pp. 1001-1005.

Nutt, S.L., and Kee, B.L. (2007). The transcriptional regulation of B cell lineage commitment. Immunity *26*, 715-725.

O'Connor, B.P., Vogel, L.A., Zhang, W., Loo, W., Shnider, D., Lind, E.F., Ratliff, M., Noelle, R.J., and Erickson, L.D. (2006). Imprinting the fate of antigen-reactive B cells through the affinity of the B cell receptor. Journal of immunology *177*, 7723-7732.

O'Flaherty, E., and Kaye, J. (2003). TOX defines a conserved subfamily of HMG-box proteins. BMC genomics *4*, 13.

Ochiai, K., Maienschein-Cline, M., Mandal, M., Triggs, J.R., Bertolino, E., Sciammas, R., Dinner, A.R., Clark, M.R., and Singh, H. (2012). A self-reinforcing regulatory network triggered by limiting IL-7 activates pre-BCR signaling and differentiation. Nature immunology *13*, 300-307.

Oestreich, K.J., Mohn, S.E., and Weinmann, A.S. (2012). Molecular mechanisms that control the expression and activity of Bcl-6 in TH1 cells to regulate flexibility with a TFH-like gene profile. Nature immunology *13*, 405-411.

Okada, T., Miller, M.J., Parker, I., Krummel, M.F., Neighbors, M., Hartley, S.B., O'Garra, A., Cahalan, M.D., and Cyster, J.G. (2005). Antigen-engaged B cells undergo chemotaxis toward the T zone and form motile conjugates with helper T cells. PLoS biology *3*, e150.

Olumi, A.F., Grossfeld, G.D., Hayward, S.W., Carroll, P.R., Tlsty, T.D., and Cunha, G.R. (1999). Carcinoma-associated fibroblasts direct tumor progression of initiated human prostatic epithelium. Cancer research *59*, 5002-5011.

Oracki, S.A., Walker, J.A., Hibbs, M.L., Corcoran, L.M., and Tarlinton, D.M. (2010). Plasma cell development and survival. Immunological reviews *237*, 140-159.

Orimo, A., Gupta, P.B., Sgroi, D.C., Arenzana-Seisdedos, F., Delaunay, T., Naeem, R., Carey, V.J., Richardson, A.L., and Weinberg, R.A. (2005). Stromal fibroblasts present in invasive human breast carcinomas promote tumor growth and angiogenesis through elevated SDF-1/CXCL12 secretion. Cell *121*, 335-348.

Orosz, A., Wisniewski, J., and Wu, C. (1996). Regulation of Drosophila heat shock factor trimerization: global sequence requirements and independence of nuclear localization. In Molecular and cellular biology, pp. 7018-7030.

Ostling, P., Bjork, J.K., Roos-Mattjus, P., Mezger, V., and Sistonen, L. (2006). Heat Shock Factor 2 (HSF2) Contributes to Inducible Expression of hsp Genes through Interplay with HSF1. In The Journal of biological chemistry, pp. 7077-7086.

Otaki, J.M., Hatano, M., Matayoshi, R., Tokuhisa, T., and Yamamoto, H. (2010). The proto-oncogene BCL6 promotes survival of olfactory sensory neurons. Developmental neurobiology *70*, 424-435.

Parekh, S., Polo, J.M., Shaknovich, R., Juszczynski, P., Lev, P., Ranuncolo, S.M., Yin, Y., Klein, U., Cattoretti, G., Dalla Favera, R., *et al.* (2007). BCL6

programs lymphoma cells for survival and differentiation through distinct biochemical mechanisms. Blood *110*, 2067-2074.

Park, J.M., Werner, J., Kim, J.M., Lis, J.T., and Kim, Y.J. (2001). Mediator, not holoenzyme, is directly recruited to the heat shock promoter by HSF upon heat shock. Molecular cell *8*, 9-19.

Pasqualucci, L., Dominguez-Sola, D., Chiarenza, A., Fabbri, G., Grunn, A., Trifonov, V., Kasper, L.H., Lerach, S., Tang, H., Ma, J.*, et al.* (2011a). Inactivating mutations of acetyltransferase genes in B-cell lymphoma. Nature *471*, 189-195.

Pasqualucci, L., Neumeister, P., Goossens, T., Nanjangud, G., Chaganti, R.S., Kuppers, R., and Dalla-Favera, R. (2001). Hypermutation of multiple proto-oncogenes in B-cell diffuse large-cell lymphomas. Nature *412*, 341-346.

Pasqualucci, L., Trifonov, V., Fabbri, G., Ma, J., Rossi, D., Chiarenza, A., Wells, V.A., Grunn, A., Messina, M., Elliot, O.*, et al.* (2011b). Analysis of the coding genome of diffuse large B-cell lymphoma. In Nature Publishing Group, pp. 830-837.

Patriarca, E.J., and Maresca, B. (1990). Acquired thermotolerance following heat shock protein synthesis prevents impairment of mitochondrial ATPase activity at elevated temperatures in Saccharomyces cerevisiae. Experimental cell research *190*, 57-64.

Paus, D., Phan, T.G., Chan, T.D., Gardam, S., Basten, A., and Brink, R. (2006). Antigen recognition strength regulates the choice between extrafollicular plasma cell and germinal center B cell differentiation. The Journal of experimental medicine *203*, 1081-1091.

Pearl, L.H., and Prodromou, C. (2006). Structure and mechanism of the Hsp90 molecular chaperone machinery. Annual review of biochemistry *75*, 271-294.

Pereira, J.P., Kelly, L.M., Xu, Y., and Cyster, J.G. (2009). EBI2 mediates B cell segregation between the outer and centre follicle. Nature *460*, 1122-1126.

Perlot, T., and Alt, F.W. (2008). Cis-regulatory elements and epigenetic changes control genomic rearrangements of the IgH locus. Advances in immunology *99*, 1-32.

Peteranderl, R., and Nelson, H.C.M. (1992). Trimerization of the Heat Shock Transcription Factor by a Triple-Stranded a-Helical Coiled-Coil. In Biochemistry, pp. 12272-12276.

Petesch, S.J., and Lis, J.T. (2008). Rapid, transcription-independent loss of nucleosomes over a large chromatin domain at Hsp70 loci. Cell *134*, 74-84.

Petesch, S.J., and Lis, J.T. (2012). Activator-induced spread of poly(ADP-ribose) polymerase promotes nucleosome loss at Hsp70. In Molecular cell, pp. 64-74.

Phan, R.T., and Dalla-Favera, R. (2004). The BCL6 proto-oncogene suppresses p53 expression in germinal-centre B cells. In Nature, pp. 635-639.

Phan, R.T., Saito, M., Basso, K., Niu, H., and Dalla-Favera, R. (2005). BCL6 interacts with the transcription factor Miz-1 to suppress the cyclin-dependent kinase inhibitor p21 and cell cycle arrest in germinal center B cells. Nature immunology *6*, 1054-1060.

Pickup, M., Novitskiy, S., and Moses, H.L. (2013). The roles of TGFbeta in the tumour microenvironment. Nature reviews Cancer *13*, 788-799.

Polo, J.M., Dell'Oso, T., Ranuncolo, S.M., Cerchietti, L., Beck, D., Da Silva, G.F., Prive, G.G., Licht, J.D., and Melnick, A. (2004). Specific peptide interference reveals BCL6 transcriptional and oncogenic mechanisms in B-cell lymphoma cells. Nature medicine *10*, 1329-1335.

Pratt, W.B., and Toft, D.O. (1997). Steroid receptor interactions with heat shock protein and immunophilin chaperones. Endocrine reviews *18*, 306-360.

Prichard, M.N., and Shipman, C., Jr. (1990). A three-dimensional model to analyze drug-drug interactions. Antiviral research *14*, 181-205.

Prodromou, C., Roe, S.M., O'Brien, R., Ladbury, J.E., Piper, P.W., and Pearl, L.H. (1997). Identification and structural characterization of the ATP/ADP-binding site in the Hsp90 molecular chaperone. Cell *90*, 65-75.

Qi, H., Cannons, J.L., Klauschen, F., Schwartzberg, P.L., and Germain, R.N. (2008). SAP-controlled T-B cell interactions underlie germinal centre formation. Nature *455*, 764-769.

Rabindran, S.K., Haroun, R.I., Clos, J., Wisniewski, J., and Wu, C. (1993). Regulation of heat shock factor trimer formation: role of a conserved leucine zipper. Science *259*, 230-234.

Ranuncolo, S.M., Polo, J.M., Dierov, J., Singer, M., Kuo, T., Greally, J., Green, R., Carroll, M., and Melnick, A. (2007). Bcl-6 mediates the germinal center B cell phenotype and lymphomagenesis through transcriptional repression of the DNA-damage sensor ATR. In Nature immunology, pp. 705-714.

Ranuncolo, S.M., Polo, J.M., and Melnick, A. (2008a). BCL6 represses CHEK1 and suppresses DNA damage pathways in normal and malignant B-cells. In Blood Cells Mol Dis, pp. 95-99.

Ranuncolo, S.M., Wang, L., Polo, J.M., Dell'Oso, T., Dierov, J., Gaymes, T.J., Rassool, F., Carroll, M., and Melnick, A. (2008b). BCL6-mediated attenuation of DNA damage sensing triggers growth arrest and senescence through a p53-dependent pathway in a cell context-dependent manner. In The Journal of biological chemistry, pp. 22565-22572.

Raychaudhuri, S., Loew, C., Korner, R., Pinkert, S., Theis, M., Hayer-Hartl, M., Buchholz, F., and Hartl, F.U. (2014). Interplay of acetyltransferase EP300 and the proteasome system in regulating heat shock transcription factor 1. Cell *156*, 975-985.

Richmond, C.S., Glasner, J.D., Mau, R., Jin, H., and Blattner, F.R. (1999). Genome-wide expression profiling in Escherichia coli K-12. Nucleic acids research *27*, 3821-3835.

Richter, K., Haslbeck, M., and Buchner, J. (2010). The Heat Shock Response: Life on the Verge of Death. In Molecular cell, pp. 253-266.

Ritossa, F. (1962). A new puffing pattern induced by temperature shock and DNP in drosophila. Experientia *18*, 571-573.

Rizzi, N., Denegri, M., Chiodi, I., Corioni, M., Valgardsdottir, R., Cobianchi, F., Riva, S., and Biamonti, G. (2004). Transcriptional Activation of a Constitutive Heterochromatic Domain of the Human Genome in Response to Heat Shock. In Molecular biology of the cell, pp. 543-551.

Robinson, M.D., McCarthy, D.J., and Smyth, G.K. (2010). edgeR: a Bioconductor package for differential expression analysis of digital gene expression data. Bioinformatics *26*, 139-140.

Rodriguez-Abreu, D., Bordoni, A., and Zucca, E. (2007). Epidemiology of hematological malignancies. Annals of oncology : official journal of the European Society for Medical Oncology / ESMO *18 Suppl 1*, i3-i8.

Roe, S.M., Prodromou, C., O'Brien, R., Ladbury, J.E., Piper, P.W., and Pearl, L.H. (1999). Structural basis for inhibition of the Hsp90 molecular chaperone by the antitumor antibiotics radicicol and geldanamycin. Journal of medicinal chemistry *42*, 260-266.

Rohlin, L., Trent, J.D., Salmon, K., Kim, U., Gunsalus, R.P., and Liao, J.C. (2005). Heat shock response of Archaeoglobus fulgidus. Journal of bacteriology *187*, 6046-6057.

Romanow, W.J., Langerak, A.W., Goebel, P., Wolvers-Tettero, I.L., van Dongen, J.J., Feeney, A.J., and Murre, C. (2000). E2A and EBF act in synergy with the V(D)J recombinase to generate a diverse immunoglobulin repertoire in nonlymphoid cells. Molecular cell *5*, 343-353.

Roschewski, M., Staudt, L.M., and Wilson, W.H. (2014). Diffuse large B-cell lymphoma-treatment approaches in the molecular era. Nature reviews Clinical oncology *11*, 12-23.

Saibil, H. (2013). Chaperone machines for protein folding, unfolding and disaggregation. Nature reviews Molecular cell biology *14*, 630-642.

Sanchez, C., Sanchez, I., Demmers, J.A., Rodriguez, P., Strouboulis, J., and Vidal, M. (2007). Proteomics analysis of Ring1B/Rnf2 interactors identifies a

novel complex with the Fbxl10/Jhdm1B histone demethylase and the Bcl6 interacting corepressor. Molecular & cellular proteomics : MCP *6*, 820-834.

Sandqvist, A., Björk, J.K., Akerfelt, M., Chitikova, Z., Grichine, A., Vourc'h, C., Jolly, C., Salminen, T.A., Nymalm, Y., and Sistonen, L. (2009). Heterotrimerization of heat-shock factors 1 and 2 provides a transcriptional switch in response to distinct stimuli. In Molecular biology of the cell, pp. 1340-1347.

Santagata, S., Hu, R., Lin, N.U., Mendillo, M.L., Collins, L.C., Hankinson, S.E., Schnitt, S.J., Whitesell, L., Tamimi, R.M., Lindquist, S.*, et al.* (2011). High levels of nuclear heat-shock factor 1 (HSF1) are associated with poor prognosis in breast cancer. Proceedings of the National Academy of Sciences of the United States of America *108*, 18378-18383.

Santagata, S., Xu, Y.-M., Wijeratne, E.M.K., Kontnik, R., Rooney, C., Perley, C.C., Kwon, H., Clardy, J., Kesari, S., Whitesell, L.*, et al.* (2012). Using the heat-shock response to discover anticancer compounds that target protein homeostasis. In ACS chemical biology, pp. 340-349.

Santos, S.D., and Saraiva, M.J. (2004). Enlarged ventricles, astrogliosis and neurodegeneration in heat shock factor 1 null mouse brain. Neuroscience *126*, 657-663.

Sarge, K.D., Murphy, S.P., and Morimoto, R.I. (1993). Activation of heat shock gene transcription by heat shock factor 1 involves oligomerization, acquisition of DNA-binding activity, and nuclear localization and can occur in the absence of stress. Molecular and cellular biology *13*, 1392-1407.

Sato, H., Saito-Ohara, F., Inazawa, J., and Kudo, A. (2004). Pax-5 is essential for kappa sterile transcription during Ig kappa chain gene rearrangement. Journal of immunology *172*, 4858-4865.

Sawarkar, R., Sievers, C., and Paro, R. (2012). Hsp90 globally targets paused RNA polymerase to regulate gene expression in response to environmental stimuli. Cell *149*, 807-818.

Scheeren, F.A., Naspetti, M., Diehl, S., Schotte, R., Nagasawa, M., Wijnands, E., Gimeno, R., Vyth-Dreese, F.A., Blom, B., and Spits, H. (2005). STAT5

regulates the self-renewal capacity and differentiation of human memory B cells and controls Bcl-6 expression. Nature immunology *6*, 303-313.

Scherz-Shouval, R., Santagata, S., Mendillo, M.L., Sholl, L.M., Ben-Aharon, I., Beck, A.H., Dias-Santagata, D., Koeva, M., Stemmer, S.M., Whitesell, L.*, et al.* (2014). The reprogramming of tumor stroma by HSF1 is a potent enabler of malignancy. Cell *158*, 564-578.

Seifert, M., Scholtysik, R., and Kuppers, R. (2013). Origin and pathogenesis of B cell lymphomas. Methods in molecular biology *971*, 1-25.

Shaffer, A.L., 3rd, Young, R.M., and Staudt, L.M. (2012). Pathogenesis of human B cell lymphomas. Annual review of immunology *30*, 565-610.

Shaffer, A.L., Yu, X., He, Y., Boldrick, J., Chan, E.P., and Staudt, L.M. (2000). BCL-6 represses genes that function in lymphocyte differentiation, inflammation, and cell cycle control. Immunity *13*, 199-212.

Shapiro-Shelef, M., and Calame, K. (2005). Regulation of plasma-cell development. Nature reviews Immunology *5*, 230-242.

Shevtsov, S.P., and Dundr, M. (2011). Nucleation of nuclear bodies by RNA. In Nature Publishing Group, pp. 1-14.

Shi, Y., Mosser, D.D., and Morimoto, R.I. (1998). Molecular chaperones as HSF1-specific transcriptional repressors. Genes & development *12*, 654-666.

Shulman, Z., Gitlin, A.D., Weinstein, J.S., Lainez, B., Esplugues, E., Flavell, R.A., Craft, J.E., and Nussenzweig, M.C. (2014). Dynamic signaling by T follicular helper cells during germinal center B cell selection. Science *345*, 1058-1062.

Siegel, P.M., and Massague, J. (2003). Cytostatic and apoptotic actions of TGF-beta in homeostasis and cancer. Nature reviews Cancer *3*, 807-821.

Smith, S.T., Petruk, S., Sedkov, Y., Cho, E., Tillib, S., Canaani, E., and Mazo, A. (2004). Modulation of heat shock gene expression by the TAC1 chromatin-modifying complex. Nature cell biology *6*, 162-167.

Staudt, L.M. (2010). Oncogenic activation of NF-kappaB. In Cold Spring Harbor perspectives in biology, pp. a000109.

Stebbins, C.E., Russo, A.A., Schneider, C., Rosen, N., Hartl, F.U., and Pavletich, N.P. (1997). Crystal structure of an Hsp90-geldanamycin complex: targeting of a protein chaperone by an antitumor agent. Cell *89*, 239-250.

Stephanou, A., and Latchman, D.S. (2011). Transcriptional modulation of heat-shock protein gene expression. Biochemistry research international *2011*, 238601.

Stogios, P.J., Cuesta-Seijo, J.A., Chen, L., Pomroy, N.C., and Prive, G.G. (2010). Insights into strand exchange in BTB domain dimers from the crystal structures of FAZF and Miz1. Journal of molecular biology *400*, 983-997.

Straus, D.B., Walter, W.A., and Gross, C.A. (1987). The heat shock response of E. coli is regulated by changes in the concentration of sigma 32. Nature *329*, 348-351.

Straussman, R., Morikawa, T., Shee, K., Barzily-Rokni, M., Qian, Z.R., Du, J., Davis, A., Mongare, M.M., Gould, J., Frederick, D.T.*, et al.* (2012). Tumour micro-environment elicits innate resistance to RAF inhibitors through HGF secretion. Nature *487*, 500-504.

Sullivan, E.K., Weirich, C.S., Guyon, J.R., Sif, S., and Kingston, R.E. (2001). Transcriptional activation domains of human heat shock factor 1 recruit human SWI/SNF. Molecular and cellular biology *21*, 5826-5837.

Szulc, J., Wiznerowicz, M., Sauvain, M.-O., Trono, D., and Aebischer, P. (2006). A versatile tool for conditional gene expression and knockdown. In Nat Meth, pp. 109-116.

Tabuchi, Y., Takasaki, I., Wada, S., Zhao, Q.L., Hori, T., Nomura, T., Ohtsuka, K., and Kondo, T. (2008). Genes and genetic networks responsive to mild hyperthermia in human lymphoma U937 cells. International journal of hyperthermia : the official journal of European Society for Hyperthermic Oncology, North American Hyperthermia Group *24*, 613-622.

Taipale, M., Jarosz, D.F., and Lindquist, S. (2010). HSP90 at the hub of protein homeostasis: emerging mechanistic insights. In Nature reviews Molecular cell biology, pp. 515-528.

Takaki, E., Fujimoto, M., Sugahara, K., Nakahari, T., Yonemura, S., Tanaka, Y., Hayashida, N., Inouye, S., Takemoto, T., Yamashita, H.*, et al.* (2006). Maintenance of olfactory neurogenesis requires HSF1, a major heat shock transcription factor in mice. In The Journal of biological chemistry, pp. 4931-4937.

Takii, R., Fujimoto, M., Tan, K., Takaki, E., Hayashida, N., Nakato, R., Shirahige, K., and Nakai, A. (2015). ATF1 modulates the heat shock response by regulating the stress-inducible heat shock factor 1 transcription complex. Molecular and cellular biology *35*, 11-25.

Takii, R., Inouye, S., Fujimoto, M., Nakamura, T., Shinkawa, T., Prakasam, R., Tan, K., Hayashida, N., Ichikawa, H., Hai, T.*, et al.* (2010). Heat shock transcription factor 1 inhibits expression of IL-6 through activating transcription factor 3. In The Journal of Immunology, pp. 1041-1048.

Tan, K., Fujimoto, M., Takii, R., Takaki, E., Hayashida, N., and Nakai, A. (2015). Mitochondrial SSBP1 protects cells from proteotoxic stresses by potentiating stress-induced HSF1 transcriptional activity. Nature communications *6*, 6580.

Tanabe, M., Sasai, N., Nagata, K., Liu, X.D., Liu, P.C., Thiele, D.J., and Nakai, A. (1999). The mammalian HSF4 gene generates both an activator and a repressor of heat shock genes by alternative splicing. The Journal of biological chemistry *274*, 27845-27856.

Tang, D., Khaleque, M.A., Jones, E.L., Theriault, J.R., Li, C., Wong, W.H., Stevenson, M.A., and Calderwood, S.K. (2005). Expression of heat shock proteins and heat shock protein messenger ribonucleic acid in human prostate carcinoma in vitro and in tumors in vivo. Cell stress & chaperones *10*, 46-58.

Taylor, J.J., Pape, K.A., and Jenkins, M.K. (2012). A germinal center-independent pathway generates unswitched memory B cells early in the primary response. The Journal of experimental medicine *209*, 597-606.

Tiberi, L., Bonnefont, J., van den Ameele, J., Le Bon, S.D., Herpoel, A., Bilheu, A., Baron, B.W., and Vanderhaeghen, P. (2014). A BCL6/BCOR/SIRT1 complex triggers neurogenesis and suppresses medulloblastoma by repressing Sonic Hedgehog signaling. Cancer cell *26*, 797-812.

Tiberi, L., van den Ameele, J., Dimidschstein, J., Piccirilli, J., Gall, D., Herpoel, A., Bilheu, A., Bonnefont, J., Iacovino, M., Kyba, M.*, et al.* (2012). BCL6 controls neurogenesis through Sirt1-dependent epigenetic repression of selective Notch targets. In Nat Neurosci, pp. 1627-1635.

Tiegs, S.L., Russell, D.M., and Nemazee, D. (1993). Receptor editing in self-reactive bone marrow B cells. The Journal of experimental medicine *177*, 1009-1020.

Toivola, D.M., Strnad, P., Habtezion, A., and Omary, M.B. (2010). Intermediate filaments take the heat as stress proteins. Trends in cell biology *20*, 79-91.

Tokoyoda, K., Egawa, T., Sugiyama, T., Choi, B.I., and Nagasawa, T. (2004). Cellular niches controlling B lymphocyte behavior within bone marrow during development. Immunity *20*, 707-718.

Toney, L.M., Cattoretti, G., Graf, J.A., Merghoub, T., Pandolfi, P.P., Dalla-Favera, R., Ye, B.H., and Dent, A.L. (2000). BCL-6 regulates chemokine gene transcription in macrophages. Nature immunology *1*, 214-220.

Trapnell, C., Pachter, L., and Salzberg, S.L. (2009). TopHat: discovering splice junctions with RNA-Seq. In Bioinformatics, pp. 1105-1111.

Trepel, J., Mollapour, M., Giaccone, G., and Neckers, L. (2010). Targeting the dynamic HSP90 complex in cancer. Nature reviews Cancer *10*, 537-549.

Trinklein, N.D., Murray, J.I., Hartman, S.J., Botstein, D., and Myers, R.M. (2004). The role of heat shock transcription factor 1 in the genome-wide regulation of the mammalian heat shock response. In Molecular biology of the cell, pp. 1254-1261.

Tunyaplin, C., Shaffer, A.L., Angelin-Duclos, C.D., Yu, X., Staudt, L.M., and Calame, K.L. (2004). Direct repression of prdm1 by Bcl-6 inhibits plasmacytic differentiation. Journal of immunology *173*, 1158-1165.

VanDemark, A.P., Blanksma, M., Ferris, E., Heroux, A., Hill, C.P., and Formosa, T. (2006). The structure of the yFACT Pob3-M domain, its interaction with the DNA replication factor RPA, and a potential role in nucleosome deposition. Molecular cell *22*, 363-374.

Vasanwala, F.H., Kusam, S., Toney, L.M., and Dent, A.L. (2002). Repression of AP-1 function: a mechanism for the regulation of Blimp-1 expression and B lymphocyte differentiation by the B cell lymphoma-6 protooncogene. Journal of immunology *169*, 1922-1929.

Victora, G.D., and Nussenzweig, M.C. (2012). Germinal centers. Annual review of immunology *30*, 429-457.

Victora, G.D., Schwickert, T.A., Fooksman, D.R., Kamphorst, A.O., Meyer-Hermann, M., Dustin, M.L., and Nussenzweig, M.C. (2010). Germinal center dynamics revealed by multiphoton microscopy with a photoactivatable fluorescent reporter. In Cell, pp. 592-605.

Vihervaara, A., Sergelius, C., Vasara, J., Blom, M.A., Elsing, A.N., Roos-Mattjus, P., and Sistonen, L. (2013). Transcriptional response to stress in the dynamic chromatin environment of cycling and mitotic cells. Proceedings of the National Academy of Sciences of the United States of America *110*, E3388-3397.

Vilenchik, M., Solit, D., Basso, A., Huezo, H., Lucas, B., He, H., Rosen, N., Spampinato, C., Modrich, P., and Chiosis, G. (2004). Targeting wide-range oncogenic transformation via PU24FCl, a specific inhibitor of tumor Hsp90. Chemistry & biology *11*, 787-797.

Voellmy, R. (2004). On mechanisms that control heat shock transcription factor activity in metazoan cells. In Cell stress & chaperones, pp. 122-133.

Vogel, J.L., Parsell, D.A., and Lindquist, S. (1995). Heat-shock proteins Hsp104 and Hsp70 reactivate mRNA splicing after heat inactivation. Current biology : CB *5*, 306-317.

Vuister, G.W., Kim, S.J., Orosz, A., Marquardt, J., Wu, C., and Bax, A. (1994). Solution structure of the DNA-binding domain of Drosophila heat shock transcription factor. Nature structural biology *1*, 605-614.

Vuori, K.A., Ahlskog, J.K., Sistonen, L., and Nikinmaa, M. (2009). TransLISA, a novel quantitative, nonradioactive assay for transcription factor DNA-binding analyses. The FEBS journal *276*, 7366-7374.

Wade, J.T., Castro Roa, D., Grainger, D.C., Hurd, D., Busby, S.J., Struhl, K., and Nudler, E. (2006). Extensive functional overlap between sigma factors in Escherichia coli. Nature structural & molecular biology *13*, 806-814.

Wang, G., Ying, Z., Jin, X., Tu, N., Zhang, Y., Phillips, M., Moskophidis, D., and Mivechi, N.F. (2004). Essential requirement for both hsf1 and hsf2 transcriptional activity in spermatogenesis and male fertility. In Genesis, pp. 66-80.

Wang, G., Zhang, J., Moskophidis, D., and Mivechi, N.F. (2003). Targeted disruption of the heat shock transcription factor (hsf)-2 gene results in increased embryonic lethality, neuronal defects, and reduced spermatogenesis. In Genesis, pp. 48-61.

Warters, R.L., and Stone, O.L. (1983). The effects of hyperthermia on DNA replication in HeLa cells. Radiation research *93*, 71-84.

Warters, R.L., and Stone, O.L. (1984). Histone protein and DNA synthesis in HeLa cells after thermal shock. Journal of cellular physiology *118*, 153-160.

Welch, W.J., and Suhan, J.P. (1985). Morphological study of the mammalian stress response: characterization of changes in cytoplasmic organelles, cytoskeleton, and nucleoli, and appearance of intranuclear actin filaments in rat fibroblasts after heat-shock treatment. The Journal of cell biology *101*, 1198-1211.

Welch, W.J., and Suhan, J.P. (1986). Cellular and biochemical events in mammalian cells during and after recovery from physiological stress. The Journal of cell biology *103*, 2035-2052.

Westerheide, S.D., Anckar, J., Stevens, S.M., Sistonen, L., and Morimoto, R.I. (2009). Stress-inducible regulation of heat shock factor 1 by the deacetylase SIRT1. In Science, pp. 1063-1066.

Whitesell, L., and Lindquist, S. (2009). Inhibiting the transcription factor HSF1 as an anticancer strategy. In Expert Opin Ther Targets, pp. 469-478.

Whitesell, L., Mimnaugh, E.G., De Costa, B., Myers, C.E., and Neckers, L.M. (1994). Inhibition of heat shock protein HSP90-pp60v-src heteroprotein complex formation by benzoquinone ansamycins: essential role for stress proteins in oncogenic transformation. Proceedings of the National Academy of Sciences of the United States of America *91*, 8324-8328.

Wilson, T.R., Fridlyand, J., Yan, Y., Penuel, E., Burton, L., Chan, E., Peng, J., Lin, E., Wang, Y., Sosman, J.*, et al.* (2012). Widespread potential for growth-factor-driven resistance to anticancer kinase inhibitors. Nature *487*, 505-509.

Wold, M.S. (1997). Replication protein A: a heterotrimeric, single-stranded DNA-binding protein required for eukaryotic DNA metabolism. Annual review of biochemistry *66*, 61-92.

Wong, R.S., and Dewey, W.C. (1982). Molecular studies on the hyperthermic inhibition of DNA synthesis in Chinese hamster ovary cells. Radiation research *92*, 370-395.

Workman, P., Burrows, F., Neckers, L., and Rosen, N. (2007). Drugging the cancer chaperone HSP90: combinatorial therapeutic exploitation of oncogene addiction and tumor stress. Annals of the New York Academy of Sciences *1113*, 202-216.

Wu, C. (1995). Heat shock transcription factors: structure and regulation. In Annu Rev Cell Dev Biol pp. 441-469.

Xavier, I.J., Mercier, P.A., McLoughlin, C.M., Ali, A., Woodgett, J.R., and Ovsenek, N. (2000). Glycogen synthase kinase 3beta negatively regulates both DNA-binding and transcriptional activities of heat shock factor 1. The Journal of biological chemistry *275*, 29147-29152.

Xiao, X., Zuo, X., Davis, A.A., McMillan, D.R., Curry, B.B., Richardson, J.A., and Benjamin, I.J. (1999). HSF1 is required for extra-embryonic development, postnatal growth and protection during inflammatory responses in mice. In The EMBO journal, pp. 5943-5952.

Xing, H. (2005). Mechanism of hsp70i Gene Bookmarking. In Science, pp. 421-423.

Xu, D., Zalmas, L.P., and La Thangue, N.B. (2008). A transcription cofactor required for the heat-shock response. In EMBO reports, pp. 662-669.

Ye, B.H., Cattoretti, G., Shen, Q., Zhang, J., Hawe, N., Waard, R.d., Leung, C., Nouri-Shirazi, M., Orazi, A., Chaganti, R.*, et al.* (1997). The BCL-6 proto-oncogene controls germinal-centre formation and Th2-type inflammation. In Nature genetics, pp. 161-170.

Ying, C.Y., Dominguez-Sola, D., Fabi, M., Lorenz, I.C., Hussein, S., Bansal, M., Califano, A., Pasqualucci, L., Basso, K., and Dalla-Favera, R. (2013). MEF2B mutations lead to deregulated expression of the oncogene BCL6 in diffuse large B cell lymphoma. Nature immunology *14*, 1084-1092.

Yoshida, T., Fukuda, T., Hatano, M., Koseki, H., Okabe, S., Ishibashi, K., Kojima, S., Arima, M., Komuro, I., Ishii, G.*, et al.* (1999). The role of Bcl6 in mature cardiac myocytes. Cardiovascular research *42*, 670-679.

Yoshida, T., Fukuda, T., Okabe, S., Hatano, M., Miki, T., Hirosawa, S., Miyasaka, N., Isono, K., and Tokuhisa, T. (1996). The BCL6 gene is predominantly expressed in keratinocytes at their terminal differentiation stage. Biochemical and biophysical research communications *228*, 216-220.

Zaarur, N., Gabai, V.L., Porco, J.A., Calderwood, S., and Sherman, M.Y. (2006). Targeting heat shock response to sensitize cancer cells to proteasome and Hsp90 inhibitors. In Cancer research, pp. 1783-1791.

Zan, H., and Casali, P. (2013). Regulation of Aicda expression and AID activity. Autoimmunity *46*, 83-101.

Zhang, J., Grubor, V., Love, C.L., Banerjee, A., Richards, K.L., Mieczkowski, P.A., Dunphy, C., Choi, W., Au, W.Y., Srivastava, G.*, et al.* (2013). Genetic

heterogeneity of diffuse large B-cell lymphoma. Proceedings of the National Academy of Sciences of the United States of America *110*, 1398-1403.

Zhang, S., Steijart, M.N., Lau, D., Schutz, G., Delucinge-Vivier, C., Descombes, P., and Bading, H. (2007). Decoding NMDA receptor signaling: identification of genomic programs specifying neuronal survival and death. Neuron *53*, 549-562.

Zhao, K., Liu, M., and Burgess, R.R. (2005). The global transcriptional response of Escherichia coli to induced sigma 32 protein involves sigma 32 regulon activation followed by inactivation and degradation of sigma 32 in vivo. The Journal of biological chemistry *280*, 17758-17768.

Zhao, Y., Liu, H., Liu, Z., Ding, Y., Ledoux, S.P., Wilson, G.L., Voellmy, R., Lin, Y., Lin, W., Nahta, R.*, et al.* (2011). Overcoming trastuzumab resistance in breast cancer by targeting dysregulated glucose metabolism. Cancer research *71*, 4585-4597.

Zhao, Y.H., Zhou, M., Liu, H., Ding, Y., Khong, H.T., Yu, D., Fodstad, O., and Tan, M. (2009). Upregulation of lactate dehydrogenase A by ErbB2 through heat shock factor 1 promotes breast cancer cell glycolysis and growth. Oncogene *28*, 3689-3701.

Zhong, M., Wisniewski, J., Fritsch, M., Mizuguchi, G., Orosz, A., Jedlicka, P., and Wu, C. (1996). Purification of heat shock transcription factor of Drosophila. Methods in enzymology *274*, 113-119.

Zobeck, K.L., Buckley, M.S., Zipfel, W.R., and Lis, J.T. (2010). Recruitment timing and dynamics of transcription factors at the hsp70 Loci in living cells. In Molecular cell, pp. 965-975.

Zotos, D., and Tarlinton, D.M. (2012). Determining germinal centre B cell fate. Trends in immunology *33*, 281-288.

Zou, J., Guo, Y., Guettouche, T., Smith, D.F., and Voellmy, R. (1998). Repression of heat shock transcription factor HSF1 activation by HSP90 (HSP90 complex) that forms a stress-sensitive complex with HSF1. Cell *94*, 471-480.

Zuehlke, A., and Johnson, J.L. (2010). Hsp90 and co-chaperones twist the functions of diverse client proteins. Biopolymers *93*, 211-217.

Zuo, J., Baler, R., Dahl, G., and Voellmy, R. (1994). Activation of the DNA-binding ability of human heat shock transcription factor 1 may involve the transition from an intramolecular to an intermolecular triple-stranded coiled-coil structure. Molecular and cellular biology *14*, 7557-7568.

Zuo, J., Rungger, D., and Voellmy, R. (1995). Multiple layers of regulation of human heat shock transcription factor 1. Molecular and cellular biology *15*, 4319-4330.